CHARACTERISTICS AND WATER PROPERTIES OF MESOSCALE EDDIES IN THE REGION OF STATION ALOHA

A THESIS SUBMITTED TO THE GRADUATE DIVISION OF THE
UNIVERSITY OF HAWAI'I IN PARTIAL FUFILLMENT
OF THE REQUIREMENTS FOR THE DEGREE OF

MASTER OF SCIENCE

IN

OCEANOGRAPHY

AUGUST 2008

By
Kellee M. Nolan

Thesis Committee:

Roger Lukas, Chairperson
Mark Merrifield
Bo Qiu

We certify that we have read this thesis and that, in our opinion, it is satisfactory in scope and quality as a thesis for the degree of Master of Science in Oceanography.

THESIS COMMITTEE

Chairperson

ACKNOWLEDGEMENTS

I am indebted to the United States Coast Guard for the opportunity to complete this work. I could not have accomplished so much in such a short time without the continued support of my advisory committee, especially Roger. The algorithm output provided by, and the collaboration with, Dudley Chelton and Michael Schlax from Oregon State University were invaluable. I would not have succeeded without the technical support of the HOT physical oceanography team members, especially Paul Lethaby and Fernando Santiago-Mandujano. I also appreciate the unyielding moral support from my family and friends.

ABSTRACT

Mesoscale eddies in the central North Pacific Subtropical Gyre have important consequences on physical phenomena and significant influence on biological and geochemical properties (Robinson, 1983). This study focuses on eddies that pass through Station ALOHA, the ~monthly sampling site of the Hawaii Ocean Time-series (HOT) Program, located at 22° 45'N and 158°W, 100 km north of Oahu. Eddies are first identified as closed contours of sea level anomalies from gridded maps of merged satellite altimetry and then tracked using an eddy identification and tracking algorithm developed by Chelton et al. (2007). From October 1992-December 2006, 76 eddies (40 cyclonic and 36 anticyclonic) passed through the 2°x2° degree box surrounding Station ALOHA and are catalogued in a database which includes information about their statistics (amplitude, radius, translation speed and axial speed). Additionally, for eddies whose passage through Station ALOHA overlapped with a HOT cruise, vertical profiles of water mass properties and ADCP measurements are analyzed to gain additional information about the characteristics of these eddies. The eddies are subject to several types of interactions that disrupt them from equilibrium including interaction with other eddies, interaction with the topography of the Hawaiian islands and interaction with the surrounding mean flow. The presence of the Hawaiian Islands greatly affects eddy trajectories in this region. Water property anomalies are greater for eddies that form east of 148°W than water property anomalies for eddies that form near Station ALOHA (west of 156°W), indicating that the eddies formed east of 148°W encapsulate water from their source region and transport it within a bolus as they translate west. The eddies that pass

through ALOHA share similar characteristics to eddies in the larger surrounding region bounded by 15°-30°N and 170°-140°W.

TABLE OF CONTENTS

LIST OF TABLES

LIST OF FIGURES

Figure Page

Figure Page

1 Introduction

Mesoscale eddies have significant impacts on localized regions (Lumpkin 1998, Sweeney et al. 2003). Because of their ability to transport momentum, salt, heat and anomalous biological and chemical properties, mesoscale eddies can affect water mass properties far from their generation point (McDonald 1999). The eddy transport of heat is crucial for balancing the global ocean heat budget (Roemmich and Gilson 2001) and eddy waters can significantly impact the biogeochemistry of a localized region (Robinson 1983, Siegel et al. 1999).

With the objective of understanding eddy characteristics and their impacts on the surrounding water north of Oahu, Hawaii, this work focuses on the region surrounding Station ALOHA (A Long-term Oligotrophic Habitat Assessment), the focus of the Hawaii Ocean Time-series (HOT) program. Station ALOHA is a 10 km radius circle centered on 22°45'N and 158°00'W, situated 100 km north of Kahuku Point on the Hawaiian island of Oahu. Eddies in this region are important mechanisms for vertical and horizontal advection; processes which have been suggested to have large impacts on the regional biogeochemical balance (Letelier et al. 2000) and interannual climate variability (Roemmich and Gilson 2001), respectively.

Several individual eddy events at ALOHA have been analyzed in detail to gain insight about both their physical (Lukas and Santiago-Mandujano 2001, Firing and Merrifield 2004) and biogeochemical properties (Letelier et al. 2000, Lukas and Santiago-Mandujano 2001), but a time-series of eddies in this region has not been developed and analyzed. Here, we use the extensive catalog of mesoscale eddies detected by an eddy-tracking algorithm that identifies eddy structures from satellite

altimetry measurements of sea surface height (Chelton et al. 2007). Tracked eddies are then analyzed in detail to build a database of characteristics for each eddy that includes the following parameters: rotation direction, radius, amplitude, speed and direction of propagation, lifetime, water mass properties and interactions with other eddies and/or topography.

Section 2 elaborates on types of vortices, general eddy dynamics, eddy genesis and distribution, eddy movement, eddy interactions and eddy transport. Section 3 further describes the HOT program, Station ALOHA and collection and analysis of HOT data. Section 3 also discusses methods used to analyze several data sources including AVISO (Archiving, Validation and Interpretation of Satellite Oceanographic data) altimetry data (AVISO 2006) and the eddy identification and tracking algorithm developed by Chelton et al. (2007). Results (Section 4) describes ALOHA eddy characteristics obtained from the identification and tracking algorithm, their spatial and temporal distribution, information about their vertical structure as obtained from the HOT data and a summary of the eddy characteristics for the larger region north and east of the Hawaiian Islands. Section 5 summarizes the characteristics of eddies at ALOHA and the eddies of the larger region surrounding the Hawaiian Islands, discusses how well ALOHA eddies behave like idealized vortices, and addresses how well the method works for eddy identification and tracking in the region of the Hawaiian Islands.

2 Scientific Background

An eddy is defined as a closed circulation where the circulation period of a water parcel moving within the structure is shorter than the lifetime of the structure (Cushman-Roisin 1994). Eddies are not the only mesoscale features that occur in the ocean, and it is important to be able to distinguish eddies from other items such as jets, current meanders and Rossby waves.

Distinguishing eddies from Rossby waves is especially important. Mesoscale eddies and Rossby waves can appear similar in altimetric data (Chelton and Schlax 1996, Chelton et al. 2007). Unlike eddies, Rossby waves are not able to transport mass and heat. In the sub-tropics, Rossby waves and mesoscale eddies propagate at similar translational speeds (~5 cm/s) and occur at nearly the same period (~100 days). Rossby waves can also manifest as closed contours in sea level anomalies from a super position of two Rossby waves together. Particular patterns of winds acting on the sea surface can also result in closed contours of sea level anomaly (SLA). Chelton and Schlax (1996) attributed mesoscale signals they found in Topex/Poseidon (T/P) data solely to Rossby waves, but after analyzing data merged from multiple altimeters, they were able to show that the mesoscale field was dominated by eddies, not Rossby waves (Chelton et al. 2007).

The major distinction between Rossby waves and eddy vortices is their duration. Superimposed Rossby waves are a transient phenomenon, which won't last more than a couple of weeks, and the complex wind patterns needed to sustain mesoscale circular closed contours of SLA are improbable whereas eddies will remain as coherent closed

contoured vortices for several weeks or more. It is this difference that is a crucial threshold of the algorithm (described in detail in Section 3.3.3) used to identify only the mesoscale eddies in the region of ALOHA. Another difference between Rossby waves and eddies is that Rossby waves are based on linear theory, while eddies are inherently nonlinear (Section 2.2).

2.1 Types of Vortices

2.1.1 Theoretical Models

There are several widely used theoretical models of a closed circulation vortex for determining the radial distribution of the azimuthal component of velocity of an eddy: those in solid body rotation, irrotational vortices, Rankine vortices and Gaussian vortices (Lumpkin 1998, Kundu and Cohen 2004). Solid body rotation occurs when the period of rotation of all particles in the vortex around the vortex center are the same, so that the angular velocity is proportional to the radius of the streamline for any point in the vortex. All fluid particles in the vortex have constant vorticity and behave as a rigid, rotating solid, thus the name "solid-body rotation". This creates an infinite-shear edge separating the vortex from the surrounding fluid of the same density, which is physically impossible (Lumpkin 1998). An irrotational vortex is characterized by "circular flow where the velocity is tangential and inversely proportional to the radius of the streamline" (Kundu and Cohen 2004). This means that vorticity is zero everywhere except at the center, where vorticity is infinite (Kundu and Cohen 2004). A Rankine vortex is an idealization of a vortex that has a solid body core and irrotational far field (Figure 2.1) (Kundu and Cohen 2004). Rankine vortices are characterized by constant vorticity within a specified

core radius and zero vorticity outside the core. A Gaussian vortex is another idealization of a vortex that does not have the vorticity discontinuity displayed in a Rankine vortex (Figure 2.1). A Gaussian eddy is assumed to be radially symmetric with a sea surface height (h) perturbation that is Gaussian shaped

$$h(r) = h_0 e^{\frac{r^2}{2L^2}} \tag{1}$$

where h_0 is the amplitude of the eddy, r is the distance from center of the eddy and L is the radius of the eddy. Assuming geostrophy, this height function gives an azimuthal velocity distribution ($v(r)$)

$$v(r) = \frac{g' h_0}{fL^2} r e^{-\frac{r^2}{2L^2}} \tag{2}$$

where g' is the reduced gravity and f is the Coriolis parameter $f = 2\Omega \sin(\theta)$.

2.1.2 Baroclinicity

Eddies can be categorized into different types. One distinction is whether an eddy is barotropic or baroclinic (Figure 2.2). In barotropic flow, density changes are a function of depth only. This means that isopycnals are flat, and therefore horizontal geostrophic velocities within the flow are unchanging with depth. A barotropic eddy is best visualized as a column of water in solid body rotation. This type of eddy is formed from a barotropic instability (Section 2.3.2).

More common are baroclinic eddies that form from baroclinic instabilities (Section 2.3.2) (Gill et al. 1974). First baroclinic mode eddies have their maximum velocities at the surface, where isopycnals are flat. Isopycnal displacement is concave upwards (bowl shaped) for an anticyclone and convex upwards (dome shaped) for a cyclone. First

baroclinic mode eddies near Station ALOHA have their maximum isopycnal displacement around 1000 m. This is the location of the zero crossing of horizontal velocities and the region of greatest shear. Below 1000 m, geostrophic velocities are in the opposite direction from the surface layer but are relatively weak (Figure 2.2) and isopycnal displacements are slightly convex for an anticyclone and slightly concave for a cyclone. Higher baroclinic mode eddies do exist (Paschini et al. 1993) but have more complex vertical structures and will not be discussed in this study, because there is evidence which suggests that the majority of the eddies near Station ALOHA are probably first baroclinic mode features (Wyrtki 1982, Chiswell 2002).

2.1.3 Mesoscale Eddies

This study will focus on mesoscale eddies, which exist in approximate geostrophic balance, generally move westward at a few cm/s (Gill 1982), have length scales on the order of 100 km and time scales of 70-90 days. Mesoscale eddies can be categorized into two basic types: surface and subsurface eddies. This study focuses on surface eddies, that is, eddies with a sea surface signature in sea level anomalies. Surface eddies can be cyclonic or anticyclonic. An example of a subsurface eddy is a mode water eddy, which will be discussed briefly.

Cyclonic eddies rotate in the same sense as the earth's rotation (Cushman-Roisin 1994), that is that they rotate counterclockwise in the Northern Hemisphere and clockwise in the Southern Hemisphere and exhibit a negative sea level anomaly. This type of eddy is associated with an elevation in isopycnals (relative to the surrounding

environment) in both the seasonal and main pycnoclines, and upwelling within the eddy structure during the formation (spin up) phase (Figure 2.3).

Anticyclonic eddies rotate clockwise in the Northern Hemisphere and counterclockwise in the Southern Hemisphere and exhibit an elevated sea level anomaly. This type of eddy depresses both the main and seasonal pycnoclines (relative to the surrounding environment) during the spin up phase (Figure 2.3).

Mode water eddies result from a mode water intrusion, which depresses the main pycnocline and elevates the seasonal pycnocline (Figure 2.3). A mode water intrusion results from a convective instability that disturbs isopycnal surfaces and creates a density gradient, which then induces a circulation in order to conserve potential vorticity. Mode water eddies rotate in the same direction as anticyclones because geostrophic velocities are dominated by the depression of the main pycnocline (McGillicuddy et al. 2007). Mode water eddies may or may not have an identifiable sea level anomaly.

There are specific types of eddies that are well documented, including Gulf Stream Rings and Meddies. Gulf Stream Rings can be cyclones or anticyclones, depending on which side of the Gulf Stream current they separate from. Eddies that form by separation from a current are common in strong western boundary current systems. Meddies are anticyclones associated with the Mediterranean outflow. These subsurface mode water eddies are on the order of 100 km in diameter, 800 m thick, centered around 1000 m in depth and can last up to several years (Knauss 1996).

2.2 Eddy Dynamics

We begin with the momentum equation

$$\rho_0\left(\frac{\partial}{\partial t}+\bar{u}\cdot\nabla\right)\bar{u}+\rho_0 2\Omega\times\bar{u}=-\nabla\bar{P}+A_h\nabla_h{}^2\bar{u}+A_v\frac{\partial^2}{\partial z^2}\bar{u} \tag{3}$$

where the first two terms on the left hand side describe the local acceleration and advection of a water parcel with velocity ($\bar{u}$). The third term on the left describes the effect of rotation, referred to as the Coriolis force. The first term on the right is the pressure gradient force, and the last two terms describe the horizontal (A_h) and vertical (A_v) eddy viscosities. If (3) is scaled for velocity (U) scales typically found in eddies located in the central North Pacific Subtropical Gyre O(0.1 m/s) (Chelton and Schlax 1996, Roemmich and Gilson 2001) and length scales (L) on the order of the radius of deformation $R_d=\frac{c}{f}\approx 50\,\text{km}$ (O(50 km)), where c is the first baroclinic mode Rossby wave speed (~2.9 cm/s near Station ALOHA), and f is the vertical component of the Coriolis force ($f=2\Omega\sin(\theta)$), then the Rossby number is about 0.1.

$$R_o=\frac{U}{fL}\approx 0.1 \tag{4}$$

A Rossby number of 0.1 would indicate that the nonlinear advective terms are an order of magnitude smaller than the Coriolis force and should be neglected. This is appropriate for eddies in background conditions that are not subject to interactions with the mean flow, with other mesoscale features or with topography (Section 2.6). In the case where the Rossby number approaches one, the nonlinear advective terms are retained, leaving

$$\frac{Du}{Dt}-fv=\frac{1}{\rho_0}\frac{\partial P}{\partial x}\ \text{and}\ \frac{Dv}{Dt}+fu=\frac{1}{\rho_0}\frac{\partial P}{\partial y} \tag{5}$$

as the horizontal momentum balance for an eddy. The first term is the material derivative, which contains the local acceleration and nonlinear advective terms and the

second term is the Coriolis force. These are balanced on the right hand side by the pressure gradient force.

It is more difficult to describe eddies that are subject to interactions (Section 2.6) and are changing size and velocity continuously as they attempt to maintain "quasi-equilibrium". In such an environment, if we Reynolds average the horizontal momentum equation (3) for large scale motions, we see that the horizontal eddy viscosity term (A_h) parameterizes eddy fluxes due to nonlinear interactions.

If the nonlinear terms are ignored but the local acceleration term is retained, the resulting balance is known as quasi-geostrophic balance, which includes linear Rossby waves as a solution (Section 2.2.3). If the local acceleration term is additionally dropped, then geostrophy dominates, which describes eddy behavior to the lowest order. If the momentum equation (3) is scaled with smaller length scales (less than 100 km), then the centrifugal force is as important as the Coriolis force. This momentum balance is referred to as cyclo-geostrophic balance and will be described in Section 2.2.2.

2.2.1 Vorticity

Eddy motions can also be described in terms of vorticity, which is derived as the curl of the momentum equation. For nonlinear solutions, vorticity is complicated. Vorticity is a dynamic tracer and a property of the flow where other tracers (like salinity or nutrients) are thermodynamic tracers and properties of the fluid (Müller 1995). Potential vorticity is the vorticity averaged over a layer of fluid, defined by

$$\frac{D}{Dt}\left(\frac{f+\zeta}{\frac{1}{\rho_0}\frac{d\rho}{dz}}\right) = \text{sources} + \text{sinks} \tag{6}$$

where ζ is the vertical component of relative vorticity $\zeta = \frac{\partial v}{\partial x} - \frac{\partial u}{\partial y}$, the spin due to the horizontal motion of the parcel. f is the planetary vorticity , or the spin due to the earth's rotation, which is approximated by $f = f_0 + \beta y$, where β is the change in f due to a change in latitude (y). Sources of potential vorticity in an eddy include wind stress curl, bottom stress curl, and turbulent stress curl. Sinks include turbulence, eddy diffusivity, the bottom boundary layer and shape distortions from interactions with other eddies.

In the rare case where the sources and sinks sum to zero, potential vorticity in an eddy is conserved. Most of the time, however, they do not, and an eddy is gaining or losing potential vorticity as it translates (Drijfhout and Hazeleger 2001, Mahadeva et al. 2008). The particulars of these higher order dynamics will not be discussed here. In this study, a linearized version of potential vorticity ($\zeta = 0$) that is density dependent known as Ertel's vorticity is used (Müller 1995), which assumes that the eddy dynamics are inherently baroclinic,

$$Q_0 = \frac{f}{\rho_0}\frac{\partial \rho}{\partial z} \tag{7}$$

2.2.2 Cyclo-geostrophic balance

The centrifugal force is due to flow along a curved trajectory. The importance of the centrifugal force in an eddy depends on its radius and velocity, $C_p = \frac{U^2}{R}$.

Cyclostrophic balance is the extreme case where the vortex is so small that the Coriolis effect can be neglected (like the flow down a drain or in a tornado). By neglecting the Coriolis force, the remaining forces are the pressure gradient and the centrifugal force. Since the centrifugal force is always directed outward, the pressure gradient force must be directed inward, and therefore only vortices with low pressure centers exist in cyclostrophic balance.

Cyclo-geostrophic balance is normally described in polar coordinates, and retains the nonlinear centrifugal force term in geostrophic balance

$$\frac{v^2}{r} + fv = g\frac{\partial h}{\partial r} \tag{8}$$

where $\frac{v^2}{r}$ is the centrifugal force, v is the azimuthal component of velocity, h is amplitude of the eddy and r is the radius.

2.2.3 Quasi-geostrophy

Quasi-geostrophy assumes geostrophic flow to the lowest order, but retains the time dependence in the vorticity equation so that the geostrophic relations for velocity can be used everywhere except in the horizontal divergence term.

$$\frac{\partial u}{\partial t} - fv = -\frac{1}{\rho_0}\frac{\partial P}{\partial x} \text{ and } \frac{\partial v}{\partial t} + fu = -\frac{1}{\rho_0}\frac{\partial P}{\partial y} \tag{9}$$

Several studies used to describe vortex motions utilize a one and a half layer, quasi-geostrophic vortices on the β–plane (McWilliams and Flierl 1979, McDonald 1999). Quasi-geostrophy is also used to describe Rossby waves.

2.2.4 Eddy force balance

In the subtropics, on length scales of the same order of magnitude as the Rossby radius of deformation $R_d = \frac{c}{f} \approx 50\text{km}$ the centrifugal force $C_p = \frac{U^2}{R}$ is the same order of magnitude as the Coriolis force and so should be considered. Cyclones are characterized by a sea level depression, so the pressure gradient force is directed inward (Figure 2.4) and is partially balanced by the outward directed centrifugal force. The outward directed Coriolis force makes up the difference. In an anticyclone, the pressure gradient force is directed outward, as is the centrifugal force, so the Coriolis must be directed inward and balance both outward forces. As a result, the orbital velocity (in cyclogeostrophic balance) of an anticyclone will be greater than that of a cyclone of the same amplitude and radius (Cushman 1994).

2.3 Eddy Genesis Regions and Mechanisms

2.3.1 North Pacific Genesis Regions

Knowledge of the temporal and spatial distribution of mesoscale eddies is required to quantify the impact of mesoscale eddies on basin scales. Roemmich and Gilson (2001) determined through XBT transects of the North Pacific that eddy variability was the dominant forcing mechanism for interannual changes in southward transport of thermocline waters. They identified 410 features across the North Pacific over an eight-year period through a combination of remote and in-situ measurements.

Though the east-central North Pacific Subtropical Gyre (NPSG) is a region characterized by weak mean flow and relatively low eddy kinetic energy compared to

regions like the Kuroshio western boundary current system, the ratio of eddy kinetic energy to mean kinetic energy is approximately 10/1 (Wyrtki et al. 1976). Though the eddies in the central NPSG are comparatively weak, they are an important part of the variability in this region.

Niiler and Hall (1988) used current meter data to study eddies at 28°N, 152°W, which were characterized by length scales of 150-175 km and periods of 40-80 days. Munch (1996) identified regions northeast of the Hawaiian Ridge that exhibited high energy variability and hypothesized that this variability was due to the presence of Rossby waves and the Musician Seamounts, but the source of this energy and its generation mechanisms remain unknown.

2.3.2 Formation Mechanisms

Eddy kinetic energy in the ocean is an important component of large scale ocean circulation. Potential energy available in the mean circulation can be converted to eddy kinetic energy through baroclinic instabilities (Gill et al. 1974, Wyrtki et al. 1976). Baroclinic instability occurs at low Rossby numbers when density surfaces are not parallel to pressure surfaces. Lateral variations in density surfaces set up a potential where the density surfaces seek to regain equilibrium with pressure surfaces and create vorticity in the process, thus initiating the formation of an eddy. Baroclinic instability depends on the vertical velocity distribution and stratification, whereas in a barotropic instability the velocities are depth independent.

A barotropic instability is one where density perturbations are a function of pressure alone, so that the instability is independent of depth and stratification. It

depends on the meridional gradient of absolute vorticity changing sign somewhere in the flow (Munch 1996). Both barotropic and baroclinic instabilities can arise in areas of horizontal shear such as western boundary currents (Gulf Stream rings) or wind shear (eddies in the lee of the Hawaiian Islands). Both types of instabilities can co-exist in a stratified fluid. Determining which type of instability is the primary formation mechanism for eddies impacting Station ALOHA is difficult with the data used in this study, but previous studies (Bernstein 1974, Wyrtki 1982) have shown that the eddies in this region are probably primarily caused by baroclinic instabilities.

2.3.3 Related regions of interest

There are particular areas of high eddy activity that have been well studied, including the rings that are pinched off from Gulf Stream meanders in the Atlantic (Knauss 1996), those that are seasonally generated in the Gulf of Tehauntepec (Zamudio et al. 2006), and the regular eddy events in the lee of the Hawaiian islands (Patzert 1969, Lumpkin 1998). Only very recently has there been a global approach to identifying eddies through satellite altimetry (Chelton et al. 2007). An improved version of this approach is used here to identify the eddies affecting Station ALOHA.

The HOT program's Atlantic Ocean counterpart is the Bermuda Atlantic Time-series Study (BATS) program. The BATS site is off Bermuda in the western boundary current recirculation region of the North Atlantic Subtropical Gyre and it has been sampled monthly since 1988. In 1994, the nearby Bermuda Testbed Mooring was added to provide a high-resolution time series with moored instrumentation (McGillicuddy et al. 1999). Several mesoscale eddies that have passed through the BATS site have been

heavily sampled to ascertain their vertical structure and composition as well as the response of the surrounding upper ocean (McGillicuddy et al. 1999, McNeil et al. 1999, Siegel et al. 1999, Sweeney et al. 2003). Sweeney et al. (2003) analyzed nine eddies that passed through the BATS site from 1993-1995, determining that eddies in this region significantly influence primary production and particle fluxes. Another study (Siegel et al. 1999) identified eddies using satellite altimetry over a four year period (1992-1996). The identified features exhibited SLA's up to 25 cm, diameters of 100-200 km, propagation speeds of 5 cm/s, and had lifetimes of several months.

Eddies that form in the lee of the Hawaiian Islands are also well investigated. Though the location of these features is within a few degrees of latitude to the eddies that pass through Station ALOHA, the lee eddies are completely different. The lee eddies are similar to a von Karman vortex street and are more frequent, more intense and more predictable (Patzert 1969, Lumpkin 1998) than eddies that pass through ALOHA. These eddies occur about every 60 days, with alternating extremes of SLA and propagate with speeds up to 10 cm/s (Holland and Mitchum 2001). Several recent case studies of particular eddy events have shown Hawaiian lee eddies to be responsible for increased silica export (Benitez-Nelson et al. 2007) and regions of biological enhancement (Seki et al. 2001).

2.4 Eddy Evolution

2.4.1 Lifecycle

An eddy lifecycle is characterized by three stages: generation, maturity, and decay. Generation, or spin-up phase, of an eddy can be the result of one of several

mechanisms. Eddies can be generated from current shear like that associated with western boundary currents, most notably the Gulf Stream Rings of the North Atlantic. Eddies can also be wind generated, like those formed in the Gulf of Tehuantepec (Zamudio et al. 2006) or in the lee of the Hawaiian Islands. A more prevalent mechanism for eddy formation is baroclinic instability, such as exists in the region between Hawaii and Taiwan (Qiu 1999). The spin up phase takes place in a particular location, known as the eddy genesis region, and it is the water properties from this region that become encapsulated in the bolus (or center) of the eddy. The transition to the mature phase occurs when the eddy reaches quasi-geostrophic balance. Finally, the decay, or spin-down phase, occurs when the eddy breaks up and transfers its energy to smaller scales where it can be dissipated.

2.4.2 Westward drift

The Coriolis force on the south side of an eddy is less than on the north side. In order to maintain geostrophic balance, the velocity on the south side will be greater than on the north side. The velocity difference results in a convergence (divergence) on the western side of the anticyclone (cyclone), which redistributes mass to the west, and thus the eddy itself moves westward (Cushman-Roisin 1994). Westward drift can also be explained in terms of conservation of potential vorticity. As a vortex rotates, it induces relative vorticity in surrounding water parcels. Disturbed parcels on the north (south) part of the eddy develop cyclonic (anticyclonic) relative vorticity. Integrating these relative vorticities at the latitude of the vortex center results in westward drift (Nof 1981, Cushman-Roisin et al. 1990).

Eddy drift velocity can be theoretically calculated using a one-and-a-half-layer, reduced gravity model on the beta-plane. In this model, quasi-geostrophic eddies with length scales on the order of the internal Rossby radius of deformation (R) propagate at the long, non-dispersive Rossby wave speed (u_R) (Nof 1981, Cushman et al. 1990),

$$u_R = -\beta_0 R^2 \tag{10}$$

where $R^2 = \frac{c}{f}$ and $\beta_0 = \frac{\partial f}{\partial y}$. The first baroclinic mode phase velocity (c_1) near ALOHA is 2.9 m/s (Chiswell 2002), so the drift velocity of first baroclinic mode quasi-geostrophic eddies is 5.5 cm/s.

2.5 Eddy Transport

Eddies have potentially important implications for local biogeochemistry because they correspond with anomalies in water mass properties (Richardson 1993). These anomalies originate from several mechanisms including vertical advection, lateral entrainment, advection of the eddy by the mean flow and bolus transport. Each of these mechanisms is described in detail in the following sections and is depicted in Figure 2.5. Also addressed is the impact of biological processes on eddy water property characteristics. Each of these processes affects the purity of water property signals that an eddy retains throughout its lifetime.

2.5.1 Vertical Advection

As eddies amplify or decay, there is a vertical velocity that displaces isopycnals to balance horizontal pressure gradients. In the amplification of an anticyclone (cyclone), the isopycnals are displaced downward (upward). This mechanism is important during

the spin up phase of the eddy and is the process that brings nutrient rich water from below into the euphotic zone in a cyclonic eddy. Another mechanism for vertical transport of water properties in eddies is enhanced diapycnal mixing (Siegel et al. 1999).

2.5.2 Lateral Entrainment

Another mechanism by which eddies can create a water mass anomaly is by horizontal advection and lateral stirring. An eddy's far field is in contact with the surrounding water mass, and as the eddy rotates, it can displace the surrounding spatial gradients of surrounding water properties. This process is the primary contributor to water mass mixing within the eddy. This process can penetrate to the center of the eddy and change the water mass signature of the eddy, especially when eddy-eddy or eddy-topography interactions are involved (Section 2.6). Multiple observations of a Gulf Stream ring (Schmitz and Vastano 1975) revealed migration of water property characteristics from the ring's periphery into its center. Recently, model simulations have shown that second order nonlinear circulation processes within an eddy are responsible for mixing water property characteristics outside of an eddy with water property characteristics within an eddy (Mahadevan et al. 2008).

2.5.3 Advection by the Mean Flow

Though eddies translate westward because of their dynamics (Section 2.4.2), they can also be carried along by background mean flow. If eddies are assumed to be in geostrophic balance, this advection of eddies by the mean flow will not occur if the mean flow is geostrophic and purely zonal or purely meridional and has a length scale much larger than the length scale of the eddy. The horizontal pressure gradient that induces

current flow (assuming a purely zonal or purely meridional current), is balanced by advection of the eddy by the mean flow. This explains why eddies in strong eastward flows like the Kuroshio extension still move westward.

2.5.4 Bolus Transport

Bolus transport is the final and most significant process by which eddies can transport water masses. The bolus is the core of the eddy, which has limited interaction with its surrounding environment once the eddy has reached steady state. This is the most interior part of the eddy and exhibits the water mass characteristics of the eddy formation region. Eddies formed in a region with a large spatial gradient of water mass properties will have a mixture across the gradient of water mass properties drawn into the bolus during formation, whereas an eddy formed in a region with small spatial gradients of water properties will have a purer signal of water mass property characteristics at its formation location. In January 2001, an extreme water mass anomaly passed through Station ALOHA and was attributed to the bolus of an eddy that formed off of Baja California in 1997 during an El Niño event (Lukas and Santiago-Mandujano 2001). This eddy remnant was identified solely by its anomalous water properties, some of which were over 30 standard deviations from average conditions at Station ALOHA.

2.6 Eddy Interactions

Eddy-eddy or eddy-topography interactions can determine how and where eddies will redistribute heat, momentum and water-mass characteristics during their life cycle. Eddy interactions are highly nonlinear and complex, and these interactions can have significant impacts on eddy behavior. For example, models that describe westward

propagation of an isolated vortex neglect to describe meridional displacements caused by interactions with topography, the mean flow, or with other mesoscale features. Mesoscale eddies are important features for transferring energy to different scales. Ocean processes predominantly transfer energy down into the smaller scales, but eddies can interact with each other, or with topographic features, or with instabilities in the mean flow, and can transfer energy back to larger scales. These interactions are an important aspect of eddy behavior but are difficult to quantify.

2.6.1 Eddy-eddy

Vortices can cause one another to move while mostly maintaining their own shape when the shear strain rate between features is less than the rotational velocity inside the vortex, where the shear strain rate

$$S = \frac{\partial u}{\partial y} + \frac{\partial v}{\partial x} \tag{11}$$

describes the deformation of the vortex. Eddy-eddy interactions require that the vortices are sufficiently separated, otherwise they will deform one another (McWilliams 2006). Weak eddy-eddy interactions can result in a meridional change in translation direction from directly west. This will cause an imbalance of forces, but the eddy can regain equilibrium by several methods. The eddy can return to its original latitude, change its vorticity (i.e. spin faster or slow down), or stretch/shrink, as per the conservation of potential vorticity. More intrusive deformation can result in the exchange of mass between two eddies. In the extreme case, deformation will cause two interacting vortices to merge. The dynamics involved in this process are more complex than will be discussed here.

2.6.2 Eddy-topography

Eddy interactions with topography are most straightforward with barotropic eddies, where the vortex is uniform throughout the water column. Using the shallow water approximation, where the length scale of the eddy is much larger than the vertical scale, as the eddy translates onto a step where the height (H) will decrease, so relative vorticity or the Coriolis parameter will also have to decrease in order for the eddy to conserve potential vorticity (Section 2.2.1) and maintain shape. Decreasing relative vorticity is an unstable solution, thus the eddy would "prefer" to move equatorward (toward a smaller f) in order to maintain equilibrium (Cushman-Roisin 1994). If an eddy encounters a vertical (meridional) wall, depending on its direction of rotation it will also seek to recover its equilibrium balance by moving equatorward (cyclones) or poleward (anticyclones).

2.6.3 Eddy-mean flow

Eddies can draw energy from the mean flow by barotropic or baroclinic instability. Eddies can also transfer energy into the mean flow that they translate through (Section 2.5.3). Baroclinic instabilities in the mean flow can work to amplify or decay an eddy (Stammer 1998). Drawing energy from the mean flow can cause an eddy to re-intensify after its initial spin-up phase and can assist in the translation of an eddy across an ocean basin. Model simulations have shown that eddies can play an important role in determining the character of the large-scale mean flow by a) limiting the amplitude of upper ocean mean flow and b) transferring energy downward into the deep ocean from the surface (Holland 1978).

2.7 Biological Impact

By advecting water property characteristics into a region with different characteristics, salinity and nutrient gradients are changed in the region impacted by the eddy. Since most of the interior ocean is nutrient limited near the surface, introducing nutrients into such an area will cause a change in primary production, which will then change the nutrient and oxygen characteristics of the eddy. Essentially this means that the biologically dependent water property characteristics of an eddy can be changing due to biology (and not a physical process) while the eddy is translating west.

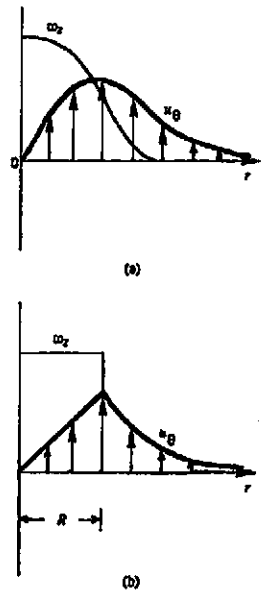

Figure 2.1: Velocity (u_θ) and vorticity (w_z) distributions in a real vortex (a) and a Rankine vortex (b). *From Kundu and Cohen (2004).*

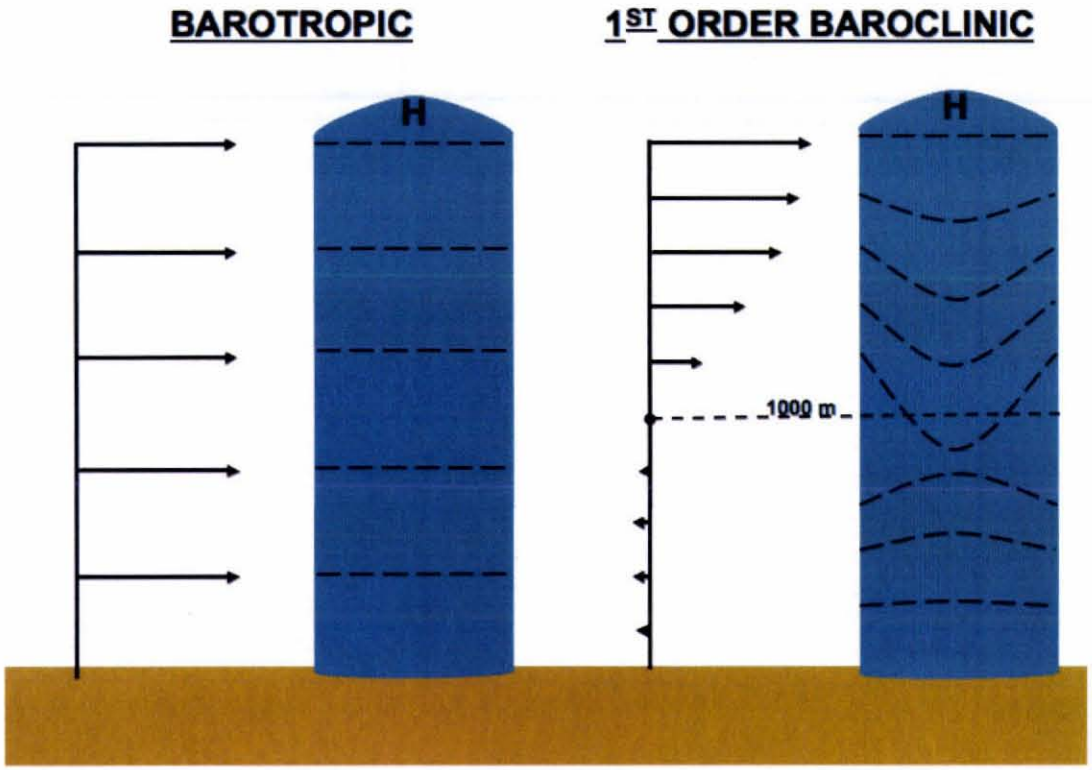

Figure 2.2: Visual representation of a barotropic (left) and a 1st mod baroclinic (right) anticyclone. The H indicates higher pressure due to a mound of water at the sea surface (positive SLA). The arrows indicate vertical distribution of geostrophic velocities (clockwise in the northern hemisphere) for the whole barotropic eddy and for the top 1000 m of the baroclinic eddy. The dashed lines indicate displacement of isopycnal surfaces.

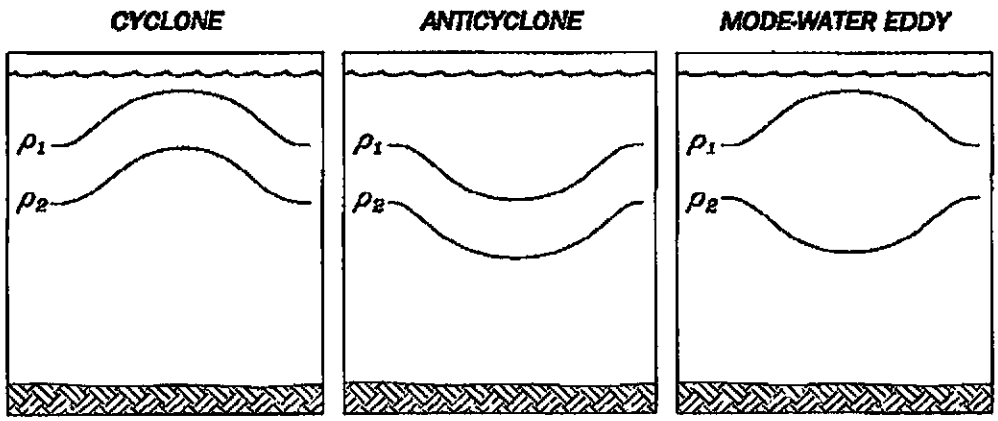

Figure 2.3: Isopycnal displacements for different types of eddies. Two isopycnal surfaces are depicted, the seasonal thermocline (ρ_1) and the permanent thermocline (ρ_2). *From McGillicuddy et al. (1999).*

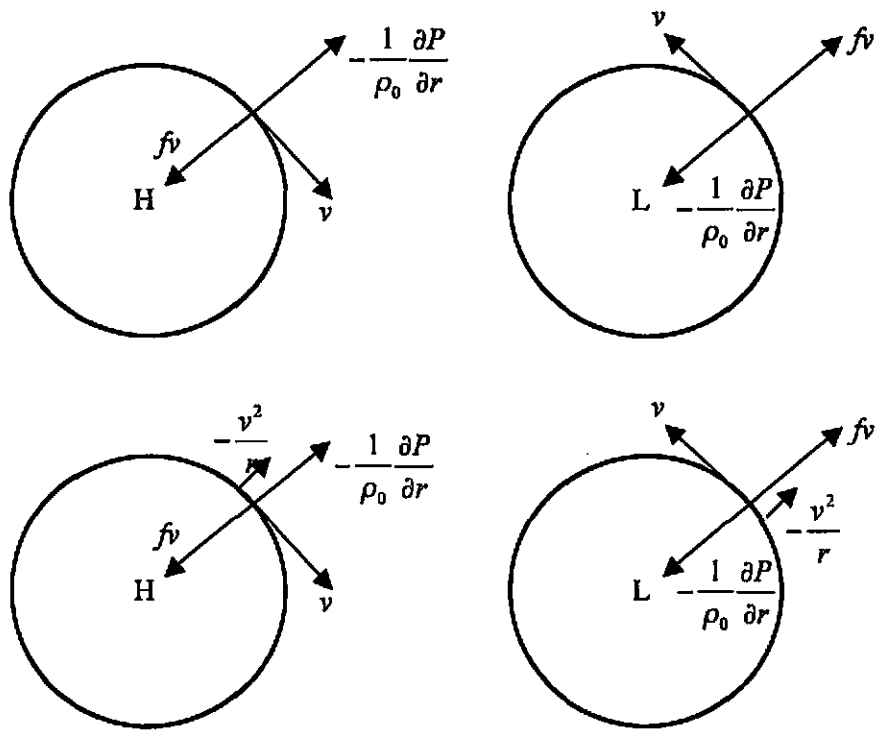

Figure 2.4: Balance of forces for vortices in the Northern Hemisphere in geostrophic (a) and cyclogeostrophic (b) balance. "H" denotes an anticyclone and "L" denotes a cyclone.

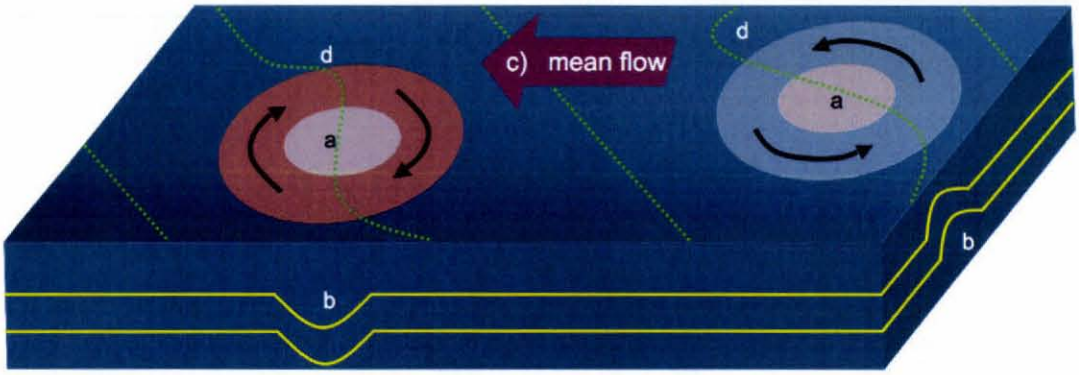

Figure 2.5: The mechanisms by which an anticyclonic (left) eddy and a cyclonic (right) eddy advect anomalous water properties: a) bolus transport, b) vertical advection, c) advection through the mean flow, and d) lateral entrainment.

3 Data & Methods

This study seeks to characterize eddies in the east-central North Pacific Subtropical Gyre (NPSG), investigate their interactions with the main Hawaiian islands and gain information about their vertical structure and water mass properties using available resources. This study focuses on the eddies that pass through Station ALOHA, the site of the Hawaii Ocean Time-series (HOT) program (Section 3.1) because of the wealth of information that can be gained from observations coinciding with the passage of an eddy and the importance of understanding the impacts of eddies on the physics and biogeochemistry of the ALOHA ecosystem. Eddies are first identified from satellite altimetry (Section 3.2) and then tracked using a sophisticated algorithm (Section 3.3) developed by Chelton et al. (2007). Analyses of algorithm output and HOT data are described in Section 3.4.

3.1 HOT Program

3.1.1 Station ALOHA

The primary objective of the HOT Program is to provide a long time-series of physical and biogeochemical observations of the NPSG (Karl and Lukas 1996). The HOT database contains ~monthly shipboard observations made at Station ALOHA since October 1988. Station ALOHA was chosen as a deep ocean station far enough from land to be free of biogeochemical and coastal ocean dynamics influences, while close enough to Honolulu to be logistically feasible (Karl and Lukas 1996). Located 100 km north of Kahuku Point, Oahu, at 22.75°N 158°W and in 4800 m of water (Figure 3.1), Station

ALOHA is two Rossby radii from the coast, and one Rossby radius from the nearest bathymetric slopes, and is thus considered a representative location within the southeastern part of the NPSG. This long-term data set has temporal resolution averaging just over four weeks.

The existence of eddies passing near Station ALOHA has been verified with a few case studies (Lukas and Santiago-Mandujano 2001, Letelier 2000, Firing and Merrifield 2004, Fong et al. 2008), but the general characterization and impacts of all eddies in this region have not been studied. The present study seeks to address this gap.

3.1.2 Hydrographic Data Collection

The HOT Program data archive contains quasi-monthly observations of temperature, salinity, dissolved oxygen (dO_2) and inorganic nutrient data ([nitrate + nitrite], phosphate and silicate). Continuous CTD profiles are conducted from 0 to 1000 m every three hours in a 36-hour long burst in order to extend over the local inertial period and three diurnal tidal cycles. Profile data are processed to 2 dbar resolution. Discrete water samples are collected during each cast at various depths to sufficiently sample across density gradients and these samples are analyzed for salinity, oxygen and nutrient content. The bottle data are used to calibrate the CTD measurements. Methods and calibration details are provided in the HOT annual reports, which can be found on the web at *http://www.soest.hawaii.edu/HOT_WOCE/data_report.html*.

3.1.3 Acoustic Doppler Current Profile (ADCP) Data

ADCP data are provided in Appendix II if it was available for HOT cruises that corresponded with eddies. Rough conditions or problems with instrumentation that

corrects ADCP velocities for gyro error can cause a bias in the ADCP velocities. ADCP data that has been flagged as having a bias has been removed and will appear as gaps in the contour plots. Availability is listed in Appendix I. There are five ADCP plots displayed for each HOT cruise. The first plot contains an arrow stick profile depicting the cruise averaged ADCP data collected on-station at ALOHA with the long term mean removed. The four depth-distance contour plots are the north and southbound legs for each HOT cruise, split into u and v components. Visual analysis (Appendix II) describes surface currents that correspond with the expected current based on the position and rotation of each eddy during the HOT cruise. Details concerning the processing of ADCP data can be found in Firing et al. (1995) and in the E. Firing ADCP Laboratory on the web at *http://currents.soest.hawaii.edu/*.

3.1.4 Data Processing and Quality Control

This analysis focuses on HOT cruises 41 through 188, which occurred during the period for which SLA was analyzed with the eddy identification and tracking algorithm (14 October 1992 through 31 December 2006). Twelve of these cruises were not included. Cruises 42 and 43 had insufficient dO_2 data, cruise 48 had no data for Station ALOHA and cruise 90 had problems with the CTD cable. Cruise 122 was characterized by a very large subsurface anomaly and has been described in detail in Lukas and Santiago-Mandujano (2001) and is removed because its salinity anomaly large enough (over 30 standard deviations from the mean) to skew the mean values of water mass property concentrations. Cruise 126 had multiple CTD problems, cruises 127-131 had bad nutrient data and cruise 177 did not have a 1000 m cast. The remaining 136 cruise

profiles were converted to anomalies by removing the mean along each potential density surface of the three previous cruises and normalizing by the standard deviation of all 136 cruises.

For the present analysis, one cruise-averaged CTD profile from the 36-hour burst sampling is used. Nutrient data at each bottle depth is averaged for the cruise and then the bottle averages are interpolated to CTD depths using a cubic spline fit. Potential density is calculated from 2 dbar CTD temperature, salinity and pressure data by first filtering with a five point triangular filter and calculating potential density using a centered difference. The cruise with the greatest potential density at its lower boundary determines the upper depth limit and the cruise with the lightest potential density measurement on its upper boundary determines the lower depth limit to be used for all cruise data. The resulting 2 dbar interval variables are then re-gridded onto potential density surfaces using a linear interpolation with 0.01 σ_θ resolution.

Water samples for the determination of dissolved inorganic nutrient concentrations were collected at predetermined depths and isopycnals as described in Tupas et al. (1993) and analyzed as described in each HOT report. Dissolved inorganic nutrients include soluble reactive phosphorus (SRP), [nitrate + nitrite] and silicate. These discrete samples were gridded onto potential density surfaces using the method described above.

For the Empirical Orthogonal Function (EOF) analysis (Sec. 3.1.5), it is important to include variables that are independent, meaning that no variable is affected by changes in another variable. It is also preferable to include variables that are not influenced by

biological variability. Oxygen, [nitrate + nitrite] and phosphate are important components in the oxidation of organic matter:

$$106\ CO_2 + 16\ HNO_3 + 1\ H_3PO_4 + 122\ H_2O \leftrightarrow [(CH_2O)_{106}\ (NH_3)_{16}\ (H_3PO_4)] + 138\ O_2$$

Broecker (1974) introduced the concept of "NO"

$$\text{"NO"} = 9\ NO_3 + O_2 \tag{12}$$

as a conservative tracer where the increase in NO_3 from nitrate introduction during respiration is balanced by the consumption of dissolved O_2. This assumes that the Redfield ratio (Redfield, 1963), in which the ratio of C:N:P = 106:16:1, is the same for all water masses. This means that for every 1 mole of NO_3 released during respiration, 9 moles of O_2 are removed.

Broecker (1974) showed this tracer to be effective in identifying different water masses in the North Atlantic. The Redfield ratio is environmentally dependent because of differences in apparent O_2 utilization and the amount of preformed NO_3 present in different water masses. Broecker (1974) also mentioned that "PO" could similarly be used, but since the ratio of NO_3 to PO_4 is nearly constant across oceans (assuming that the Redfield ratio holds), then "NO" and "PO" should yield similar information.

The assumption of whether the Redfield ratio holds at Station ALOHA is crucial to the applicability of using NO as a water mass tracer. Karl et al. (1999) analyzed the first nine years of HOT data and found that for dissolved inorganic nutrients, the N:P ratio varied on a seasonal, annual and perhaps even decadal cycle. N:P ratios were shown to be much lower than the Redfield ratio nearer the surface, but were consistently

lower than the Redfield ratio throughout the upper 1000 m over the period of study. "NO" is probably a more conservative tracer than "N" or "O" individually, but quantifying how much more conservative is beyond the scope of this study. Results are presented with individual nutrient profiles for comparison with climatological maps of spatial gradients of nutrients on particular potential density surfaces (Figure 3.2). Appendix II shows vertical profiles of normalized water property anomalies for each eddy that corresponded with a HOT cruise. 136 cruise profiles were averaged over time along each density surface to create a mean profile and standard deviation. The anomaly profile is the cruise profile (x_k) minus the mean of the 3 previous cruises where k is the cruise of interest, divided by the standard deviation (σ).

$$x' = \frac{x_k - \overline{x_{k-3} + x_{k-2} + x_{k-1}}}{\sigma} \tag{13}$$

By removing the long term mean, the influence of other processes that occur on shorter time scales is not removed. Anomalies relative to the long term mean will thus not show water mass anomalies due only to the passage of an eddy. That is why the profiles in Appendix II have only the mean of the 3 previous cruises (approximately 3-4 month average) removed, so most of the shorter time scale variability not related to the eddy is removed from these profiles. This also means that the baseline changes for each eddy, which may or may not make it easier to compare different eddies.

3.2 AVISO Sea Level Data

3.2.1 Importance

In-situ measurement of every eddy is virtually impossible because of the rigorous sampling that is necessary in both space and time. Fortunately, due to the improvement of satellite altimetry to measure mesoscale variability (Ducet et al. 2000, Le Traon et al. 1992), it is possible to combine remote observations with in-situ sampling (Siegel et al. 1999, Roemmich and Gilson 2001) to glean information about specific mesoscale features. The altimeter products used in this work were produced by the multimission altimeter data processing system operated by Segment sol multimissions d'ALTimetrié d'Orbitographie et de localization précise and distributed by AVISO, with support from the Centre Nationale d'Etudes Spatiales.

Data from a single satellite is inadequate for accurately describing the mesoscale because of the large separation between measurements, in space and/or time. The ground tracks for various altimetry missions at ALOHA are shown in Figure 3.3. The ground track separation is 287 km for the 10-day repeat orbit of T/P and Jason-1, and 72 km for the 35-day repeat orbit of ERS-1/2 and Envisat. Individually, the 10-day repeat track altimeters cannot spatially resolve mesoscale features, and the 35-day repeat track altimeters cannot temporally resolve mesoscale features (Ducet et al. 2000). Merging data from different missions has been shown to significantly improve the ability to resolve mesoscale features like eddies in both space and time (Le Traon et al. 1992, Pascual et al. 2006, Chelton et al. 2007).

3.2.2 Merging Process

In order to merge multiple satellite missions, the SSH data must be homogeneous and intercalibrated. Because of the uncertainty in the geoid, data must be referenced to a mean profile obtained from repeat-track analysis, and measurements from all satellites to be merged must be corrected from the data of the satellite used for the repeat-track analysis (Ducet et al. 2000). The mean profile used for this study is a seven year mean (1993-1999) from T/P data (AVISO 2006). The largest contribution to errors when mapping space and time varying data to a grid using optimal interpolation methods are long-wavelength errors that can induce artificial eddy signals (Le Traon and Morrow 2001). This is avoided by removing these long-wavelength signals prior to mapping.

Merging data from two altimeters reduces the mapping errors by a factor greater than 2 (Ducet et al. 2000) and doubles the resolution (Chelton and Schlax 2003). For a space scale of 150 km and a time scale of 20 days, the mapping error is less than 3% of the variance (Le Traon and Dibarboure 1999). Signal variance at ALOHA is 61 cm, and calculating the error as less than 3% of the signal variance results in errors less than 1.8 cm (Le Traon and Dibarboure 1999). The result is that errors should have a minor impact on the oceanographic interpretation of the merged SLA maps (Ducet et al. 2000).

Additional altimetry errors occur in proximity to coastlines. Mitchum (1994) did a global survey comparing tide gauge data to T/P data and found on average, an rms error of 5 cm. The following year, a follow up study focusing on one tidal gauge station in the equatorial Atlantic (Verstraete and Park, 1995) showed that the accuracy of T/P data comparison was highly sensitive to the tidal model used on the T/P data, and by using a different tidal model, the error was reduced to 2 cm rms, which is of similar order as the

mapping errors. It is difficult to draw uniform conclusions on the altimetry error near land masses due to the limited amount of data. A study of the California current system estimated altimetry errors out to 30 km or more for the coast, and removed the AVISO data in this range and replaced it with in situ tidal gauge data (Strub and James 2000).

3.2.3 Product Generation

AVISO products are generated using a four-step process. Repeat-track analysis removes the 1993-1999 mean profile, cross-validation removes outliers, filtering is done by means of a Lanczos filter and finally data is projected onto a 1/3° x 1/3° grid using an advanced global suboptimal space and time objective analysis (AVISO 2006, Ducet et al. 2000). For a more detailed description of the mapping process, refer to Le Traon et al. (1999). Data from TOPEX/Poseidon (T/P), ERS-1,2, Jason-1 and ENVISAT were used, with availability as shown in Figure 3.4, (AVISO 2006).

3.3 Eddy Identification and Tracking Algorithm

3.3.1 Previous Methods

Prior to the 1970's, information about the presence of eddies in the ocean was limited to sparse in situ observations of rings and other suggestive evidence (Robinson 1983). The following decades provided the opportunity for more vigorous sampling techniques, which allowed for measurements with increased spatial and temporal resolution. The first major breakthrough in eddy observations was the space-borne Advanced Very High Resolution Radiometer (AVHRR) to remotely observe quasi-synoptic images of eddies in sea surface temperature and characterize the temporal and

spatial scales of eddies (Isoda and Saitoh 1988). Another major breakthrough in eddy observation followed the advent of sea surface height measurements by satellite altimetry. However, several significant mapping issues had to be overcome before satellite altimetry could be considered to have sufficient spatial and temporal resolution to accurately sample mesoscale features (Section 3.2).

The next hurdle was how to best identify individual eddies from sea surface height measurements. Several methods have been employed over the past decade (Isern Fontanet 2003, Chelton et al. 2007). The two methods most recently applied to identification of mesoscale eddies on a global scale are to track a specified contour of the Okubo-Weiss (W) parameter (Isern Fontanet 2003, Chelton et al. 2007) or to define closed contours of sea level anomalies (D. Chelton, unpublished proposal). The W parameter is a measure of the relative importance of deformation and rotation (Chelton et al. 2007) and is defined for horizontally nondivergent flow in the ocean as

$$W = 4\left[\left(\frac{\partial u}{\partial x}\right)^2 + \frac{\partial v}{\partial x}\frac{\partial u}{\partial y}\right] \tag{14}$$

where velocity components were computed geostrophically from altimeter data by

$$u = -\frac{g}{f}\frac{\partial h}{\partial y} \text{ and } v = \frac{g}{f}\frac{\partial h}{\partial x} \tag{15}$$

where h is the SSH, g is gravitational acceleration and f is the Coriolis parameter (Chelton et al. 2007). Since vorticity dominates strain for eddies, W will be negative inside an eddy. The defining of closed contours method is preferred for its simplicity and its freedom from being limited to a chosen threshold value, which would limit the number of features identified from SSH maps (D. Chelton, unpublished proposal). Also,

the fact that the W parameter is the product of a second derivative of the SSH field, makes analyses of SSH fields highly susceptible to noise. This study uses the method of finding closed contours, the details of which are presented in the next section.

3.3.2 Eddy Identification

The following discussion regarding details of the eddy identification and tracking algorithm relies heavily on information provided by Dudley Chelton (D. Chelton, unpublished proposal). The algorithm used to identify the eddies in this study utilized fifteen years (1992-2006) of unfiltered, merged (2 altimeters) sea level anomaly data from AVISO to isolate regions of Sea Surface Height (SSH) contained within closed contours of SSH . For geostrophic flow around localized features such as eddies, streamlines in the absence of background mean currents correspond to closed contours of SSH. The algorithm defines an eddy as a connected region bounded by a closed SSH contour that meets three criteria. First, there must be at least one interior SSH extreme; second, there must be at least one interior grid point, and third, the distance between any pair of points within the enclosed region must be less than 400 km (Figure 3.5). A point is interior if it's four nearest neighbors are also in the region bounded by the closed contour and a point is a local maximum (minimum) if it is interior and has SSH greater (less) than its four nearest neighbors.

The next step is to identify the area of the eddies. Cyclonic eddies are locally concave upward, so the SSH field is partitioned stepwise in to regions that fall below a given threshold, beginning with an initial value of +30 cm and proceeding downward in 1 cm successive increments to lower thresholds. A large initial threshold allows for

detection of relatively small-amplitude eddies propagating on a larger scale positive background SSH field, thus effectively spatially high pass filtering the SSH field. At each step in the progression to lower thresholds, connected regions within which SSH is less than the current threshold are defined and examined to see if the three criteria (described in preceding paragraph) are met. If so, the accepted region is identified as an eddy. This procedure identifies the outermost closed contour of SSH for each cyclonic eddy. Anticyclonic eddies are concave downward, so the initial threshold is -30 cm and the process steps upward, thus identifying anticyclones by their outermost closed SSH contour.

The eddy center is defined to be the centroid of SSH within the closed contour of SSH. The centroid is defined as the center of mass of the enclosed eddy. The contour of SSH that defines an eddy depends on the shape and size of the eddy, as well as the larger-scale background SSH and SSH signature of nearby eddies. A consistent method must be used for the definition of eddy amplitude and scale. The algorithm assumes that the SSH signature (h) of each eddy is radially symmetric and Gaussian. Amplitude (A) is defined as the absolute value of the difference (in cm) between of the average SSH of the perimeter of the enclosed region and the extreme value of SSH within the closed contour of the eddy. The eddy diameter for a cyclone is defined as the diameter of a circle with area equal to that of the pixels with SSH at most A/e below the maximum value of SSH for the eddy, where e is Euler's constant. Similarly, the diameter of an anticyclone is the pertinent area containing pixels with SSH at least A/e above the minimum value of SSH within the eddy. The radius of the eddy (r) is then half the diameter. Assuming a

Gaussian SSH signature for each eddy, the axial (ax), or rotational, speed of the eddy is defined as

$$ax = \frac{g}{|f|}\frac{A}{r} \tag{16}$$

3.3.3 Eddy Tracking

Once eddies are identified for each time step in the sequence of SSH maps, the tracking procedure is applied to determine the trajectory and lifetime of each eddy. The algorithm finds the closest eddy (using a specified narrow search region) in the next time-step that has an amplitude and area that falls within ½-2 times the original eddy. If no closed contour region can be found in the subsequent time-step, then the procedure is carried out up to three time steps ahead of time zero. If still no closed region is identified, then the eddy track is dropped at the last time closed contours were identified. Translation speed is then defined as the distance (in km) between the location of the eddy center at one time step to the next and divided by the time (in seconds) between time steps, which is seven days for AVISO gridded products.

The algorithm amplitude threshold is 1 cm, but AVISO two-satellite altimetry can only has 2-3 cm accuracy. With only one altimeter (as is the case for certain periods during 1994-1996 (Figure 3.4)), AVISO accuracy is only 5-6 cm. Eddies that are tracked with the algorithm having amplitudes less than the AVISO resolution may or may not be real eddies, and need to be individually verified for quality control (Section 3.4.2).

3.4 Analysis Methods

3.4.1 ALOHA eddy sampling

The algorithm is applied to global SSH maps, but the focus of this study is the region around Station ALOHA, defined as the 2° x 2° boxed region bounded by 21.75°N – 23.75°N and 159°W – 157°W. The location of the box surrounds the ALOHA sampling site for the HOT Program so it is possible to gain information about the vertical structure of eddies that pass through this area. The box was chosen to be one degree in width in each direction around Station ALOHA to ensure that the center of eddies with a radius on the order of 100 km would be retained for the analysis. Any eddy whose center passed through the box at least once, whose radius overlapped the 10 km radius around Station ALOHA and whose lifetime was at least 4 weeks was retained for this analysis and is referred to as an ALOHA eddy.

The larger regional analysis described in Section 4.7 is bounded by 15°N – 30°N and 170°W – 130°W. This region encompasses the southeast Hawaiian Islands and the region where eddies that pass through ALOHA are formed. It is a good representation of the central part of the North Pacific Subtropical Gyre.

In addition to analysis of eddy parameters derived from the algorithm output, a detailed visual comparison of the algorithm results with unfiltered, merged AVISO data was completed. This step was used to quality control the eddies identified by the algorithm by pulling out only robust eddy features, that is, features that look and behave like real eddies and are not an ambiguous feature picked up by the algorithm. A single

time step snapshot of this analysis and the region of interest around Station ALOHA can be seen in Figure 3.6.

3.4.2 Visual Analysis

Of the original 85 eddies, four were determined to be the continuation of a previously tracked eddy. One track erroneously jumped to a different eddy feature, and four features tracked by the algorithm did not resemble eddy structures in the unfiltered SSH data. The four eddy tracks that were considered to be the continuation of another eddy were combined with the original feature to make one continuous eddy track. The four features that did not visually resemble eddies were discarded from the analysis. To remain conservative the one track that appeared to jump to another feature was visually ambiguous and was also dropped from the analysis. There are four visually identified features that pass through the region surrounding Station ALOHA but are not tracked by the algorithm. Two of these events occur during the time when the altimetry maps are determined by one altimeter. These four features are also not long lived (less than 10 weeks) and they may not be eddies.

It was also visually determined that seventeen eddies were formed at least four weeks before the tracking algorithm acquired them. Ten of these eddy tracks were replaced with corresponding tracks from the algorithm's previous iteration, the details of which can be found in Chelton et al. (2007). By replacing these tracks and visually comparing the difference in how these ten eddies were tracked by the previous version of the tracking algorithm, it was determined that the same feature was similarly tracked, but the track begins closer to the time and place that the eddy actually formed.

This visual analysis also concluded that an additional seven eddies (15C, 19A, 27C, 45A, 64A, 67C, 75C) were not really eddy features because they were short-lived (less than 10 weeks) and never developed a circular shape with several closed contours. Increasing the time coherence constraint to 10 weeks only precludes the detection of locally generated eddies if they decay within 10 weeks, but the visual analysis showed that no locally generated features that looked like an eddy were precluded from the analysis. These features were dropped from the rest of the analysis. There were eight other eddies with lifetimes less than 10 weeks, (03A, 08A, 14C, 23C, 32A, 38C, 56C, 66C) but the visual analysis determined that these features were more likely the remnant of a previously tracked eddy. These features are retained only in the analysis of the vertical distribution of water properties because of their potential to contain bolus water property anomalies from the original eddy source region. These eddies are not included in the analysis of other eddy properties including amplitude, radius, translation speed and axial speed. Finally, to be conservative, three other features were dropped from the analysis (37C, 58C, 75A) because after visual inspection, their sea level signature and tracked behavior did not resemble that of the other eddies, and were not convincing features. The remaining 58 "robust" eddies are the focus of the remainder of this analysis, with the exception of the eddy remnant features, which are analyzed for their vertical water property anomalies.

3.4.3 Empirical Orthogonal Function (EOF) Analysis of water mass properties

Empirical Orthogonal Function (EOF) analysis is another name for Principal Component Analysis (PCA) (Preisendorfer 1981, Wilks 1995). The advantage of using

PCA as a multivariate statistical technique is to compact a data set with several variables into a new data set containing fewer variables that hopefully represent the larger fractions of variability of the original data set. These new variables are called the principal components (Wilks 1995). This analysis can be a useful tool for extracting spatial and temporal variability of a large, multivariable data set.

In this study, EOF analysis is performed using HOT data to attempt extraction of eddy signals from other variability. The data must be prepared so that the calculation of the principal components will render useful information for eddies. First, it is necessary to calculate the non-seasonal variance of the gridded variables (Section 3.1.4). This is accomplished by removing the annual and semiannual cycles from all data. Next, each variable is divided by its standard deviation (on each isopycnal surface). Finally, the normalized anomalies are assembled together in one large matrix. The normalization eliminates arbitrary units and differences of scale between variables.

The EOF analysis is based on the correlation matrix (correlated in space), which is the square matrix of the normalized observations times its transpose. The eigenvalues of the correlation matrix are then formed from

$$Ax = \lambda x \tag{17}$$

where A is the correlation matrix, λ are the eigenvalues that satisfy the equation and x are the eigenvectors. The resulting eigenvectors are then algebraically manipulated to recreate the data as a function of spatial distribution (vertical profile (p)) and time (t). The amplitude matrix ($a_i(t)$) is defined as the projection of each eigenvector ($x_i(p)$) onto the observations. Each eigenvector is a mode of the EOF, where the first mode is the

eigenvector with the corresponding eigenvalue that describes the largest amount of variance, the second mode describes the second largest amount of variance, etc.

The vertical structure of each mode is created by using the relationship $\sigma_a x$ where σ_a is the standard deviation of the amplitude. The associated time series for each mode is described by $\frac{a}{\sigma_a}$. In order to find the actual value of the variables described for each mode, it is necessary to multiply the time series by the vertical structure, that is, the amplitude times the eigenvector (ax) will give the data values for the first mode at a particular point in time.

In addition to the EOF analysis, it is possible to rotate the results so that the resulting eigenvectors are a linear combination of the original results. Unfortunately for physical interpretations, the required orthogonality of each EOF mode to one another can result in several physical processes being lumped into the same mode, or of one physical process being split into several modes (Mitchum 1993, Wilks 1995). Rotation can help to isolate one physical process into a single mode by correlating the amplitudes while the eigenvectors remain orthogonal. The hope is that by relaxing the condition that the eigenvectors explain the maximum amount of variance, they instead resemble the modes of the data that make physical sense (assuming any exist). This study does such a rotation and compares the results with the unrotated versions for completeness (Section 4.6.1).

We consider two types of significance with EOF analyses. The first is the modal significance, that is, which modes describe an amount of variance different from random noise. The second is the event significance, that is, which events within a particular

mode are considered significant. The applicability of these factors to the HOT data EOF analysis are presented in Section 4.6.1.

3.4.4 Displacement of Isopycnals at Station ALOHA

The average displacement of isopycnals (z') over the upper water column (from ~100-1000 m for this study) was calculated from hydrographic data obtained during each HOT cruise. For each CTD cast, salinity, temperature and pressure measurements obtained every 2 dbar were used to calculate potential density at depths ranging over the upper 1000 m of the water column. The depths (z) of the observed isopycnals were then averaged over the cruise in order to remove the effects of internal waves. These depths (z) were then contoured to a density-time grid (every 0.1 σ_θ - monthly). Next, the time averaged depth ($\bar{z}$) was removed from each isopycnal surface to get z'.

$$z' = z - \bar{z} \tag{18}$$

The resulting time series was then subsampled using a linear interpolation to the time series of eddy SLA at ALOHA that corresponded to HOT cruises. Eddy SLA is described in Section 4.2.2. Finally, the correlation between the two time series was calculated. The results of this analysis are discussed in Section 4.5.

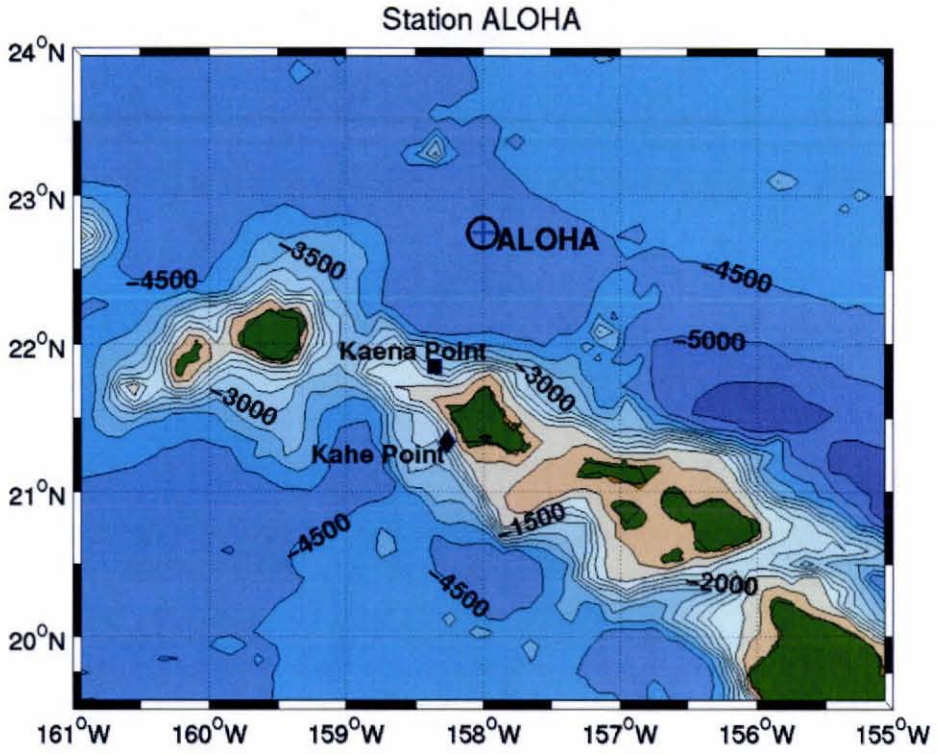

Figure 3.1: Station ALOHA, located at 22° 45' N and 158°W, site of the Hawaii Ocean Time-series Program data collection. Also shown are other stations visited during HOT cruises and the regional bathymetry (Smith and Sandwell 1997). In green are the islands of Oahu (center), Molokai (right) and Kauai (left).

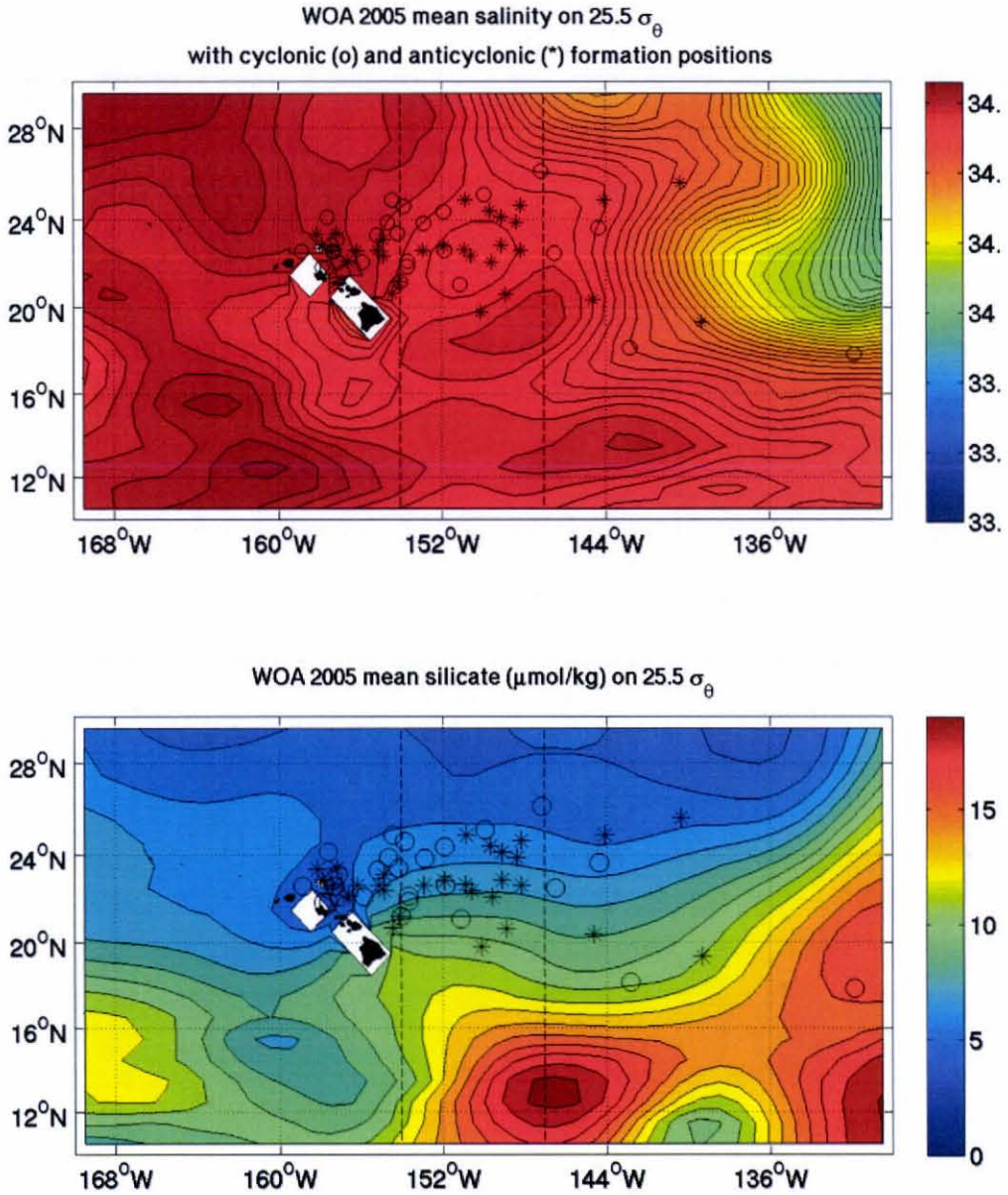

Figure 3.2: Spatial gradient of salinity *from Antonov et al. 2006* (top) and silicate *from Garcia et al. 2006* (bottom) on 25.5σ_θ. Formation location of ALOHA eddies are denotes as circles (cyclones) and stars (anticyclones).

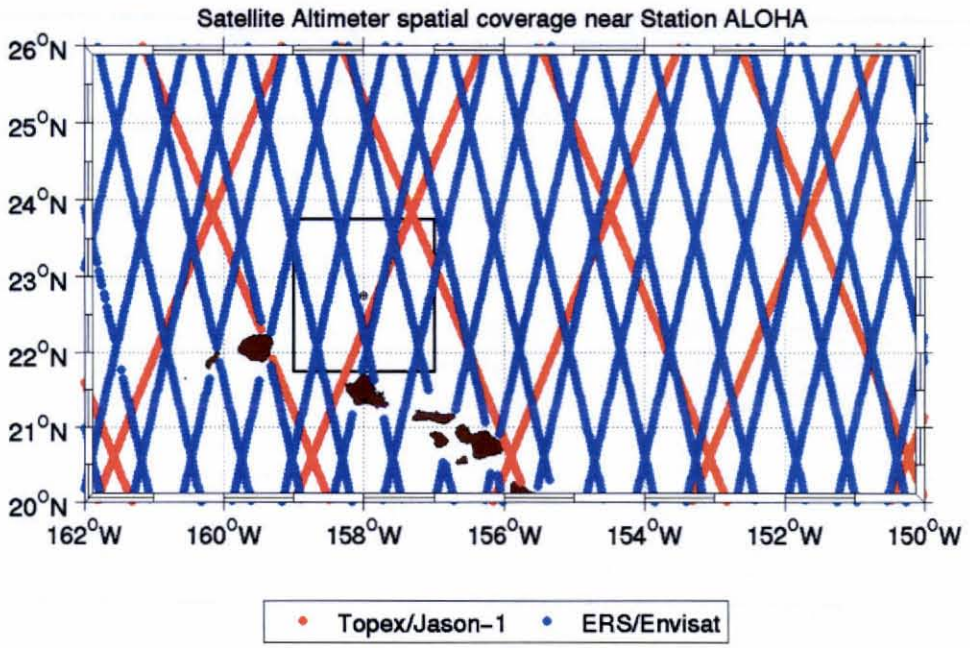

Figure 3.2: Satellite ground tracks near Station ALOHA.

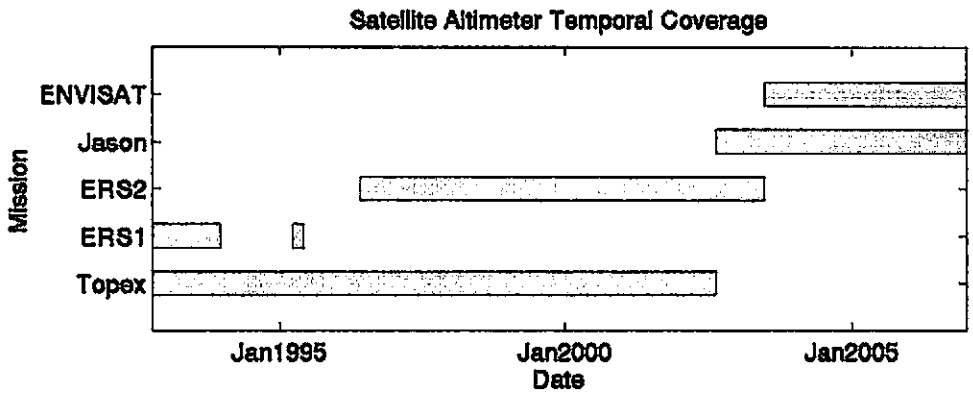

Figure 3.3: Satellite altimetric data availability for each mission as used in AVISO's homogeneous gridded data product.

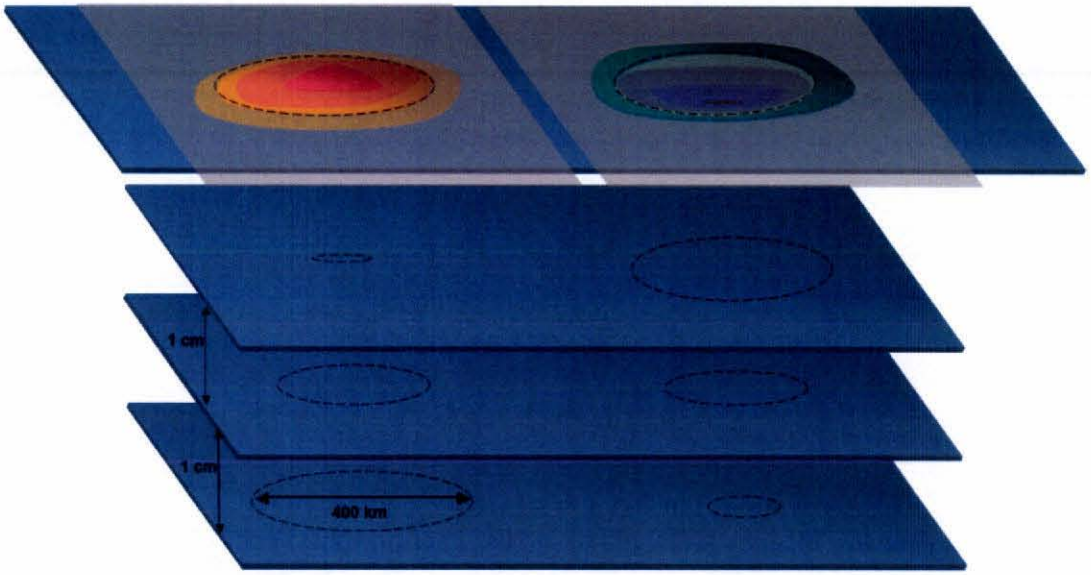

Figure 3.5: Visual representation of how the eddy identification and tracking algorithm works. The anticyclone (left) is identified by starting at -30 cm and isolating regions of closed contours of sea surface height that meet the criteria described in Section 3.3.2 and working upwards at 1 cm intervals. The cyclone (right) is identified using the same process, but starting from +30 cm and working downward in 1 cm intervals.

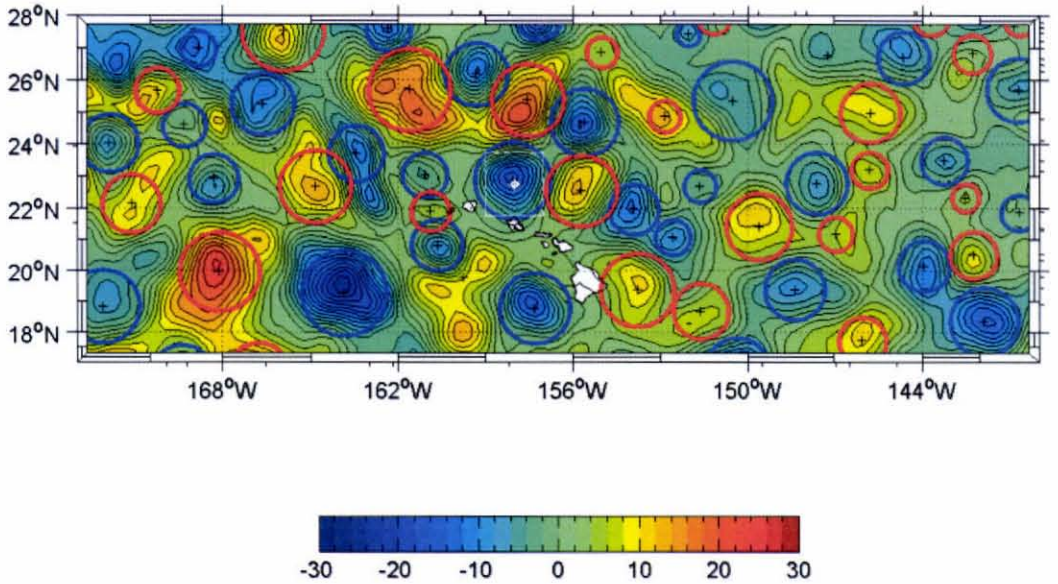

Figure 3.6: Snapshot of unfiltered AVISO sea level anomalies (cm), overlaid with eddy algorithm output on 22 February 2006. Station ALOHA is marked as the white cross and the surrounding 2°x2° degree white box represents the region through which all ALOHA eddies pass through. The larger region studied (Section 4.7) is encompassed by the limits of this map. Blue circles are cyclonic eddies and red circles are anticyclonic eddies.

4 Results

4.1 Organization

This section is organized such that the eddies directly impacting ALOHA are described first, including their characteristics, spatial and temporal distribution, information about their vertical structure and water property characteristics. These results are then compared to surrounding eddy field of the central North Pacific to determine whether the ALOHA eddies are typical of eddies in the central NPSG.

4.2 ALOHA Eddy Characteristics

4.2.1 Algorithm output

156 eddies were identified between 21 October 1992 and 31 December 2006 by the eddy tracking algorithm. These were eddies that had their center pass through the ALOHA box described in Section 3.4.1. Of those 156 eddies, 85 had their edge intersect the Station ALOHA circle and had a lifetime of at least four weeks. Next, a visual comparison of the algorithm output of each eddy at each timestep to unfiltered, merged Sea Level Anomalies (SLA) provided by AVISO was completed. On this basis the set of eddies impacting Station ALOHA was refined to a total of seventy-six features, 40 cyclonic and 36 anticyclonic. The comprehensive analysis of each eddy is provided in Appendix II but a summary of the important observations is provided here.

4.2.2 Appendices description

Appendix I contains at-a-glance data for all 76 eddies. The ID column lists the eddy ID assigned to each feature. This ID also matches with each eddy plot and description contained in Appendix II. The eddy IDs are assigned in chronological order according to when the eddy passes by Station ALOHA, and the letter designator indicates cyclonic (C), or anticyclonic (A). The "Dates at ALOHA" columns list the date that the radius of the eddy first overlapped Station ALOHA circle (in), the last date that the radius overlapped Station ALOHA (out), and the number of weeks between these two dates (wks). The Closest Point of Approach (CPA) of the eddy is defined as the position of the eddy with the smallest distance between the center of the eddy and Station ALOHA. The "part of eddy" field describes the part of the eddy that was over ALOHA at the time of CPA. The "average eddy height" (in cm) given is the average of the eddy SLA over ALOHA during its time at ALOHA (h) and the "maximum eddy height" is the maximum eddy SLA over ALOHA where

$$h(d) = Ae^{-\frac{d^2}{2R^2}} \tag{19}$$

h is calculated by assuming the eddy has a Gaussian shape and that the radius contains 95% of the eddy where d is the distance from the eddy center to Station ALOHA and R is the eddy radius. The "HOT cruise information" field includes the cruise number(s) that corresponded with the passage of an eddy, and the part of the eddy that was sampled during those cruises. "ADCP availability" denotes which eddies have ADCP plots in Appendix II. "Sat. cvrg" is satellite coverage and lists which satellite information is contained in the SSH maps used to identify each eddy. The last "of Note" column gives

brief information about HOT cruises that weren't used in the analysis (Section 3.1.2), and which eddies (after visual inspection) were dropped from the analysis (Section 4.2.1).

Appendix II contains visual and written descriptions for each of the 76 eddies listed in Appendix I. The first page includes a Mercator projection map with the eddy center position and eddy radius plotted for each time step. These plots show how the eddy grows in size and where it moves during its lifetime. They also show where the eddy passes in relation to Station ALOHA. The bottom two plots on this page show the calculated radii, amplitude, axial speed and translation speed as a function of longitude. Since the eddies move primarily west, reading these plots from right to left approximately shows the evolution of each parameter over the lifetime of the eddy. The bottom of the page contains the descriptions from the visual analysis. The next page is included if the passage of the eddy over ALOHA corresponded with a HOT cruise. The first plot shows a normalized vertical profile of water property anomalies, as described in Section 3.1.4. The standard deviation values for each variable are as follows: salinity: $\sigma = 0.056$, silicate: $\sigma = 1.62$ μmol/kg, phosphate: $\sigma = 0.78$ μmol/kg, [nitrate+nitrite]: $\sigma = 0.95$ μmol/kg, and dissolved oxygen: $\sigma = 8.00$ μmol/kg. The second plot shows ADCP data (if available) for the HOT cruise (Section 3.1.4).

Appendix III contains a brief analysis of the output from version 5 (v.5) of the eddy identification and tracking algorithm. It lists the differences between ALOHA eddies in v.4 (released in December 2007 and the focus of this study) and v.5 (released in April 2008). A description of the track numbers in v.5 that do not correspond with an eddy in v.4 are discussed. Additionally, a brief summary of the ALOHA eddy statistics in v.5 is given. This cursory analysis shows that the characteristics (amplitude, radius

and translation speed) of ALOHA eddies found in v.5 are not significantly different in the characteristics of ALOHA eddies found in v.4.

4.2.3 ALOHA eddy characteristics

The most distinguishing feature among eddy characteristics is the direction of rotation. Figure 4.1 shows plots for the mean of each characteristic for ALOHA cyclonic and anticyclonic eddies separately. The error bars denote the 95% confidence interval for the mean of N=58 eddies, calculated using two times the standard error of the mean,

$$\sigma_{\text{mean}} = \frac{2\sigma}{\sqrt{N}} \tag{20}$$

Two was determined to be the appropriate multiplier for a student's t distribution with 58 degrees of freedom (N). Also plotted are stars that show the maximum and minimum values of each variable. ALOHA eddy statistic means and standard errors are provided in Table (4.1) separately for cyclonic and anticyclonic eddies, and for all ALOHA eddies. Using the chi-square test, the distributions for each eddy statistic (amplitude, translation speed, axial speed and radius) separately for rotation sense were not significantly different at 95% confidence. This means that the characteristics of cyclones are not significantly different from the characteristics of anticyclones. The chi-square test was used because it is a test of independence between the distributions of two variables. It is useful for comparing statistics whose theoretical distribution is unknown. These statistics are based on 58 discrete eddies, or 58 degrees of freedom.

Table 4.1 Mean and standard error of the mean for ALOHA eddy statistics for all eddies. cyclonic eddies only, and anticyclonic eddies only.

ALOHA eddy statistics	Total	Cyclonic	Anticyclonic
Amplitude (cm)	6.94 ± 4.14	6.89 ± 4.32	6.98 ± 3.98
Radius (km)	101.6 ± 26.9	99.6 ± 27.02	103.4 ± 26.73

Translation Speed (cm s^{-1})	6.21 ± 2.47	6.38 ± 2.47	6.06 ± 2.46
Axial Speed (cm s^{-1})	12.6 ± 6.0	13.03 ± 6.2	12.27 ± 5.9

These eddy statistics were also compared to identify any correlations among them. This was done using a linear regression analysis of combinations of the four statistics (amplitude, radius, translation speed and axial speed) for cyclonic and anticyclonic eddies separately (Figure 4.2) and for the average of each eddy in the dataset as a whole (Figure 4.3). The only correlations above 0.2 were between axial speed and amplitude, radius and axial speed, and amplitude and radius. However, all of these are ensured due to the inclusion of amplitude in the definition for radius and the dependence of axial speed on both amplitude and radius (Section 3.3.2).

4.3 Spatial Distribution

4.3.1 ALOHA eddy trajectories

Figure 4.4 shows a spaghetti diagram of eddy trajectories and formation locations (defined as the position from the first timestep of an eddy trajectory), for the 58 "robust" eddies in the analysis (Section 3.4.2). 16 eddies formed near (west of 153°W) the Hawaiian Islands, whereas 42 others form farther away (east of 153°W) from the Hawaiian Islands to the east, and translated to ALOHA over time. The distribution of where eddies formed is discussed in further detail in the following Section (4.3.2). 16 eddies came from the north and had to translate southwestward in order to pass through the regions around ALOHA. Additionally, 7 eddies formed at a latitude south of Station ALOHA and had to translate northwestward in order to pass through the boxed region of interest. The remaining 35 eddies formed at a latitude within one degree of ALOHA and translated westward through Station ALOHA. All of the eddies passed through the

region surrounding ALOHA from east to west and continued westward past ALOHA. Once the eddies passed clear of the main Hawaiian Islands, the majority (41) decayed quickly. Of those that remained, 12 decayed farther west (near 165°W) and only 5 continued west out of the region of analysis.

4.3.2 ALOHA eddy formation regions

Figure 4.5 shows the eddy formation locations split into six regions 1, 2, 3, 4, 5, and 6. Regions 1 through 4 split the eddy genesis areas into four longitudinal areas, with region 4 being over ALOHA and progressing east to region 1. Regions 5 and 6 were chosen for the composite analysis (Section 3.4.1) in case water property spatial gradients run latitudinally instead of longitudinally. Region 1 contains 9 eddies that were formed east of 148°W. Region 2 contains 19 eddies formed east of 153°W and west of 148°W. Region 3 contains 14 eddies formed between 153°W and 156°W, and region 4 contains 16 eddies that formed west of 156°W. Regions 5 and 6 cover the same area as regions 1 and 2, but give the number of eddies (21 and 7, respectively) that formed east of 153°W and north of 22°N or south of 22°N. 8 of the eddies formed in regions 3 and 4 are actually remnants of other eddy features that were generated in regions 1 or 2 (or regions 5 or 6). Unfortunately, eddy center position and eddy characteristics information are not available for the whole lifetime of these "eddy remnants", but they may still contain bolus characteristics from the eddy's original formation region. Appendix II describes the eddies that appear to fit into this category and discusses whether these eddy remnants appear to contain bolus anomalies based on their associated vertical profiles of water

mass anomalies from the HOT data. The discussion also elaborates on this possibility (Section 5.3).

4.4 Temporal Distribution

On average, eddies pass through the 2° x 2° region surrounding ALOHA every 10 weeks. The Hawaiian lee eddies have a frequency of approximately 90 days, and since ALOHA is about 5 degrees north of these eddies, the shorter interval of 70 days is appropriate for the increase in latitude (greater f). Mitchum (1996) looked at the first two years of Topex/Poseidon data over Station ALOHA and identified an intra-annual signal with a period on the order of 100 days that propagated northwest past ALOHA and then due west once it was west of the islands. He hypothesized the signal was attributed to doppler-shifted Rossby waves, but we can now reasonably attribute that the signal he was tracking was from the ALOHA eddies. Additionally, the size and frequency of ALOHA eddies are similar to those studied by Niiler and Hall (1988) (Section 2.3.1).

The time series of eddies passing through Station ALOHA and the amount of time each eddy spends "directly impacting" ALOHA is shown in Figure 4.6. "Directly impacting," means that the eddy area (defined as the region 2π times the eddy radius (r) around the eddy center position) is overlapping the 10 km radius circle centered on Station ALOHA.

There appear to be periods when there is increased/decreased eddy activity. Figure 4.7 shows the cumulative distribution of sea level perturbations due to the eddies at ALOHA and there are definite periods of predominately cyclonic activity and periods of anticyclonic activity. Most recently, there has been a period of extended anticyclonic

activity, with some cyclonic eddies occurring, but the two large cyclonic eddy events in 2006 have brought the cumulative distribution back to zero.

4.5 Vertical Structure

Figure 4.8 shows the results of the isopycnal displacement analysis described in Section 3.4.4 before averaging over isopycnal surfaces and Figure 4.9 shows the time series after vertical averaging compared to the ALOHA sea level perturbation for each eddy. The correlation coefficient of eddy SLA (Section 4.2.2) at ALOHA with the average isopycnal displacements from HOT is 0.70, with a p-value much less than 0.001, which is significant at the 99% confidence interval. Note the isopycnal displacements are plotted on a scale that is two orders of magnitude larger than the eddy SLA. From these measurements, we can confirm that the passage of a cyclone is associated with a local shoaling of isopycnal surfaces and the passage of an anticyclone is associated with a local depression of isopycnal surfaces. These displacements are not necessarily due to upwelling or downwelling of isopycnals at ALOHA, but rather may well be due to advection of the horizontal density gradients within the eddy.

Examination of eddy water mass property characteristics on potential density surfaces (next Section) will attempt to clarify the process that is predominately responsible. Observing water mass property anomalies on potential density surfaces removes variability caused by vertical advection, and instead shows variability caused by lateral advection and mixing.

4.6 Water Property Characteristics

4.6.1 EOF Analyses

EOF analyses of different water properties and over different time periods were done in order to find the best way to identify water property anomalies due to the passage of an eddy. First, the EOF isopycnal distributions of salinity, [nitrate + nitrite], dissolved oxygen, silicate and potential vorticity were examined for the first four modes. This was done for different sub-records to see how robust the results were depending on which HOT cruises were used in the analysis. Using all HOT cruises from 1 to 188 (except the 12 with problems discussed in Section 3.1.2) versus using only HOT cruises 41 to 188 showed little difference. The vertical structure of the first four modes was the same, as were the significant events in each mode after 1992. The difference in the percentage of variance for each mode between the different length time-series was less than 2%. Additionally, the EOF results from analyzing HOT cruises 41 through 188 (136 cruises) were compared to using only the HOT cruises that corresponded with the passage of an eddy (68 cruises). Again, the vertical structure, amount of variance described and the significant amplitude peaks in the time series were very similar. Since the dominant modes of variability for these water mass properties don't change significantly based on which HOT cruises are used, the 136 HOT cruises (Section 3.1.2) were used for the remainder of the EOF analysis because these are the HOT cruises that occurred within the same time period as the eddy algorithm output, from 21 October 1992 to 31 December 2006.

Biological processes can affect how well the properties of [nitrate + nitrite] and dissolved oxygen act as water mass tracers so several EOF analyses were done using different properties to see what combination of water properties best corresponds to eddy events. Only the first four modes were examined in detail because they individually describe more than 5% of the total variance. The first four modes of each group were analyzed for the larger peaks in the time-series. The larger peaks were first denoted as those with absolute magnitudes greater than $|1|$. The number of peak events in each time series that are significant is determined by assuming the time series is normally distributed and identifying the peaks that have less than 5% chance of occurrence based on the standard deviation of the time series.

The method described above for evaluating peaks in the EOF mode time series was validated by determining how different the time-series of amplitudes are from a normal distribution. Values of skewness and kurtosis were calculated to test the null hypothesis that each mode time series is normally distributed (Table 4.2).

Table 4.2: Values of skewness and kurtosis for water mass EOF time series. Values that are significantly different from a normal distribution (see text) are shown in italics. Negative skewness values mean the series is skewed towards negative amplitudes.

All variable	Unrotated					Rotated			
Mode	**1**	**2**	**3**	**4**		**1**	**2**	**3**	**4**
skewness	*0.44*	-0.17	0.06	*-0.24*		*1.00*	*-1.03*	0.15	*0.43*
kurtosis	2.98	3.19	3.09	2.83		*7.5*	*5.99*	*3.63*	*3.85*

Sal & PV	Unrotated					Rotated			
Mode	**1**	**2**	**3**	**4**		**1**	**2**	**3**	**4**
skewness	0.1	*-0.46*	*0.95*	0.04		*0.85*	*0.78*	*0.76*	-0.2
kurtosis	*3.75*	*3.83*	*5.2*	*3.64*		*6.38*	*4.28*	*4.25*	*3.88*

We reject the null hypothesis when the skewness is greater than the standard error of skewness (ses) $ses = \sqrt{\frac{6}{N}} = 0.21$ (Tabachnick 1996) and N is the degrees of freedom (136 HOT cruises), and when the kurtosis is greater/lesser than 3± the standard error of kurtosis (sek), where $sek = \sqrt{\frac{24}{N}} = 0.42$ (Tabachnick 1996). Significant values of kurtosis indicate that the distribution of amplitudes is prone to outliers. Outliers are considered to be event-like, as is the passage of an eddy.

Several of the significant EOF amplitude peaks correspond to eddy events. Figures 4.10 through 4.25 show the EOF analyses results for two groups of water properties. The first series of EOFs included salinity, potential vorticity, silicate, [nitrate + nitrite] and dissolved oxygen. The second series included only salinity and potential vorticity. Peaks in the time series with an eddy number by it indicate significant peaks that corresponded with an eddy. These two groups of variables are not the only groups that were analyzed, but they display the greatest number of large events attributed to eddies, and all of the eddies that appear as large peaks in the four modes of the other EOFs also appear in these EOFs. Some of the other groups of variables that were analyzed included:

- salinity and silicate
- salinity and "NO"
- salinity, potential vorticity, silicate and "NO"
- salinity only
- salinity, silicate, [nitrate +nitrite] and dissolved oxygen

Additionally, a rotation of the EOFs was done for these two groups of variables (Section 3.4.3). The rotation results are presented alongside the unrotated results (Figures 4.10 through 4.25). The rotation changed the vertical structures, which

realigned which mode that certain eddies would appear in with a large amplitude. The five variable (salinity, dissolved oxygen, silicate, [nitrate + nitrite] and potential vorticity) EOF vertical structure of mode 1 really only changed sign during the rotation and the two variable (salinity and potential vorticity) EOF vertical structure of mode 1 did not change as a result of the rotation.

The EOF analysis showed that the dominant modes of variability (those explaining over 5% of the amount of variance) of water property anomalies at ALOHA are the same regardless of which group of cruises are used. This analysis also showed that EOFs can isolate distinct events like eddies. Because of the small number of cases and the potential significance of eddy-eddy interactions (Section 5.3) for water property anomalies within an eddy, the EOF analysis was not able to group eddies with similar water property anomaly characteristics by formation region, direction of rotation, or any other obvious characteristic.

4.6.2 Composite profiles

A simpler way to look at water property anomalies based on eddy characteristics is to look at composite profiles (Section 3.1.4). Composite profiles are a less sophisticated method of grouping water mass variability than the EOF analysis but approaches the same question from a different angle. Instead of trying to separate the water mass characteristics from all of the eddies, composites allow us to start with a hypothesis that all eddies with certain similar properties, such as direction of rotation or region of formation, will have similar water mass property anomaly characteristics.

Figure 4.26 shows composites of normalized water property anomalies for cyclonic and anticyclonic eddies. Figures 4.27 through 4.32 show composite profiles of normalized water property anomalies, based on the eddy's region of formation (Section 4.3.2). Anticyclones have larger water property anomalies than cyclones do. Most noticeable are the increased nutrients in anticyclones at $25.25\sigma_\theta$ and $26.7\sigma_\theta$, the reduced salinity at $25.5\sigma_\theta$ and decreased dO_2 over the entire profile. The cyclones are characterized by anomalies that are at most 2 standard deviations with increased dO_2, a salinity maximum at $26.3\sigma_\theta$ and a silicate maximum at $27.2\sigma_\theta$. Hypotheses for why profiles would be different based on the direction of rotation are presented in Section 5.6.

The composite profiles (Figures 4.27 -4.32) that are divided by eddy formation region are defined as in Section 4.3.2. None of these water mass property composite profiles are as large as the composites based on rotation direction, with the largest anomalies found in region 6, which is comprised of eddies that formed south of 22°N and east of 153°W. Eddies formed in region 1 (east of 148°W) have maximum normalized water property anomalies of about 1.5 standard deviations, whereas eddies formed in region 4 (west of 156°W) have maximum anomalies of only 0.5 standard deviations. Regions 1 and 2 combined were also split into regions 5 (encompassing north of 22°N and east of 153°W) and 6 (encompassing south of 22°N and east of 153°W). The region 6 composite had the largest water property anomalies of all the regional composites. We expect eddies that form in region 1 would have larger anomalies than those formed in region 4 if the spatial gradient of water properties is such that the water mass characteristics in region 1 are different from region 4. Water mass spatial gradients (Antonov et al. 2006, Garcia et al. 2006), were interpolated onto select potential density

surfaces. The 25.5σ_θ surface for salinity and silicate is shown in Figure 3.2 along with the formation locations of the ALOHA eddies. Both silicate and salinity show the largest differences from values at ALOHA to the southeast, in region 6.

4.6.3 ALOHA eddy current structure

Currents in forty eddies that that were sampled by HOT cruises were also measured by shipboard ADCP. Twenty two of the eddies exhibit currents in the direction expected based on the portion of the eddy over ALOHA at the time of the cruise. The current profiles of several eddies decrease in magnitude with depth (26C, 34A, 36A, 37C, 41C, 55C, 56C, 57A, 59C, 60A, 62C, 65A, 66C, 76C). Three of the larger eddies (31A, 44A, 71C) exhibited stronger currents that are uniform over the upper 300 m, depending on which part of the eddy was sampled by the HOT cruise. Eight of the eddies have ADCP profiles that do not make sense with the plotted position of the eddy during the HOT cruise. The remaining eight eddies exhibited currents that are indiscernible, whether because the eddy itself is weaker, the eddy was sampled along its periphery, or the presence of some other ocean process confused the eddy current signal.

The north and southbound tracks between the island of Oahu and Station ALOHA provide additional information about the cross sectional portion of an eddy through which the ship transited. Three eddies moved fast enough, and were strong enough that the northbound transit currents are noticeably different from the southbound currents. A few eddies exhibit vertical current shear in the on station profiles that corresponds with changes in the eddy's water property anomaly vertical profiles, which might provide some insight into the shape of the eddy (Section 5.3). Details of the eddy current

observations for each eddy, along with the ADCP profiles can be found within the eddy descriptions of Appendix II.

4.7 Eddy statistics of East-Central North Pacific

The last part of this study broadens its scope to look at eddies in the North Pacific Subtropical Gyre, in the vicinity of the Hawaiian Islands. By applying some of the methods used to characterize ALOHA eddies, it is worthwhile to learn how eddies affect the Hawaiian Islands, and not just Station ALOHA.

4.7.1 Eddy characteristics

The eddies in the vicinity of the Hawaiian Islands are those that pass through the larger box described in Figure 3.6. The distributions of each characteristic (amplitude, radius, translation speed and axial speed) are similar to those of ALOHA eddies (Figure 4.33). The larger region provides a much larger sample size with which to calculate some of the statistics looked at in Section 4.2, but these eddies have not been visually inspected to ensure that the features captured by the algorithm are all real, unique eddies. This probably causes a slight overestimation in the number of features. It is also important to keep in mind that the larger region encompasses parts of eddy tracks as well as complete tracks because eddies translate into and out of this region, beyond the geographical limits of this study. This can cause a disconnect between the number of eddies seen in the region at any particular time and the number of eddies that are formed in the region (Section 4.7.2).

Figure 4.34 shows a similar statistical display to that of Figure 4.3. With the larger sample size, the correlation between latitude and translation speed is more evident,

as latitude decreases, the translation speed increases. Again, the relationship between amplitude and radius is ensured by the definition of the radius (Section 3.3.2) because they are linearly dependent. To see how the eddies in the vicinity of the Hawaiian Islands compare to those of ALOHA, the primary focus is on the temporal distribution. Figure 4.35 shows the total number of eddies per year that passed by ALOHA and the total number of eddies per year (divided by 106) that passed through the larger region. The region is approximately 106 times the size of the 2°x2° box around ALOHA (minus the area of the Hawaiian Islands), so dividing by 106 scales the number of eddies per year to a level appropriate for comparison. The number of eddies per year for the larger region appears constant, so that an increased number of eddies at ALOHA in a particular year is more likely explained by randomness due to unpredictable physical processes such as instabilities or eddy-eddy interactions.

Biological observations at Station ALOHA indicated that a regime shift in the NPSG occurred in 1977, but that effects from that did not manifest until a decade later (Karl 1999). To further explore the possibility of a decadal shift in the gyre affecting the presence of eddies in our region of interest, the total number of eddies per year that occurred from 1993-1997 were compared to the number of eddies per year occurring from 1998-2006 (Figure 4.36). Again, the larger region totals are divided by 106. The difference in the number of eddies per year between the two time periods is not significant.

Also examined were the number of cyclones versus anticyclones. The ALOHA eddies showed a slight but insignificant surplus of cyclones (Figure 4.37) when looking at all 76 features. If only the 58 "robust" cases are examined, then there is no bias for

rotation. The larger region (again totals are divided by 106) also showed no bias for rotation.

4.7.2 Spatial distribution

Figure 4.38 shows the distribution of average number of eddies per year in the region surrounding the Hawaiian Islands, and their average translation speed and direction. It is interesting to note that the region immediately northeast of the islands has fewer features than the region further northeast, and an associated eddy trajectory change from due west to the northwest. The average translation direction of the eddies that pass through the region around ALOHA (Figure 4.38 arrows) show that eddies approaching the islands have a slight tendency to move northwest along the ridge, then resume a westward trajectory once clear of the islands. There is a strong possibility that this deviation from westward propagation is due to eddy interaction with the mean flow of the North Hawaiian Ridge Current (NHRC) or due to eddy interaction with the topography of the Hawaiian Islands, discussed in further detail in Section 5.5.

Figure 4.39 shows the formation locations of eddies that occur within the larger region of interest. The ALOHA eddy formation locations are annotated as black dots. Other than in the lee of the big island of Hawaii, the distribution of eddy genesis appears to be pretty random. It is also interesting to note that there are eddies that form east of Station ALOHA, at the same latitude as Station ALOHA, but which do not pass through Station ALOHA, due to disturbances in their westward trajectory. Recall that these eddies have not been subject to a visual analysis that might reveal that some of the eddies in this larger region are not really eddies, or are remnants from other features.

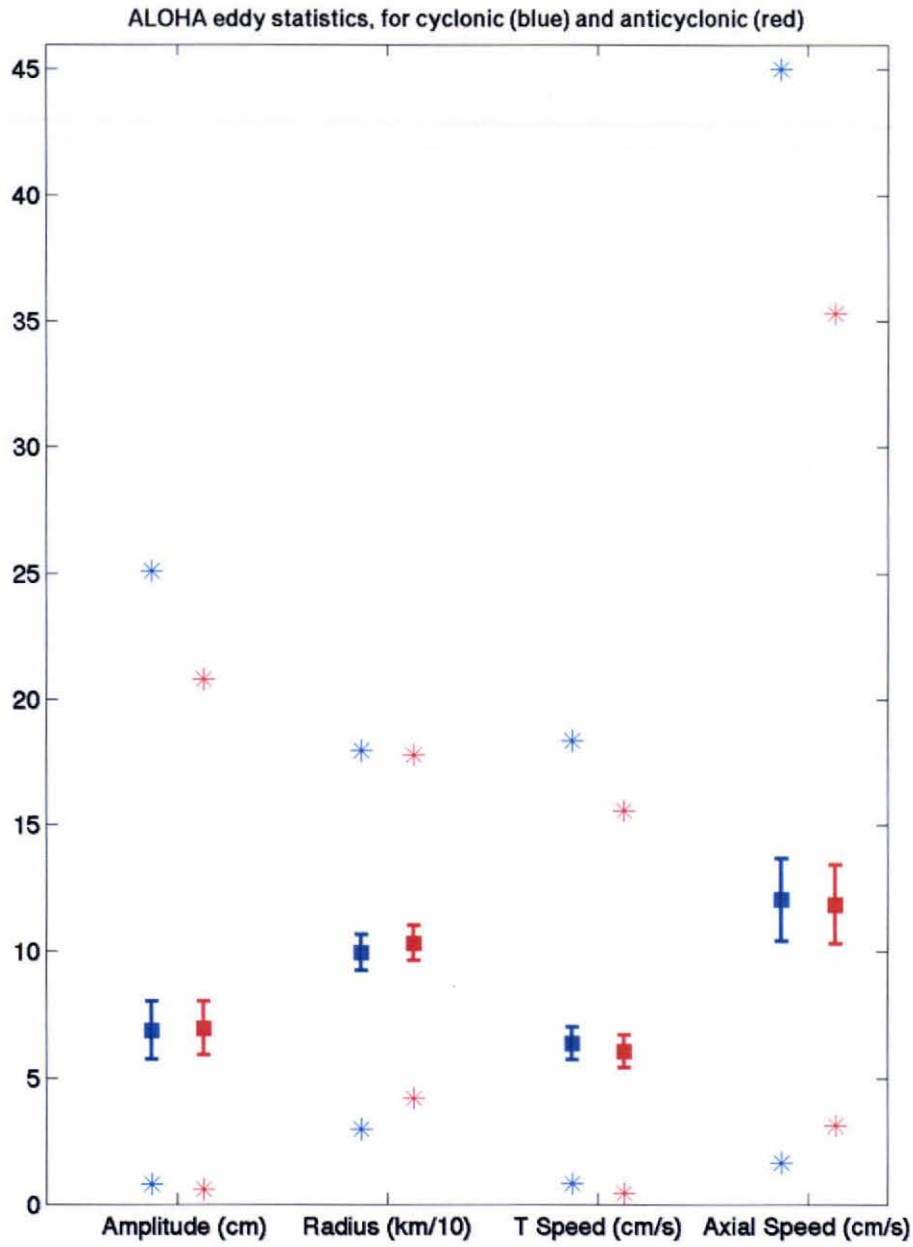

Figure 4.1: ALOHA eddy statistics of amplitude (cm), radius(km/10), translation (T) speed (cm/s) and axial speed (cm/s). The squares denote the mean and the error bars describe the standard error of the mean at 95% confidence for 58 eddies. The stars denote the maximum and minimum values of each parameter. Blue symbols are for cyclones and red symbols are for anticyclones.

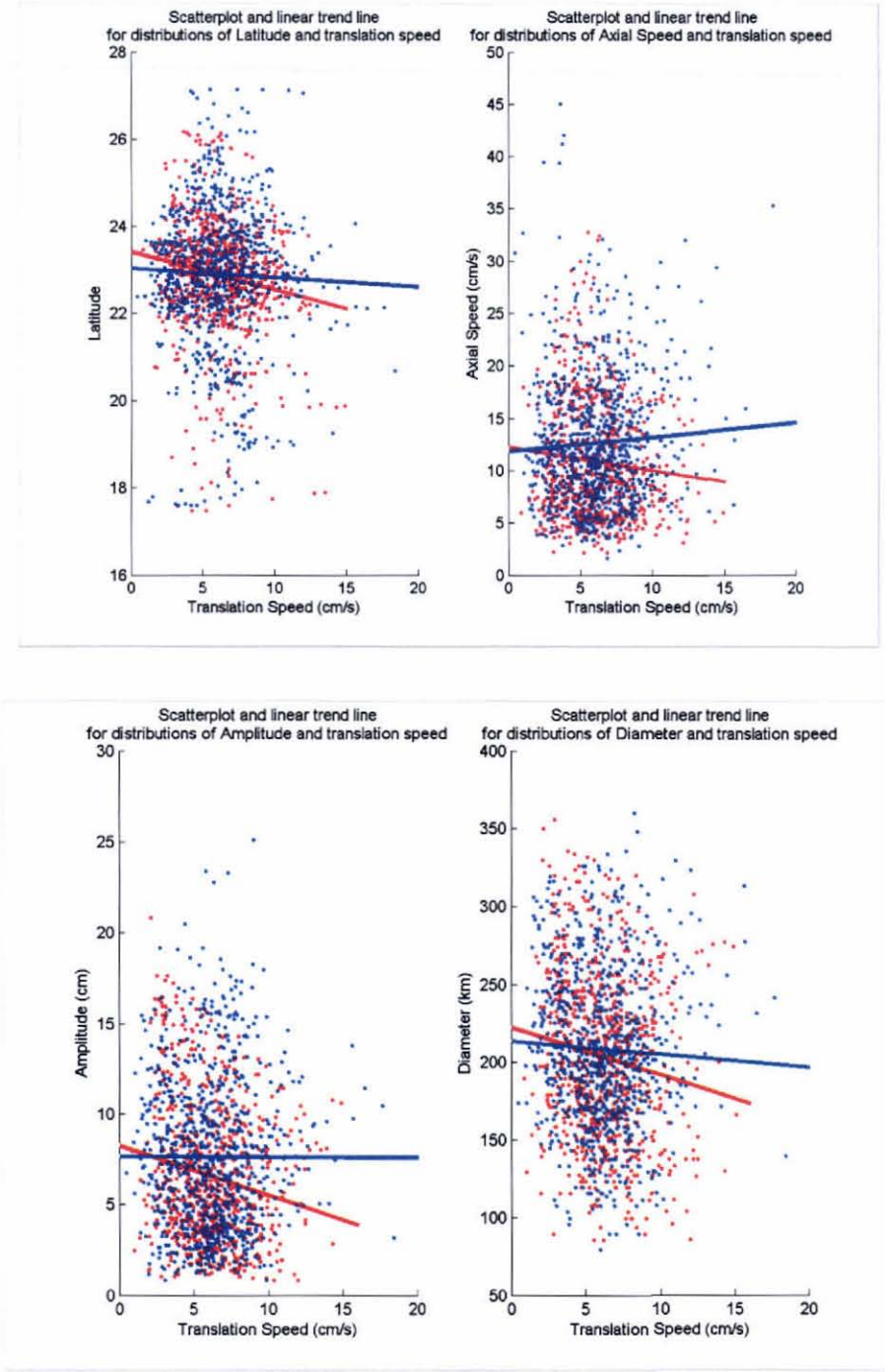

Figure 4.2: Scatter plots of ALOHA eddy statistics. Line slope indicates regression coefficient for anticyclonic eddy parameters (red) and cyclonic eddy parameters (blue).

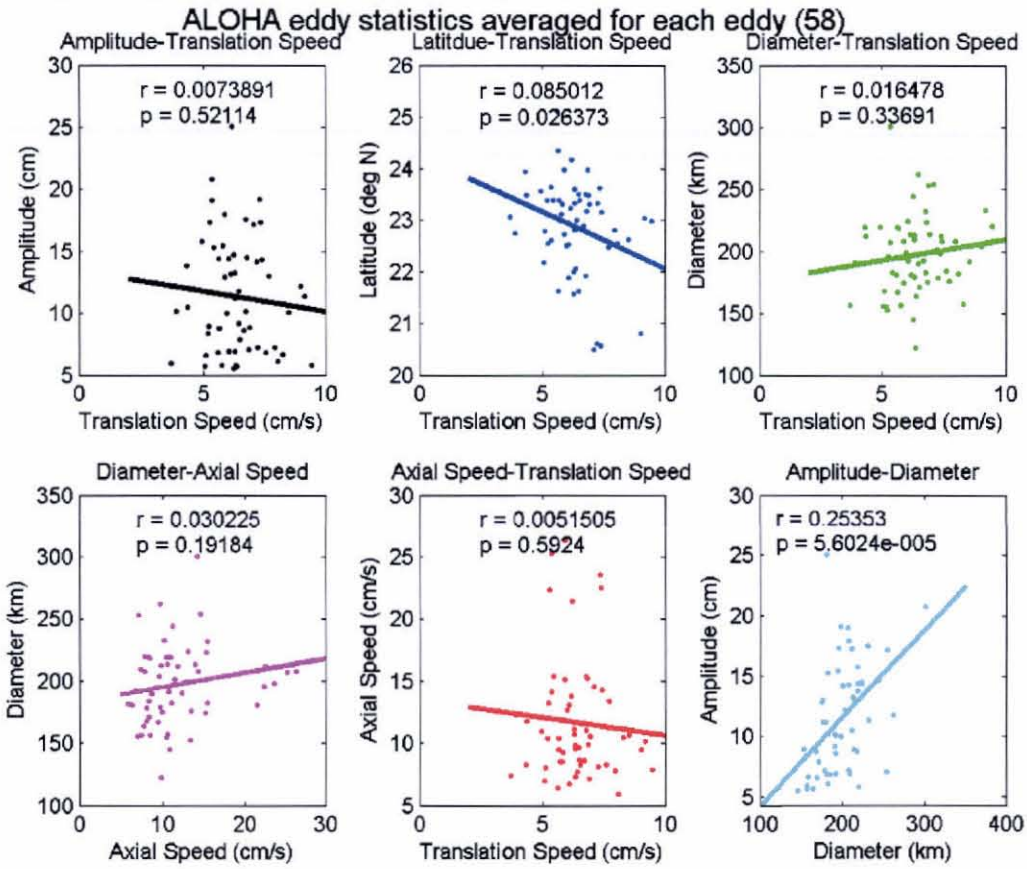

Figure 4.3: Scatterplots of eddy average parameters for 58 ALOHA eddies.

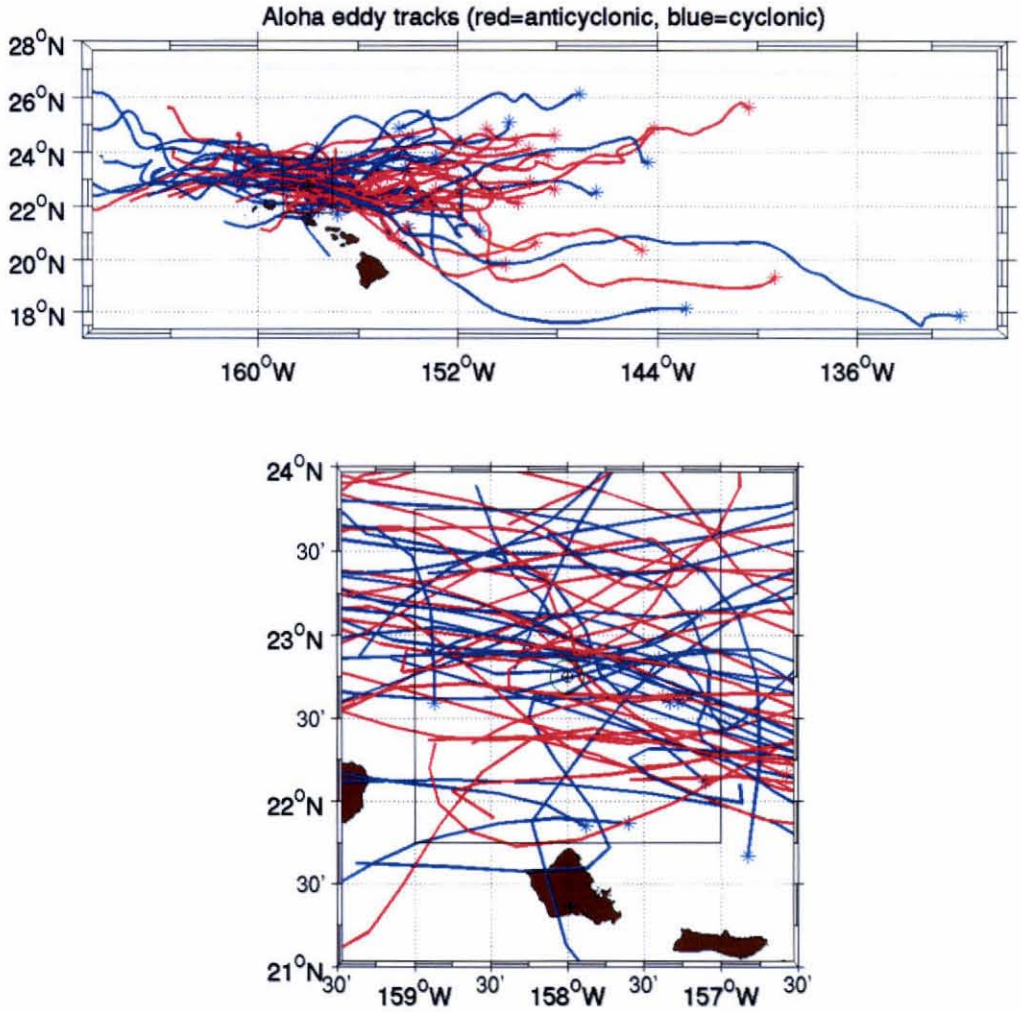

Figure 4.4: Eddy origin locations and eddy tracks. "*"marks represent the origin location, red are anticyclonic eddies and blue are cyclonic eddies. The bottom plot shows a closer view of the region around Station ALOHA.

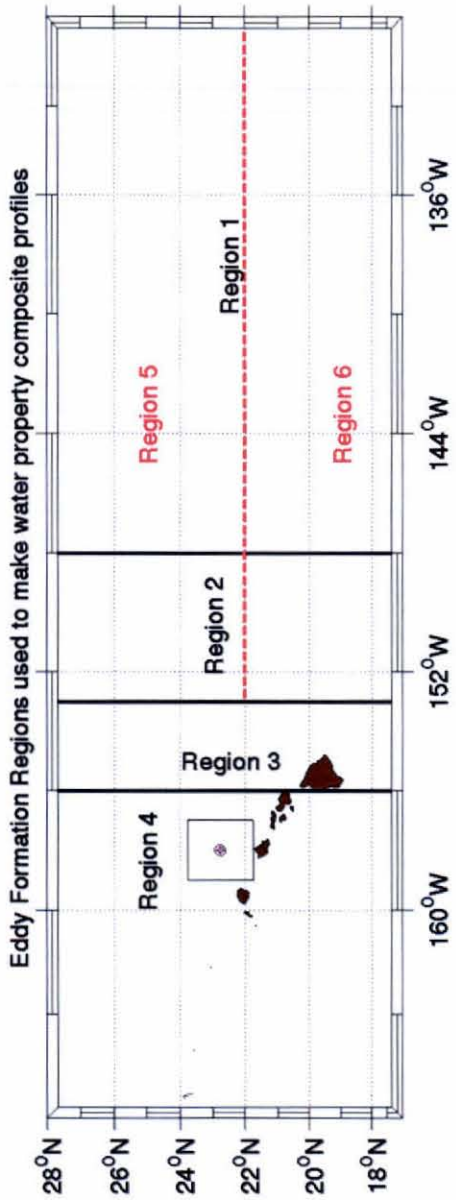

Figure 4.5: Regions of eddy formation. Dashed line separates Regions 5 and 6 and vertical solid lines separate Regions 1 thorugh 4. The study area is depicted by the square box and maker in the center

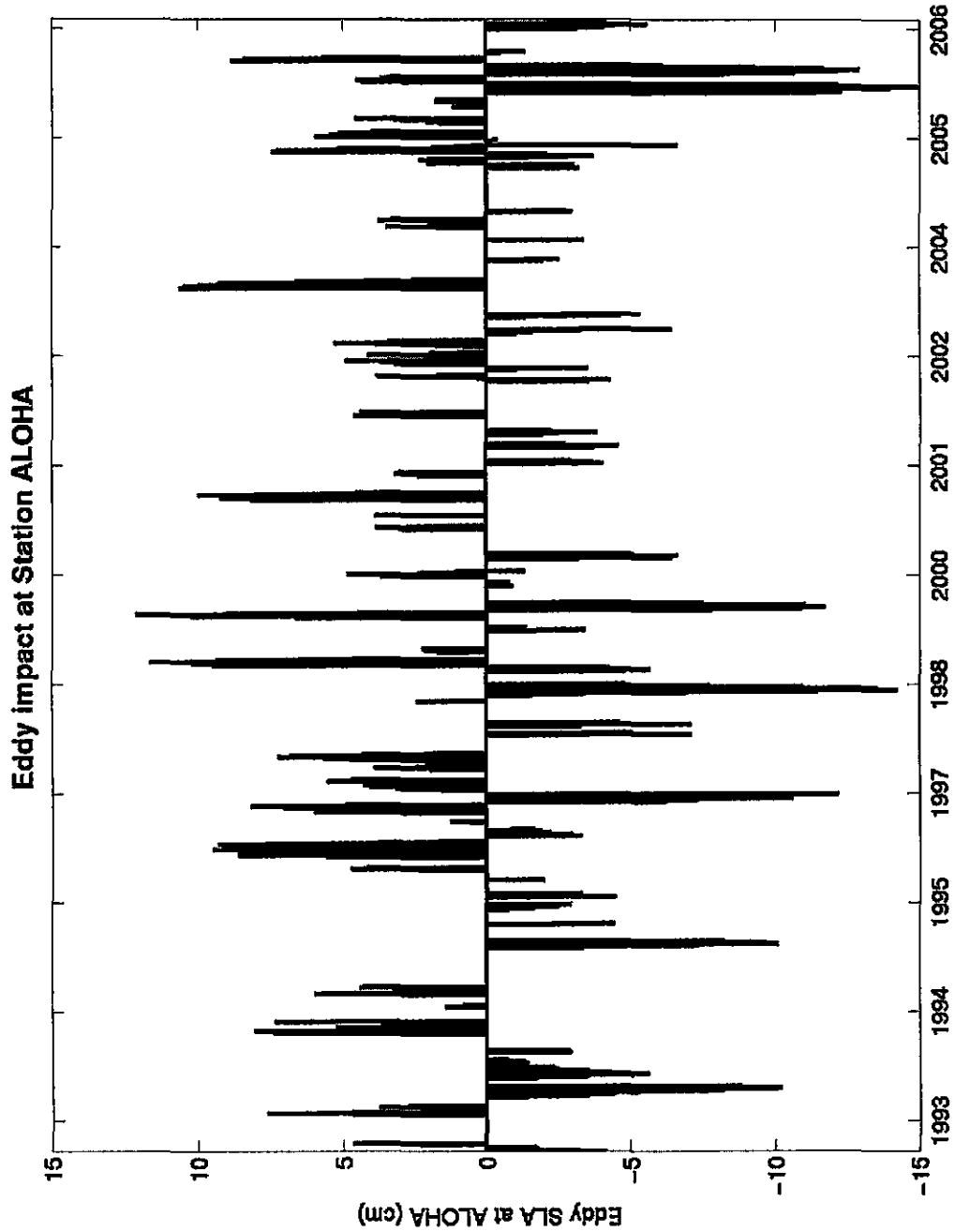

Figure 4.6: Time series of eddy events at ALOHA plotted as the sea level perturbation due to the eddy over Station ALOHA. Zero values indicate no eddy present, negative values are cyclones and positive values are anticyclones.

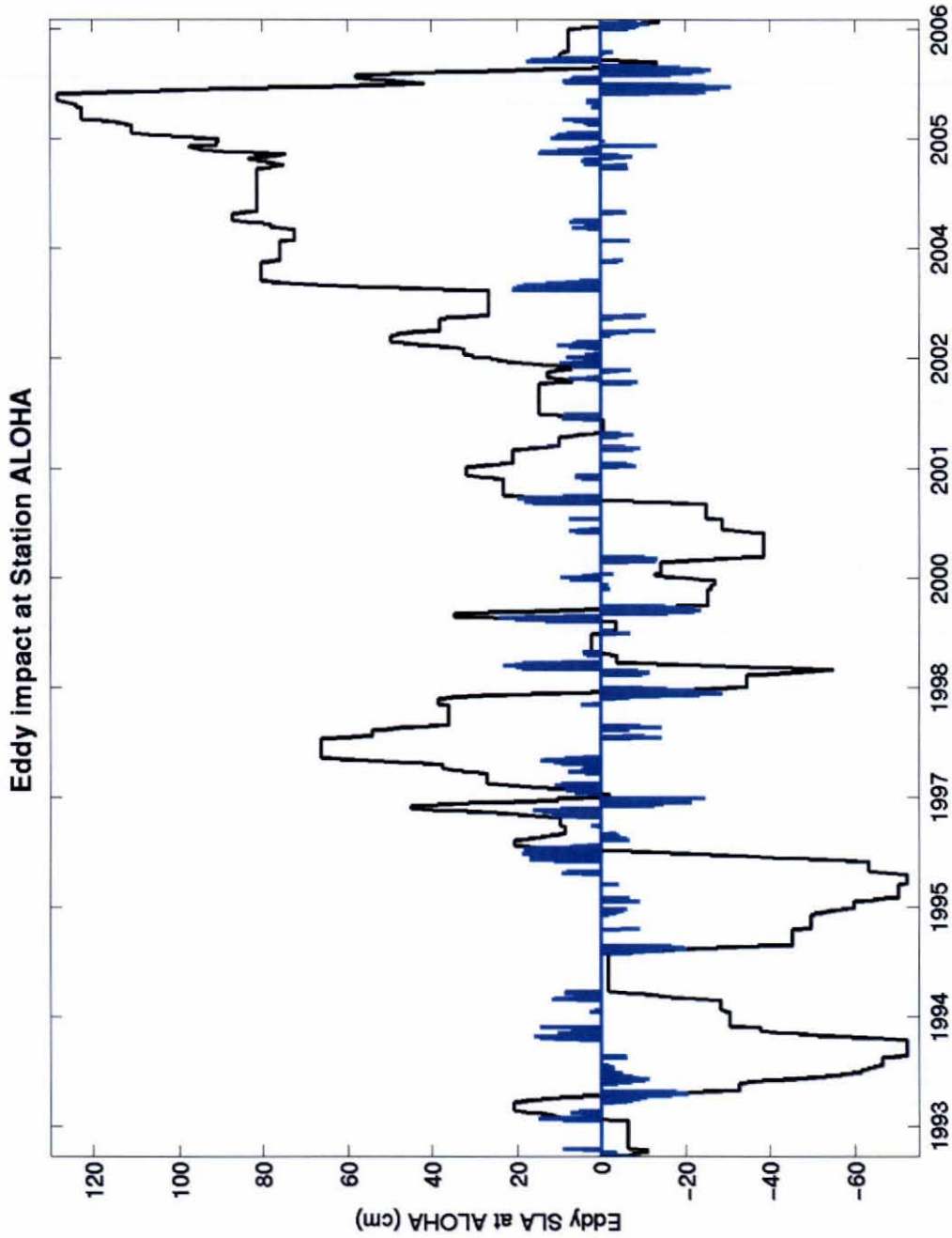

Figure 4.7: Figure 4.6 shown in blue, and black time series denotes cumulative distribution of sea level perturbation due to eddies at Station ALOHA.

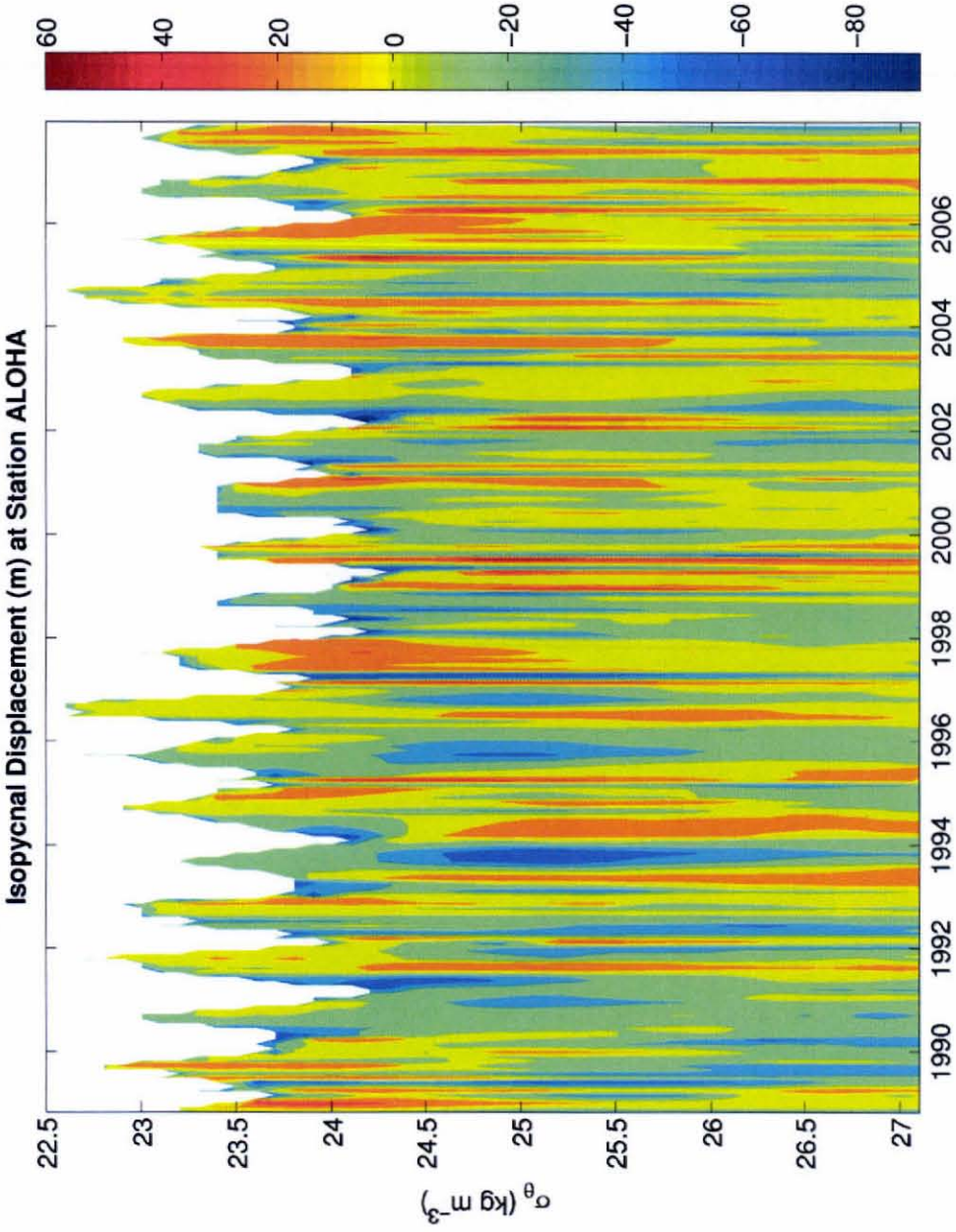

Figure 4.8: Contoured isopycnal displacements (in meters) over the upper ~800 m at Station ALOHA. Positive isopycnal displacement indicates a depression of isopycnal surfaces and a negative displacement indicates an uplift in isopycnal displacement.

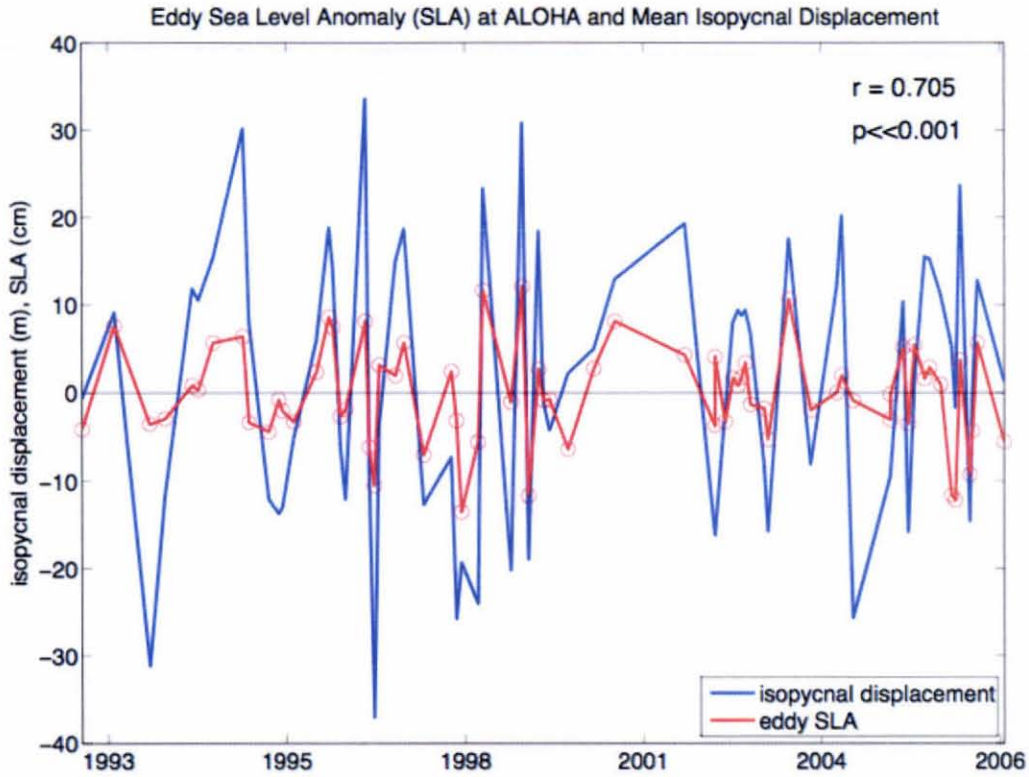

Figure 4.9: Eddy sea level perturbation at Station ALOHA (red) and average isopycnal displacement at ALOHA (blue). (r) is the correlation coefficient and (p) is the p-value.

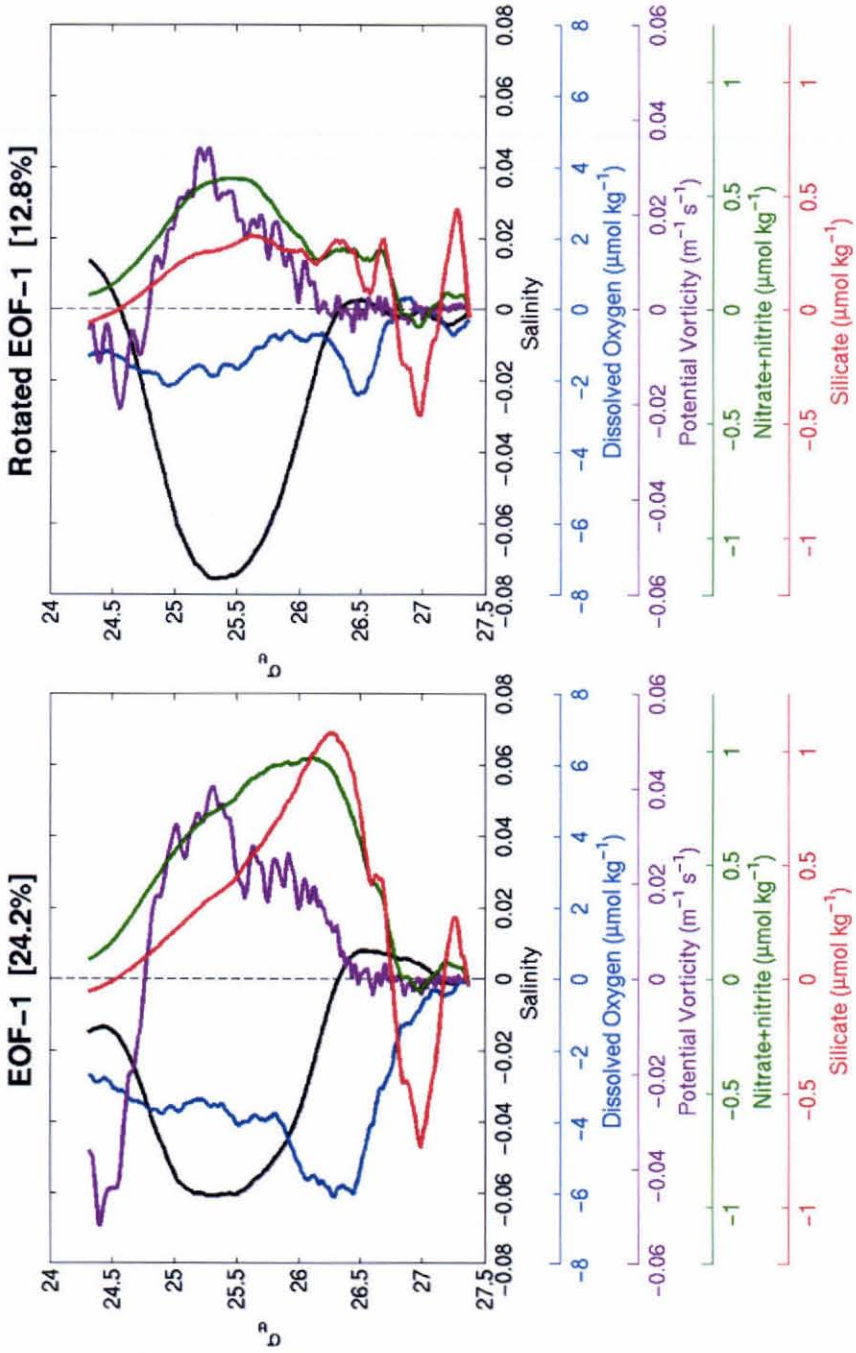

Figure 4.10: Vertical structure of water property anomalies for mode 1 of the unrotated (left) and rotated (right) EOF analysis of salinity, dissolved oxygen, potential vorticity, [nitrate + nitrite], and silicate.

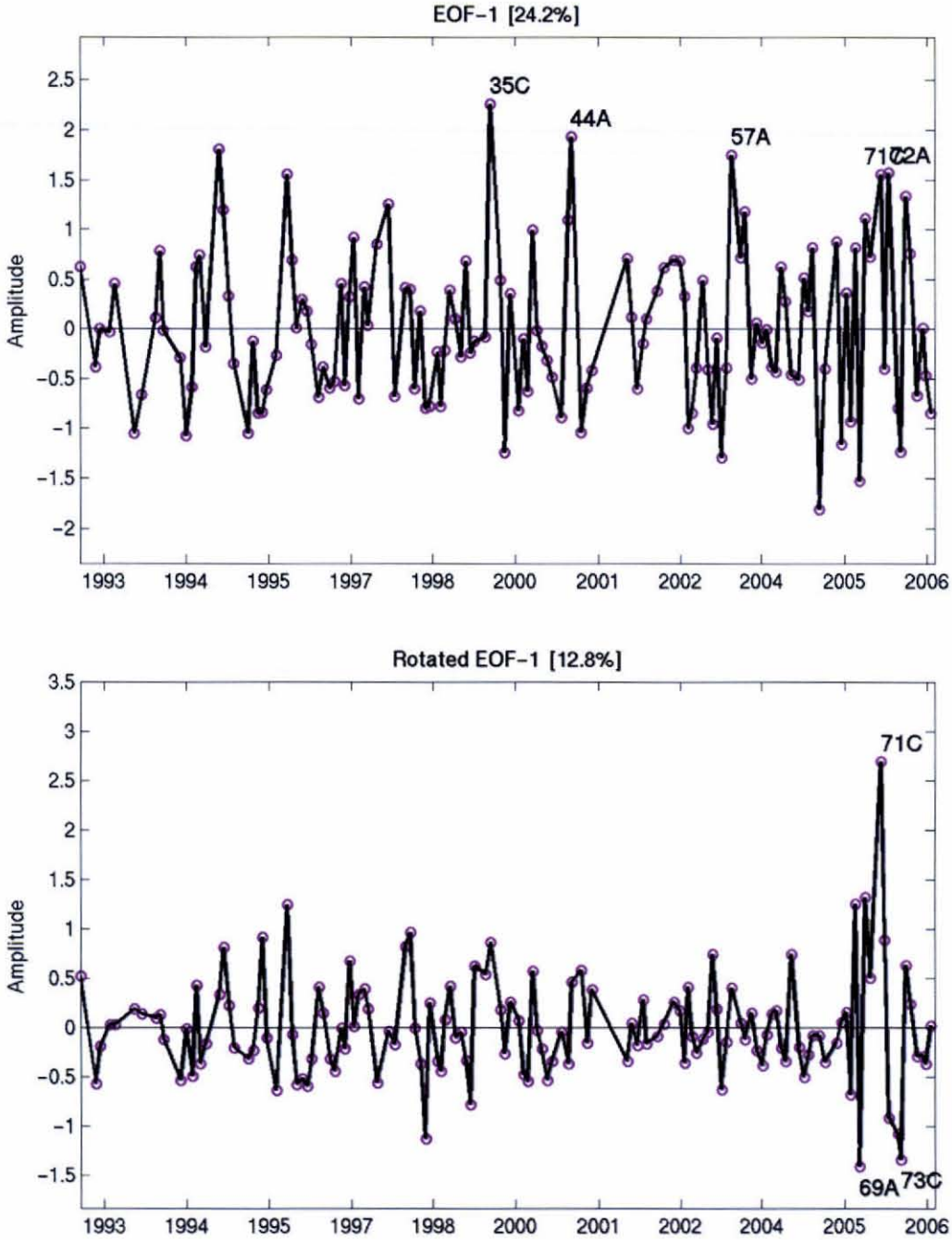

Figure 4.11: Time series of normalized amplitudes for mode 1 of the unrotated (top) and rotated (bottom) EOF analysis of salinity, dissolved oxygen, potential vorticity, [nitrate + nitrite], and silicate.

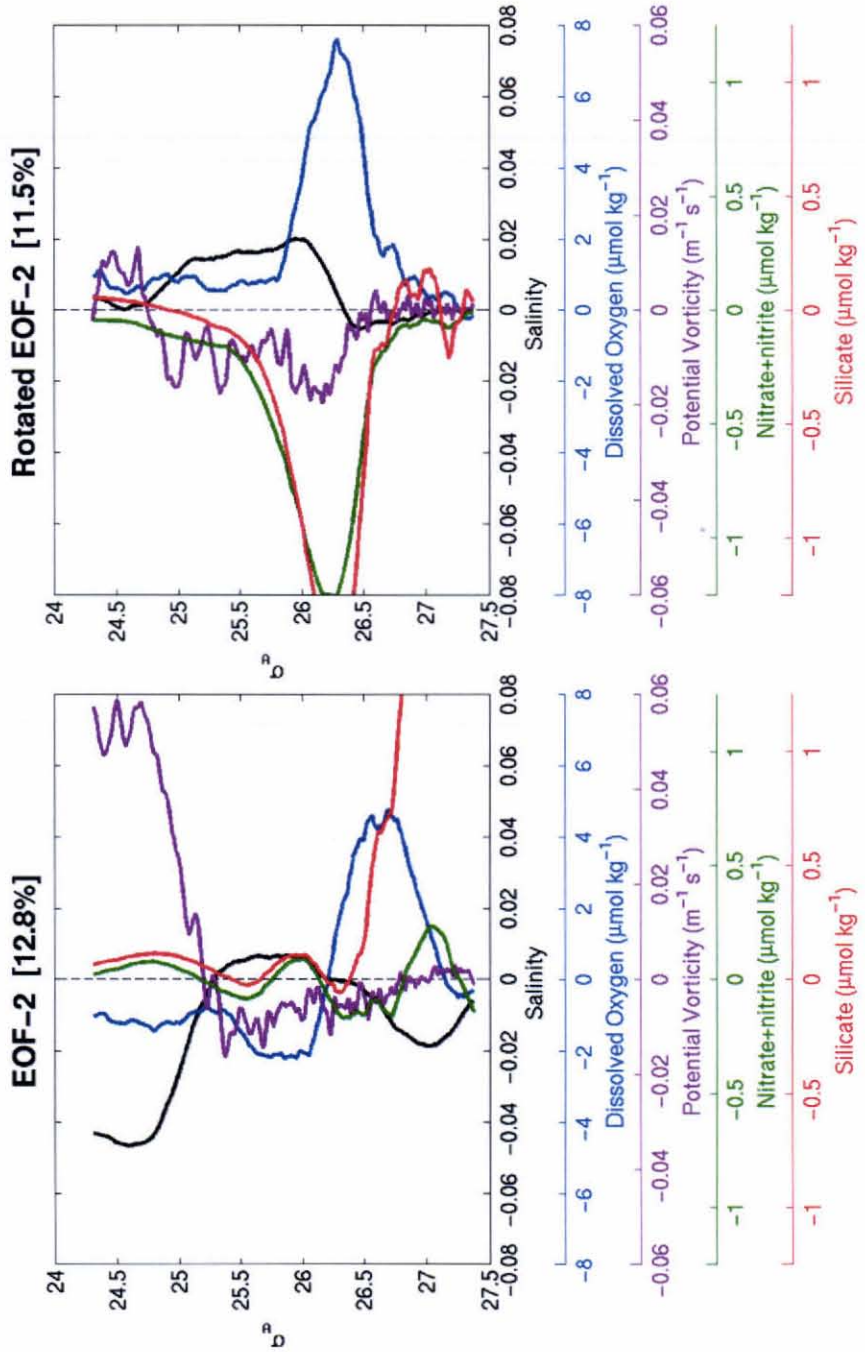

Figure 4.12: Vertical structure of water property anomalies for mode 2 of the unrotated (left) and rotated (right) EOF analysis of salinity, dissolved oxygen, potential vorticity, [nitrate + nitrite], and silicate.

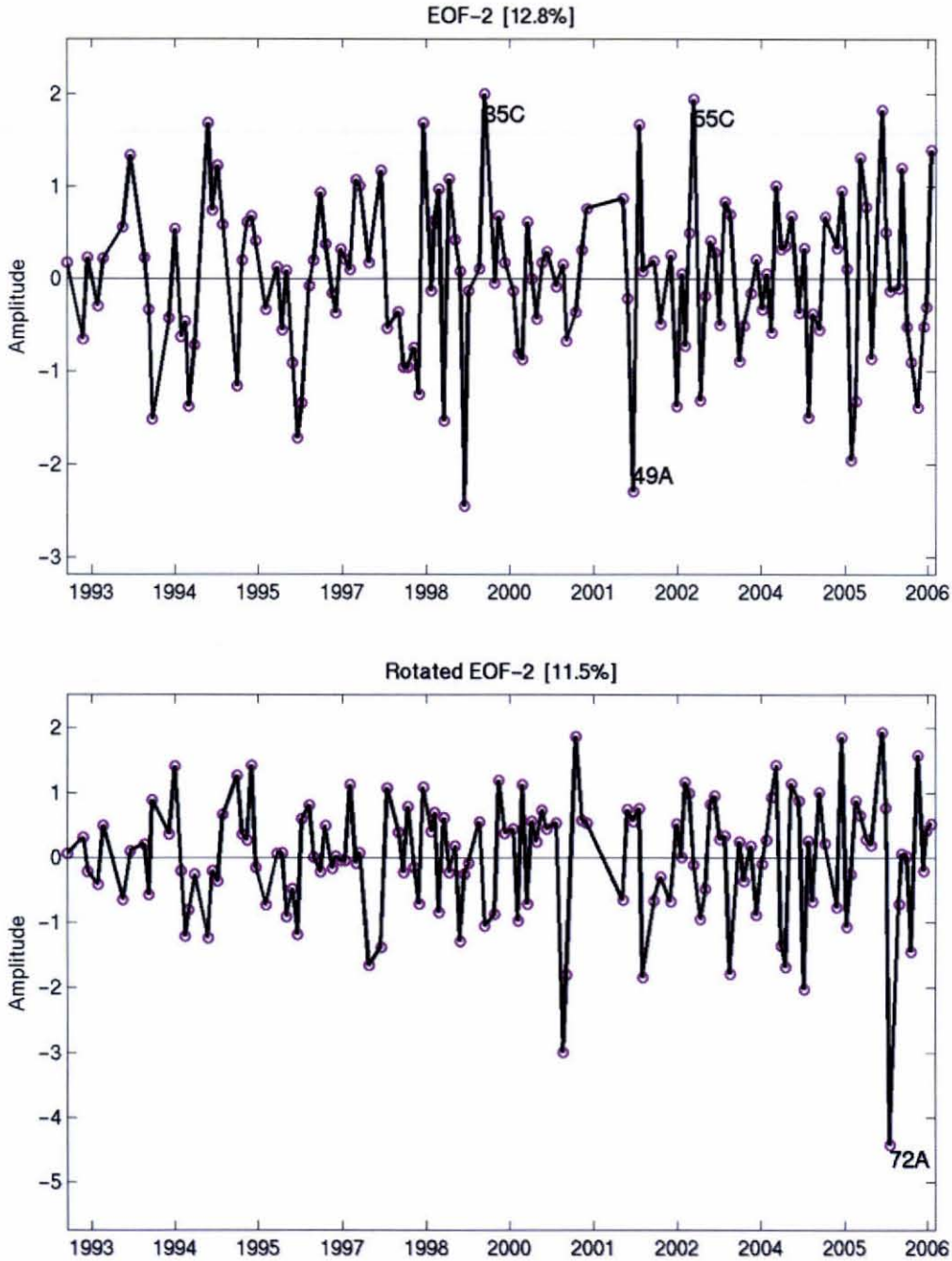

Figure 4.13: Time series of normalized amplitudes for mode 2 of the unrotated (top) and rotated (bottom) EOF analysis of salinity, dissolved oxygen, potential vorticity, [nitrate + nitrite], and silicate.

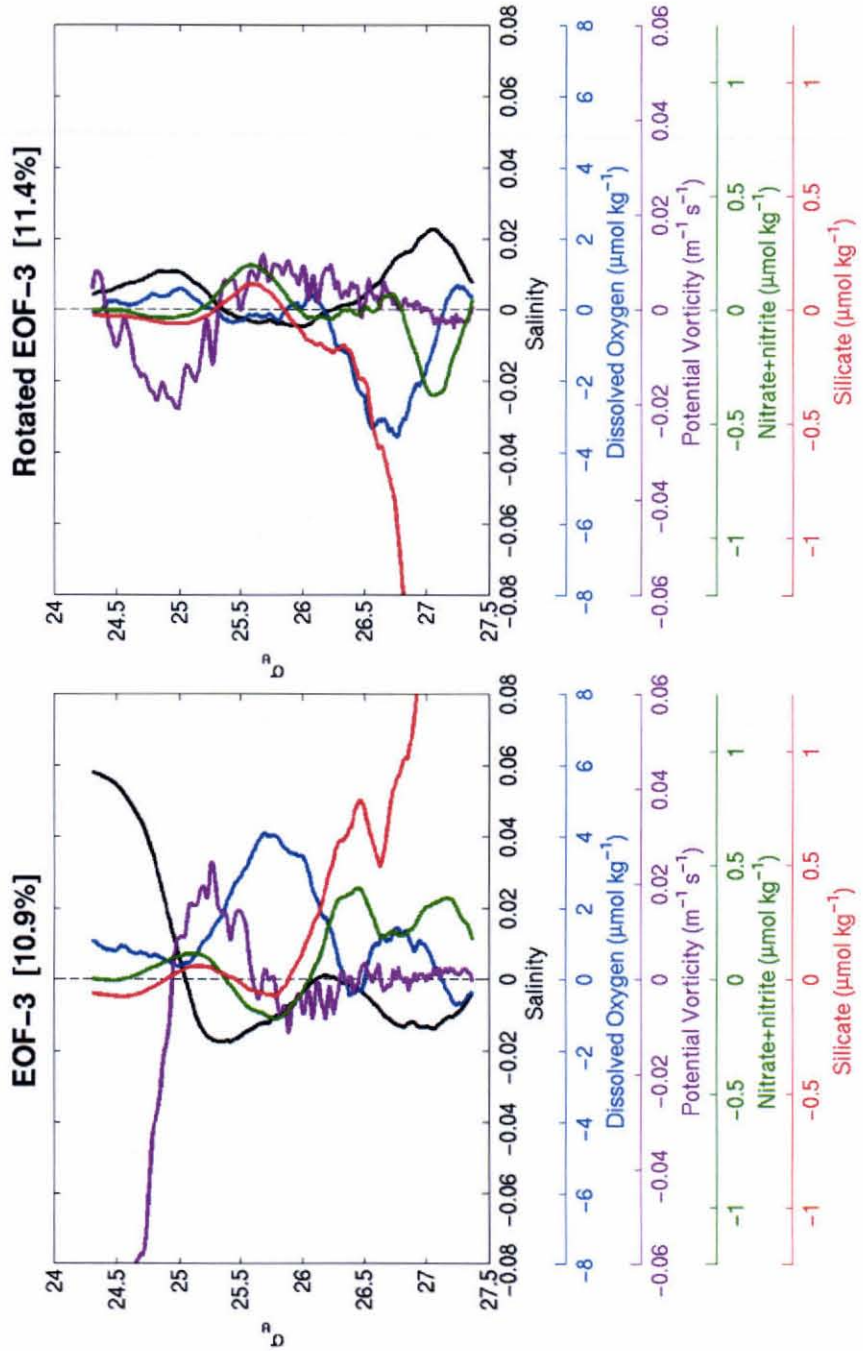

Figure 4.14: Vertical structure of water property anomalies for mode 3 of the unrotated (left) and rotated (right) EOF analysis of salinity, dissolved oxygen, potential vorticity, [nitrate + nitrite], and silicate.

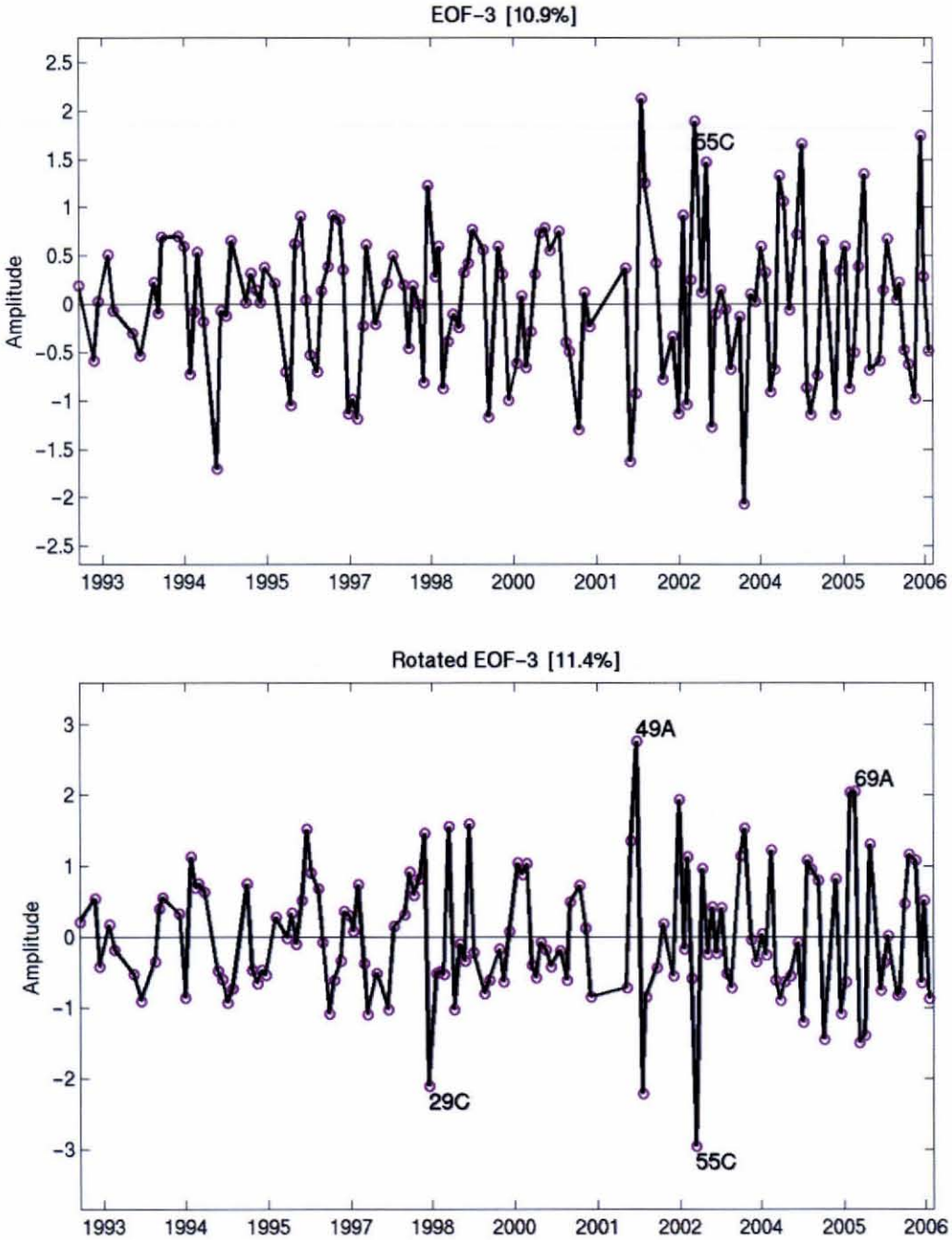

Figure 4.15: Time series of normalized amplitudes for mode 3 of the unrotated (top) and rotated (bottom) EOF analysis of salinity, dissolved oxygen, potential vorticity, [nitrate + nitrite], and silicate.

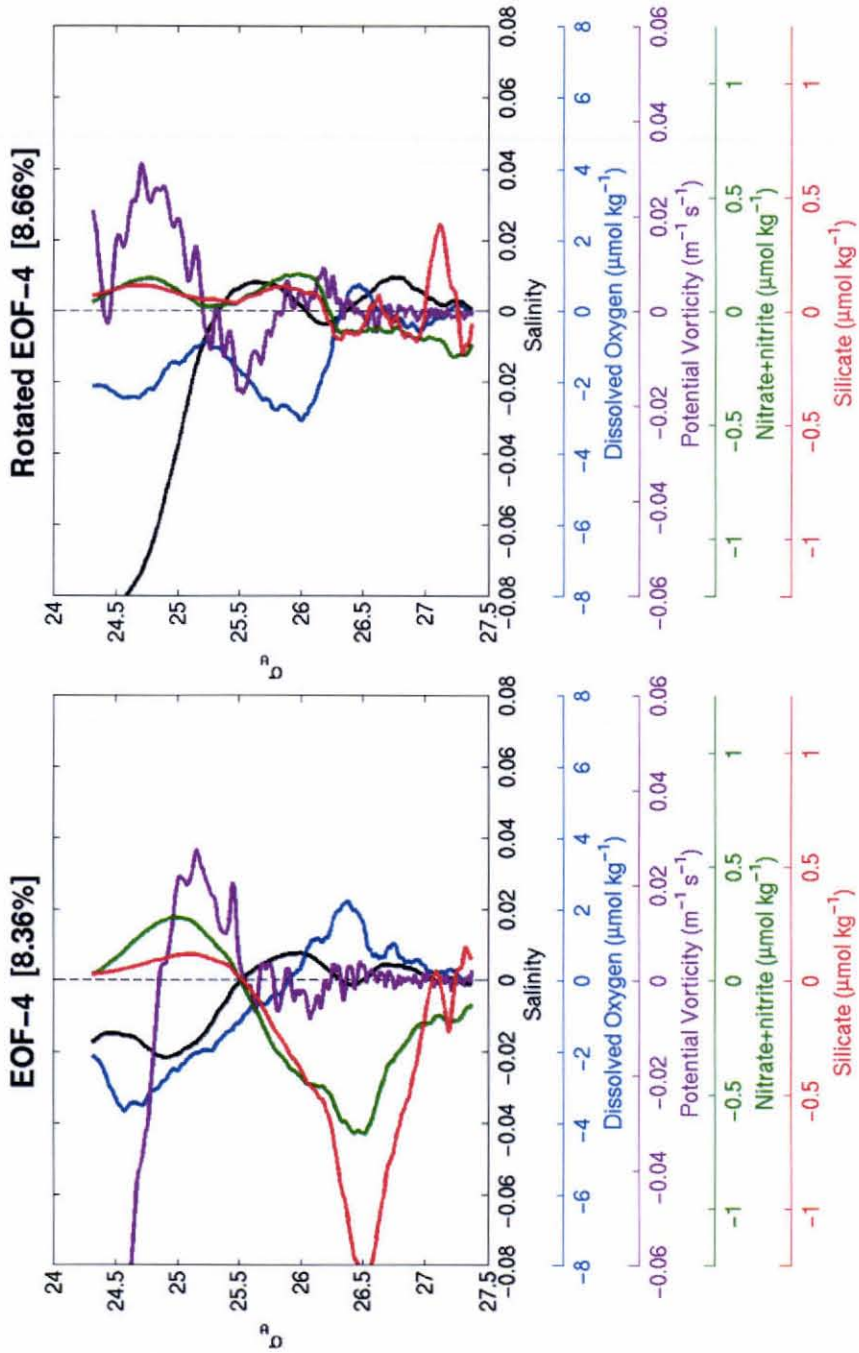

Figure 4.16: Vertical structure of water property anomalies for mode 4 of the unrotated (left) and rotated (right) EOF analysis of salinity, dissolved oxygen, potential vorticity, [nitrate + nitrite], and silicate.

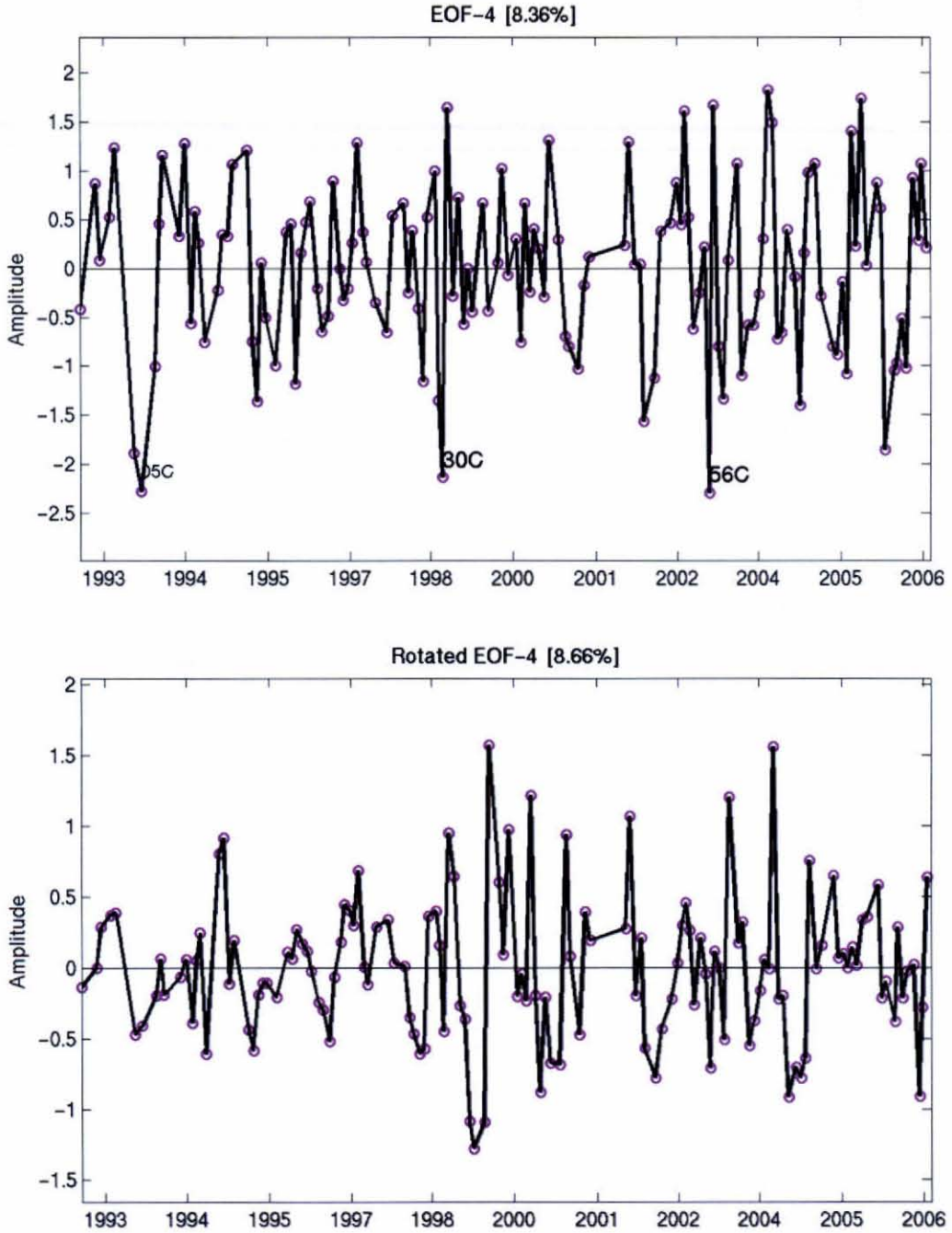

Figure 4.17: Time series of normalized amplitudes for mode 4 of the unrotated (top) and rotated (bottom) EOF analysis of salinity, dissolved oxygen, potential vorticity, [nitrate + nitrite], and silicate.

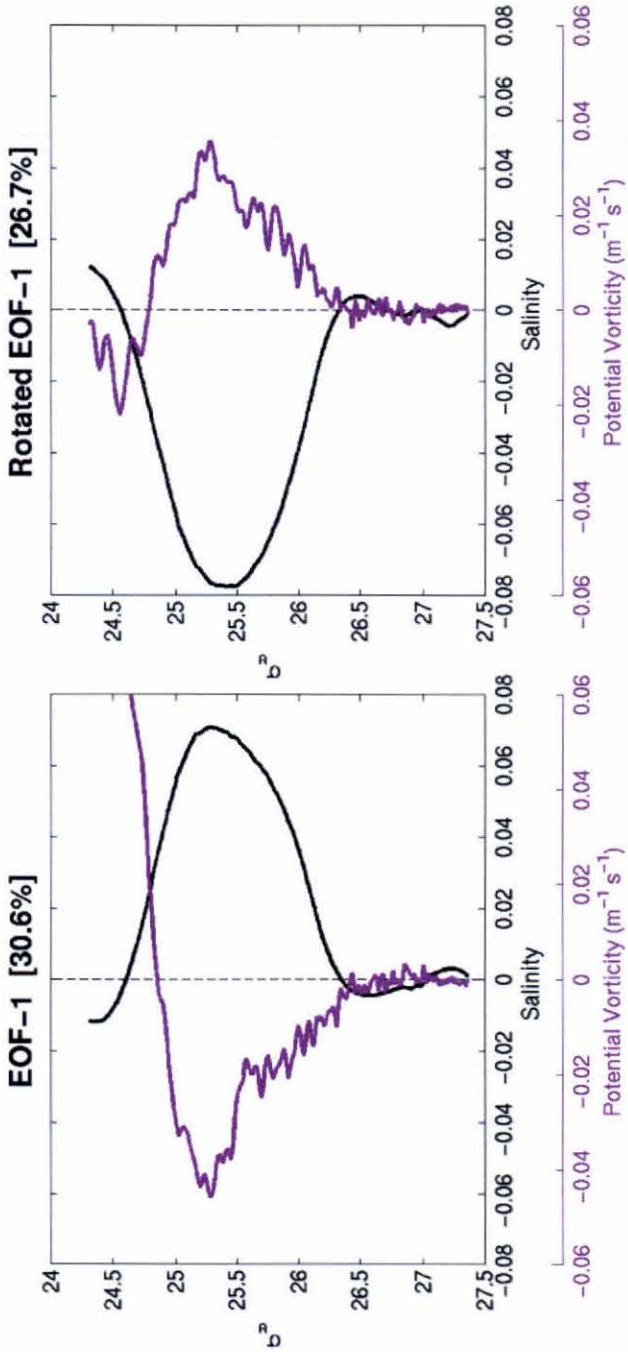

Figure 4.18: Vertical structure of water property anomalies for mode 1 of the unrotated (left) and rotated (right) EOF analysis of salinity and potential vorticity.

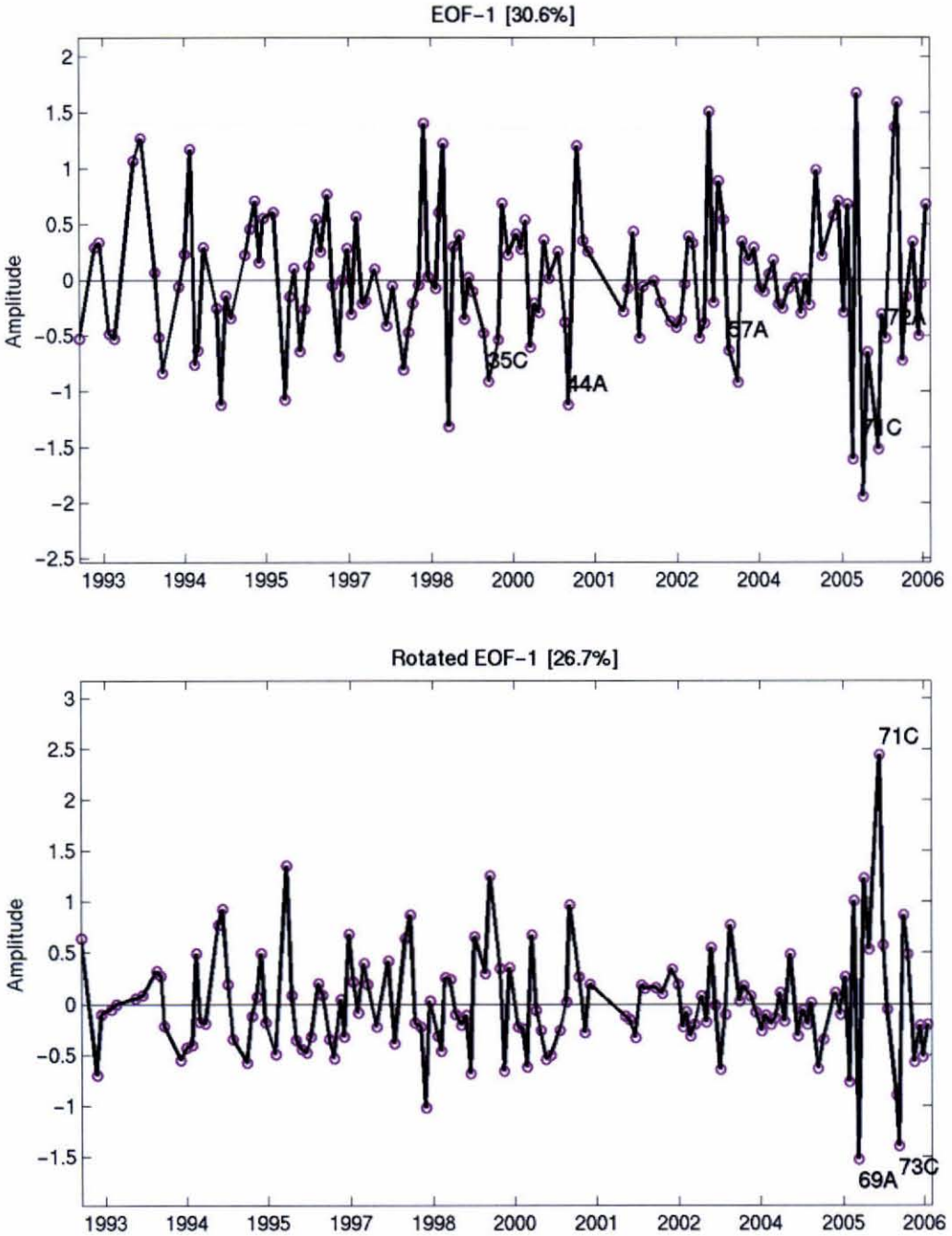

Figure 4.19: Time series of normalized amplitudes for mode 1 of the unrotated (top) and rotated (bottom) EOF analysis of salinity and potential vorticity.

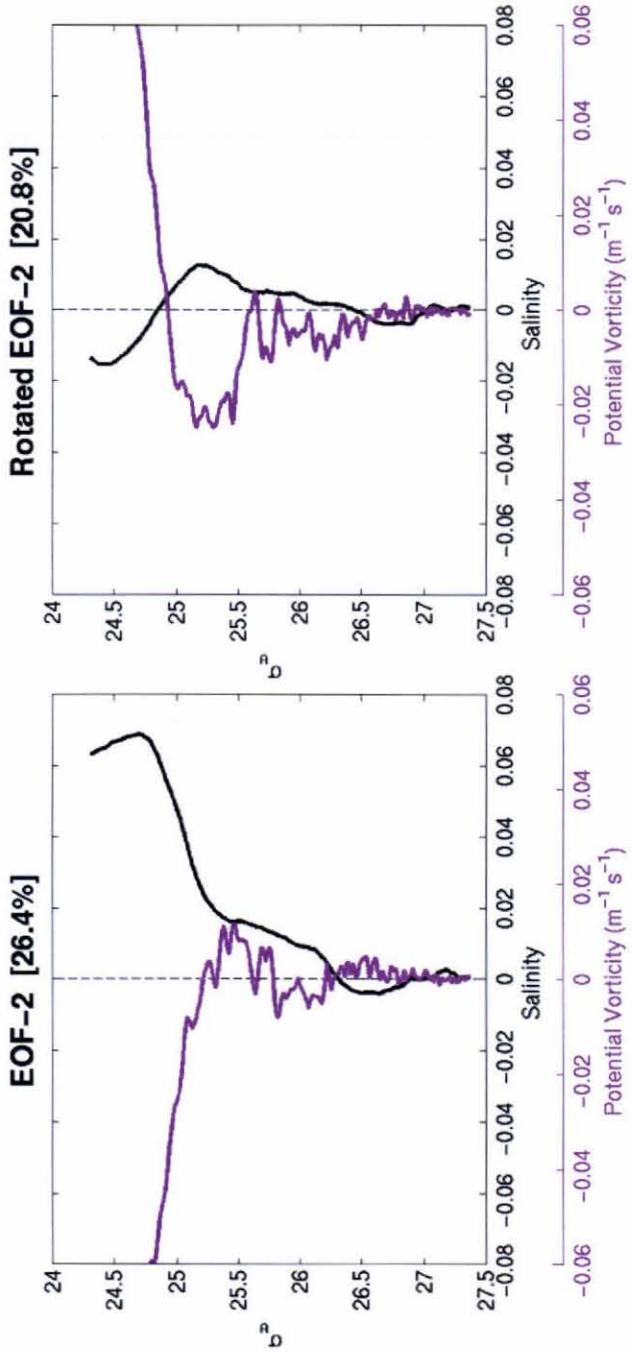

Figure 4.20: Vertical structure of water property anomalies for mode 2 of the unrotated (left) and rotated (right) EOF analysis of salinity and potential vorticity.

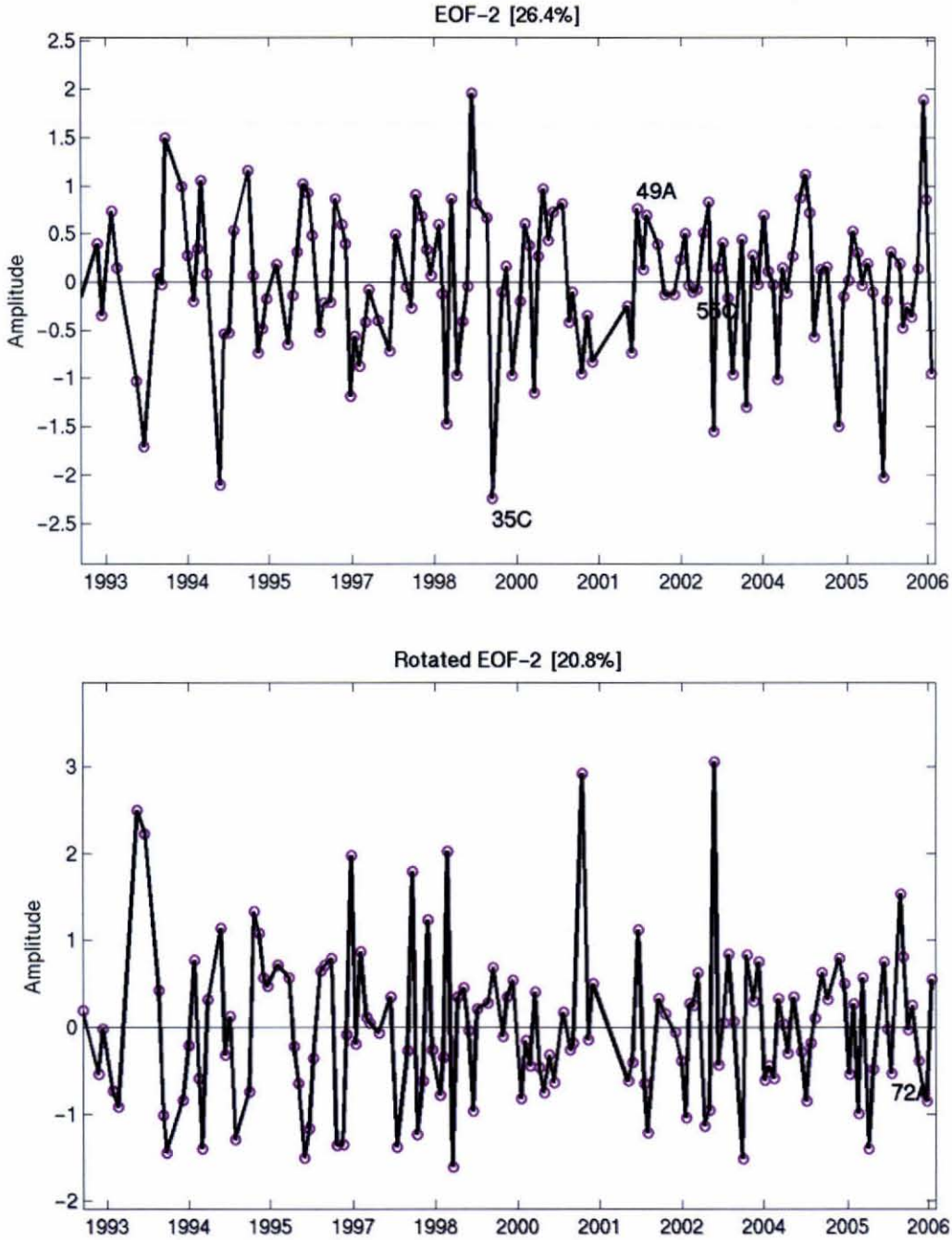

Figure 4.21: Time series of normalized amplitudes for mode 2 of the unrotated (top) and rotated (bottom) EOF analysis of salinity and potential vorticity.

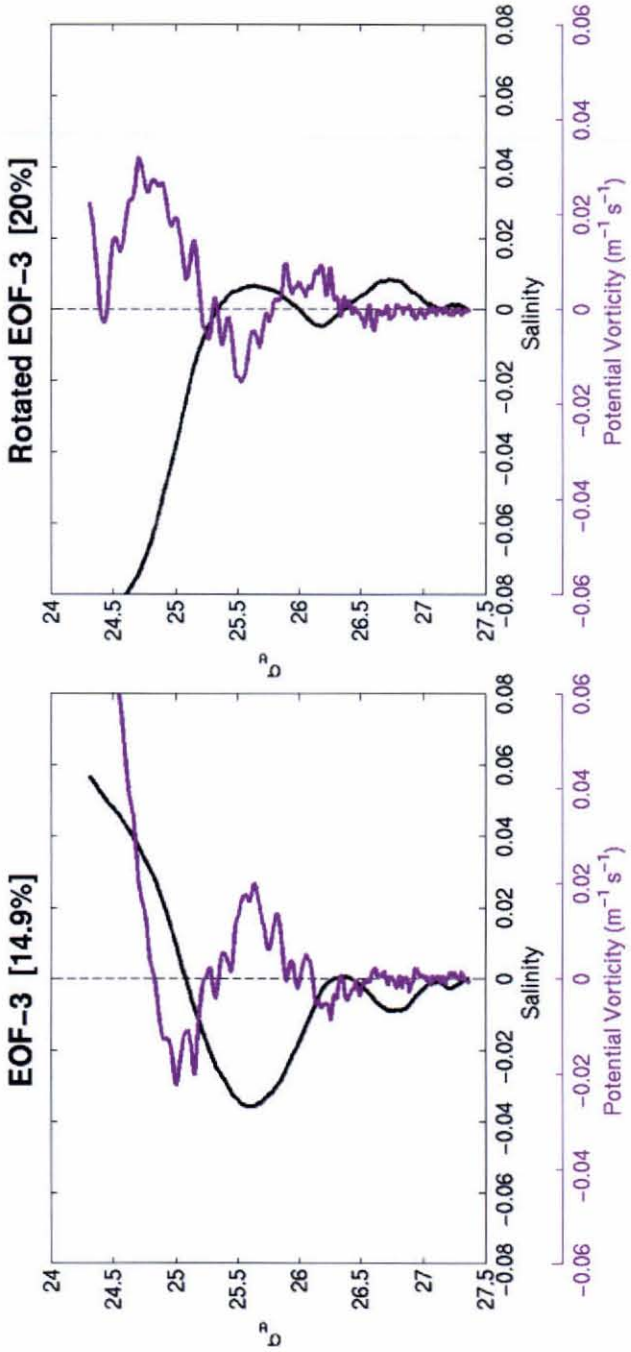

Figure 4.22: Vertical structure of water property anomalies for mode 3 of the unrotated (left) and rotated (right) EOF analysis of salinity and potential vorticity.

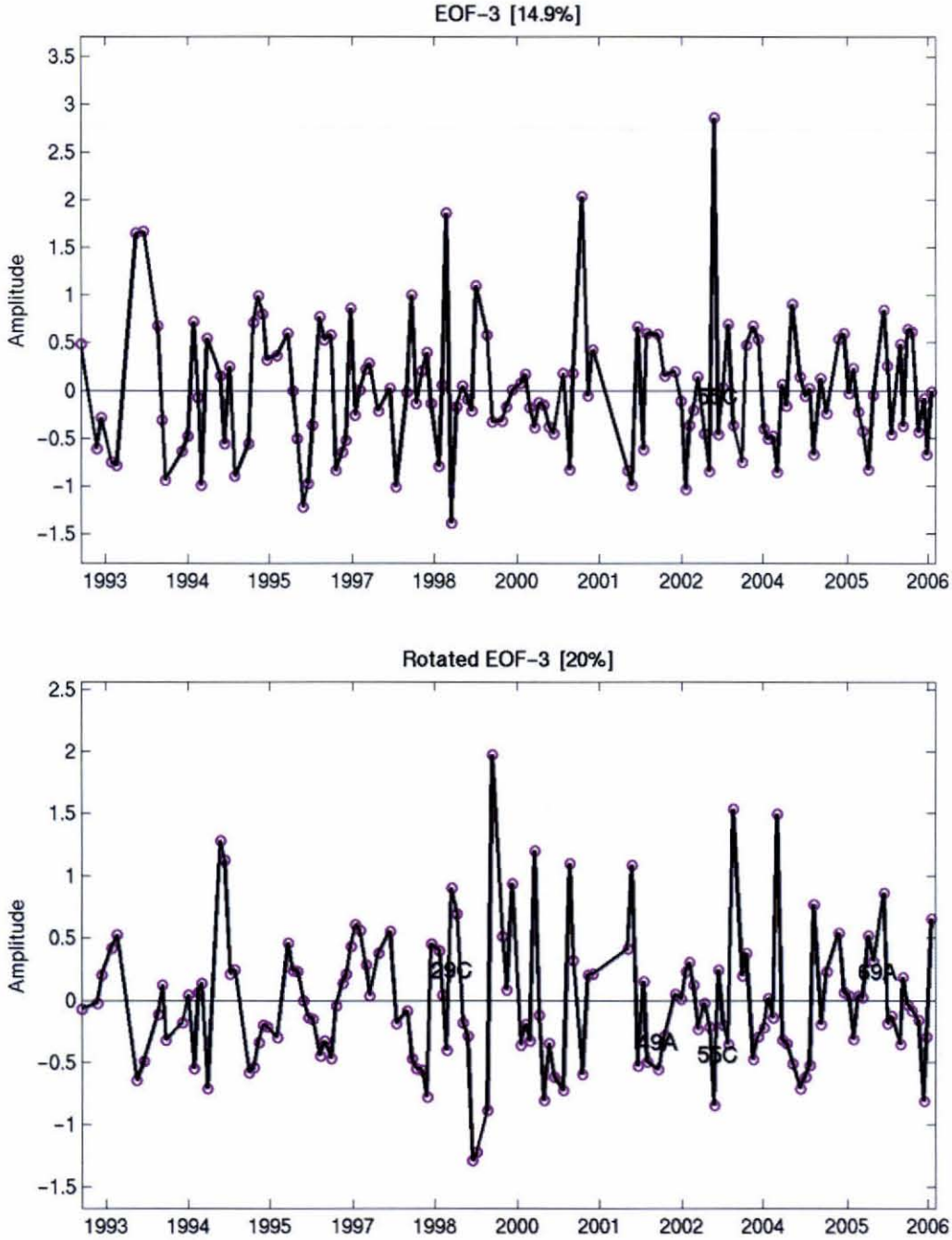

Figure 4.23: Time series of normalized amplitudes for mode 3 of the unrotated (top) and rotated (bottom) EOF analysis of salinity and potential vorticity.

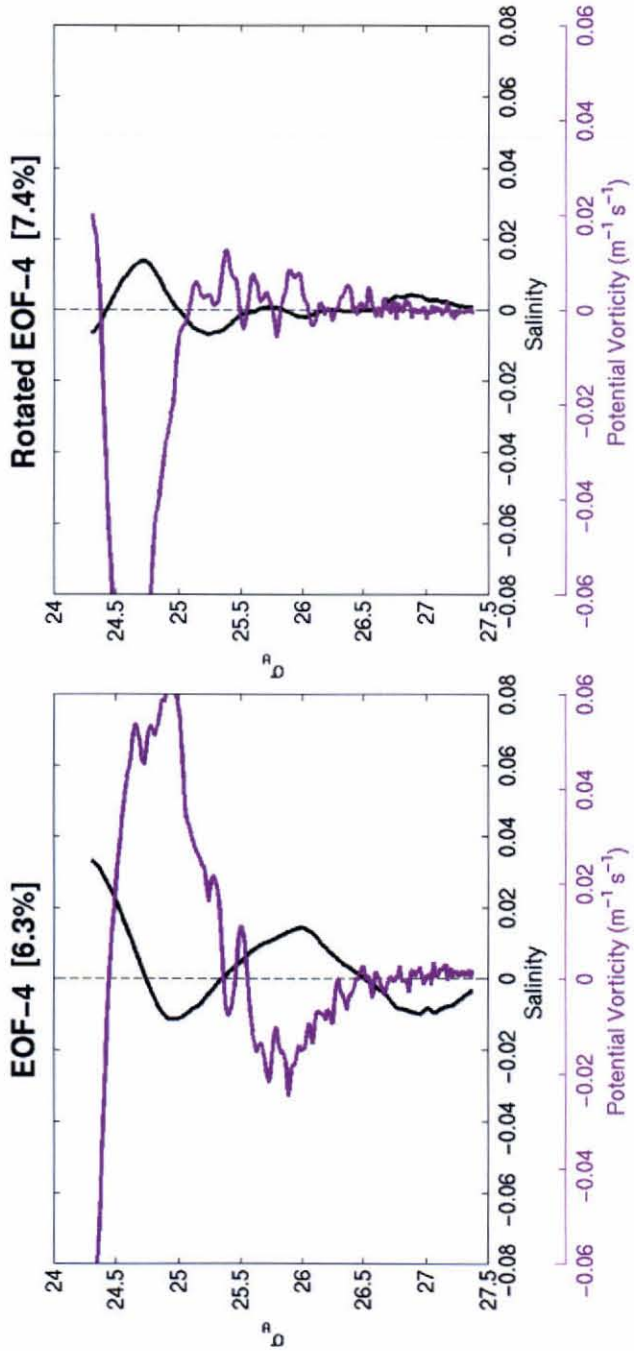

Figure 4.24: Vertical structure of water property anomalies for mode 4 of the unrotated (left) and rotated (right) EOF analysis of salinity and potential vorticity.

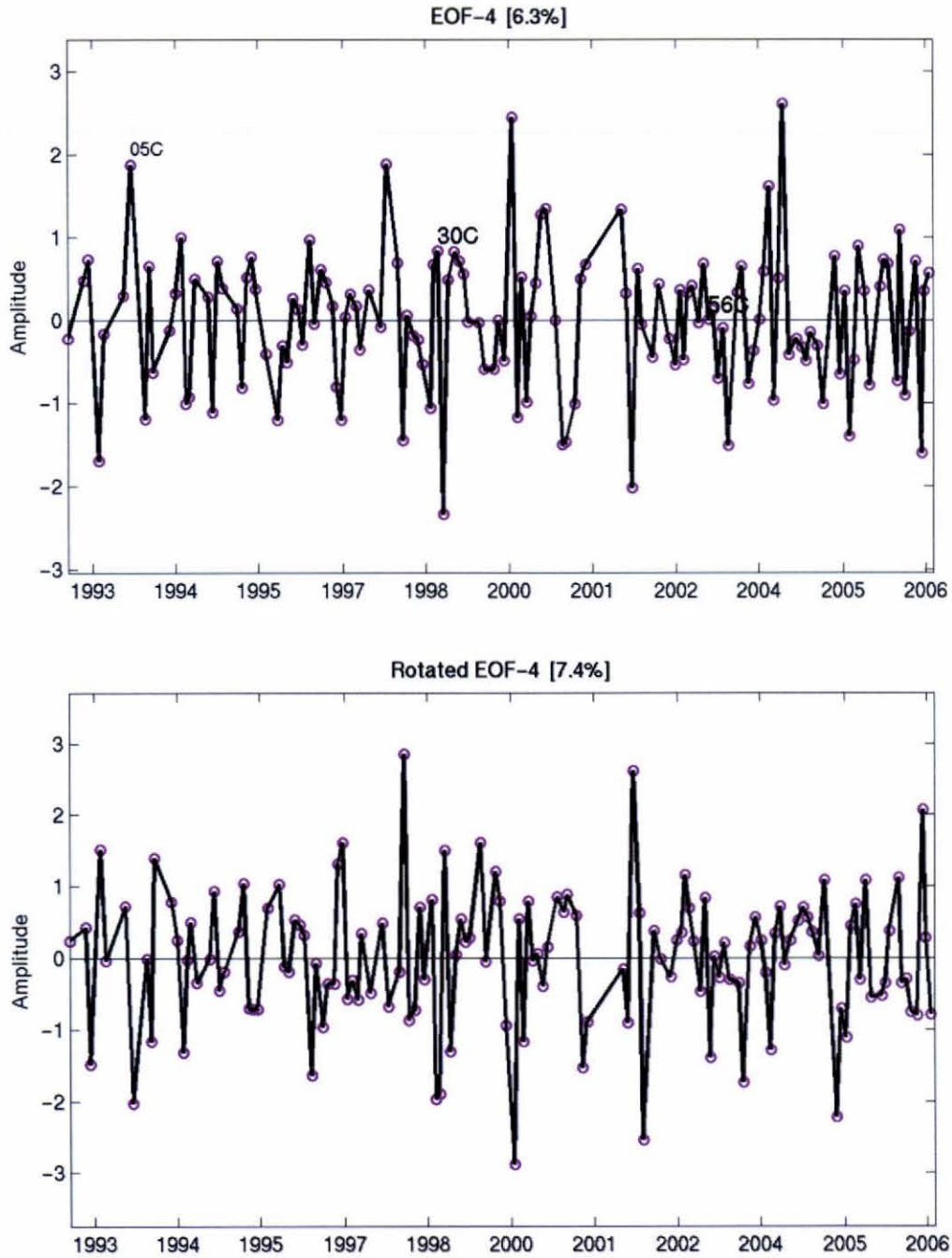

Figure 4.25: Time series of normalized amplitudes for mode 4 of the unrotated (top) and rotated (bottom) EOF analysis of salinity and potential vorticity.

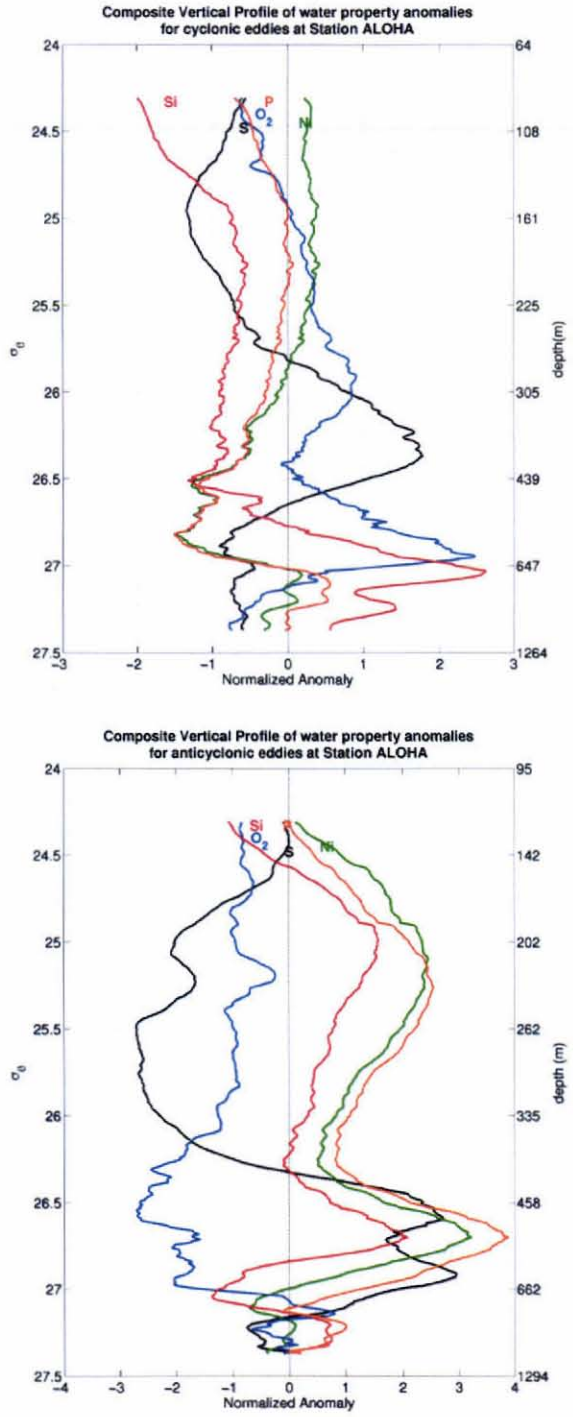

Figure 4.26: Composite vertical profiles of water mass property anomalies for cyclonic (top) and anticyclonic (bottom) ALOHA eddies.

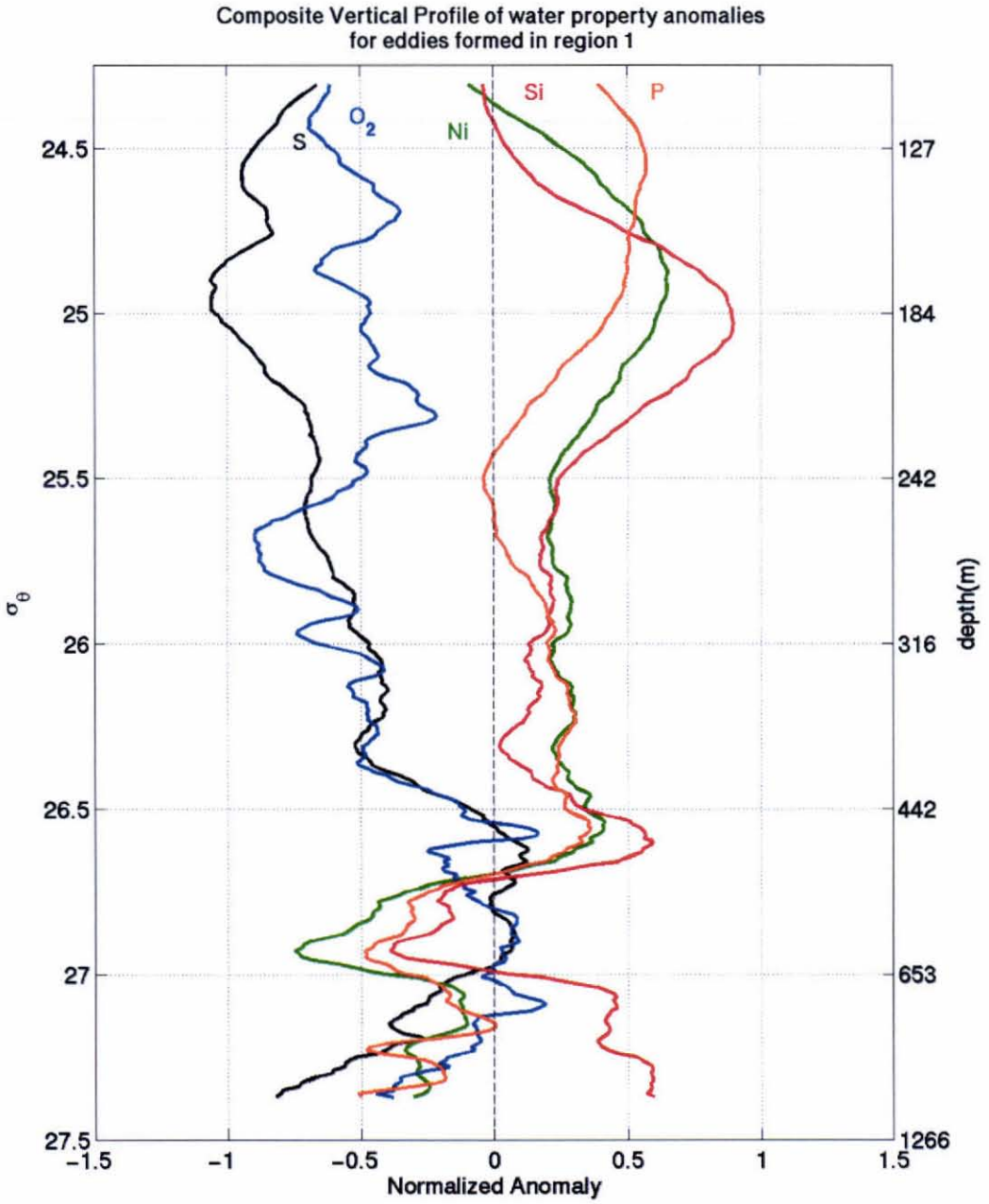

Figure 4.27: Composite vertical profile of vertical water mass property anomalies for eddies formed east of 148°W.

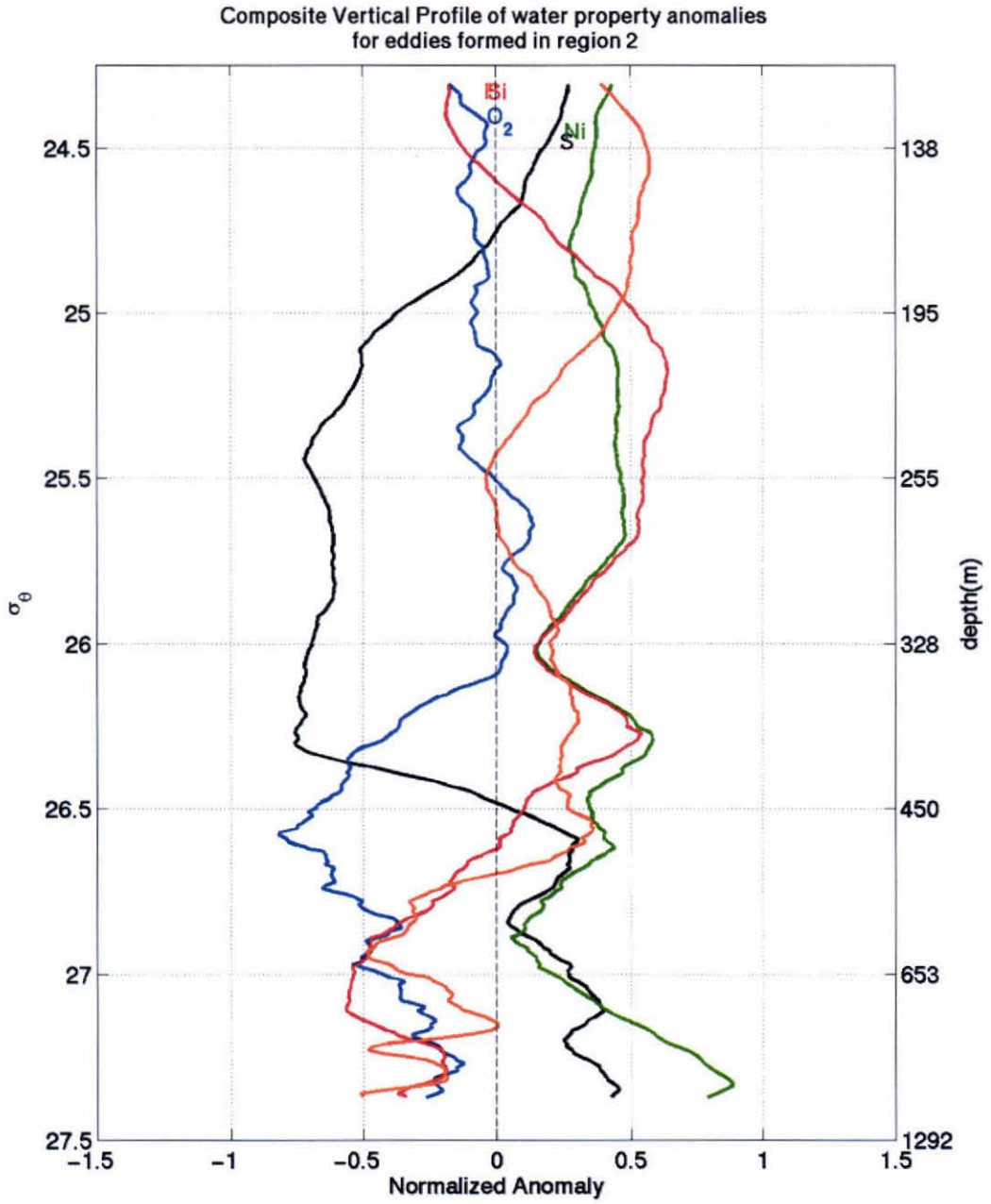

Figure 4.28: Composite vertical profile of vertical water mass property anomalies for eddies formed east of 153°W and west of 148°W.

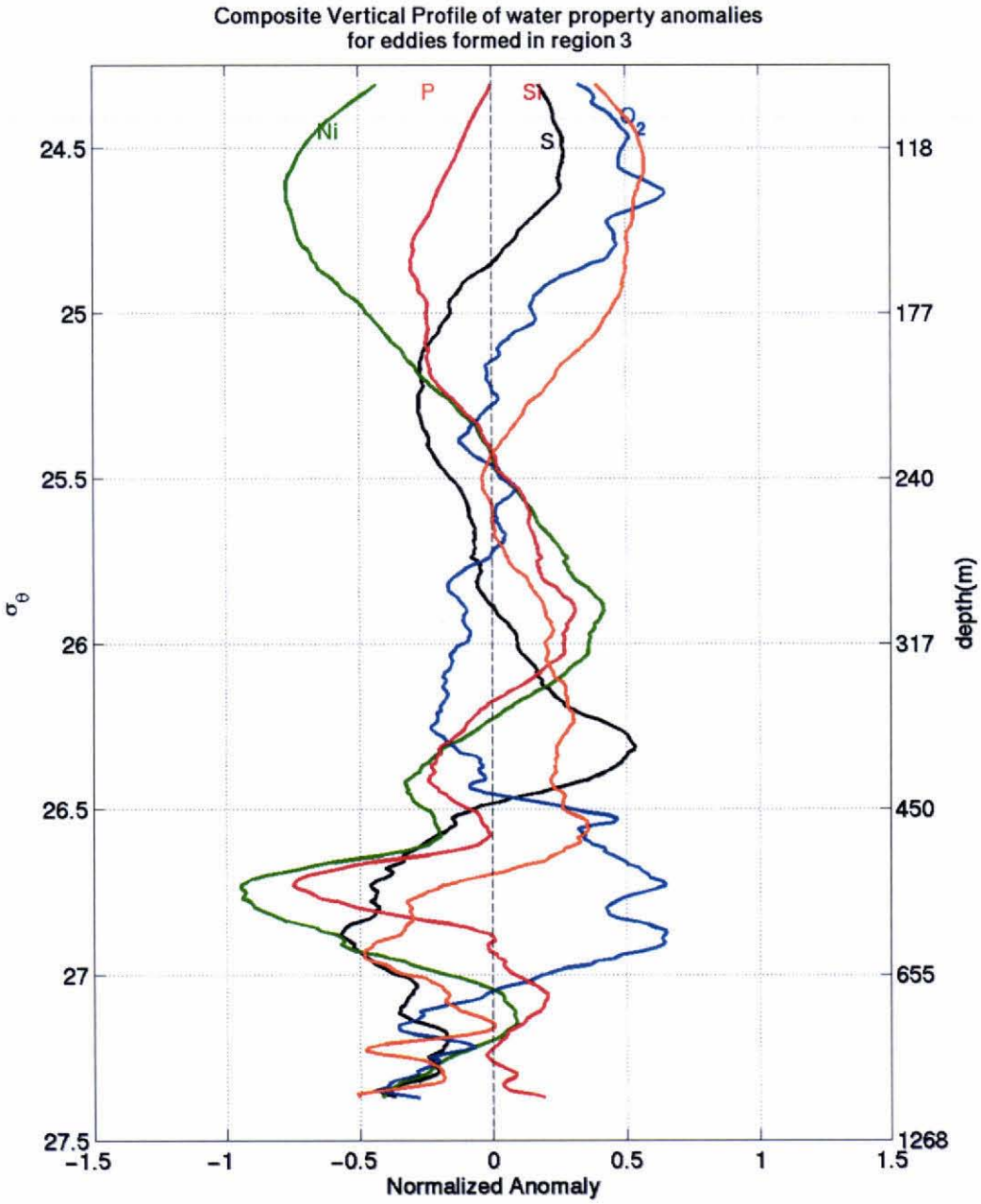

Figure 4.29: Composite vertical profile of vertical water mass property anomalies for eddies formed east of 156°W and west of 153°W.

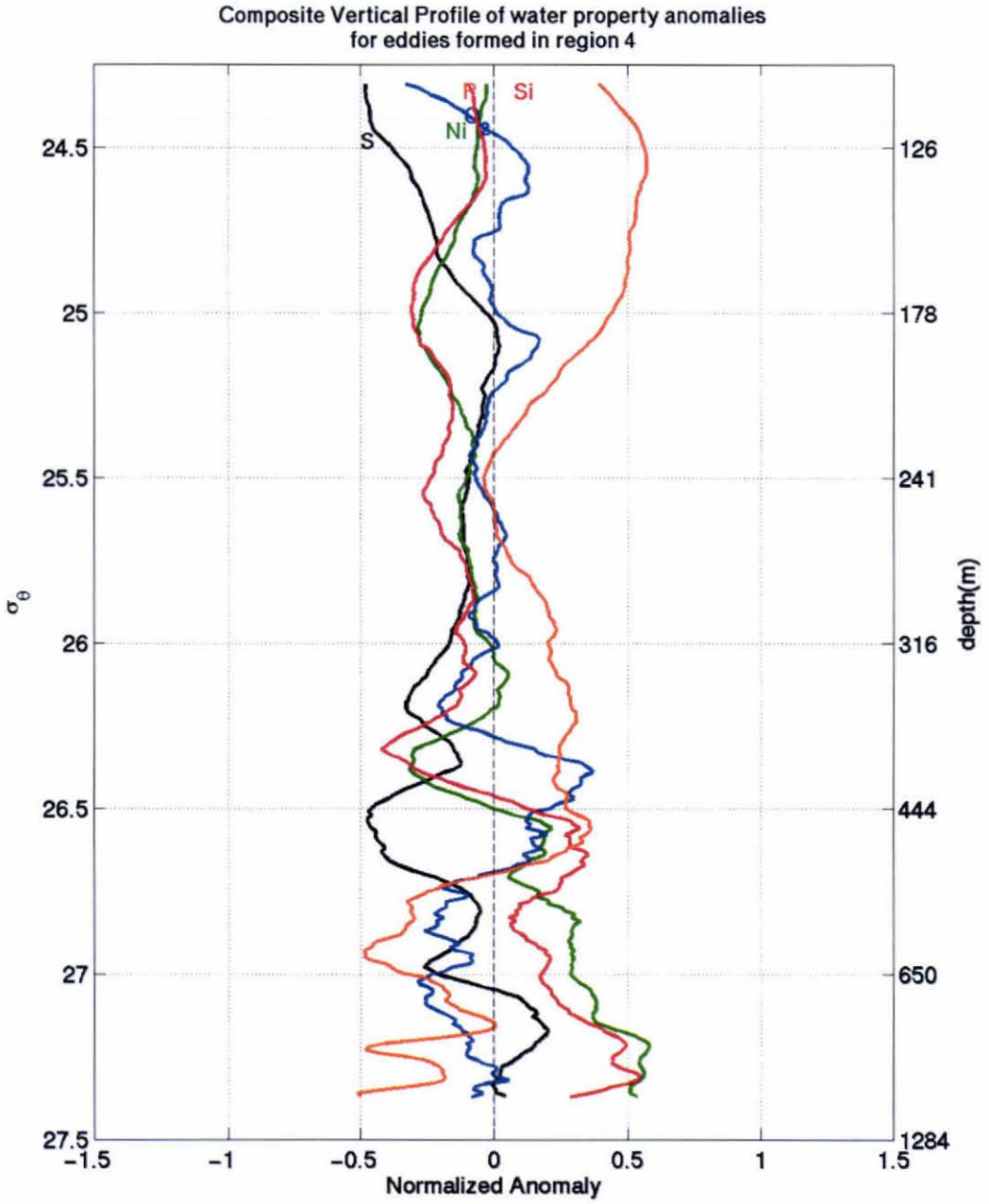

Figure 4.30: Composite vertical profile of vertical water mass property anomalies for eddies formed west of 156°W.

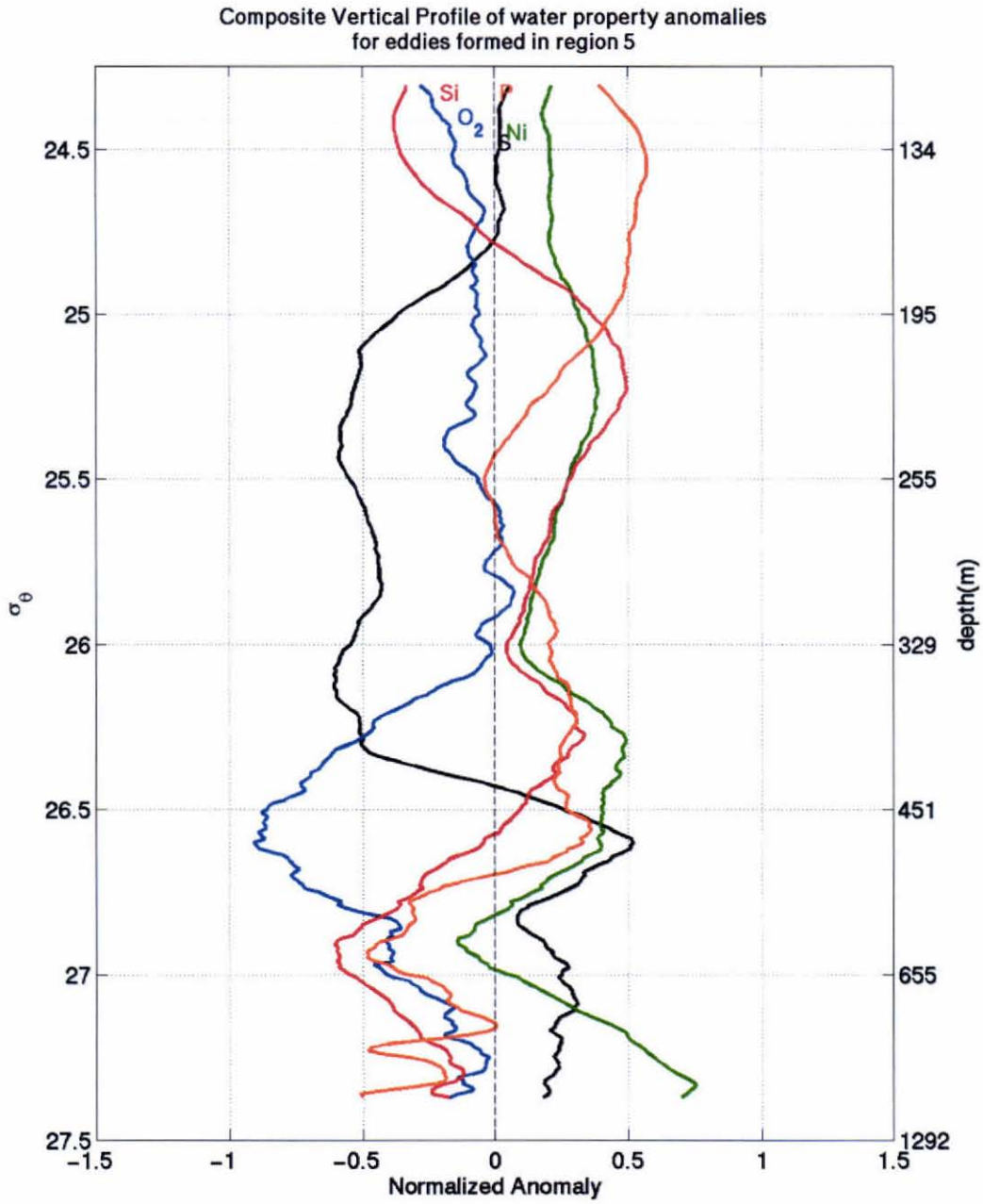

Figure 4.31: Composite vertical profile of vertical water mass property anomalies for eddies formed east of 153°W and north of 22°N.

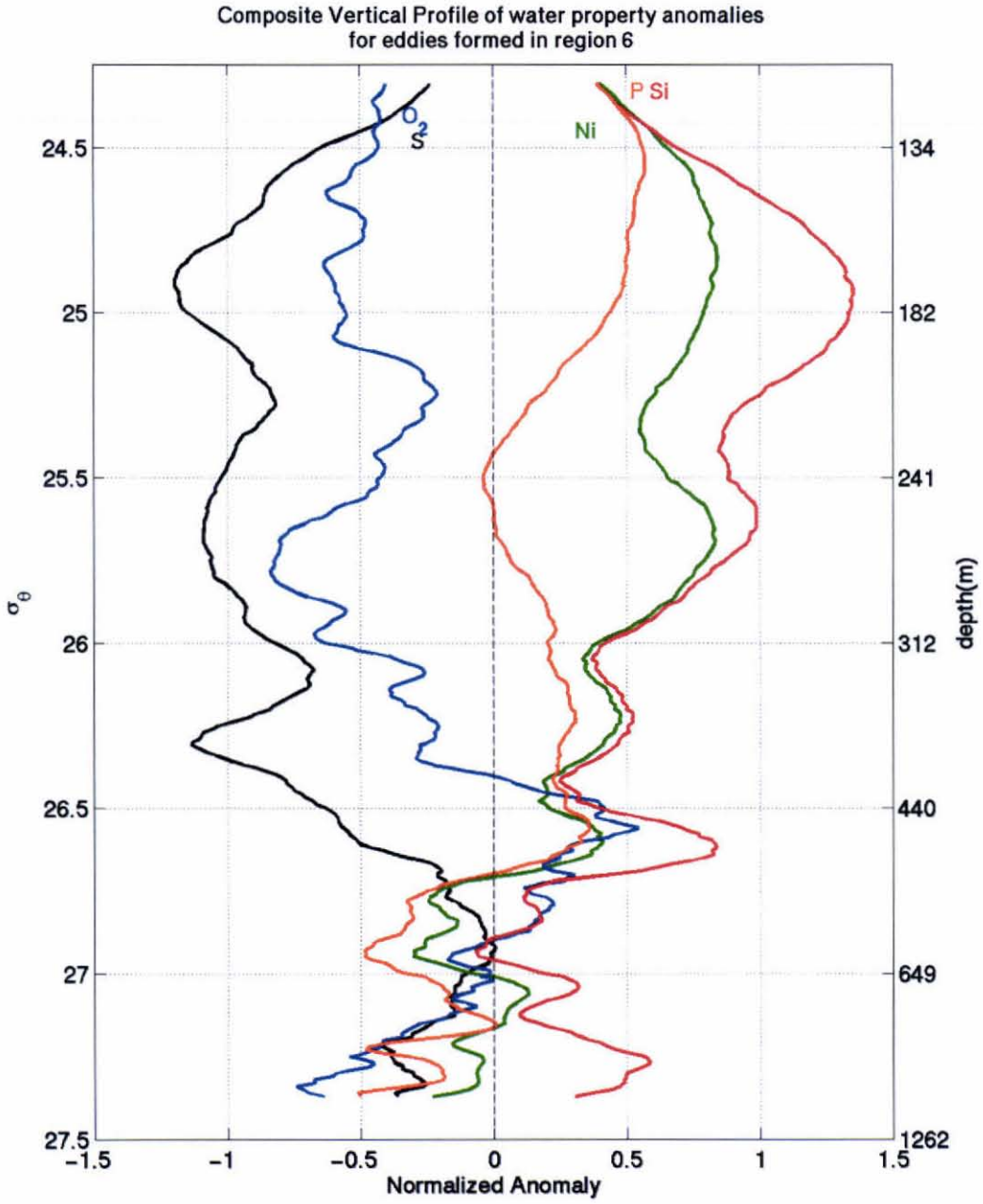

Figure 4.32: Composite vertical profile of vertical water mass property anomalies for eddies formed east of 153°W and south of 22°N.

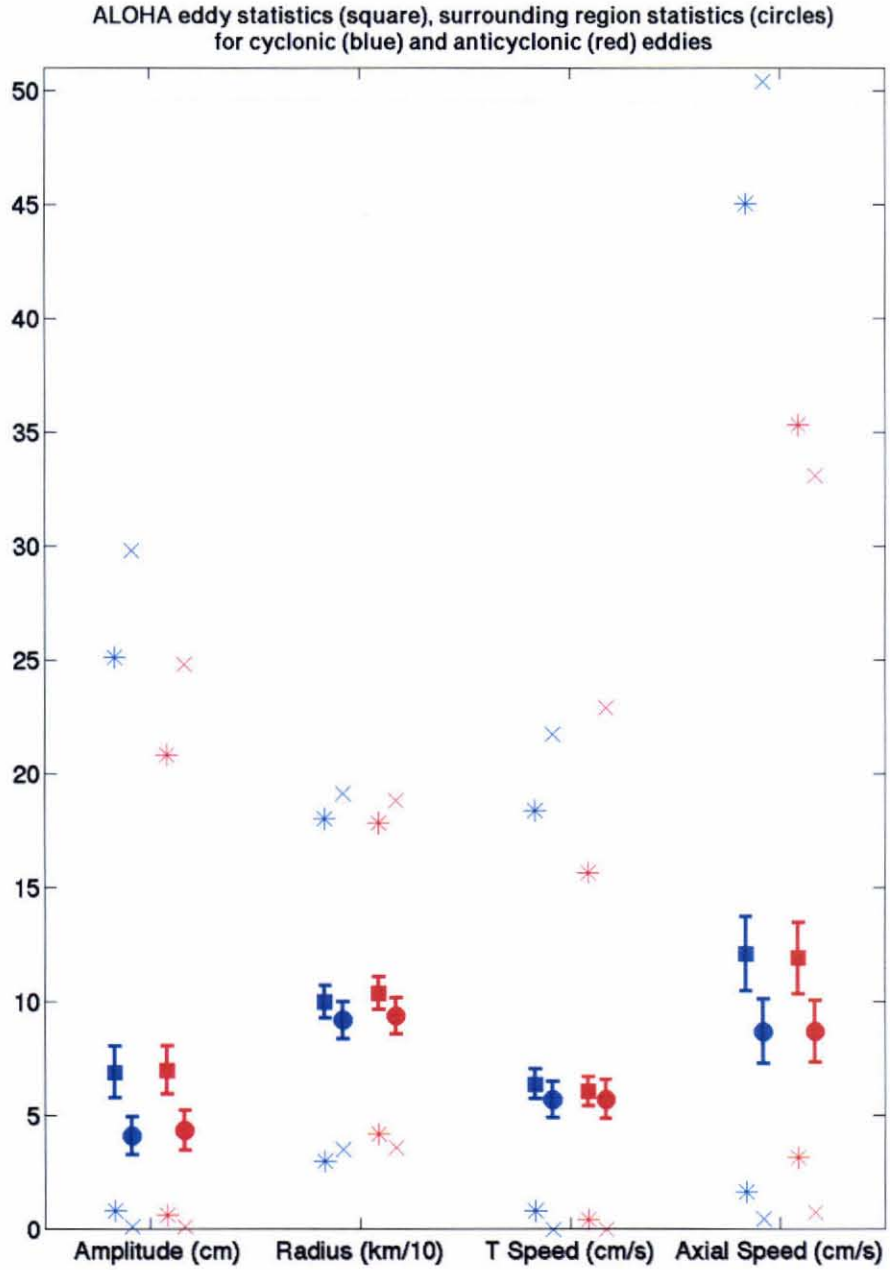

Figure 4.33: Eddy statistics for ALOHA eddies (squares and stars) and eddies in the surrounding region (circles and x's). Statistics include Amplitude (cm), Radius (km/10), translation "T" speed (cm/s) and axial speed (cm/s). The solid shapes denote the mean, error bars denote the standard error of the mean at 95% confidence. Line shapes indicate maximum and minimum values. Blue symbols denote cyclones and red symbols denote anticyclones.

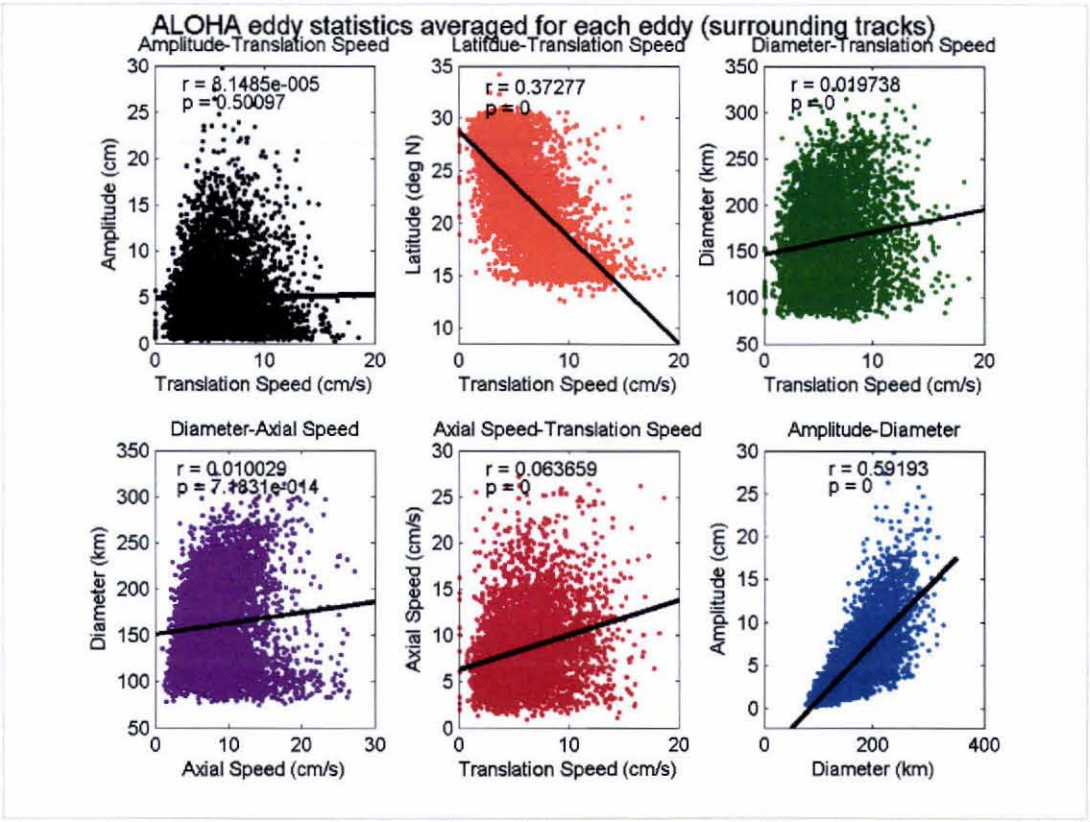

Figure 4.34: Eddy averaged scatterplots of characteristics of eddies from larger region of analysis.

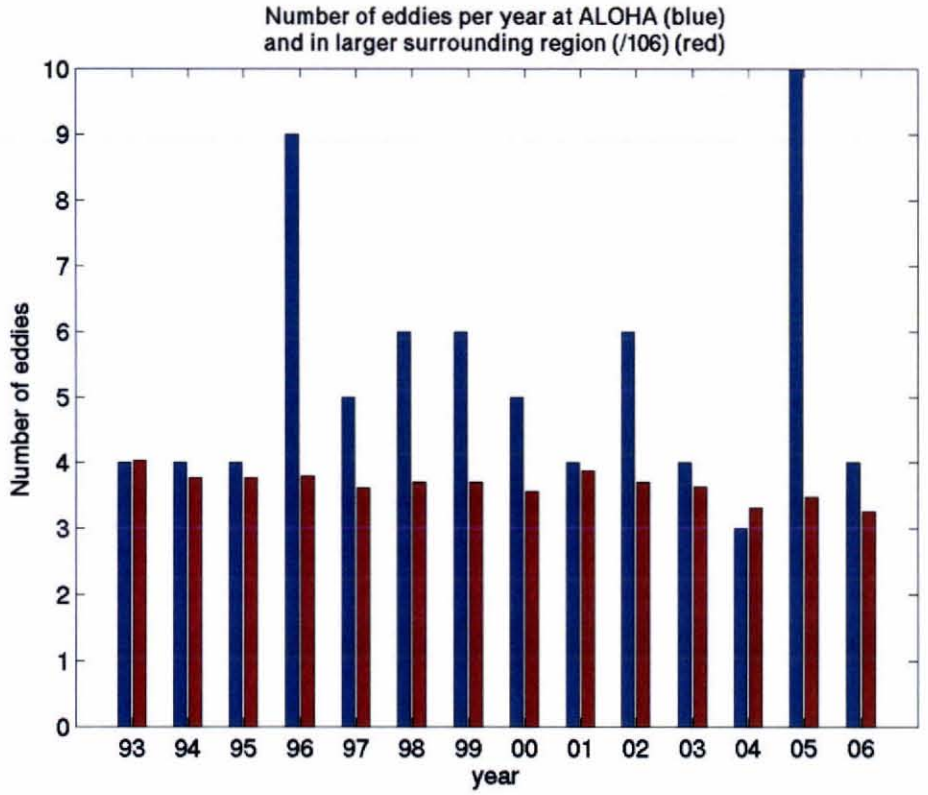

Figure 4.35: Histogram of the number of eddies per year that pass through the 2x2 region surrounding ALOHA (blue) and the number of eddies per year in the larger region of interest, divided by 106 (red).

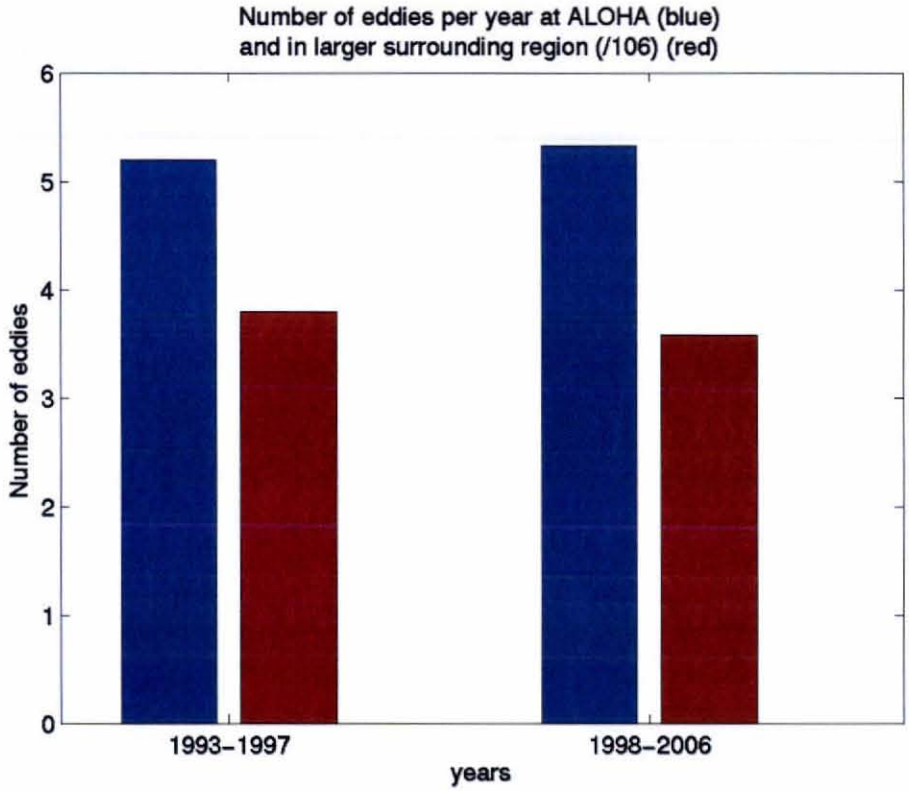

Figure 4.36: Histogram of the number of eddies for two bins spanning seven years. Eddies that passed through ALOHA are in blue and the number of eddies from the larger region (divided by 106) are shown in red.

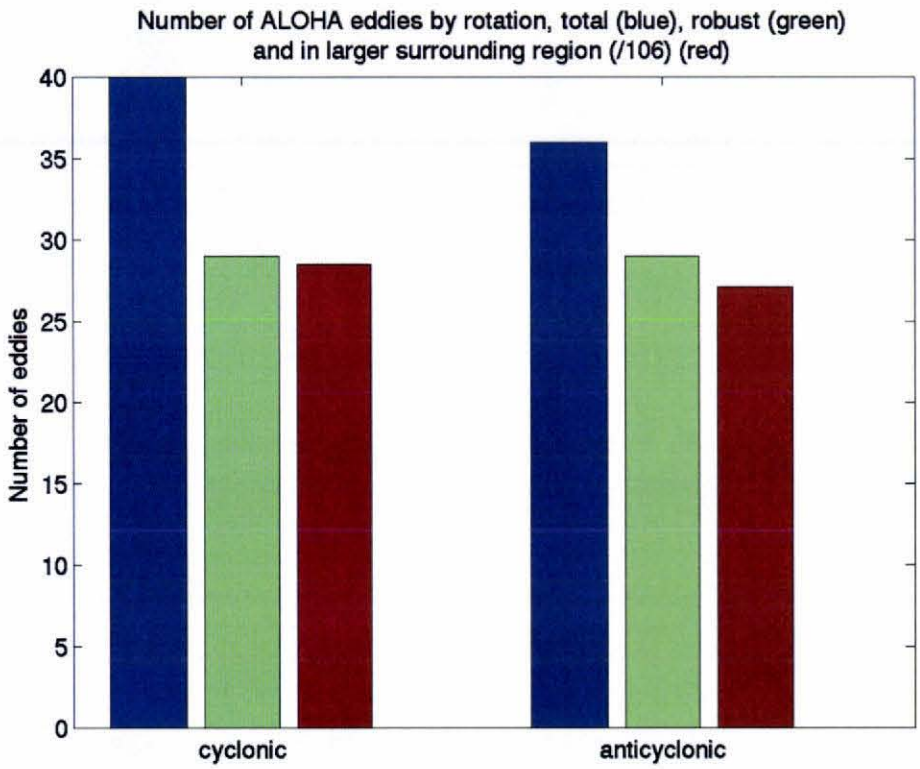

Figure 4.37: Bar graph of number of eddies based on direction of rotation. Blue is the number of eddies that passed through the 2x2 region around Station ALOHA, green is the number of eddies that remained after the visual analysis and red is the number of eddies from the larger region of interest divided by 106.

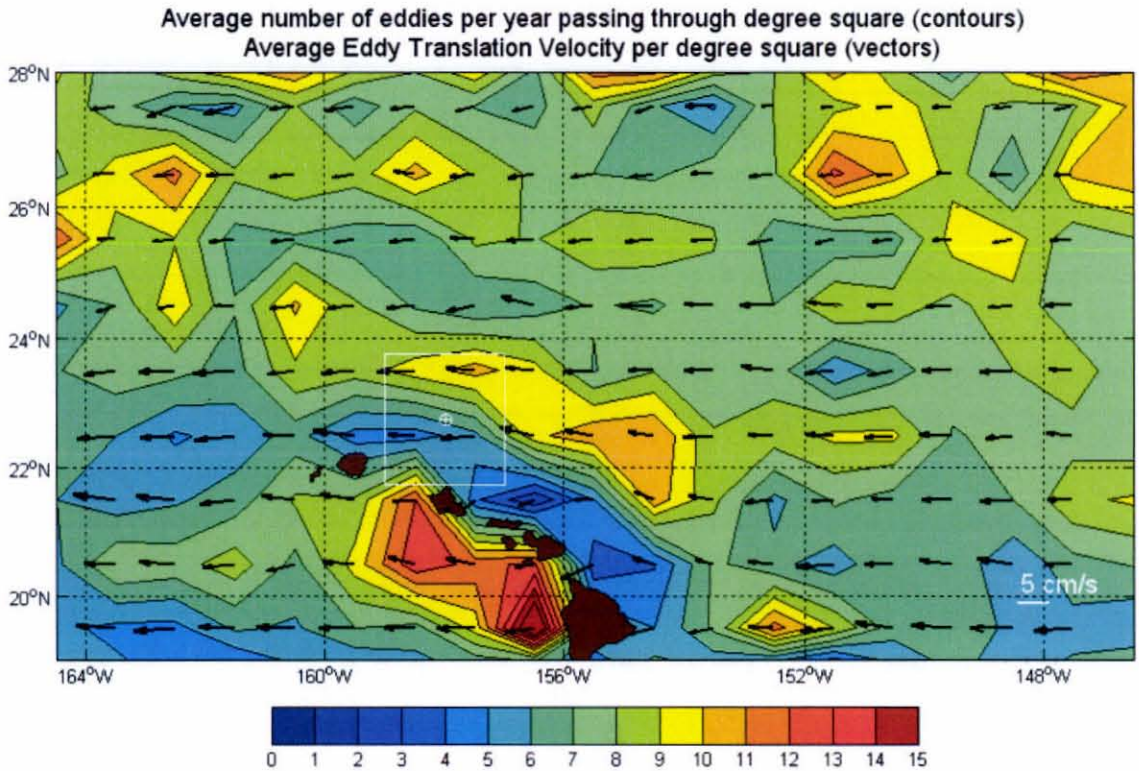

Figure 4.38: Plot showing the average number of eddies in each 1°x1° degree square per year (contours) and the average eddy translation velocity for all of the eddies that passed through each degree square over the 14 year period of study.

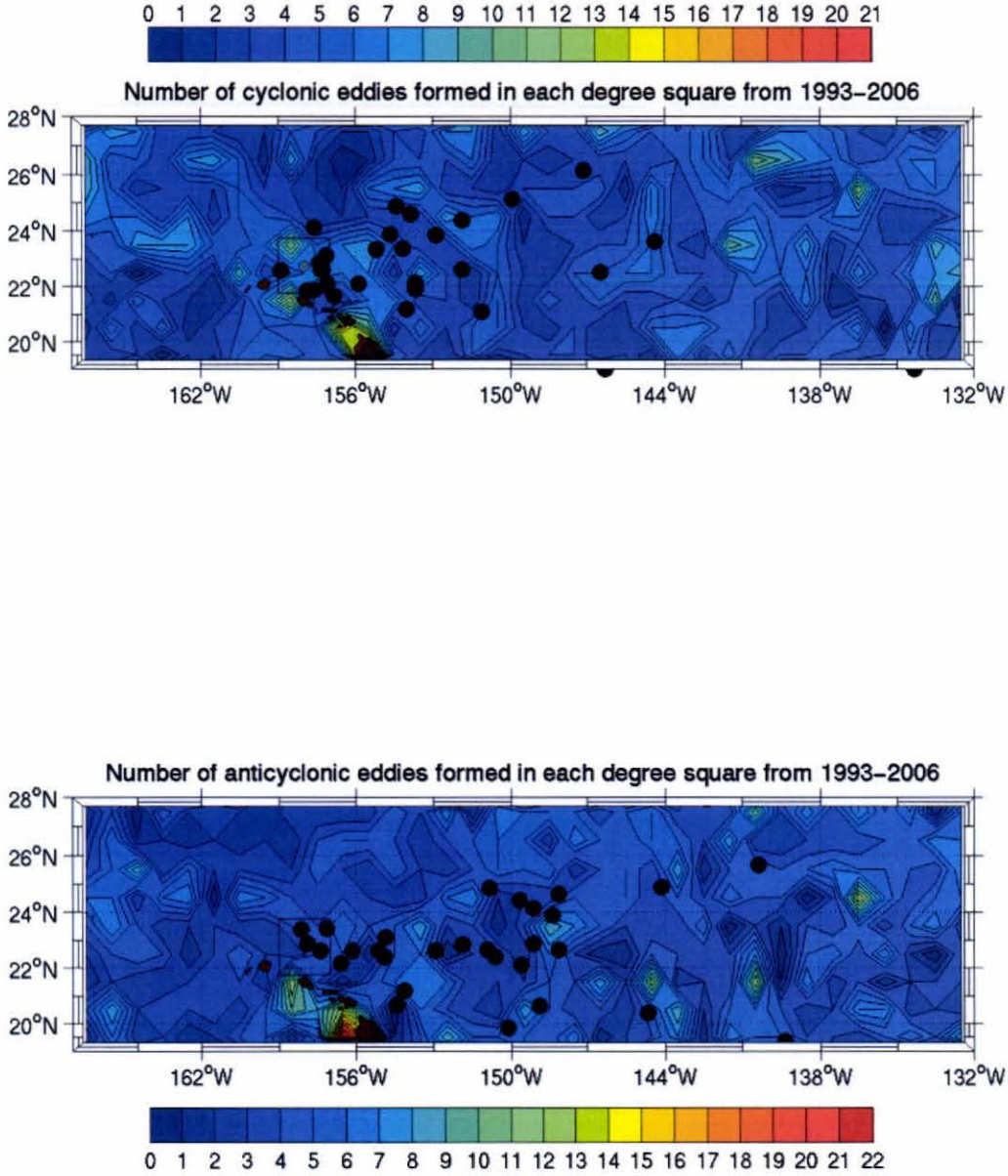

Figure 4.39: Formation locations of ALOHA eddies (large black circles) and number of eddies formed in each 1°x1° degree square in the surrounding region from January 1993 to December 2006.

5 Discussion

5.1 Algorithm Effectiveness

The eddy identification and tracking algorithm used in this study proved to be a valuable tool for identifying and tracking mesoscale eddies in the region of Station ALOHA. The algorithm slightly overestimates the number of features that are eddies, but did not miss identifying any visually robust eddy features. The algorithm used for this study was the fourth iteration (v.4) of a continuously evolving product and the visual analysis (Section 3.4.2) provided valuable feedback to the algorithm creators.

Near completion of this study, results from version 5 (v.5) of the eddy identification and tracking algorithm were released. Appendix III contains the summary of the differences between the results presented in this study and the new output. Only one "robust" eddy (33C) was not tracked in v.5. The eddy characteristics (amplitude, radius, translation speed and axial speed) in v.5 are not significantly different at 95% confidence than the results presented here for v.4.

Eddies that deform when encountering the Hawaiian Islands are not tracked as well as eddies translating in regions away from land. The inaccuracy of AVISO data near coastlines (Section 3.2.2) is an issue (Ducet et al. 2000, Strub and James 2000), which probably contributes to the algorithm having difficulty tracking the eddies near the Hawaiian Islands. It is difficult to accurately observe whether an eddy actually passes through the Kauai or Kaiwi Channels but based on the visual analysis, five eddies passed through these channels, these are discussed in more detail in Section 5.2.2.

Since the detection algorithm is based on satellite altimetry, it is prudent to reiterate the accuracy of the merged SLA maps, which are correlated in space and time. As described in Section 3.2.2, on length scales of 150 km and time scale of 20 days, SLA rms errors in the merged maps are approximately 1.8 cm. ALOHA eddies are of length scale 200 km and at least 30 days in duration, so the probability of the algorithm tracking a feature that is not really an eddy is small. 10 eddies occur during the period with only one altimeter in operation. These 10 eddies translate at approximately 6 cm/s (5 km/day) in a region of satellite ground track separation on the order of 300 km. These eddies will be in between ground tracks for longer than 30 days, but less than 10 weeks, so the further analysis in which we filtered out eddies less than 10 weeks in duration (Section 3.4.2), greatly reduces the probability that eddies are artifacts of serial correlations in space or time in the altimetric maps.

5.2 Regions of Formation and Decay

5.2.1 Formation Regions

Baroclinic instability is the predominant formation mechanism for ALOHA eddies (Section 2.3.2). Several eddies appear to have formed from the merging of two other vortices or a split in two from another eddy, but all of the ALOHA eddies formed in a region of the ocean where there is no strong current shear, wind shear, or significant changes in topography (Wyrtki 1982, Munch 1996). The eastern central North Pacific has been shown to be characterized by regions of baroclinic instability (Wyrtki et al. 1976, Roemmich and Gilson 2001). In the absence of strong shear, the amplitude of these eddies should be less than eddies associated with strong shear, such as Gulf Stream

rings, or eddies that form within the Kuroshio current system in the Western Pacific. These western boundary current eddies have typical amplitudes of 20-30 cm, almost double the average amplitude of ALOHA eddies.

Assuming that the background variability of a region does not change, all eddies that form in a particular region should encapsulate the same source water during their spin up phase. The characteristics of the water properties encapsulated within the eddy bolus is highly dependent on several factors (Section 4.6). The EOF analyses aimed to segregate the water mass variability and attempt to group eddies with similar water property anomalies to see if any patterns emerged. Idealized, isolated vortices should group so that eddies from the same region of formation and of the same sign appear as peaks of similar amplitudein the same mode. The EOF results of this study did not reveal these distinct groups. Each EOF mode only identified 2-3 significant peaks, per mode and the first four modes combined explain less than 50% of water mass variability at ALOHA.

All eddies formed in a particular region should have similar water property anomalies and by taking a step back and using the more rudimentary analysis of compositing to group ALOHA eddy water mass variability, some general patterns do emerge. Eddies formed in regions 1 and 2 (also 5 & 6) exhibit larger water property anomalies than eddies formed in regions 3 and 4, (see Figure 4.5 for the region boundaries). Succinctly, eddies that formed east of 148°W have larger water property anomalies than eddies that formed to the west of the same longitude. Regions 5 and 6 divide region 1 into north of 22°N and south of 22°N. Eddies with the largest water property anomalies formed east of 148W and south of 22°N.

5.2.2 Regions of Decay

At the other end of an eddy's lifecycle is where the eddy decays or breaks up. ALOHA eddies tend to decay in three areas. The majority of ALOHA eddies decay around 160°W, just west of Kauai. A few eddies break up along the north side of the islands, probably due to being too close to the island topography and deforming to the point where they can no longer retain their circulation. A couple of eddies remain as eddies past the islands and decay due to interactions with other eddies between 165°W and 170°W. Redistribution of eddy energy into other eddies and into the mean flow are the predominant processes in eddy decay.

The Hawaiian Islands serve as a partial sink for ALOHA eddies. Ten eddies approached too close to the islands as they translated northwestward along the north side of the Hawaiian Ridge, resulting in deformation that eventually reached a level of deformity that they couldn't recover from, resulting in these eddies breaking apart. Five eddies approached the islands from the east or northeast and appeared to track through the Kauai or Kaiwi Channels. Four additional eddies that came from the northeast broke apart as they collided with the Hawaiian Islands. Presumably, the angle at which they impacted the Hawaiian Ridge was too steep for the eddy to change trajectory direction from southwestward to northwestward and recover equilibrium quickly enough to remain coherent. One eddy came from the east-northeast and managed to bounce off of Maui (50C) and continue its westward translation past the islands. Another eddy (52C) is a remnant of an eddy that bounced from Maui from an eddy that collided with the islands. Additionally, three eddies that passed west through Station ALOHA then collided with the island of Kauai where they broke apart.

5.3 ALOHA Eddy Variability

A major aim of this study is to characterize eddies passing through Station ALOHA and in the greater region of the central North Pacific Subtropical Gyre. The eddies of this region are not as intense as their western boundary current counterparts. The number of eddies in this region do not vary significantly over time. There is no apparent seasonality to the number of eddies that are found in the region. The eddies also exhibit no significant bias for rotation direction.

The water mass rotated EOF results indicate only eddies that maintained a strong bolus anomaly appear as significant peaks in the amplitude time series. These results provide insight into the vertical structure of a few distinct cases as described in Appendix II, but these few results are not sufficient to generally characterize the water property anomalies of ALOHA eddies. The eddies that exhibited a strong bolus anomaly share some behavioral characteristics. These are eddies that are formed far enough away from Station ALOHA so that the water properties of the eddy bolus are quite different from the typical water property characteristics at Station ALOHA. These eddies also exhibited limited interaction with other eddies and were not deformed as a result of interaction with island topography. Since there are only 6 eddies that fit into this category, it's difficult to determine whether or not rotation direction is a factor in how well the eddy maintains its bolus (explained in greater detail is Section 5.6).

The majority of eddies did exhibit some type of interaction, with either another eddy, the islands, or possibly the mean flow, and they have less distinct water property anomalies. This indicates that eddy mass transport is generally more complex than described by an isolated bolus. The large amount of variability in ALOHA eddy water

property anomalies indicates that most eddies entrain and mix water properties throughout their lifetime. The variability in non-conservative water properties (that are affected by biological processes) introduces another level of complexity in characterizing eddies based on water property anomalies.

Another aspect of eddy dynamics to consider is the possible existence of an eddy wake and its effect on the water mass property characteristics at Station ALOHA. Since an eddy displaces surrounding waters as it translates, the water mass characteristics in the lee of the eddy will be subject to increased mixing. This temporary increased mixing can affect the water mass properties at Station ALOHA. The water mass property variability induced by an eddy wake can be especially important if another eddy passes through ALOHA immediately after the wake of an eddy. Removing the mean of the three previous HOT cruises may not remove variability due to an eddy wake.

5.4 ALOHA Eddy Behavior Compared to Theoretical Vortex Behavior

An isolated geostrophic eddy on the beta plane is a model to which ALOHA eddies can be compared. A theoretical first baroclinic mode eddy will translate west at the first baroclinic mode linear Rossby wave speed (Section 2.4.2), which is 5.5 cm/s at ALOHA. ALOHA eddies translate at an average of 6 ± 2 cm/s, which is comparable to the Rossby wave speed. ALOHA eddies travel generally westward over most of their lifetime, but they do experience occasional periods of meridional translation. The effect of the presence of the Hawaiian Islands on eddy trajectory is discussed in the next section.

ALOHA eddy translation direction is also greatly affected by the presence of other eddies. An idealized vortex which conserves potential vorticity is isolated from the

surrounding environment and would remain in "steady state" after it had achieved equilibrium. For an eddy to decay, it would require energy to be dissipated, which requires turbulent mixing. However, if turbulent mixing is dissipating energy, then potential vorticity is not conserved (Mahadevan 2008). All of the abrupt changes in eddy trajectory direction distant from the islands are visually attributed to the nearby presence of another eddy. The presence of another eddy can also cause an amplification or a decrease in an eddy's amplitude, which then contributes to a change in radius and, by definition, axial speed (Section 3.3.2).

Idealized vortices that are conserving potential vorticity are also not exchanging water mass properties with the surrounding environment, thus the properties of the water mass that they transport solely from their region of formation. This study has shown that isolated bolus water property anomalies are not generally the case with ALOHA eddies. ALOHA eddies are not conserving potential vorticity, and are not linear. Non-linear eddies have important second order dynamics that allow for water mass property circulation between the eddy's periphery and the surrounding environment (Mahadevan 2008), which will degrade the pureness of source water eddy bolus transport.

5.5 Eddy Convergence at ALOHA

The convergence of eddies that come from the east, north and south to pass through the limited region of study is the combined result of eddy interactions with other eddies, topography and the mean flow. Which type of interaction is responsible for this convergence is a difficult question to answer. One theory is the interaction of the eddies with the mean flow. There is strong evidence (Firing 1996, Qiu et al. 1997) for the

presence of the North Hawaiian Ridge Current (NHRC) in this region due to the presence of the Hawaiian Islands in the gyre circulation. Qiu et al. (1997) used drifter data and a 2-1/2 layer model to estimate the current speed of the NHRC at 0.1-0.15 m/s, with a current width on the order of 100 km. These results are consistent with those of Firing (1996), who analyzed HOT ADCP data. These results indicate that the northern limit of the NHRC region may affect Station ALOHA. Price et al. (1994) contested the existence of the NHRC, instead describing a field of eddies instead of a ridge current in the region north of Oahu from XBT and AVHRR data. The presence of the NHRC would explain the tendency for the eddies that come from latitudes south of ALOHA to change from a westward trajectory to one that is more northwesterly as the eddies approach the island chain.

Another explanation for the deviation from pure westward translation is eddy interaction with topography. The steep topography of the Hawaiian Islands can be considered similar to that of a vertical wall. Using the method of images (Kundu and Cohen 2004), when an eddy encounters such a barrier, it will "self advect" along the barrier in a direction along the wall. This "self advection" direction depends on the direction of rotation of the eddy. An anticyclone will move north along a vertical wall and a cyclone will move south. We do not see any eddies that move south along the ridge, all of the ALOHA eddies move northwest along the ridge, regardless of direction of rotation.

The interaction of eddies with island topography is much more complex than the vertical wall example. The islands do have slopes, as seen in the bathymetric map north of Oahu (Figure 3.1). Also, the Hawaiian Ridge is not a solid barrier, but contains gaps

between the islands. The behavior of eddies in the vicinity of these channels is not a focus of this study, but the visual analysis descriptions do discuss the five eddies that appear to pass through a channel. This only occurs with severe degradation of the eddy structure so none of the eddies are tracked through channel. Eddies with tracks that pass through a channel or over an island are occurrences where the eddy was tracked before it transited through the channel, then was picked up again within three time steps (Section 3.3.3) if it reformed in the lee of the islands.

Eddy translation direction is also affected by the presence of other eddies. These eddy-eddy interactions are responsible for abrupt changes in eddy direction (Section 2.6.1). Eddy-topography interactions are primarily responsible for northward meridional translation of eddies and eddy-eddy interactions are primarily responsible for the southward change in translation direction for the eddies that come from north of the latitude of ALOHA. Several eddies that formed due east of ALOHA (Figure 4.39) did not pass through the box region, the pure westward translation of these features may have been disrupted by another eddy.

5.6 Vertical Structure of ALOHA Eddies

Sampling constraints of this study prevent observing a complete vertical cross section across the breadth of the ALOHA eddies, instead, most eddies are observed through a single, discrete vertical profile at one location within the eddy. Eight eddies were covered by two cruises, but in all of these cases, the first cruise captured the leading edge of the eddy and the second cruise captured the trailing edge. In these cases, the

HOT cruises used in this study are the cruises corresponding to the trailing edge, because these cruises exhibit larger water property anomalies.

There are several explanations for why the trailing edge of the eddy would have larger water property anomalies. One hypothesis is that there is a lag between the sea level perturbation due to the eddy as observed by satellite altimetry and its transport of water mass property anomalies (Roemmich and Gilson 2001) as observed by the HOT cruise. The vertical structure of the eddy would be such that the eddy is tilted so that its leading edge vertical profile only captures the top of the eddy and the trailing edge vertical profile captures more of the thermocline portion of the eddy and its associated water mass property anomalies. A second hypothesis is that the trailing edge vertical profile is really capturing the eddy wake as described in Section 5.3. It is not possible to distinguish which of these processes is responsible for the larger water property anomalies in the trailing edge of the eight eddies that were double sampled. Continuous vertical observations over the whole passage of the eddy would be necessary in order to determine which process has the dominant effect.

If eddies are encapsulating source water as their bolus in their region of formation, then direction of rotation shouldn't matter, but the composite profiles for cyclones and anticyclones indicate that this is not the case. Anticyclones have noticeably greater water mass property anomalies than cyclones. If we recall the non-linear forces in an eddy (Section 2.2.4) one force that becomes increasingly important at smaller radii is the apparent centrifugal force outward from the center of a rotating eddy. In a cyclone, the pressure gradient force is inward and both the Coriolis and centrifugal forces are outward. It is difficult for the pressure gradient force to balance both forces, so cyclones are more

unstable. Anticyclones, however, have an outward pressure gradient force and an inward Coriolis force. This Coriolis force can balance the pressure gradient force and the centrifugal force, so anticyclones will tend to remain intact.

The strong correlation ($r = 0.7$) between isopycnal displacements at ALOHA (Figure 4.9) and eddy height at ALOHA is an indicator that the features selected by the eddy identification algorithm are dominated by baroclinic features, but cannot definitively distinguish between eddies and Rossby waves. Eddies that have a sea level signature and a vertical displacement of isopycnals that changes sign around 1000 m are likely first mode baroclinic eddies (Figure 4.8). Eddies that show no vertical displacement in isopycnals are likely barotropic eddies and features that show multiple changes in sign in the displacement of isopycnals are likely higher mode baroclinic eddies.

Based on the average isopycnal displacement over the top ~1000 m, the majority of eddies in this study are probably first baroclinic mode eddies. There are a couple of eddies whose sea level perturbation at ALOHA is the opposite sign as the isopycnal displacement, but in these cases, the eddy height at ALOHA is small (less than 2 cm) and may be due to noise. Most of the eddies have a sea level perturbation to isopycnal displacement ratio of approximately 1/100, but three eddies (68A, 71C, 73C) have much larger sea level anomalies at ALOHA than expected by the average isopycnal displacement.

The ADCP data shows that most of the eddies have maximum velocities close to the surface and decreased velocity at depths greater than 300 m. Several of the larger eddies show no velocity shear over the top 300 m, indicative of a barotropic eddy, but without

velocity measurements deeper into the water column it is impossible to tell by the available current measurements alone whether an eddy is barotropic or baroclinic.

6 Conclusions

ALOHA eddies often do not behave like theoretical isolated vortices. Isolated vortices do not interact with one another or with the mean flow and thus cannot gain energy, whereas ALOHA eddies do change, as evidenced by their fluctuating amplitude and varying translation vectors. Eddy-eddy interactions are responsible for an eddy's deviation from westward propagation east of the Hawaiian Islands.

ALOHA cyclonic eddy characteristics are not significantly different from ALOHA anticyclonic eddy characteristics. Both types of eddies exhibit statistically similar amplitudes, radii, and translation speeds. This could be due to the limited number of eddies analyzed for the region north of the Hawaiian Islands. ALOHA eddies also do not conform to the tendency for anticyclones to translate equatorward and cyclones to translate poleward (Chelton et al. 2007). This may be due to the small latitude range used for this study.

The presence of the Hawaiian Islands affects the trajectories of eddies in the central North Pacific. Regardless of eddy characteristics including direction of rotation, size and region of formations, eddies that translated westward and encountered the Hawaiian Islands deviated from westward translation. Most eddies deviated to the northwest and translate along the Hawaiian Ridge, then resumed a westward trajectory once clear of Kauai. Others did not deviate and dissipated from their collision with the islands. A few

of the dissipated features appeared to have their remnants swept through the channels into the lee of the islands.

The five eddies that form east of 148°W and south of 22°N and have few interactions with other eddies exhibit larger water property anomalies at ALOHA. The degree of interaction with topography and other eddies is important for maintaining isolated bolus transport.

The continued cataloging of eddies affecting ALOHA is critical for understanding the ocean processes that affect Hawaii Ocean Time-series variability. Correlating the eddies resulting from this study with biological variability at Station ALOHA would be especially beneficial. This may help to sort out how well inorganic nutrients act as conservative water mass tracers within an eddy. Additionally, other multivariate methods should be applied to the HOT water mass characteristics to better characterize variability in the water properties. Q-mode factor analysis has been shown to be successful in delineating water masses in the Pacific Ocean from hydrographic data (Hamann and Swift 1991).

Further study is needed to gain additional information about the vertical structure of eddies affecting ALOHA. This can be largely accomplished using the eddy identification and tracking algorithm in parallel with a model such as the Navy Coastal Ocean Model, which utilizes satellite altimetry and incorporates eddy dynamics. A model that can accurately identify, track and possibly predict mesoscale eddy activity will have significant impact on marine operations including search and rescue, scientific sampling and ship navigation.

7 References

Archiving, Validation, and Interpretation of Satellite data in Oceanography (AVISO), (2006), AVISO SSALTO/DUACS User Handbook: (M)SLA and (M)ADT Near-Real Time and Delayed Time Products, Publishing SALP-MU-P-EA-21065-CLS, 8th edition, 50 pp.

Antonov, J. I., R. A. Locarnini, T. P. Boyer, A. V. Mishonov, and H. E. Garcia (2006), World Ocean Atlas 2005, Volume 2: Salinity. S. Levitus, Ed. NOAA Atlas NESDIS 62. U.S. Government Printing Office, Washington, D.C., 182 pp.

Benitez-Nelson, C.R., R.R. Bidigare, T.D. Dickey, M.R. Landry, C.L. Leonard, S.L. Brown, F. Nencioli, Y.M. Rii, K. Maiti, J.W. Becker, T.S. Bibby, W. Black, W-J Cai, C.A. Carlson, F. Chen, V.S. Kuwahara, C. Mahaffey, P.M. McAndrew, P.D. Quay, M.S. Rappe, K.E. Selph, M.P. Simmons and E.J. Yang (2007), Mesoscale eddies drive increased silica export in the Subtropical Pacific Ocean. *Science*, **316**, 1017-1021.

Bernstein, R. (1974), Mesoscale eddies in the North Pacific: Westward propagation. *Science*, **183**, 71-72.

Broecker, W.S. (1974), "NO", A Conservative Water-Mass Tracer. *Earth and Planetary Science Letters*, **23**, 100-107.

Chelton, D.B. and M.G. Schlax (1996), Global Observations of oceanic Rossby Waves. *Science*, **272**, 234-238.

Chelton, D.B. and M.G. Schlax (2003), The Accuracies of Smoothed Sea Surface Height Fields Constructed from Tandem Satellite Altimeter Datasets. *Journal of Atmospheric and Oceanic Technology*, **20**, 1276-1302.

Chelton, D.B., M.G. Schlax, R.M. Samelson, and R.A. de Szoeke (2007), Global Observations of large oceanic eddies. *Geophysical Research Letters*, **34**, L15606.

Chiswell, S.M. (2002), Energy Levels, Phase, and Amplitude Modulation of the Baroclinic Tide off Hawaii. *Journal of Physical Oceanography*, **32**, 2640-2651.

Cushman-Roisin, B. (1994), *Introduction to Geophysical Fluid Dynamics*. Prentic Hall, New Jersey, 320 pp.

Cushman-Roisin,B., E.P. Chassignet and B. Tang (1990), Westward Motion of Mesoscale Eddies. *Journal of Physical Oceanography*, **20**, 758-768.

Drijfhout, S.S., and W. Hazeleger (2001), Eddy Mixing of Potential Vorticity versus Thickness in an Isopycnic Ocean Model. . *Journal of Physical Oceanography*, **31**, 481-505.

Ducet, N., P.Y. LeTraon, and G. Reverdin (2000), Global high-resolution mapping of ocean circulation from TOPEX/Poseidon and ERS-1 and -2. *Journal of Geophysical Research*, **105**, 19477-19498.

Firing, E., Ranada, J., Caldwell, P. (1995), Processing ADCP data with the CODAS software system version 3.1, User's manual. (Manual and software available electronically at ftp://noio.soest.hawaii.edu/pub/codas3.).

Firing, E. (1996), Currents observed north of Oahu during the first five years of HOT. *Deep Sea Research*, **43**, 281-303.

Firing, Y.L. and M.A. Merrifield (2004), Extreme sea level events at Hawaii: Influence of mesoscale eddies. *Geophysical Research Letters*, **31**, L24306.

Garcia, H. E., R. A. Locarnini, T. P. Boyer, and J. I. Antonov, 2006. *World Ocean Atlas 2005, Volume 4: Nutrients (phosphate, nitrate, silicate)*. S. Levitus, Ed. NOAA Atlas NESDIS 64, U.S. Government Printing Office, Washington, D.C., 396 pp.

Gill, A.E., J.S.A. Green, and A.J. Simmons (1974), Energy partition in the large-scale ocean circulation and the production of mid-ocean eddies. *Deep-Sea Res.*, **21**, 499-528.

Gill,A.E. (1982), *Atmosphere-Ocean Dynamics*, Elsevier Academic Press, San Diego, 662 pp.

Hamann, I.M. and J.H. Swift (1991), A consisten inventory of water mass factors in the intermediate and deep Pacific Ocean derived from conservative tracers. *Deep Sea Res.*, **38**, S129-S169.

Holland, W.R. (1978), The role of mesoscale eddies in the general circulation of the ocean-numerical experiments using a wind-driven quasi-geostrophic model. *J. Phys. Oceano.*, **8**, 363-393.

Holland, C. and G.T. Mitchum (2001), Propagation of Big Island eddies. *J. Geophys. Res.*, **106**, 935-944.

Isern-Fontanet, J., E. Garcia-Ladona, and J. Font (2003), Identification of Marine Eddies from Altimetric Maps. *Journal of Atmospheric and Oceanic Technology*, **20**, 772-778.

Isoda, Y. and S. Saitoh (1988), Variability of the sea surface temperature obtained by the statistical analysis of AVHRR imagery. *J. Oceanography*, **44**, 52-59.

Karl, D.M. and R. Lukas (1996), The Hawaii Ocean Time-series (HOT) program: Background, rationale and field implementation. *Deep Sea Research-II*, **43**, 129-156.

Karl, D.M. (1999), A sea of change: biogeochemical variability in the North Pacific Subtropical gyre. *Ecosystems*, **2**, 181-214.

Knauss, J.A. (1996). *Introduction to Physical Oceanography.* Prentice Hall, 309 pp.

Kundu, P.K. and I.M. Cohen (2004), *Fluid Mechanics Third Edition*, Elsevier Academic Press, San Diego, 759 pp.

Letelier, R.M., D.M. Karl, M.R. Abbott, P. Flament, M. Freilich, R. Lukas, and T. Strub (2000), Role of late winter mesoscale events in the biogeochemical variability of the upper water column of the North Pacific Subtropical Gyre. *Journal of Geophysical Research*, **105**, 28,723-28,739.

Le Traon, P.Y. and F. Hernandez (1992), Mapping the Oceanic Mesoscale Circulation: Validation of Satellite Altimetry Using Surface Drifters. *Journal of Atmospheric and Oceanic Technology* **9**, 687-698.

Le Traon, P.Y., and G. Dibarboure (1999), Mesoscale mapping capabilities from multiple altimeter missions. *J. Atm. Ocean. Tech.* **16**, 1208-1223.

Le Traon, P.Y., and R. Morrow (2001), Ocean Currents and Eddies *Satellite Altimetry and Earth Sciences* , edited by L-L Fu and A. Cazenave, Academic Press, San Diego, pp. 171-215.

Lukas, R. and F. Santiago-Mandujano (2001), Extreme water mass anomaly observed in the Hawaii Ocean Time-series *Geophysical Research Letters*, **28**, 2931-2934.

Lumpkin, C.F. (1998), Eddies and currents of the Hawaiian Islands. Ph.D. Dissertation, Univ. of Hawaii, 281 pp.

Mahadevan, A., L.N. Thomas and A. Tandon (2008), Comment on "Eddy/Wind Interactions Stimulate Extraordinary Mid-Ocean Plankton Blooms". *Science*, **320**, 448b.

McDonald R. (1999), The motion of geophysical vortices. *Phil. Trans. R. Soc. Lond.*, **357**, 3427-3444.

McGillicuddy, D.J., R. Johnson, D.A. Siegel, A.F. Michaels, N.R. Bates, and A.H. Knap (1999), Mesoscale variations of biogeochemical properties in the Sargasso Sea. *Journal of Geophysical Research*, **104**, 13,381-13,394.

McGillicuddy, D.J., L.A. Anderson, N.R. Bates, T. Bibby, K.O. Buesseler, C.A. Carlson, C.S. Davis, C. Ewart, P.G. Falkowski, S.A. Goldthwait, D.A. Hansell, W.J. Jenkins, R. Johnson, V.K. Kosnyrev, J.R. Ledwell, Q.P. Li, D.A. Siegel, and D.K. Steinberg (2007), Eddy/Wind interactions stimulate extraordinary mid-ocean plankton blooms. *Science*, **316**, 1021-1026.

McNeil, J.D., H.W. Jannasch, T. Dickey, D.J. McGillicuddy, M. Brzezinski, and C.M. Sakamoto (1999), New chemical, bio-optical and physical observations of upper ocean response to the passage of a mesoscale eddy of Bermuda. *Journal of Geophysical Research*, **104**, 15537-15548.

McWilliams, J.C. and G.R. Flierl (1979), On the Evolution of Isolated, Nonlinear Vortices. *Journal of Physical Oceanography*, **9**, 1155-1182.

McWilliams, J.C. (2006), *Fundamentals of Geophysical Fluid Dynamics*, Cambridge Univ. Press, 249 pp.

Mitchum, G. T. (1993), Principal component analysis: Basic methods and extensions. *Aha Hulioko'a: Statistical Methods in Oceanography,* P. Muller and D. Henderson, Eds., SOEST Publication Services, 185–199.

Mitchum, G.T. (1994), Comparison of TOPEX sea surface height and tide gauge sea levels. *J. Geophys. Res.*, **99**, 24514-24554.

Mitchum, G.T. (1996), On using satellite altimetric heights to provide a spatial context for the Hawaii Ocean Time-series measurements. *Deep Sea Research-II*, **43**, 257-280.

Muller, P. (1995), Ertel's Potential Vorticity Theorem in Physical Oceanography. *Reviews of Geophysics*, **33**, 67-97.

Munch, C.L. (1996), The effect of the Hawaiian Ridge on mesoscale variability: results from Topex/Poseidon, Masters Thesis, Univ. of Hawaii, 125 pp.

Niiler, P.P. and M.M. Hall (1988), Low-Frequency Eddy Variability at 28N, 152W in the Eastern North Pacific Subtropical Gyre. *J. Phys. Oceano.*, **18**, 1670-1685.

Nof,D. (1981), On the β-Induced Movement of Isolated Baroclinic Eddies. *Journal of Physical Oceanography*, **11**, 1662-1672.

Paschini, E., A. Artegiani, and N. Pinardi (1993), The mesoscale eddy field of the Middle Adriatic Sea during fall 1988. *Deep Sea Res.*, **40**, 1365-1377.

Pascual, A., Y. Faugere, G. Larnicol, and P.Y. Le Traon (2006), Improved description of the ocean mesoscale variability by combining four satellite altimeters. *Geophysical Research Letters*, **33**, L02611.

Patzert,W.C. (1969), Eddies in Hawaiian waters. Technical Report 69-8, Hawaiian Institute of Geophysics, University of Hawaii at Manoa.

Preisendorfer, R.W., F.W. Zwiers, and T.P. Barnett (1981), Foundations of Principal Component Selection Rules. *SIO Reference Series*, #81-4, Scripps Inst. of Oceanography, La Jolla, CA.

Price, J.M., M.L. van Woert, M. Vitousek (1994), On the possibility of a ridge current along the Hawaiian Islands. *Journal of Geophysical Research*, **99**, C7, 14101-14112.

Qiu, B., D.A. Koh, C. Lumpkin, and P. Flament (1997), Existence and Formation Mechanism of the North Hawaiian Ridge Current. *Journal of Physical Oceanography*, **27**, 431-444.

Qiu, B. (1999), Seasonal Eddy Field Modulation of the North Pacific Subtropical Countercurrent: TOPEX/Poseidon Observations and Theory. *Journal of Physical Oceanography*, **29**, 2471-2486.

Redfield, A.C., B.H. Ketchum and F.A. Richards (1963), The influence of organisms on the composition of sea-water. In: M.N. Hill, Editor, *The Sea: Ideas and Observations on Progress in the Study of the Seas*, Wiley, New York, pp. 26–77.

Richardson, P.L. (1993), A census of eddies observed in North Atlantic SOFAR float data. *Progress in Oceanography*, **31**, 1-50.

Robinson, A.R., Ed. (1983), *Eddies in Marine Science*, Springer-Verlag, 609 pp.

Roemmich, D. and J. Gilson (2001), Eddy Transport of Heat and Thermocline Waters in the North Pacific: A Key to Interannual/Decadal Climate Variability? *Journal of Physical Oceanography*, **31**, 675-687.

Schmitz, J.E. and A.C. Vastano (1975), Entrainment and Diffusion in a Gulf Stream Cyclonic Ring. *J. Phys. Oceano.*, **5**, 93-98.

Seki, M.P., J.J. Polovina, R.E. Brainard, R.R. Bidigare, C.L. Leonard and D.G. Foley (2001), Biological enhancement at cyclonic eddies tracked with GOES thermal imagery in Hawaiian waters. *Geophys. Res. Let.*, **28**, 1583-1586.

Siegel, D.A., D.J. McGillicuddy, and E.A. Fields (1999), Mesoscale eddies, satellite altimetry, and new production in the Sargasso Sea. *Journal of Geophysical Research*, **104**, 13,359-13,379.

Smith, W. H. F., and D. T. Sandwell (1997), Global seafloor topography from satellite altimetry and ship depth soundings. *Science*, **277**,1957-1962.

Stammer, D. (1998), On Eddy Characteristics, Eddy Transports, and Mean Flow Properties. *J. Phys. Ocean.*, **28**, 727-739.

Strub, P.T. and C. James (2000), Altimeter derived variability of surface velocities in the California Current System: 2. Seasonal circulation and eddy statistics. *Deep Sea Res. II*, **47**, 831-870.

Sweeney, E.N., D.J. McGillicuddy, and K.O. Buesseler (2003), Biogeochemical impacts due to mesoscale eddy activity in the Sargasso Sea as measured at the Bermuda Atlantic Time-series Study (BATS). *Deep Sea Research II*, **50**, 3017-3039.

Tabachnick, B.G., and L.S. Fidell (1996), *Using Multivariate Statistics.* Harper Collins College, New York, 880 pp.

Tupas, L., F. Santiago-Mandujano, D. Hebel, R. Lukas, D. Karl and E. Firing. Hawaii Ocean Time-series Program Data Report 4, 1992. SOEST Tech. Report 93-14, School of Ocean and Earth Science and Technology, Univ. of Hawaii, Honolulu, HI, 248 pp.

Verstraete, J-M. and Y-H Park (1995), Comparison of Topex/Poseidon altimetry and in situ sea level data at Sao Tome Island, Gulf of Guinea. *J. Geophys. Res.*, **100**, C12, 25129-25134.

Wilks, D.S. (1995). *Statistical Methods for the Atmospheric Sciences.* Academic Press, New York, 648 pp.

Wyrtki, K., L. Magaard, J. Hager (1976), Eddy Energy in the Oceans. *J. Geophys. Res.*, **81**, 2641-2646.

Wyrtki, K. (1982), Eddies in the Pacific North Equatorial Current. *J. Phys. Ocean.*, **12**, 746-749.

Zamudio, L., H.E. Hurlburt, E.J. Metzger, S.L. Morey, J.J. O'Brien, C.E. Tilburg and J.Zavala-Hidalgo (2006), Interannual variability of Tehuantepec eddies. *J. Geophys. Res.*, **111**, C05001, doi:10.1029/2005JC003182.

ID	Dates at ALOHA			CPA		Amplitude (cm)		HOT cruise		ADCP	Sat. cvrg	of Note
	in	out	wks	distance (km)	part of eddy	maximum	average	number	part sampled	avail.		
01C	14-Oct-92	25-Nov-92	6	17.12	center	-4.18	-2.74	41	NW corner		T/P & ERS1	
02A	18-Nov-92	18-Nov-92	1	124.71	south edge	4.67	4.67	42	na		T/P & ERS1	HOT standard data not collected
03A	31-Mar-93	19-May-93	7	25.61	center	7.60	3.86	46	S-center		T/P & ERS1	
04C	30-Jun-93	18-Aug-93	8	17.70	center	-10.22	-6.69	48	na		T/P & ERS1	HOT cruise aborted
05C	22-Sep-93	29-Dec-93	13	8.40	center	-5.64	-2.80	50	east		T/P & ERS1	
06C	19-Jan-94	2-Feb-94	3	71.78	north	-2.85	-2.92	51	north		T/P	
07A	13-Apr-94	15-Jun-94	7	72.07	south	8.04	5.97	NaN	na		T/P	
08A	29-Jun-94	24-Aug-94	4	50.99	north	1.44	1.12	55	NW corner		T/P	
09A	12-Oct-94	16-Nov-94	7	38.41	center	5.88	4.43	58	W-center		T/P	
10A	28-Mar-95	28-Mar-95	NaN	132.91	southwest	NaN	NaN	62	south border		T/P	
11C	17-May-95	7-Jun-95	6	18.60	center	-10.11	-7.27	63	west border		T/P	
12C	23-Aug-95	30-Aug-95	2	35.59	east	-4.47	-4.47	65	east border		T/P	
13C	11-Oct-95	22-Nov-95	7	18.78	center	-2.94	-2.00	67/68	west/east		T/P	
14C	27-Dec-95	17-Jan-96	3	29.24	center	-4.48	-3.50	69	east		T/P	
15C	7-Feb-96	20-Mar-96	3	14.33	N-center	-2.02	-2.02	NaN	na		T/P	drop
16A	1-May-96	22-May-96	2	63.35	south	4.74	4.47	72	SE corner		T/P	
17A	3-Jul-96	11-Sep-96	11	8.26	center	9.48	7.63	74/75	W-center/S-center		T/P & ERS2	
18C	2-Oct-96	6-Nov-96	5	14.72	center	-3.32	-2.42	76/77	W-end/center		T/P & ERS2	
19A	4-Dec-96	11-Dec-96	3	79.14	north	1.24	1.24	78	NW corner		T/P & ERS2	drop
20A	29-Jan-97	26-Feb-97	8	38.73	N-center	6.15	5.86	80	N-center		T/P & ERS2	
21C	12-Mar-97	23-Apr-97	8	22.28	center	-12.23	-9.37	81/82	west/east		T/P & ERS2	
22A	30-Apr-97	11-Jun-97	7	13.36	W-center	7.58	4.73	83	west		T/P & ERS2	
23C	11-Jun-97	2-Jul-97	2	65.63	south	-2.08	-2.06	NaN	na		T/P & ERS2	
24A	6-Aug-97	27-Aug-97	5	98.99	south	3.93	2.60	86	SW edge		T/P & ERS2	
25A	24-Sep-97	22-Oct-97	6	44.92	W-center	7.22	5.76	87	W-center		T/P & ERS2	
26C	7-Jan-98	21-Jan-98	3	62.63	southwest	-7.09	-6.08	89	SW corner	X	T/P & ERS2	
27C	18-Feb-98	11-Mar-98	4	17.72	center	-7.08	-4.52	90	na		T/P & ERS2	drop
28A	10-Jun-98	17-Jun-98	4	80.71	north	2.42	2.42	94	NW corner	X	T/P & ERS2	
29C	22-Jul-98	2-Sep-98	10	41.27	center	-14.26	-9.12	95/96	W-end/center	X	T/P & ERS2	
30C	28-Oct-98	18-Nov-98	4	21.11	center	-5.85	-5.05	99	center	X	T/P & ERS2	
31A	2-Dec-98	23-Dec-98	6	90.05	S-center	11.66	10.20	100	S-center	X	T/P & ERS2	
32A	27-Jan-99	24-Feb-99	3	22.62	center	2.26	2.05	102	east border	X	T/P & ERS2	
33C	5-May-99	19-May-99	7	44.23	W-center	-3.41	-1.96	105	NW corner	X	T/P & ERS2	
34A	23-Jun-99	21-Jul-99	4	19.16	center	12.13	9.53	106	center	X	T/P & ERS2	
35C	11-Aug-99	8-Sep-99	9	24.40	center	-11.74	-9.97	107	W-center	X	T/P & ERS2	
36A	6-Oct-99	6-Oct-99	1	114.51	NW	NaN	NaN	108	N edge	X	T/P & ERS2	
37C	10-Nov-99	12-Jan-00	4	82.67	southwest	-2.07	-1.50	109	west border	X	T/P & ERS2	
38C	1-Dec-99	22-Dec-99	2	61.18	east	-0.80	-0.80	110	east border	X	T/P & ERS2	
39A	12-Jan-00	26-Jan-00	4	17.34	center	5.39	4.04	NaN	na		T/P & ERS2	
40C	2-Feb-00	23-Feb-00	4	94.63	north	-1.33	-1.33	111	north edge	X	T/P & ERS2	
41C	29-Mar-00	26-Apr-00	4	4.56	center	-6.60	-6.06	113	southwest	X	T/P & ERS2	
42A	9-Aug-00	30-Aug-00	4	23.54	center	3.86	3.23	118	east	X	T/P & ERS2	
43A	8-Nov-00	8-Nov-00	1	108.15	south	3.80	3.80	NaN	na		T/P & ERS2	
44A	20-Dec-00	14-Feb-01	6	52.49	S-center	9.98	8.01	121	W-center	X	T/P & ERS2	
45A	11-Apr-01	25-Apr-01	3	18.84	center	3.18	2.86	126	W-center	X	T/P & ERS2	drop
46C	30-May-01	20-Jun-01	8	103.11	south	-4.08	-3.58	127	south border		T/P & ERS2	bad nutrients cruise
47C	15-Aug-01	12-Sep-01	4	95.84	center	-4.61	-3.71	NaN	na		T/P & ERS2	
48C	10-Oct-01	7-Nov-01	7	26.04	center	-3.83	-2.63	131	center		T/P & ERS2	bad nutrient cruise
49A	26-Dec-01	6-Feb-02	6	40.43	S-center	4.64	3.83	134	S-center	X	T/P & ERS2	

ID	Dates at ALOHA			CPA		Amplitude (cm)		HOT cruise		ADCP	Sat. cvrg	of Note
	in	out	wks	distance (km)	part of eddy	maximum	average	number	part sampled	avail.		
50C	8-May-02	10-Jul-02	3	74.25	center	-4.31	-3.87	138	east border	X	T/P & ERS2	
51A	3-Jul-02	24-Jul-02	3	48.63	north	4.10	3.23	138	west border	X	T/P & ERS2	
52C	7-Aug-02	28-Aug-02	2	67.32	north	-3.53	-2.79	139	NE edge	X	JSN1 & ERS2	
53A	4-Sep-02	30-Oct-02	9	18.96	center	4.92	3.18	140	center	X	JSN1 & ERS2	
54A	16-Oct-02	18-Dec-02	9	18.94	S-center	5.30	3.34	141-143	south		JSN1 & ERS2	
55C	22-Jan-03	19-Feb-03	4	40.44	S-center	-6.42	-2.91	144	SE corner	X	JSN1 & ERS2	
56C	26-Mar-03	23-Apr-03	3	32.37	E-center	-5.33	-3.80	146/147	SW corner/Eend	X	JSN1 & ERS2	
57A	3-Sep-03	8-Oct-03	7	71.13	N-center	10.63	7.68	151	west border	X	JSN1 & ENVT	
58C	17-Dec-03	31-Dec-03	3	8.40	center	-2.54	-2.26	154	center		JSN1 & ENVT	
59C	24-Mar-04	7-Apr-04	1	66.25	south	-3.40	-3.40	159	south border	X	JSN1 & ENVT	
60A	19-May-04	30-Jun-04	10	88.82	north	3.78	2.92	160	NE edge	X	JSN1 & ENVT	
61C	4-Aug-04	1-Sep-04	2	68.17	west	-2.97	-2.86	162	NW corner	X	JSN1 & ENVT	
62C	2-Mar-05	16-Mar-05	3	89.14	east	-3.05	-3.05	168	east border	X	JSN1 & ENVT	
63C	23-Feb-05	27-Apr-05	4	32.85	center	-3.71	-2.99	168	W-center	X	JSN1 & ENVT	
64A	16-Mar-05	6-Apr-05	4	41.68	north	2.33	2.08	NaN	na		JSN1 & ENVT	drop
65A	4-May-05	1-Jun-05	5	43.18	N-center	7.43	4.56	169	N-center	X	JSN1 & ENVT	
66C	15-Jun-05	15-Jun-05	1	94.73	west	-6.61	-6.61	170	west border	X	JSN1 & ENVT	
67C	29-Jun-05	27-Jul-05	3	21.50	south	-0.40	-0.40	NaN	na		JSN1 & ENVT	drop
68A	13-Jul-05	17-Aug-05	5	38.58	N-center	5.95	5.14	171	west border	X	JSN1 & ENVT	
69A	14-Sep-05	5-Oct-05	6	35.60	center	4.56	2.87	173/174	Wedge/Eedge	X	JSN1 & ENVT	
70A	9-Nov-05	28-Dec-05	8	12.55	center	1.78	1.41	176	center	X	JSN1 & ENVT	
71C	8-Feb-06	8-Mar-06	7	14.67	center	-15.31	-12.31	178	center	X	JSN1 & ENVT	
72A	22-Mar-06	19-Apr-06	4	21.97	center	4.55	3.98	180	center	X	JSN1 & ENVT	
73C	3-May-06	31-May-06	7	21.45	center	-12.96	-10.17	181	W-center	X	JSN1 & ENVT	
74A	28-Jun-06	12-Jul-06	4	18.48	center	8.85	7.64	183	E-center	X	JSN1 & ENVT	
75C	2-Aug-06	9-Aug-06	2	43.92	southeast	-1.38	-0.94	NaN	na		JSN1 & ENVT	drop
76C	22-Nov-06	20-Dec-06	5	76.06	south	-5.60	-4.31	188	south	X	JSN1 & ENVT	

9 APPENDIX II Eddy Descriptions

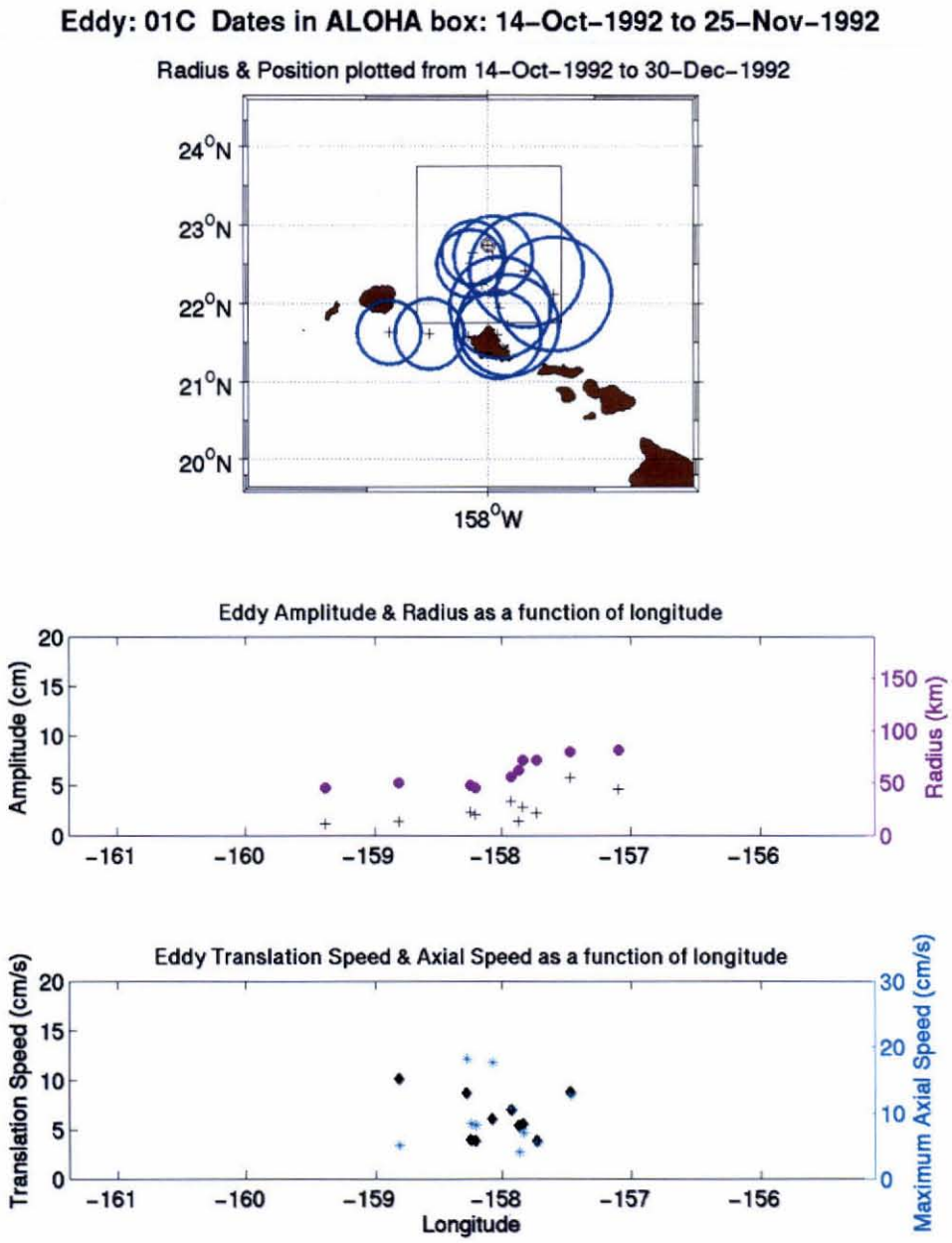

EID: 01C

This eddy formed before the initial date of the period of study. Surface currents during HOT 41 concur with expected velocities to the southwest.

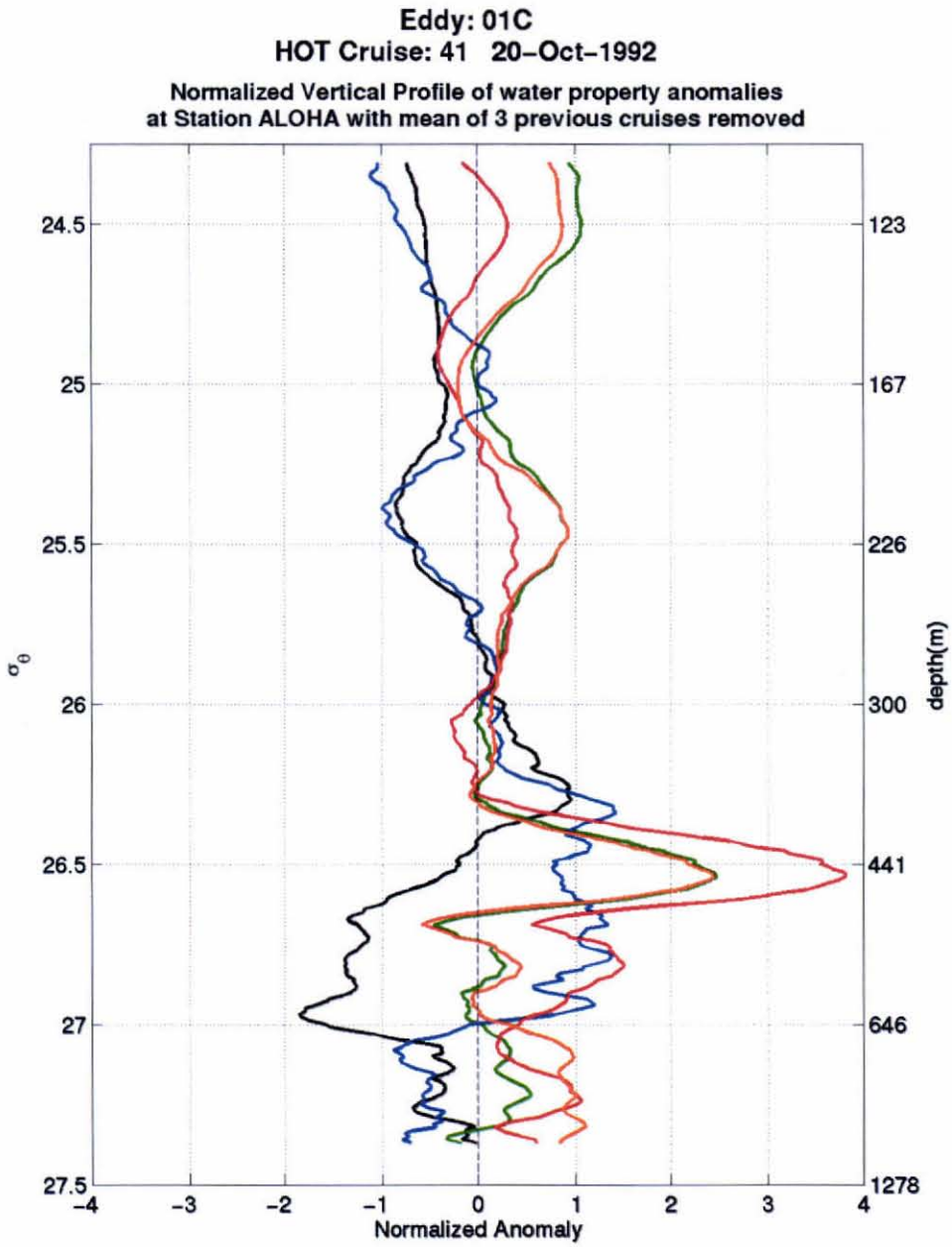
Eddy: 01C
HOT Cruise: 41 20-Oct-1992
Normalized Vertical Profile of water property anomalies
at Station ALOHA with mean of 3 previous cruises removed
24.5
25
25.5
26
26.5
27
27.5
σ_θ
123
167
226
300
441
646
1278
depth(m)
-4
-3
-2
-1
0
1
2
3
4
Normalized Anomaly

Eddy: 02A Dates in ALOHA box: 18-Nov-1992 to 18-Nov-1992

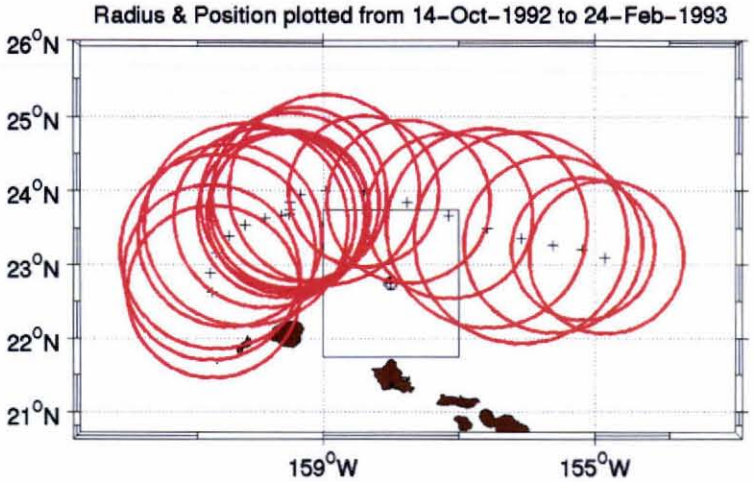

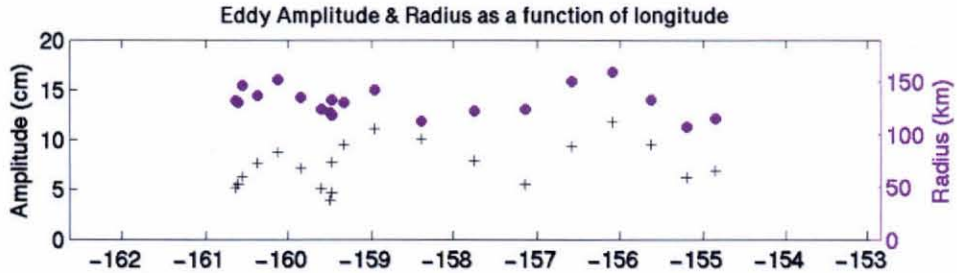

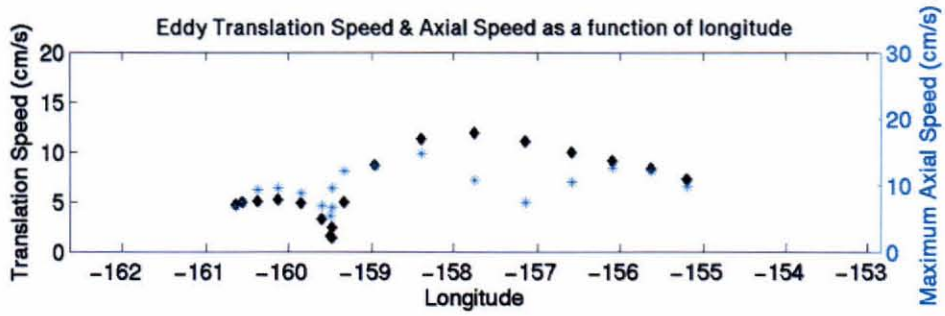

EID: 02A

This eddy forms at 155W, passes north of ALOHA, weakens north of Kauai. Slight northward track over ALOHA may be from interaction with 01C. Southern edge of eddy barely grazes ALOHA. The track is dropped when the eddy splits. The eddy later re-intensifies SW of the island chain.

Eddy: 03A Dates in ALOHA box: 31-Mar-1993 to 19-May-1993

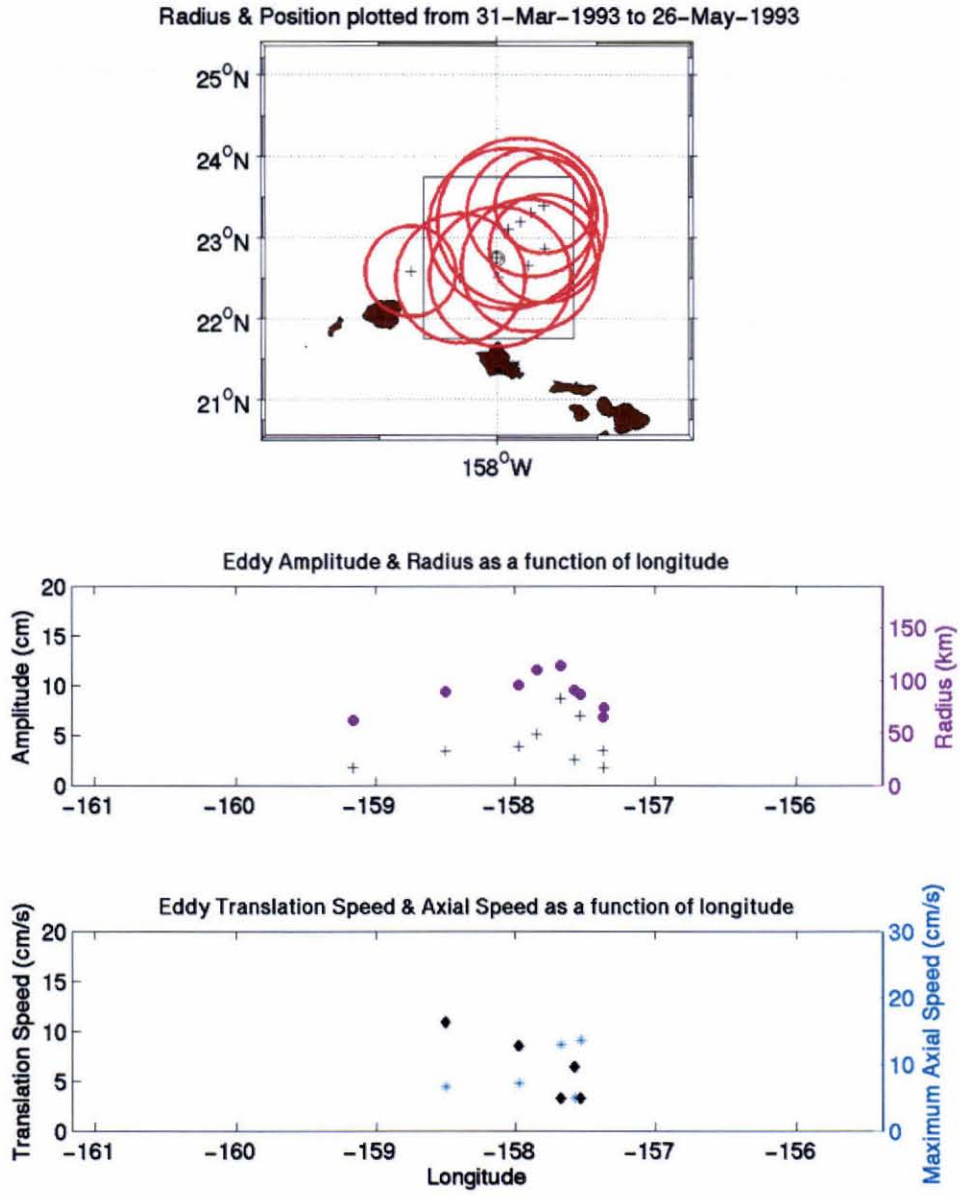

EID: 03A

This eddy is an offshoot from another eddy of unknown formation that weakens over ALOHA. ADCP surface currents concur with expected strong westward currents. Eddy is short lived and does not translate away from ALOHA.

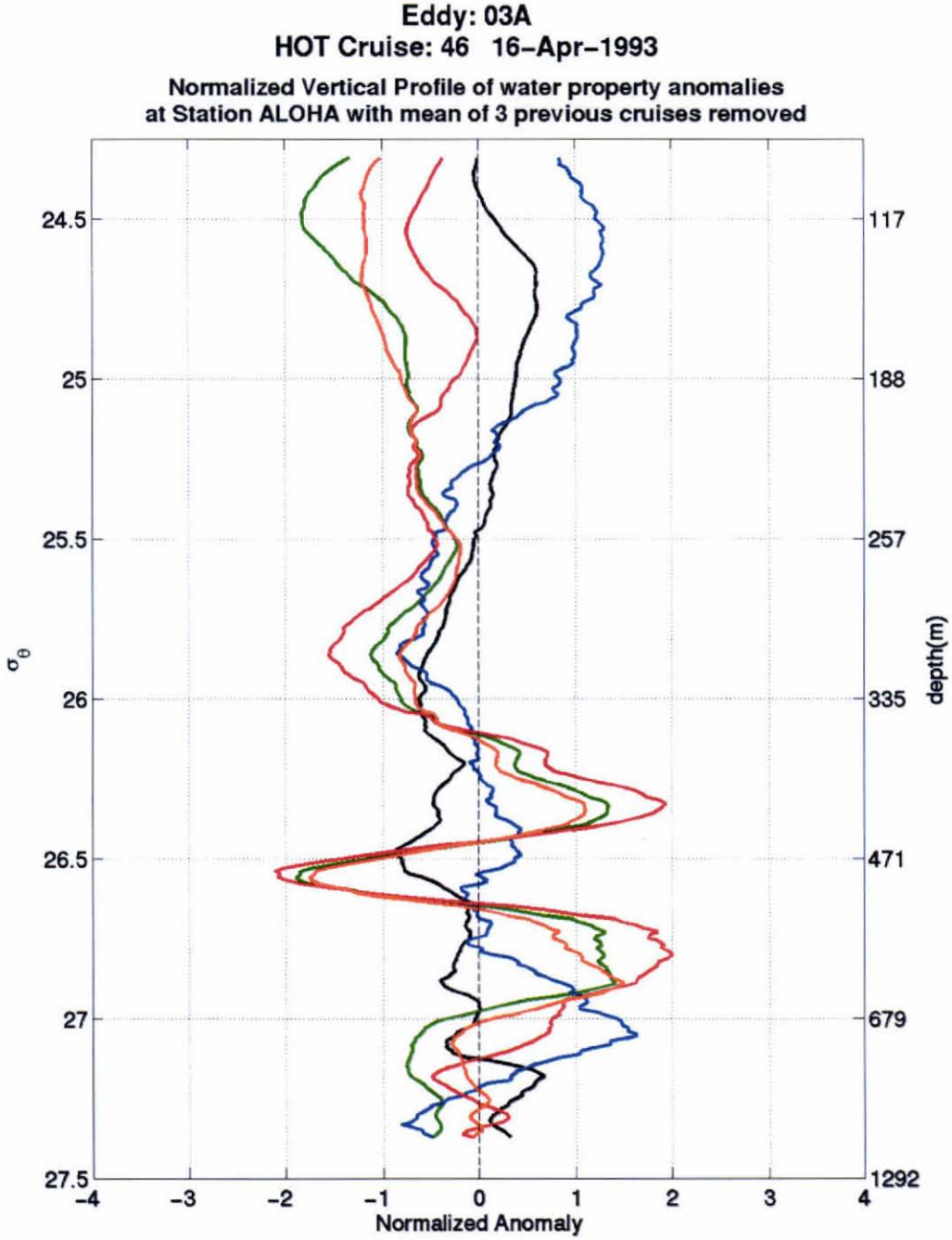
Eddy: 03A
HOT Cruise: 46 16-Apr-1993
Normalized Vertical Profile of water property anomalies
at Station ALOHA with mean of 3 previous cruises removed
24.5
25
25.5
26
26.5
27
27.5
σ_θ
117
188
257
335
471
679
1292
depth(m)
-4
-3
-2
-1
0
1
2
3
4
Normalized Anomaly

Eddy: 04C Dates in ALOHA box: 30-Jun-1993 to 18-Aug-1993

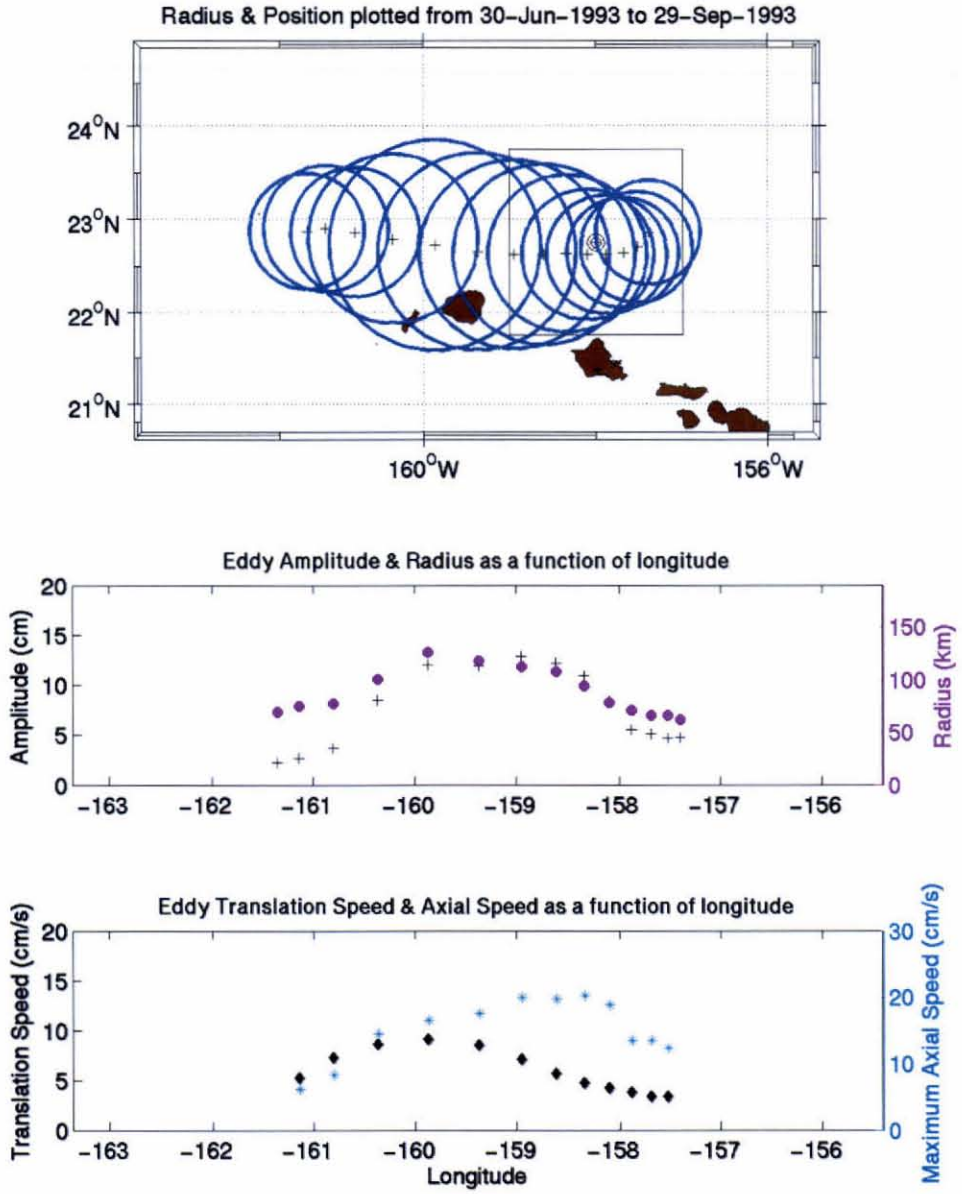

EID: 04C

This eddy is an offshoot from another feature that exhibits slow translation speeds as it spins up, interacts with island of Kauai as it grows. Interactions with another eddy appear to cause the eddy to dissipate at 162W.

Eddy: 05C Dates in ALOHA box: 22-Sep-1993 to 29-Dec-1993

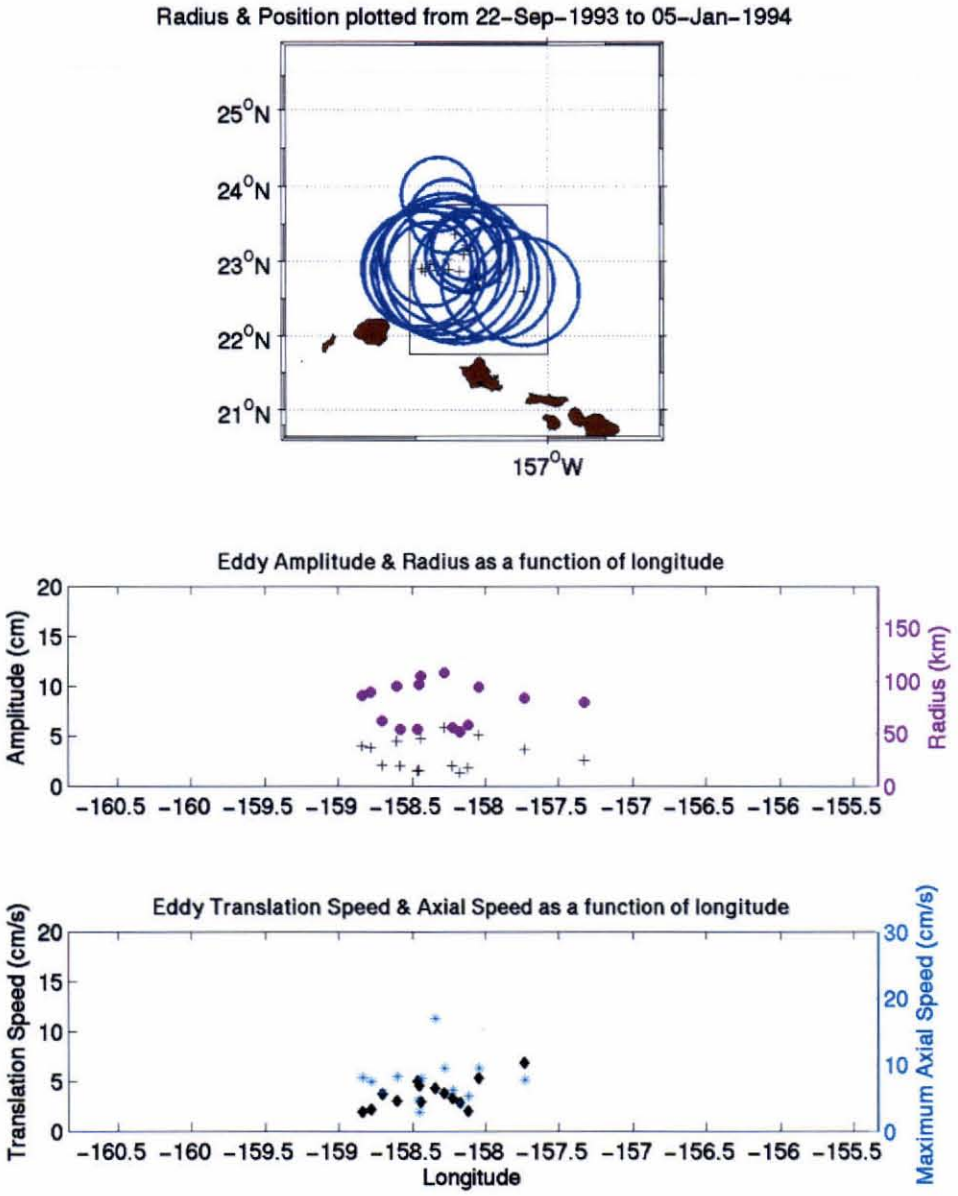

EID: 05C

This eddy track may have jumped to another feature as a result of eddy-eddy interactions. Formed from 2 interacting eddies, splits after HOT cruise and dissipates over Kauai. Do not expect a clear signature in water property anomalies or in current profile due to high degree of interactions with other eddies.

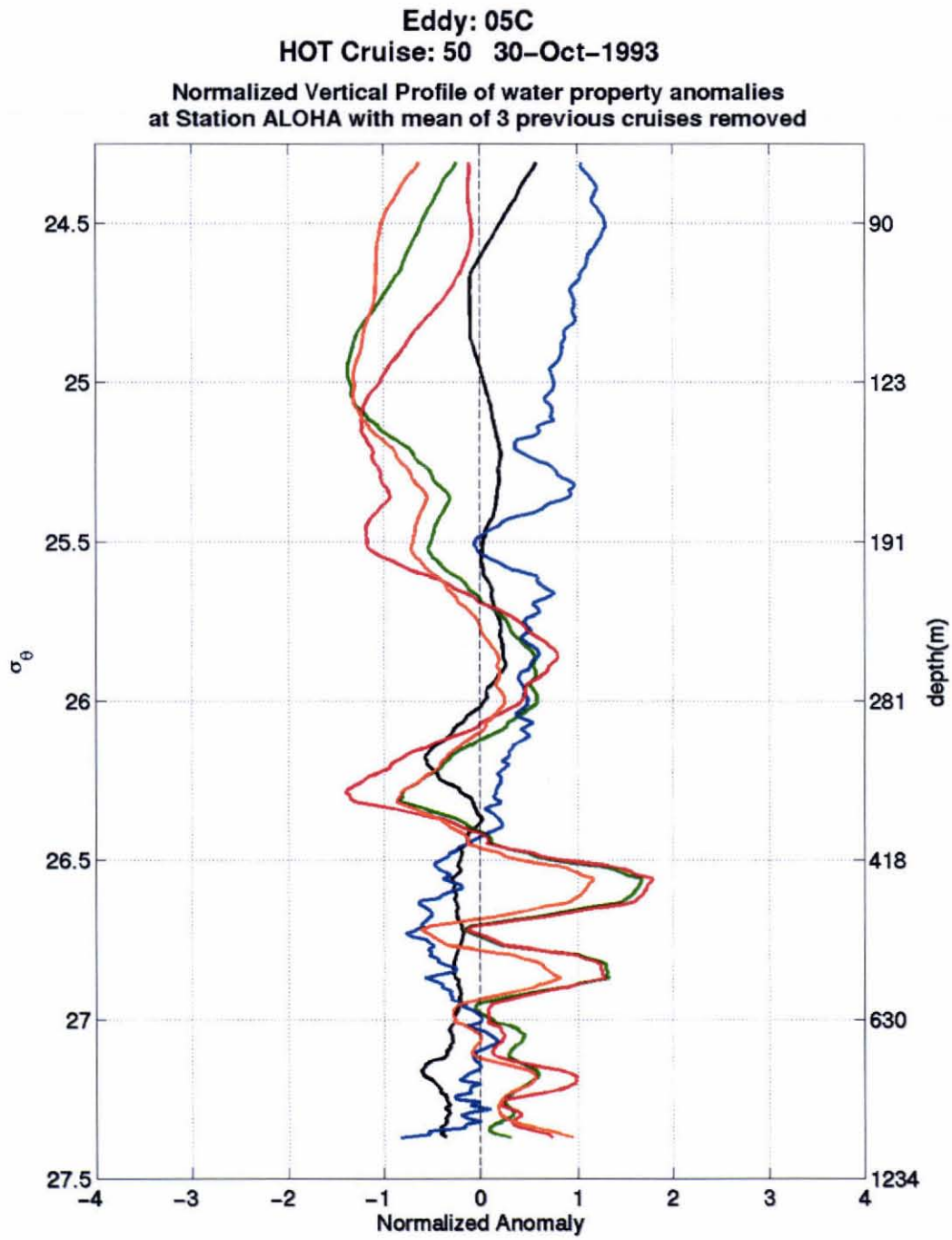
Eddy: 05C
HOT Cruise: 50 30-Oct-1993
Normalized Vertical Profile of water property anomalies
at Station ALOHA with mean of 3 previous cruises removed
24.5
25
25.5
26
26.5
27
27.5
σ_θ
90
123
191
281
418
630
1234
depth(m)
-4
-3
-2
-1
0
1
2
3
4
Normalized Anomaly

Eddy: 06C Dates in ALOHA box: 19-Jan-1994 to 02-Feb-1994

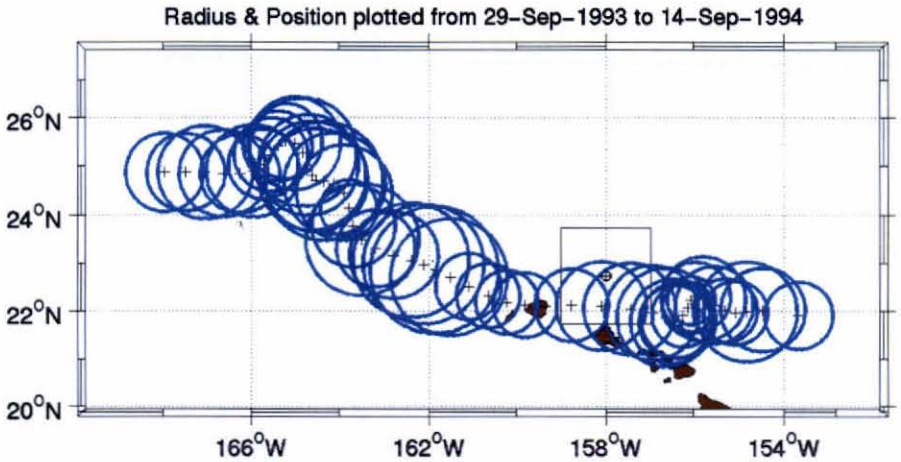

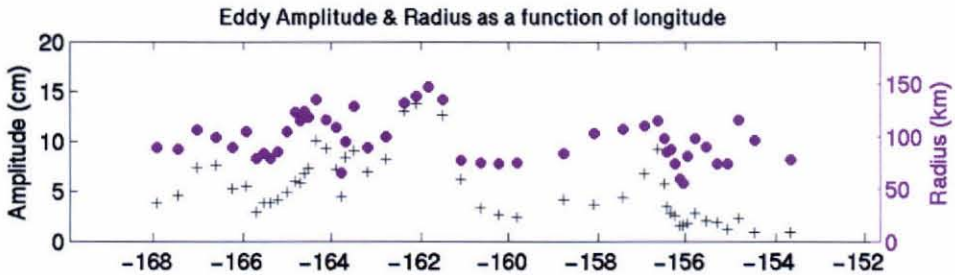

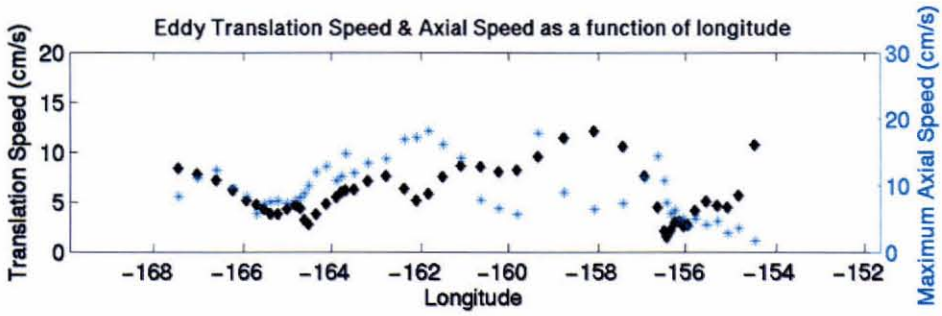

EID: 06C

This eddy formed from a series of interacting cyclonic eddies coming from the east, rapidly intensifies at 162W, radius and amplitude increase during this time. Passes south of ALOHA, distorted due to strong island interaction. Changes direction to the NW after interaction with anticyclone. Drawn up into larger eddy west of Kauai.

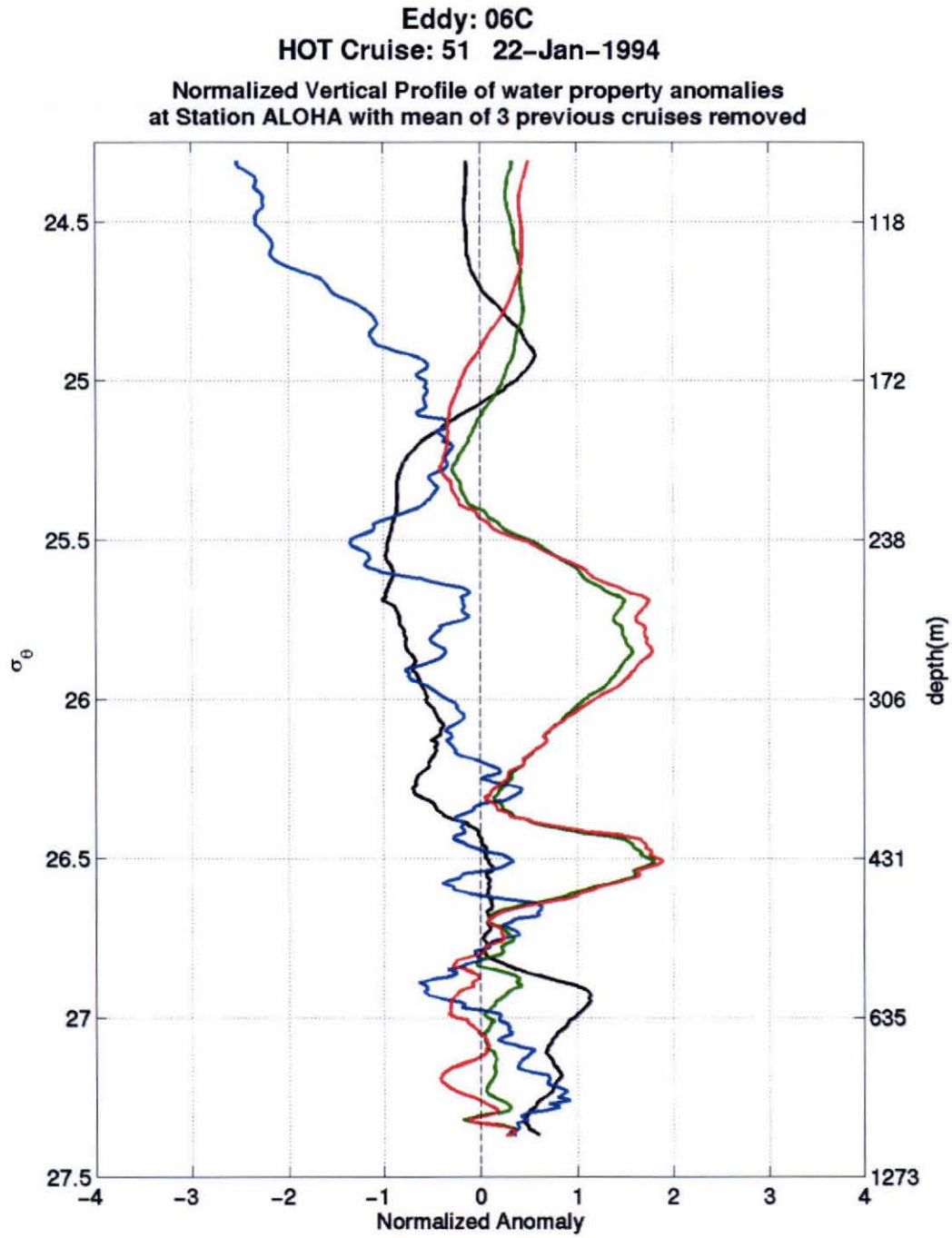
Eddy: 06C
HOT Cruise: 51 22-Jan-1994
Normalized Vertical Profile of water property anomalies
at Station ALOHA with mean of 3 previous cruises removed
24.5
25
25.5
26
26.5
27
27.5
σ_θ
118
172
238
306
431
635
1273
depth(m)
-4
-3
-2
-1
0
1
2
3
4
Normalized Anomaly

Eddy: 07A Dates in ALOHA box: 13-Apr-1994 to 15-Jun-1994

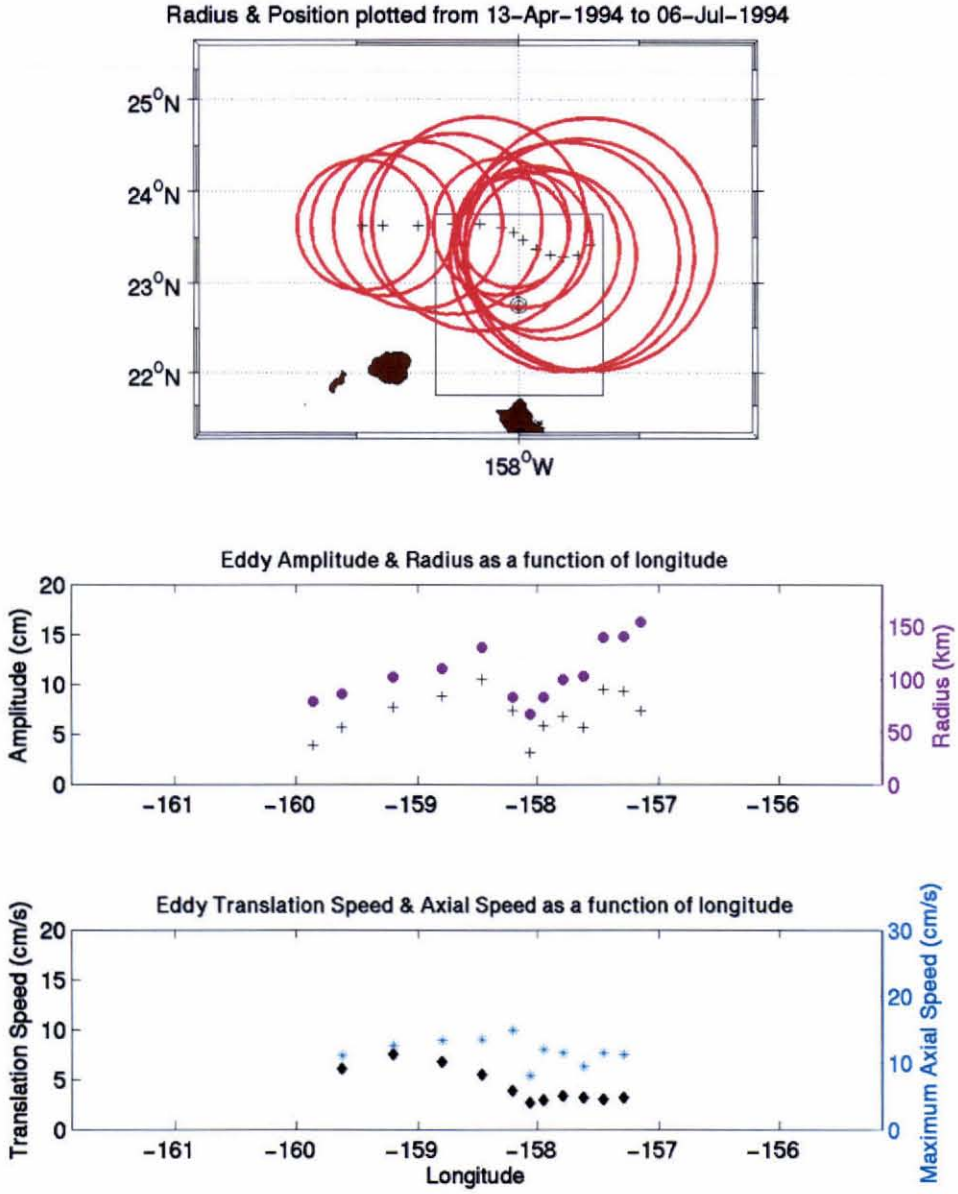

EID: 07A

This slow-translating eddy formed from two eddies merging, combines with 08A at end of its short lifetime.

Eddy: 08A Dates in ALOHA box: 29-Jun-1994 to 24-Aug-1994

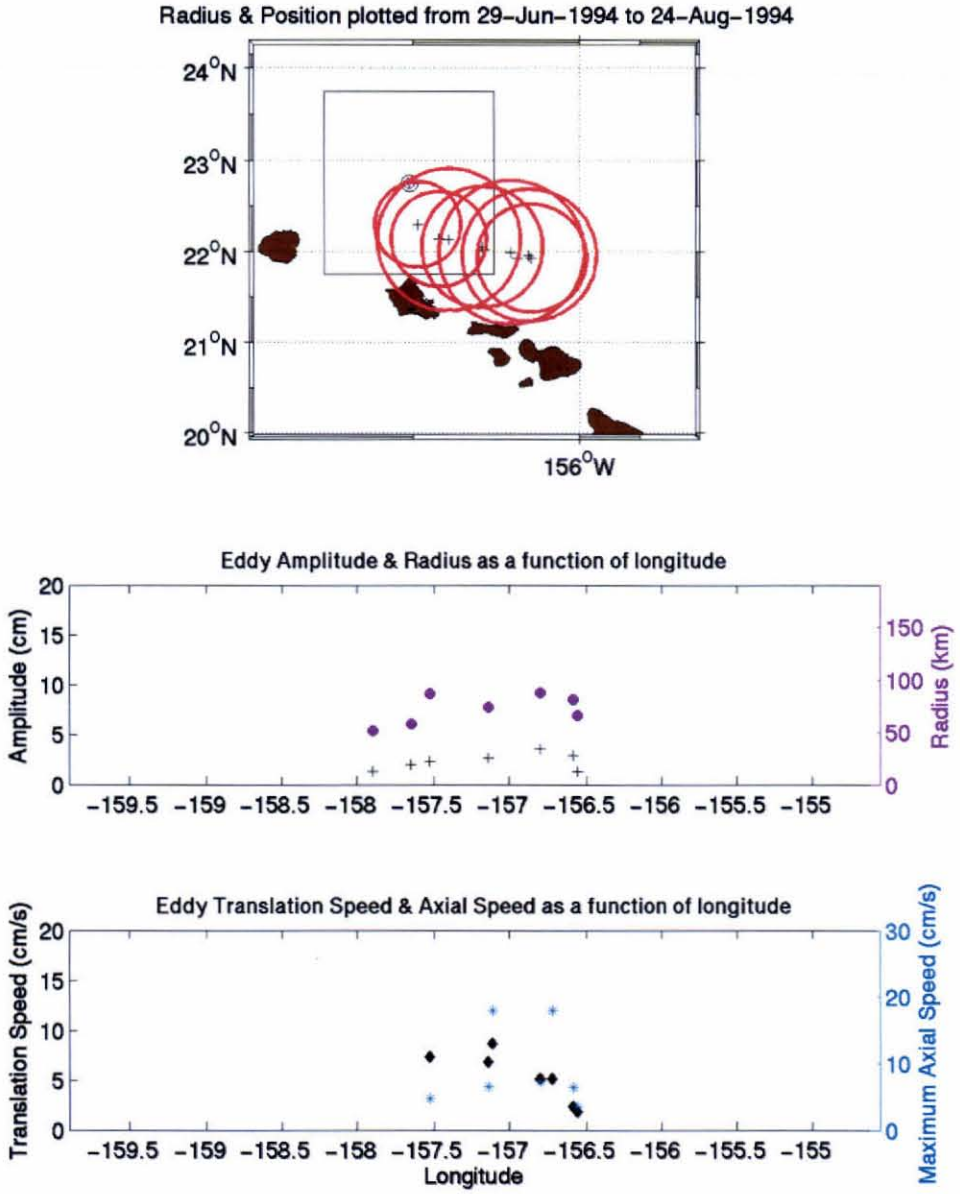

EID: 08A

This eddy spurred from two anticyclonic eddies interacting with the island chain and dissipates as it reaches ALOHA, expect any anomalies to be a result of mixing from the eddy-eddy and eddy-island interactions.

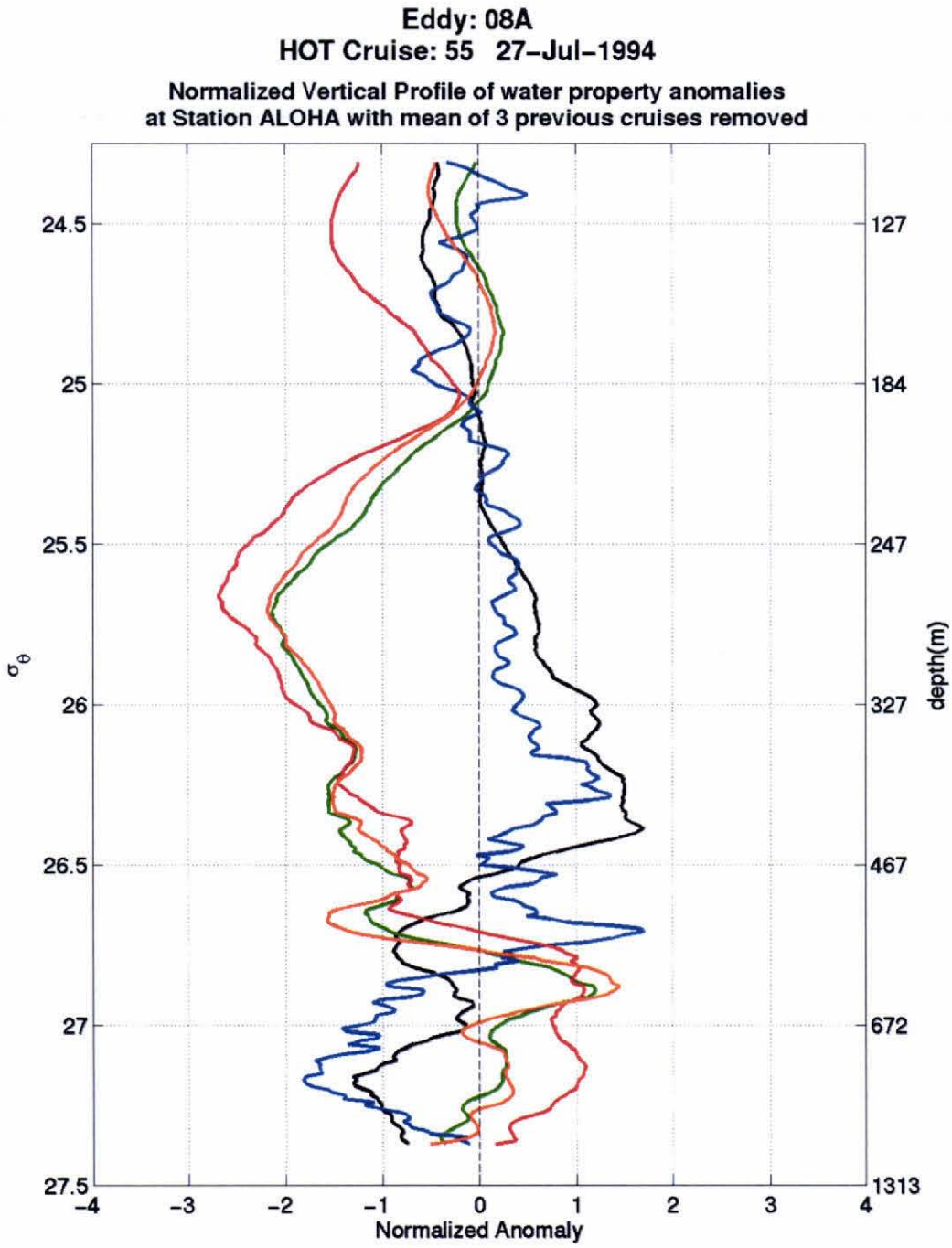
Eddy: 08A
HOT Cruise: 55 27-Jul-1994
Normalized Vertical Profile of water property anomalies
at Station ALOHA with mean of 3 previous cruises removed
24.5
25
25.5
26
26.5
27
27.5
σ_θ
127
184
247
327
467
672
1313
depth(m)
-4
-3
-2
-1
0
1
2
3
4
Normalized Anomaly

Eddy: 09A Dates in ALOHA box: 12-Oct-1994 to 16-Nov-1994

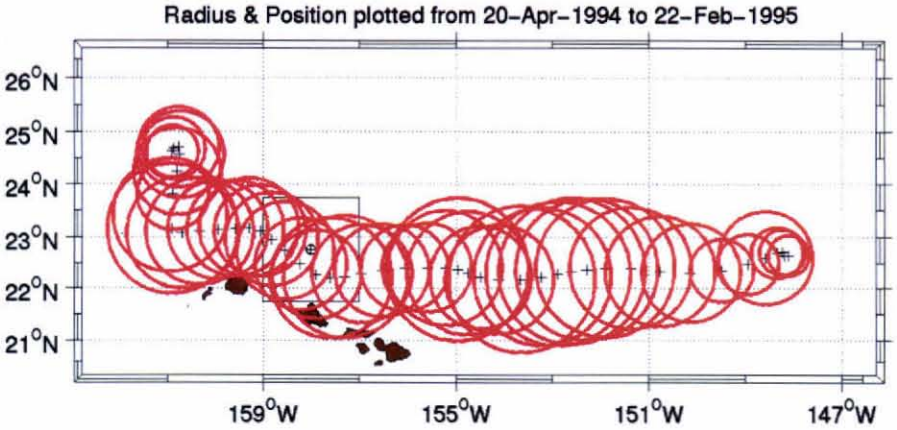

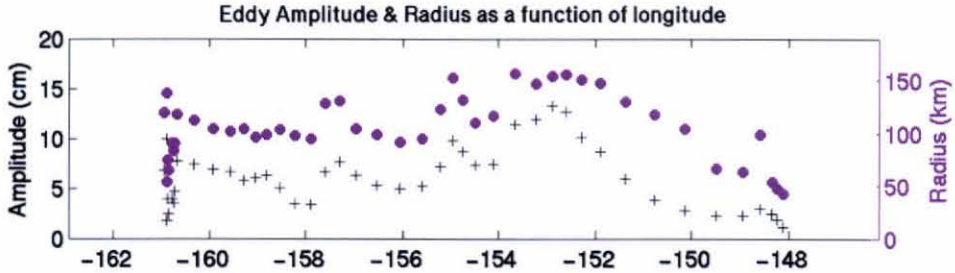

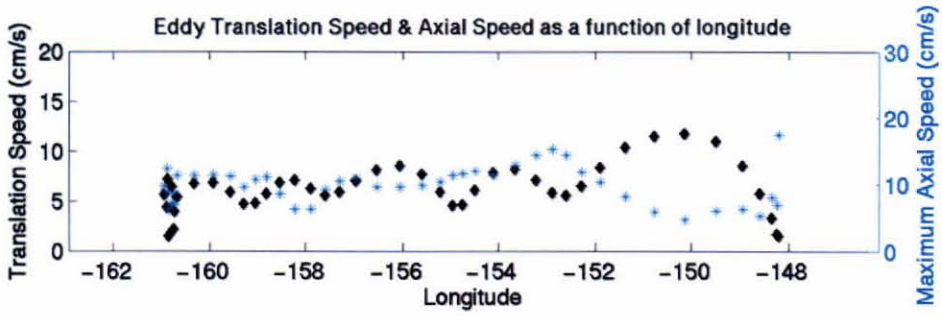

EID: 09A

This eddy spent 2-3 weeks spinning up and growing in size. Translates west and changes course to the NW when it reaches island chain, most likely because of interaction with topography. Eddy splits at 162W and track is dropped when the N moving split is drawn into another eddy. ADCP surface currents concur with expected northward velocities. Passes to the south of ALOHA, southern part of eddy interacts with islands of Maui and Oahu.

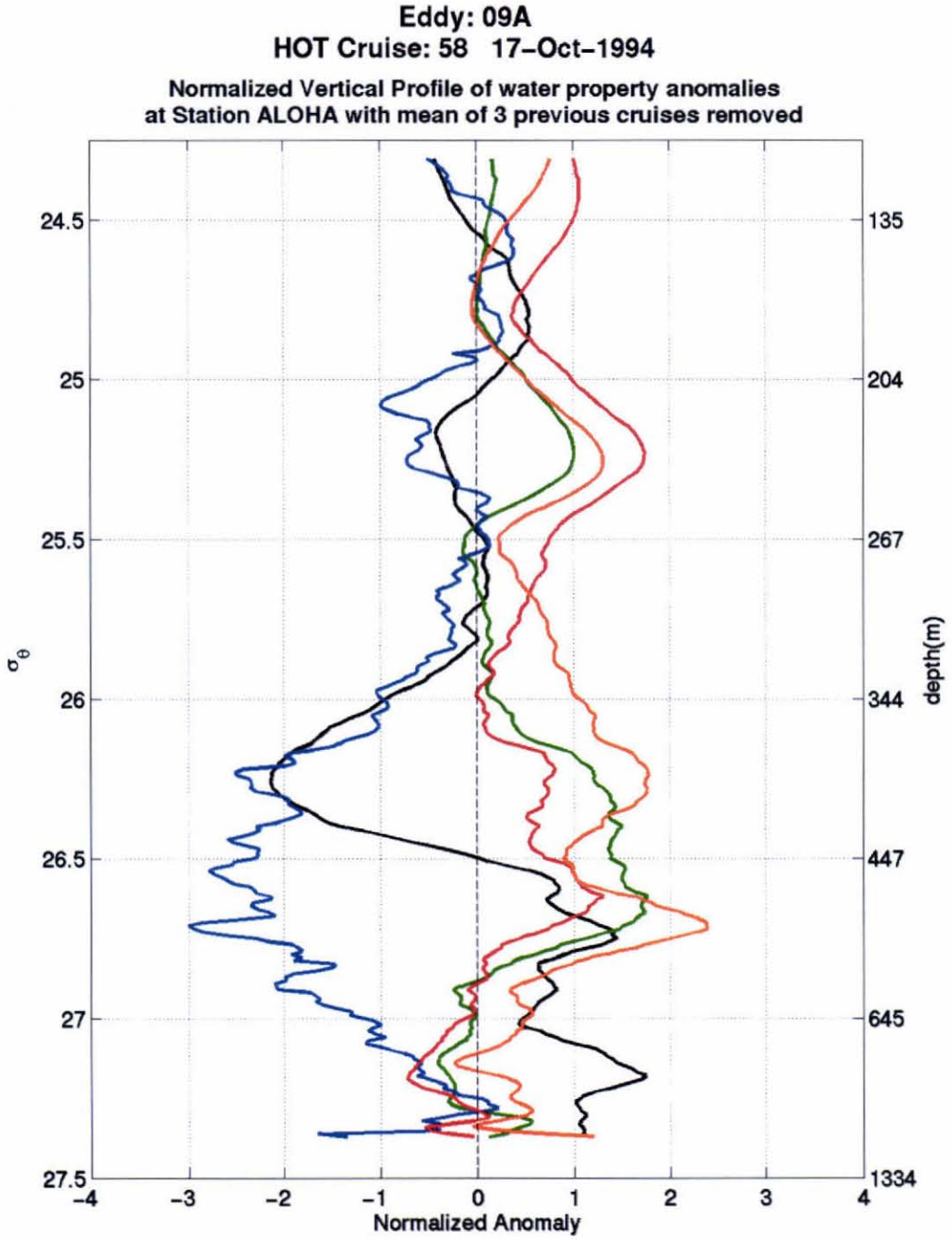
Eddy: 09A
HOT Cruise: 58 17-Oct-1994
Normalized Vertical Profile of water property anomalies
at Station ALOHA with mean of 3 previous cruises removed
24.5
25
25.5
26
26.5
27
27.5
σ_θ
135
204
267
344
447
645
1334
depth(m)
-4
-3
-2
-1
0
1
2
3
4
Normalized Anomaly

Eddy: 10A Dates in ALOHA box: 29-Mar-1995 to 29-Mar-1995

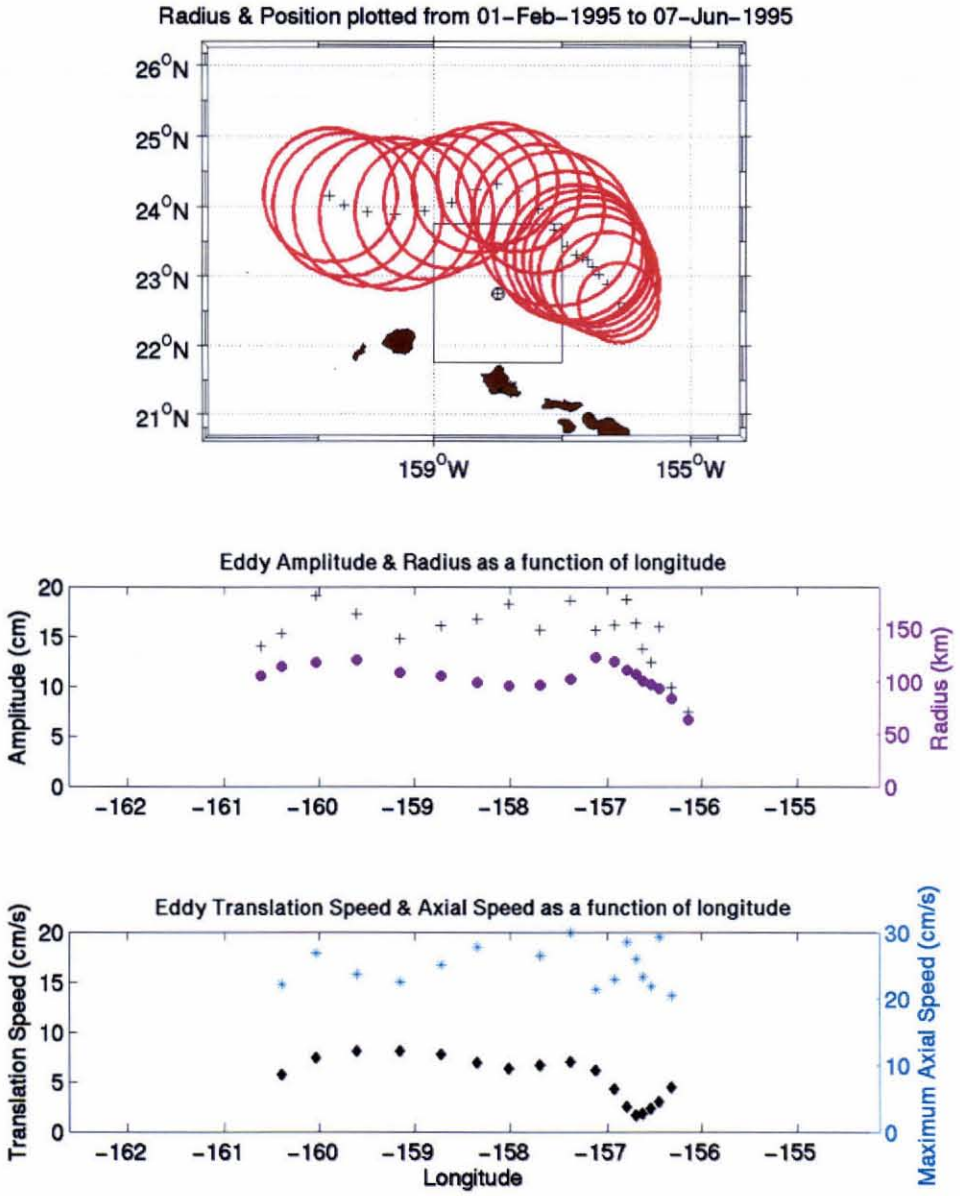

EID: 10A

The southern edge of this eddy barely grazed ALOHA. This eddy has a larger amplitude compared to most features. It is preceded by a cyclonic eddy with which it interacts. It is this interaction that forces the eddy to the north just before it reaches ALOHA. Impact on ALOHA is expected to be minimal, vertical profile of water properties shows no large anomalies.

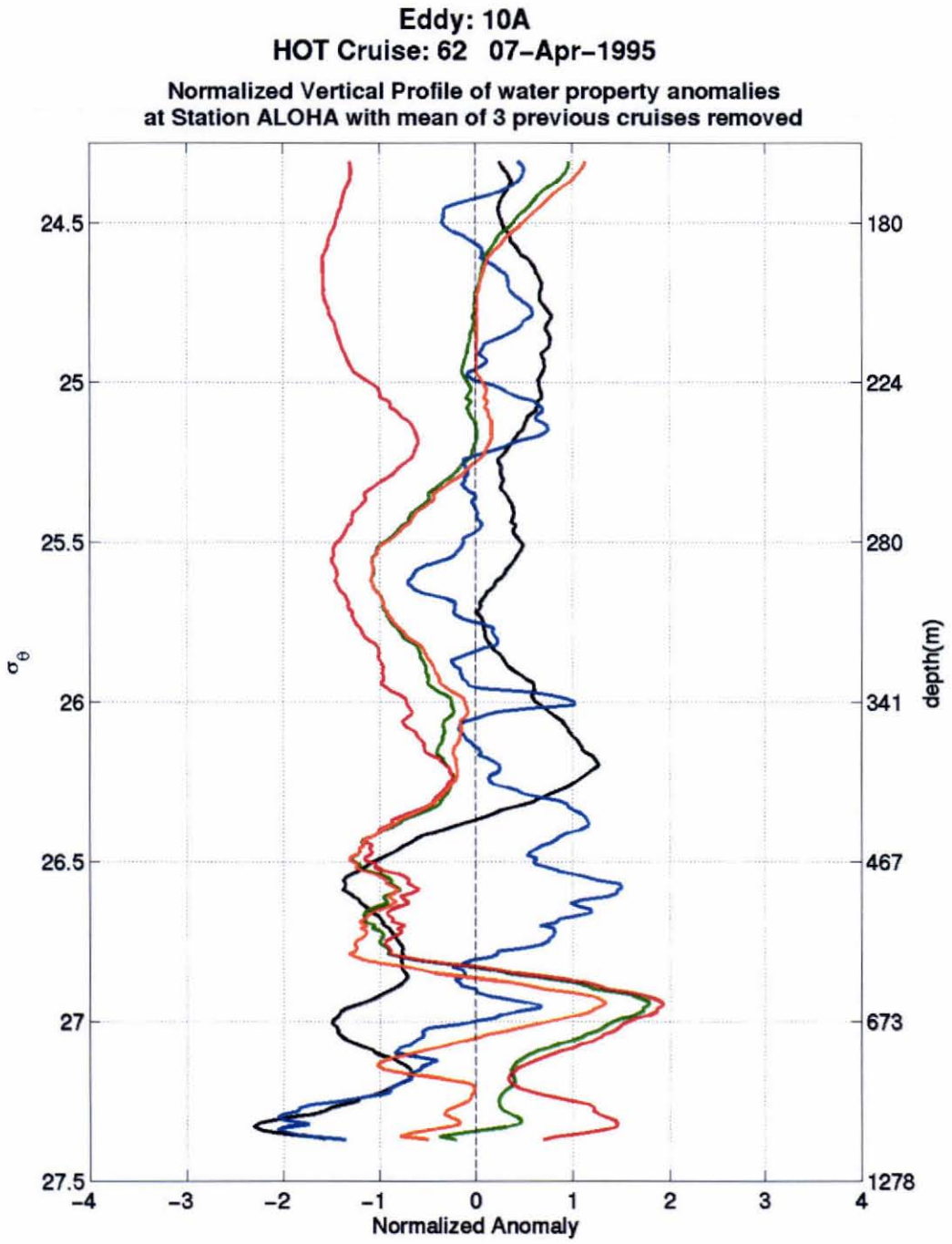
Eddy: 10A
HOT Cruise: 62 07-Apr-1995
Normalized Vertical Profile of water property anomalies
at Station ALOHA with mean of 3 previous cruises removed
24.5
25
25.5
26
26.5
27
27.5
σ_θ
180
224
280
341
467
673
1278
depth(m)
-4
-3
-2
-1
0
1
2
3
4
Normalized Anomaly

Eddy: 11C Dates in ALOHA box: 17-May-1995 to 07-Jun-1995

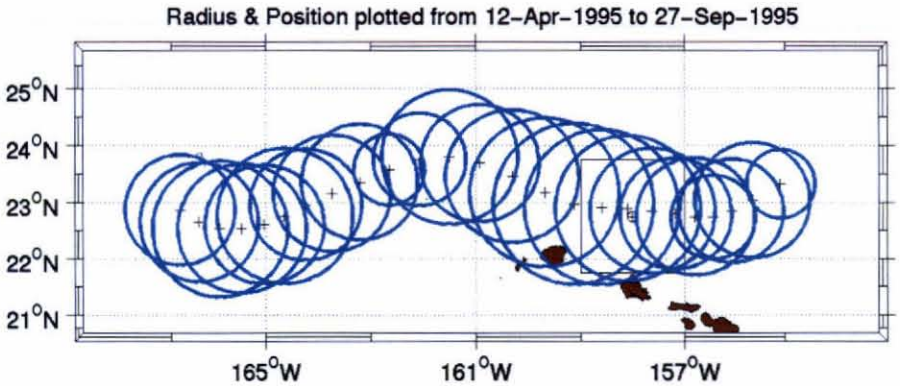

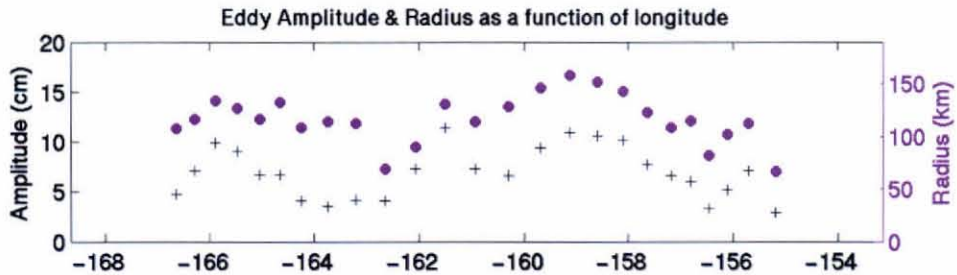

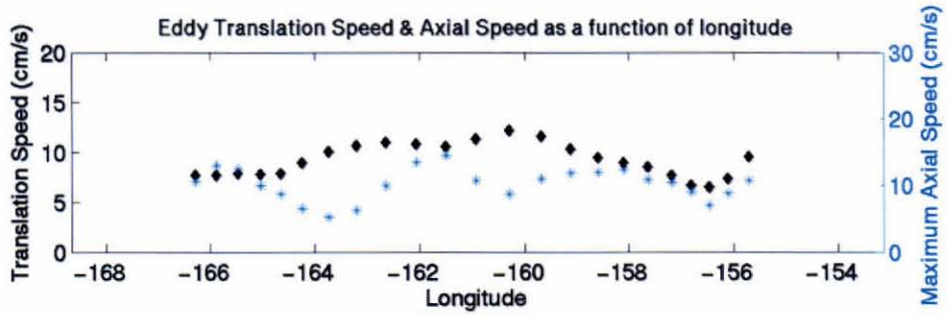

EID: 11C

This eddy formed at 156W in between two anticyclonic eddies. It remains sandwiched between these two eddies as it passes through ALOHA. Direction change to the SW at 162W due to "bouncing off" an anticyclonic eddy to the north.

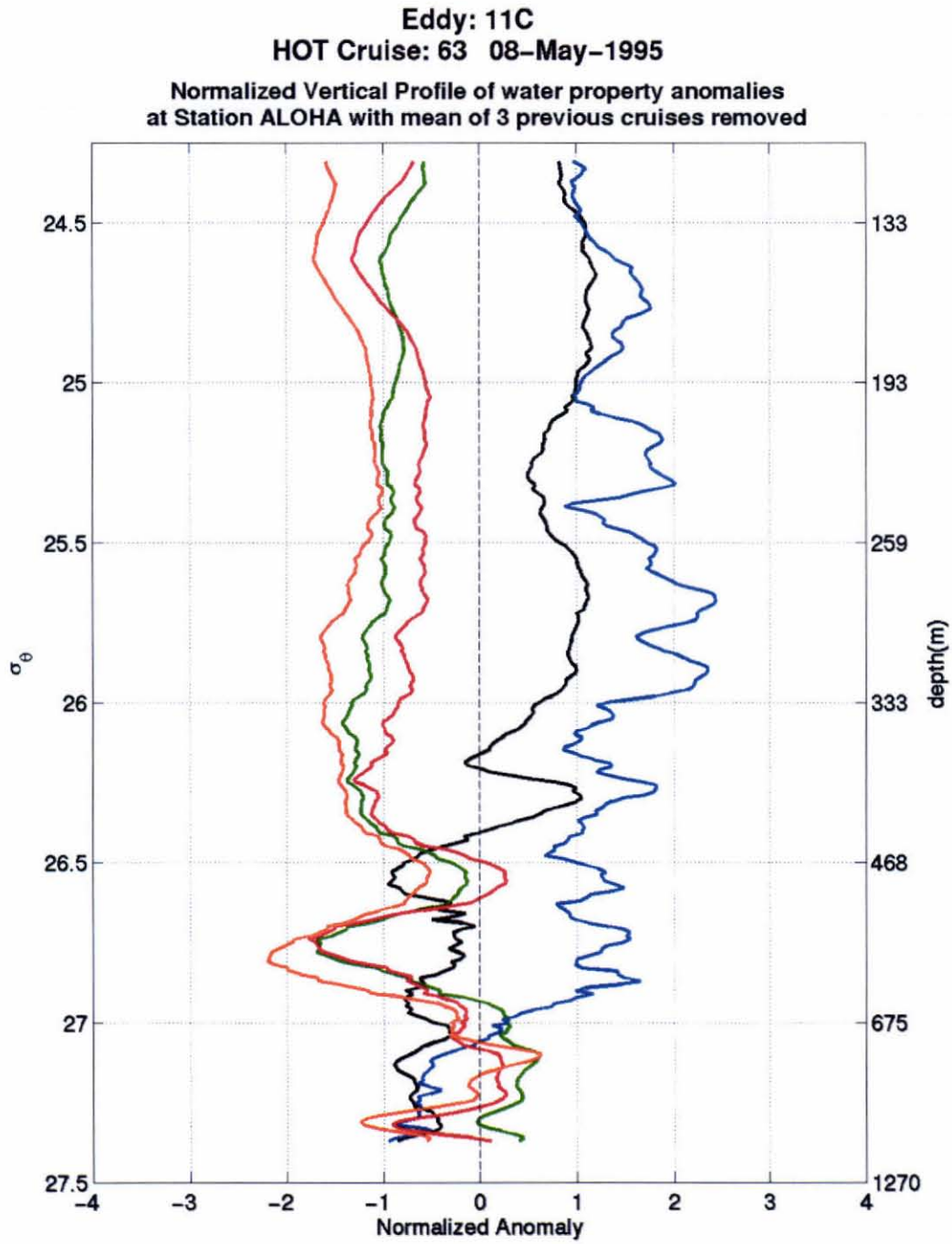
Eddy: 11C
HOT Cruise: 63 08-May-1995
Normalized Vertical Profile of water property anomalies
at Station ALOHA with mean of 3 previous cruises removed
24.5
25
25.5
26
26.5
27
27.5
σ_θ
133
193
259
333
468
675
1270
depth(m)
-4
-3
-2
-1
0
1
2
3
4
Normalized Anomaly

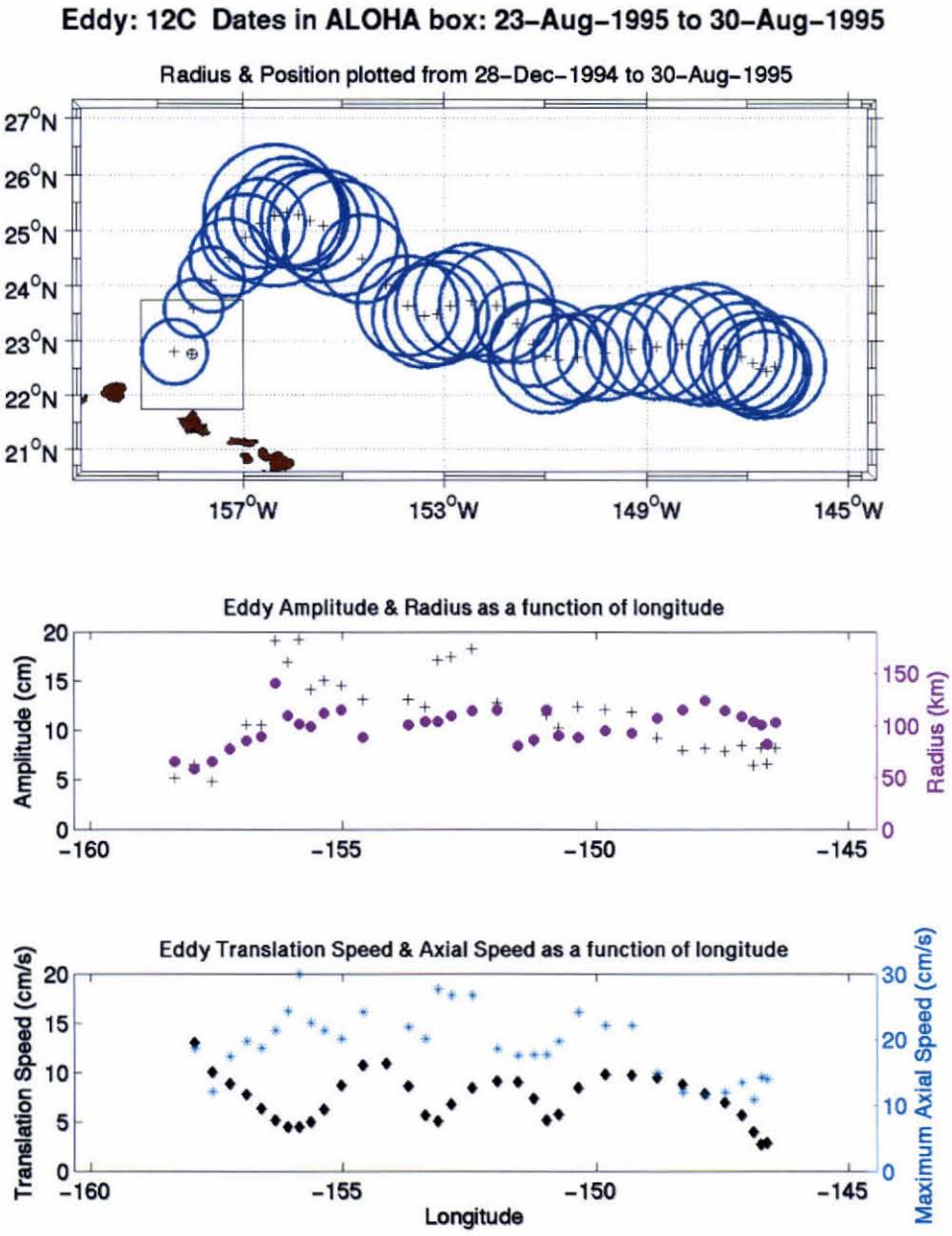

EID: 12C

This eddy was formed in a region of other eddy-eddy interactions and is squeezed south between two anticyclonic eddies, decays and breaks up as it reaches ALOHA.

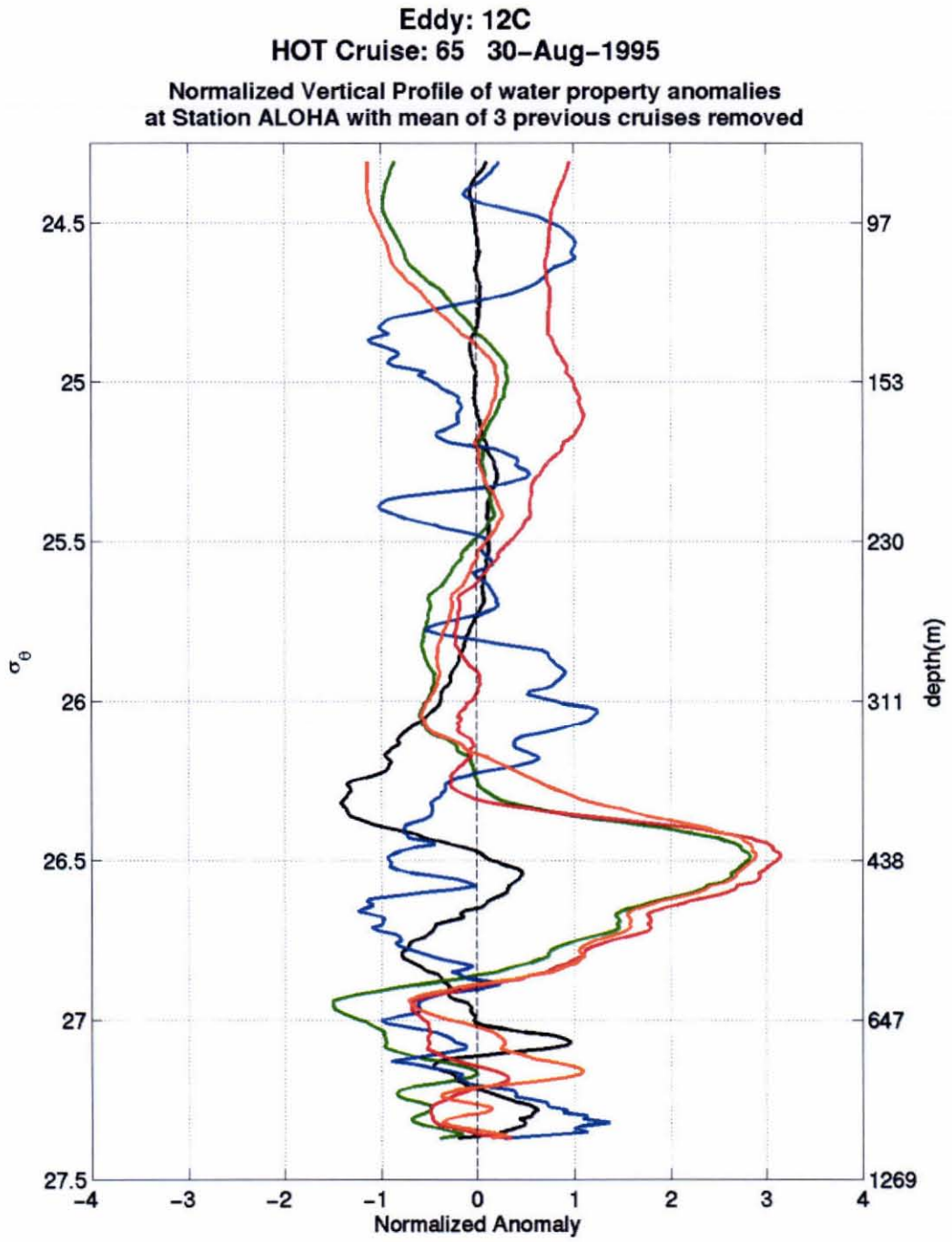
Eddy: 12C
HOT Cruise: 65 30-Aug-1995
Normalized Vertical Profile of water property anomalies
at Station ALOHA with mean of 3 previous cruises removed
24.5
25
25.5
26
26.5
27
27.5
σ_θ
97
153
230
311
438
647
1269
depth(m)
-4
-3
-2
-1
0
1
2
3
4
Normalized Anomaly

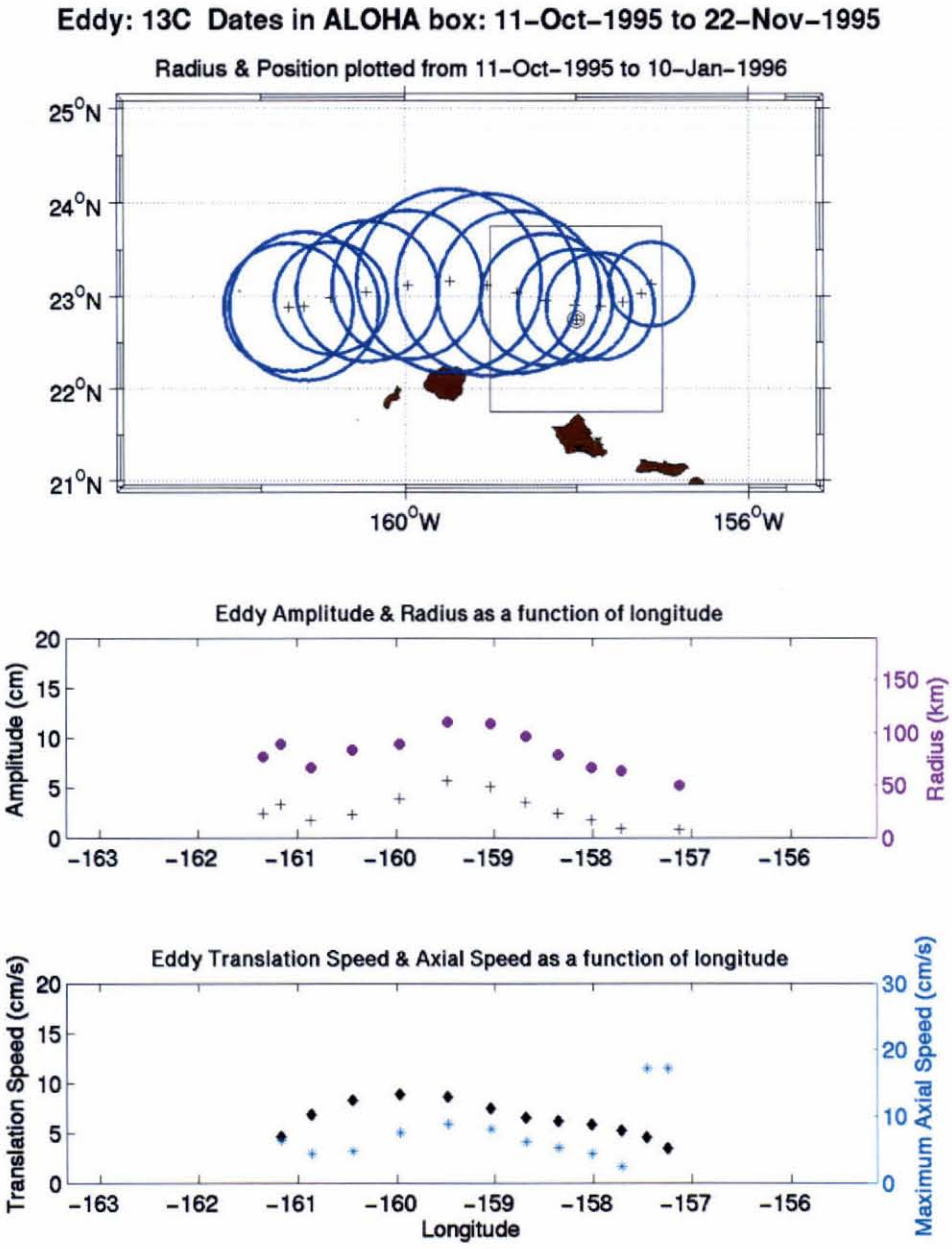

EID: 13C

This eddy is an offshoot from the break up of 12C, is short-lived and not remarkable.

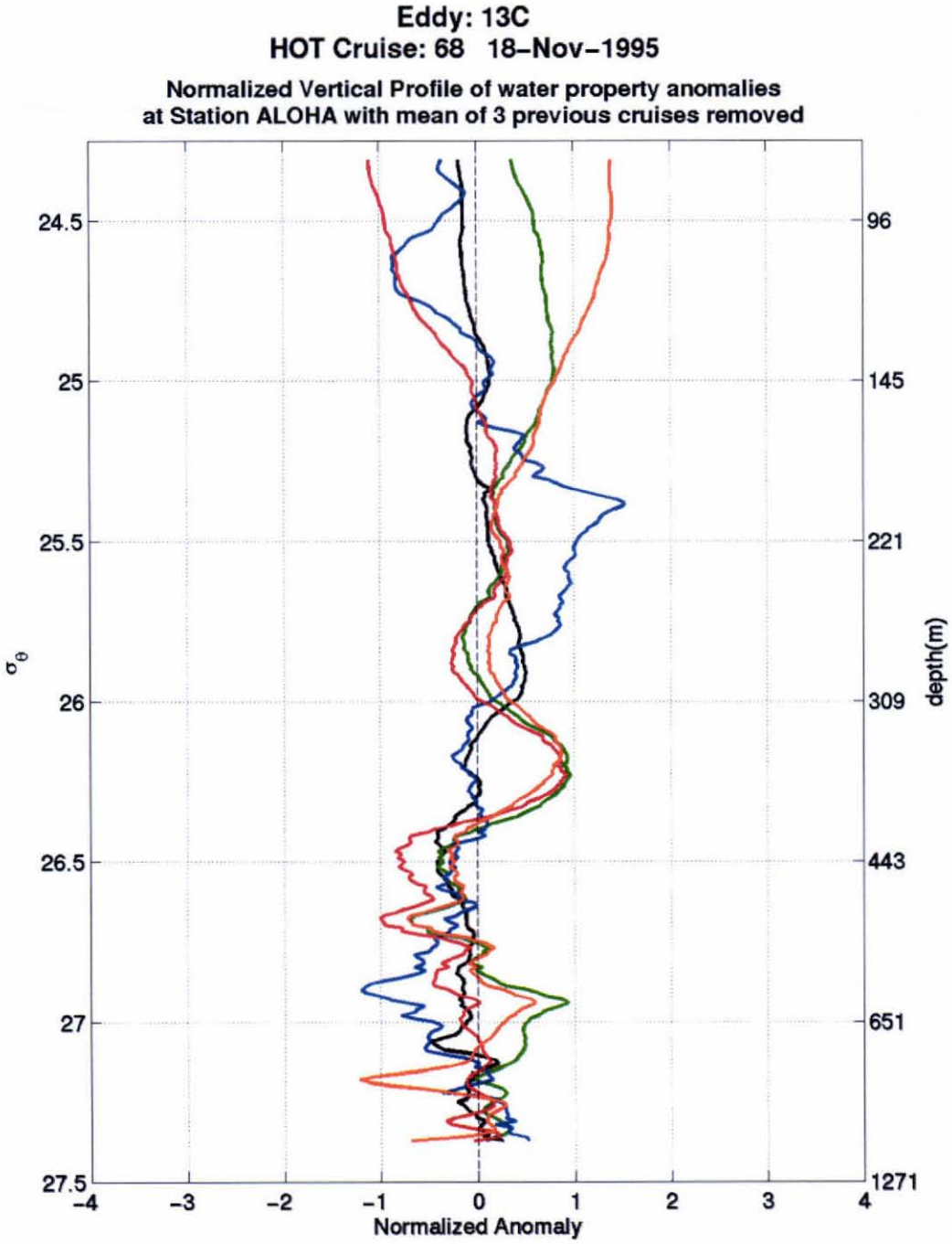
Eddy: 13C
HOT Cruise: 68 18-Nov-1995
Normalized Vertical Profile of water property anomalies
at Station ALOHA with mean of 3 previous cruises removed
24.5
25
25.5
26
26.5
27
27.5
σ_θ
96
145
221
309
443
651
1271
depth(m)
-4
-3
-2
-1
0
1
2
3
4
Normalized Anomaly

Eddy: 14C Dates in ALOHA box: 27-Dec-1995 to 17-Jan-1996

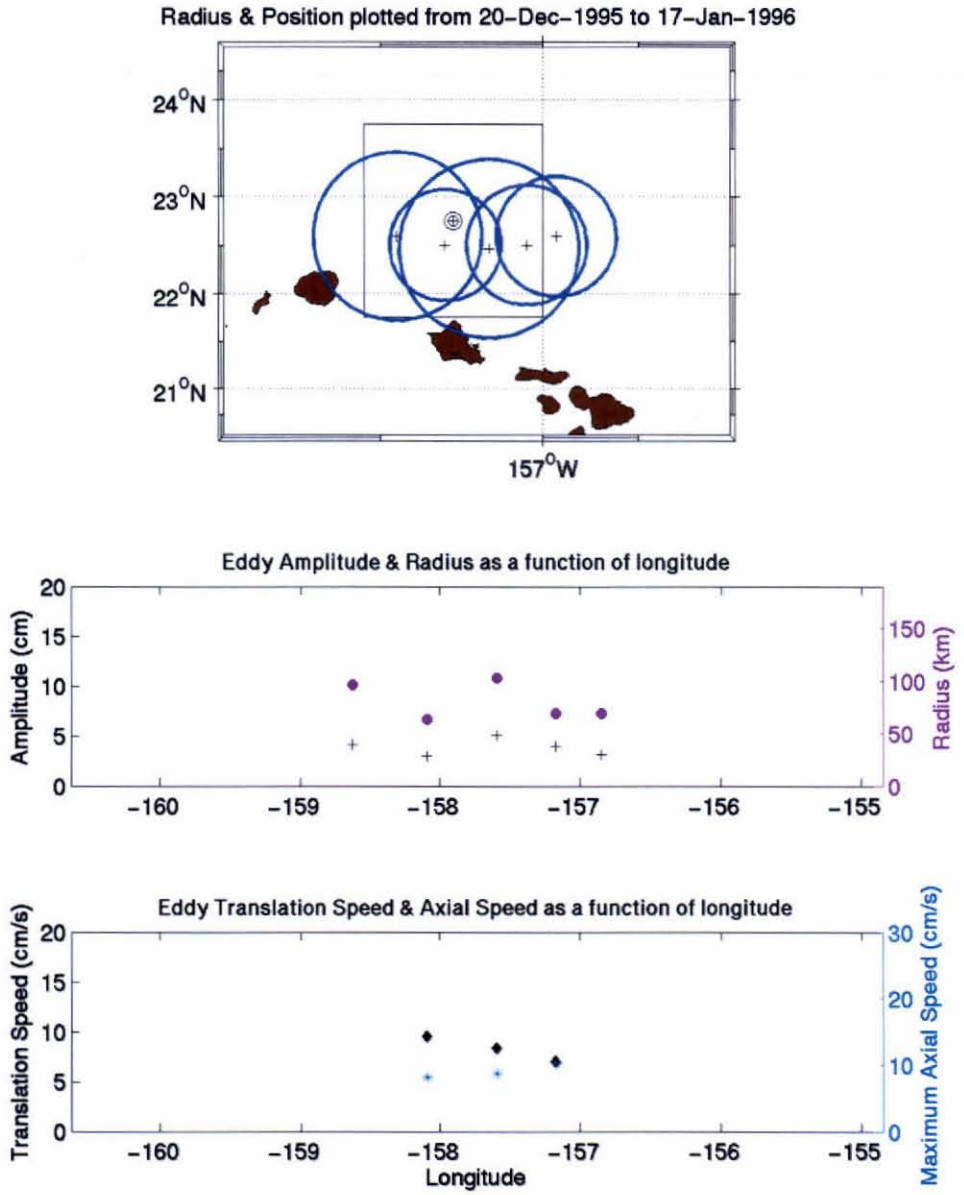

EID: 14C

This eddy appears to be the remnant of a feature that formed at 142W, vertical profile of water anomalies (salinity and dissolved oxygen) indicates there may be some remaining bolus transport on the 26.5σ_θ level.

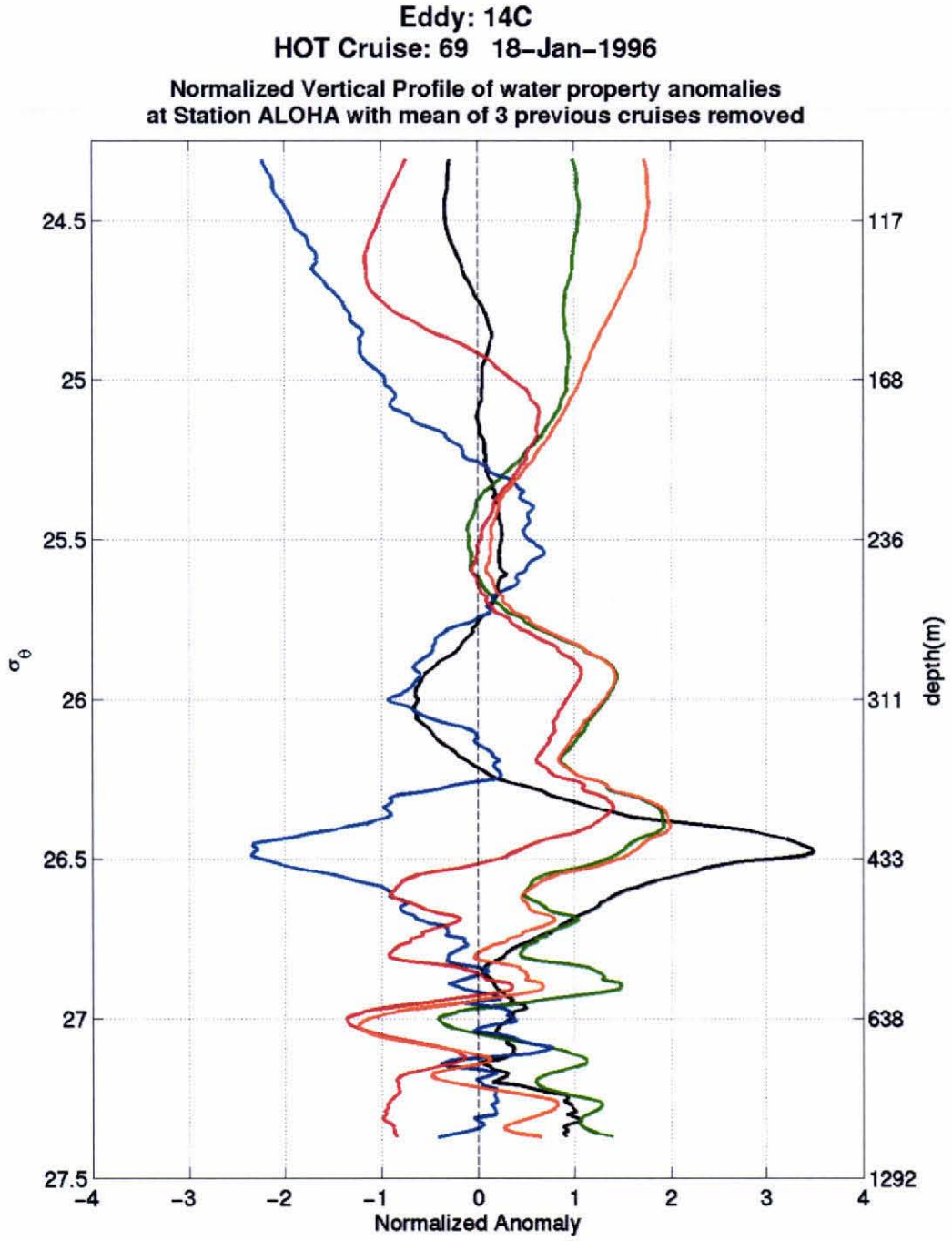
Eddy: 14C
HOT Cruise: 69 18-Jan-1996
Normalized Vertical Profile of water property anomalies
at Station ALOHA with mean of 3 previous cruises removed
24.5
25
25.5
26
26.5
27
27.5
σ_θ
117
168
236
311
433
638
1292
depth(m)
-4
-3
-2
-1
0
1
2
3
4
Normalized Anomaly

Eddy: 15C Dates in ALOHA box: 07-Feb-1996 to 20-Mar-1996

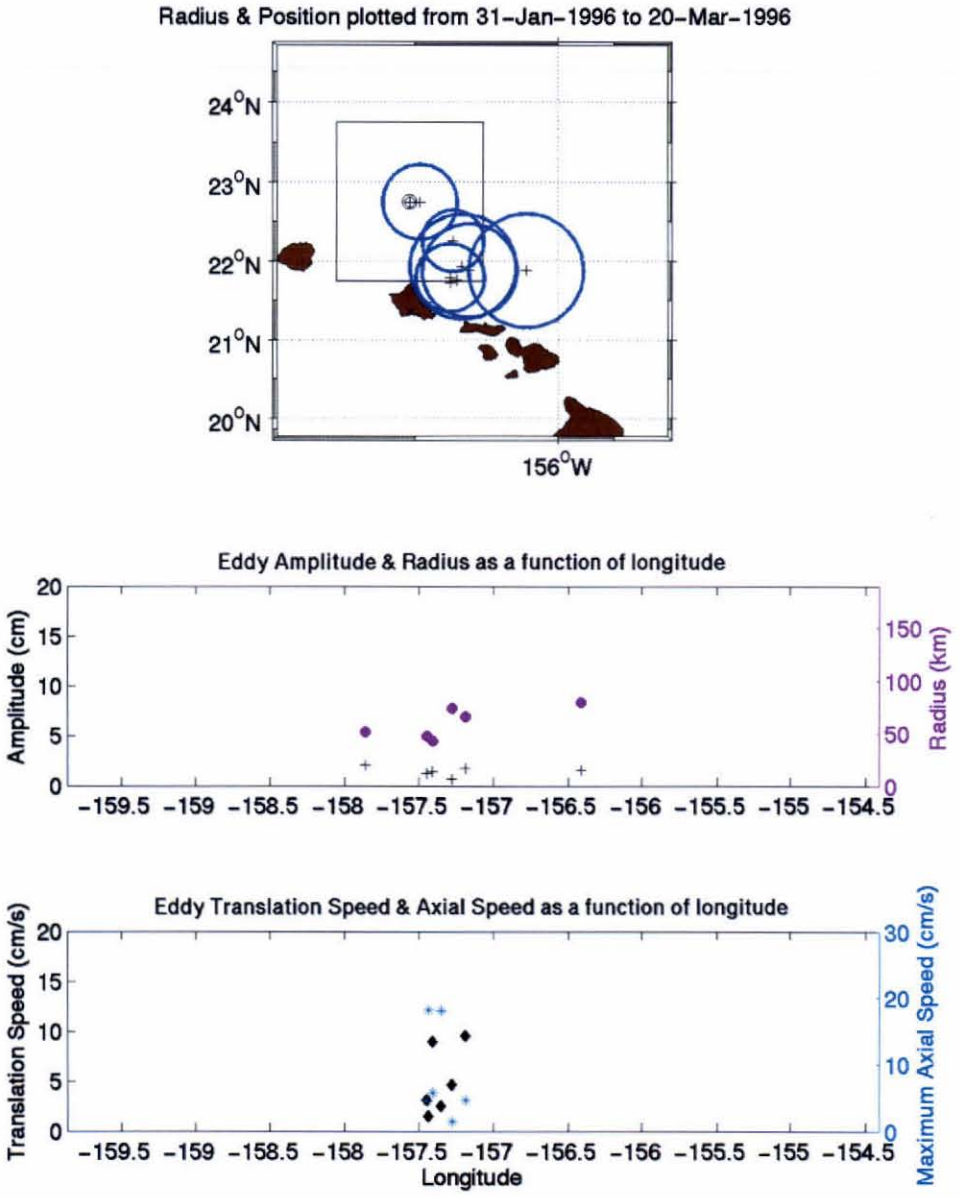

EID: 15C

This questionable eddy is an offshoot from an elongated eddy that formed around 140W that interacts with several eddies as it translates west. This elongated eddy visually collides with the islands of Oahu and Maui and appears to translate through Kaiwi Channel after the track is dropped. The last time step tracks the eddy over ALOHA, but this is doubtful and is probably the tracking algorithm jumping features.

Eddy: 16A Dates in ALOHA box: 01-May-1996 to 22-May-1996

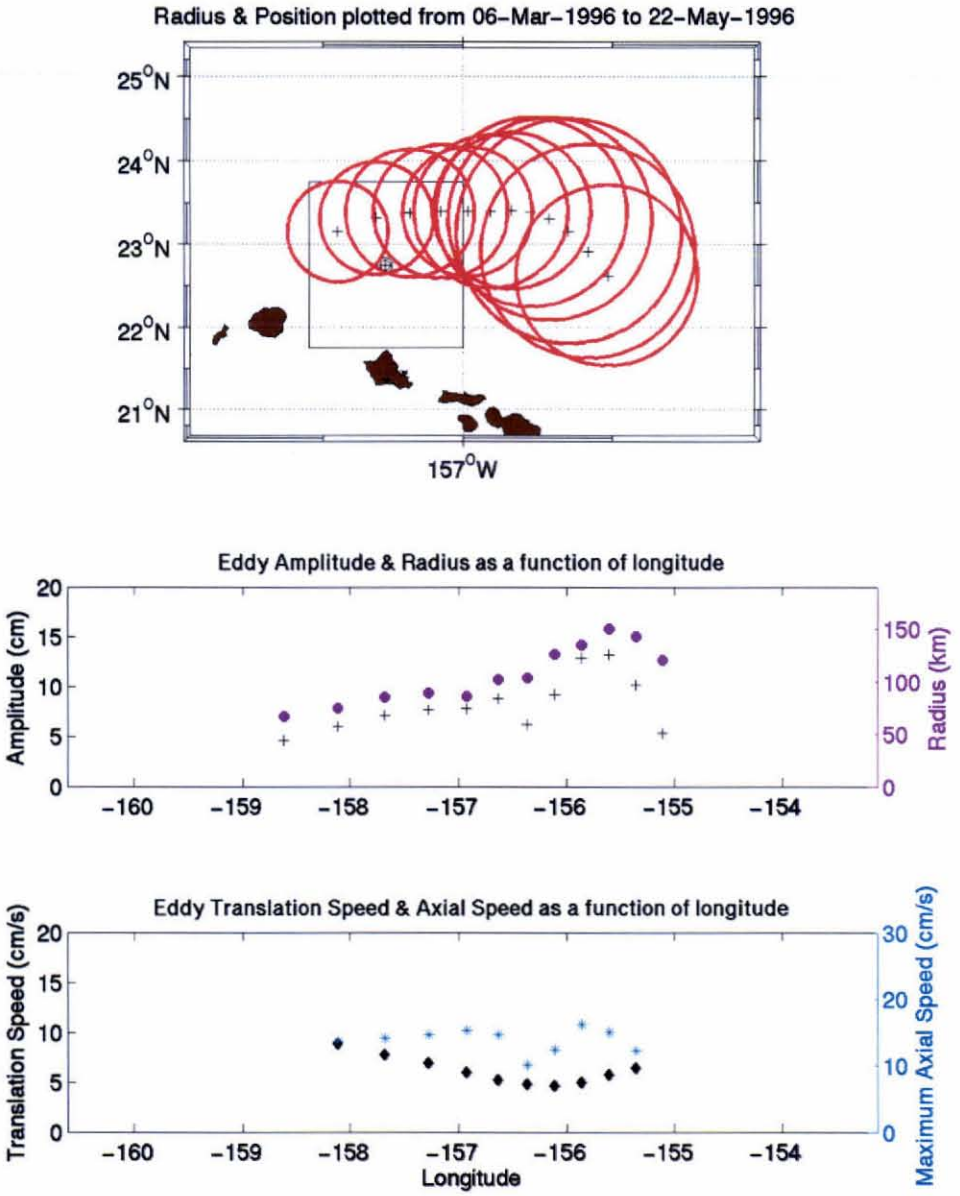

EID: 16A

This eddy formed at 155W and moves NW as it gained shape, then moved west and passed north of ALOHA and dissipated.

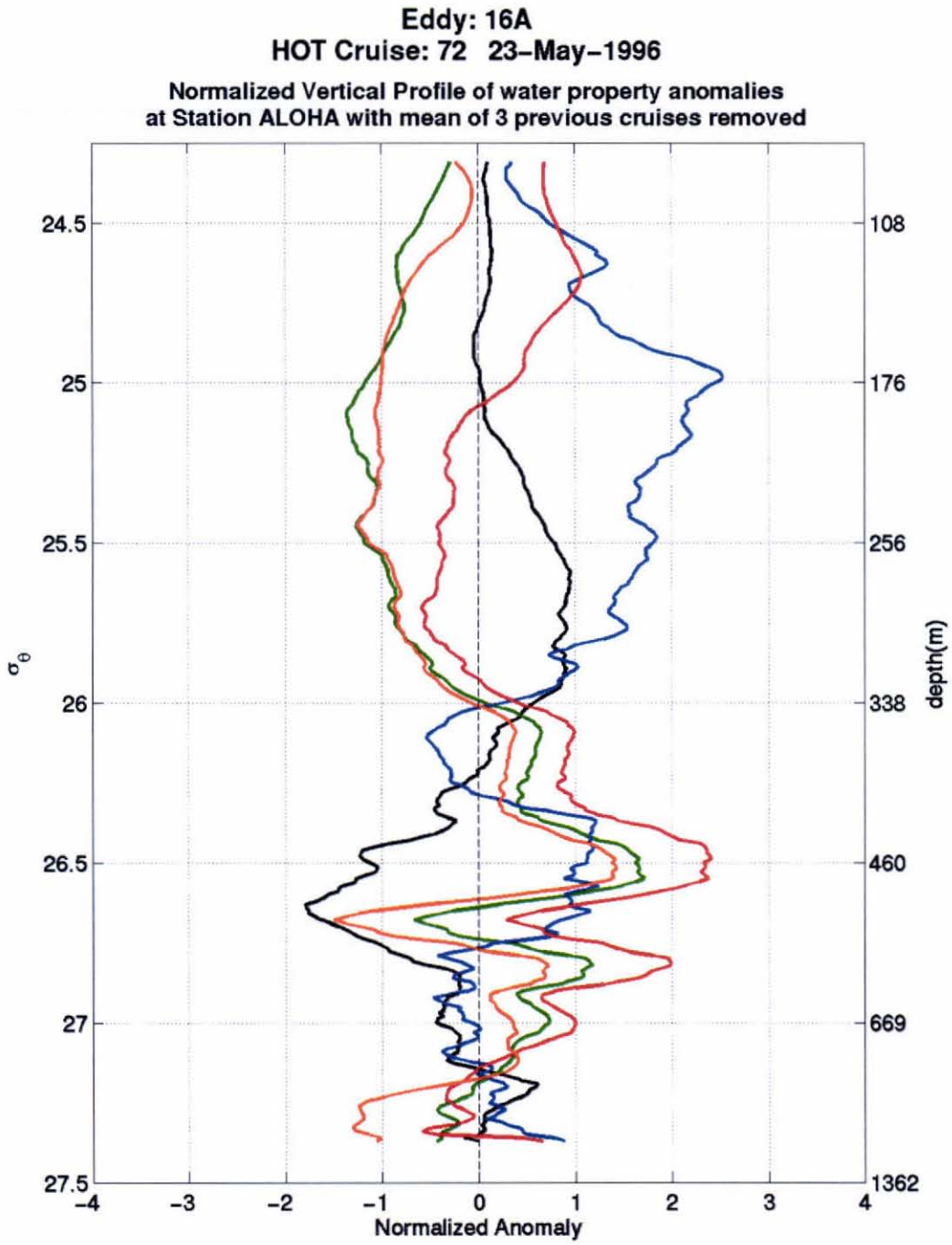
Eddy: 16A
HOT Cruise: 72 23-May-1996
Normalized Vertical Profile of water property anomalies
at Station ALOHA with mean of 3 previous cruises removed
24.5
25
25.5
26
26.5
27
27.5
σ_θ
108
176
256
338
460
669
1362
depth(m)
-4
-3
-2
-1
0
1
2
3
4
Normalized Anomaly

Eddy: 17A Dates in ALOHA box: 03-Jul-1996 to 11-Sep-1996

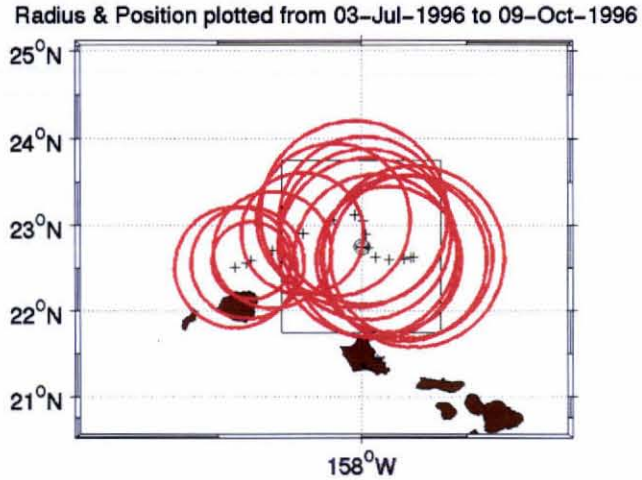

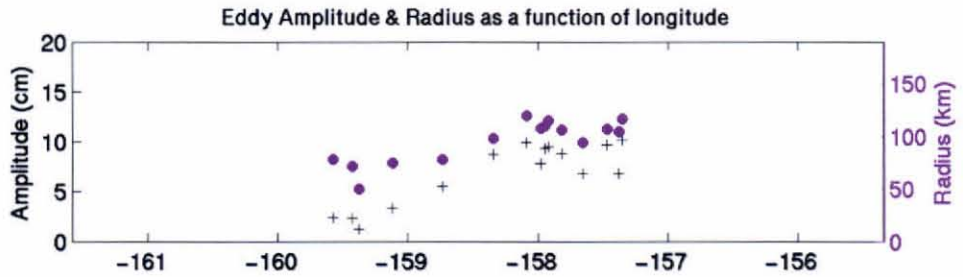

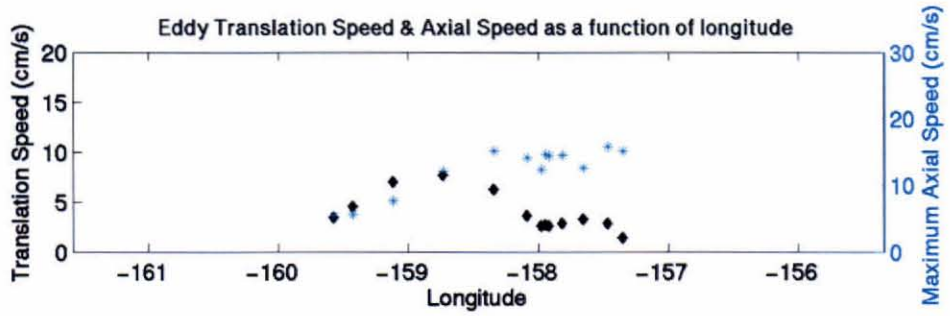

EID: 17A

This slow moving eddy formed and spent most of its short lifetime in the region around ALOHA. Eddy appeared to dissipate as a result of interacting with Kauai.

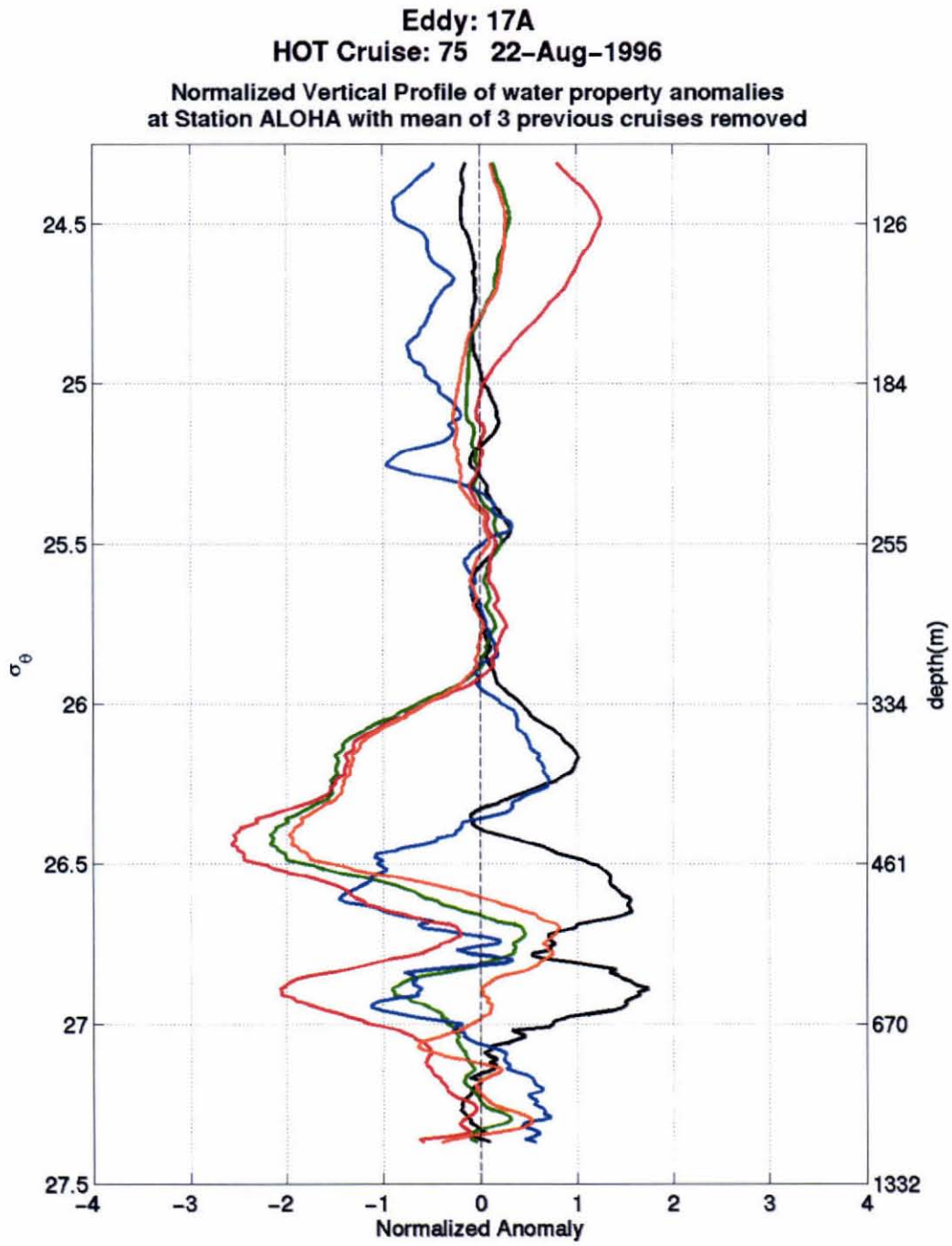
Eddy: 17A
HOT Cruise: 75 22-Aug-1996
Normalized Vertical Profile of water property anomalies
at Station ALOHA with mean of 3 previous cruises removed
24.5
25
25.5
26
26.5
27
27.5
σ_θ
126
184
255
334
461
670
1332
depth(m)
-4
-3
-2
-1
0
1
2
3
4
Normalized Anomaly

Eddy: 18C Dates in ALOHA box: 02-Oct-1996 to 06-Nov-1996

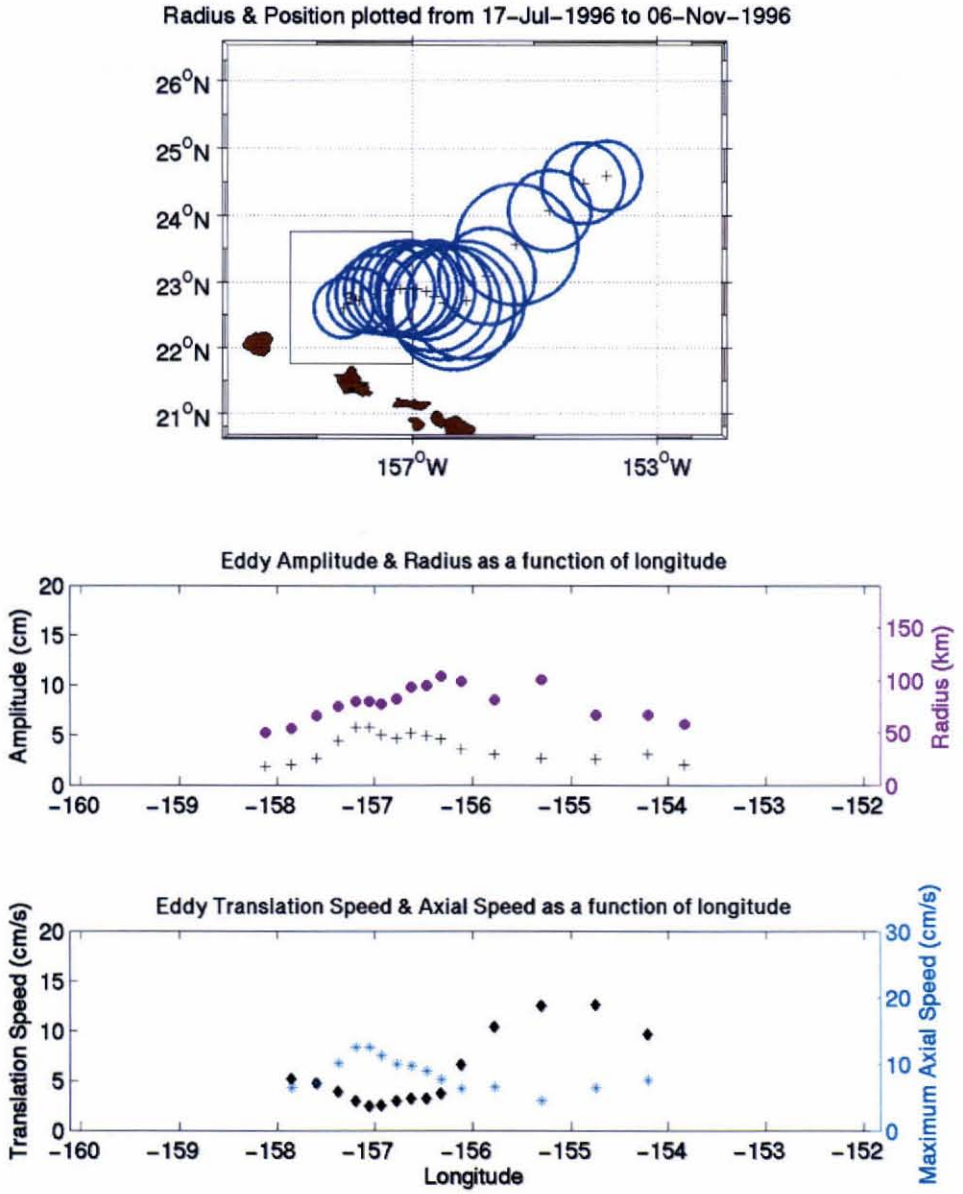

EID: 18C

This eddy may have formed as an offshoot of an eddy from the north. It stalled at the east end of the boxed region and re-intensified. Appeared to interact with Oahu after passing over ALOHA and track was dropped. Dissipated as a result of the island interaction.

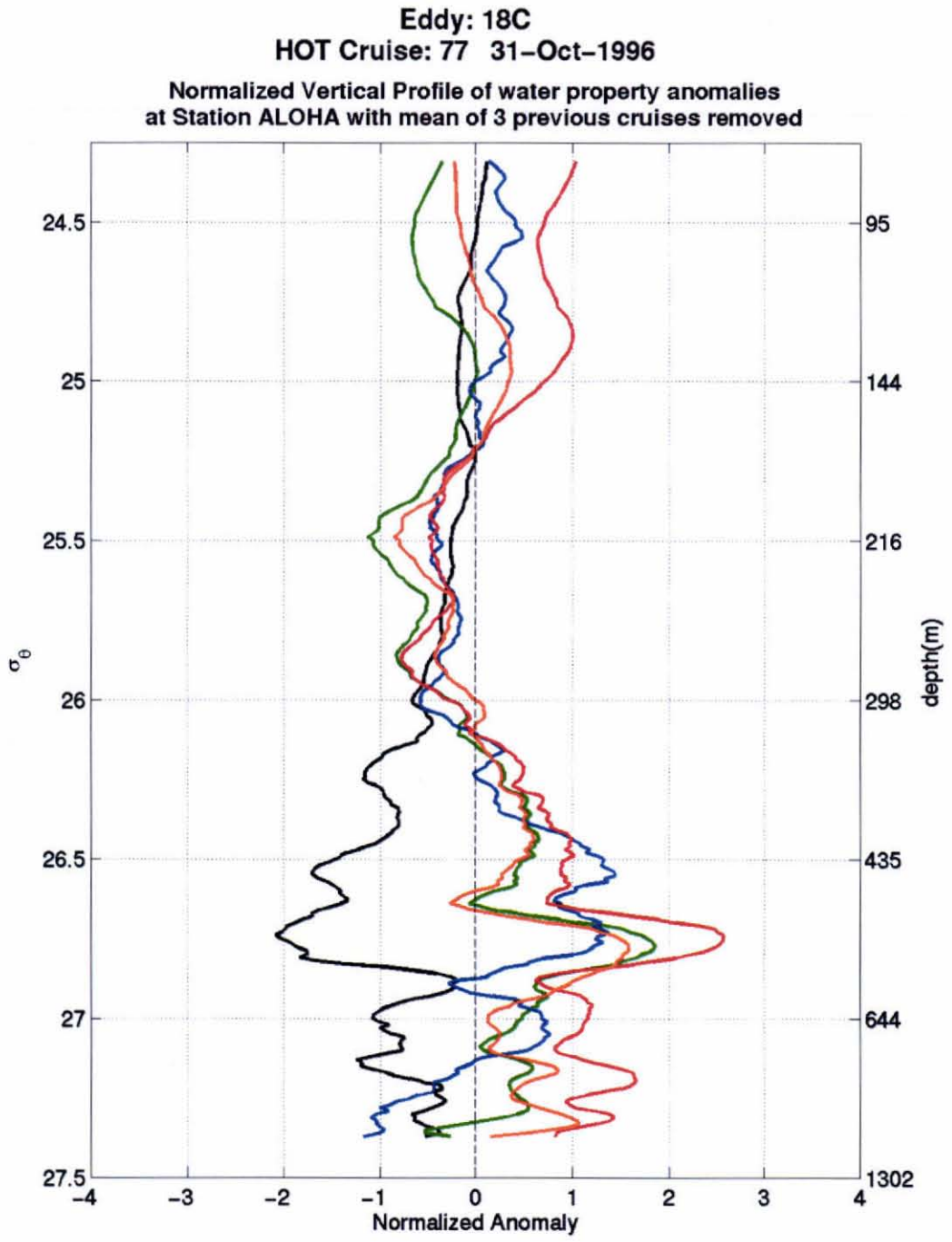
Eddy: 18C
HOT Cruise: 77 31-Oct-1996
Normalized Vertical Profile of water property anomalies
at Station ALOHA with mean of 3 previous cruises removed
24.5
25
25.5
26
26.5
27
27.5
σ_θ
95
144
216
298
435
644
1302
depth(m)
-4
-3
-2
-1
0
1
2
3
4
Normalized Anomaly

Eddy: 19A Dates in ALOHA box: 04-Dec-1996 to 11-Dec-1996

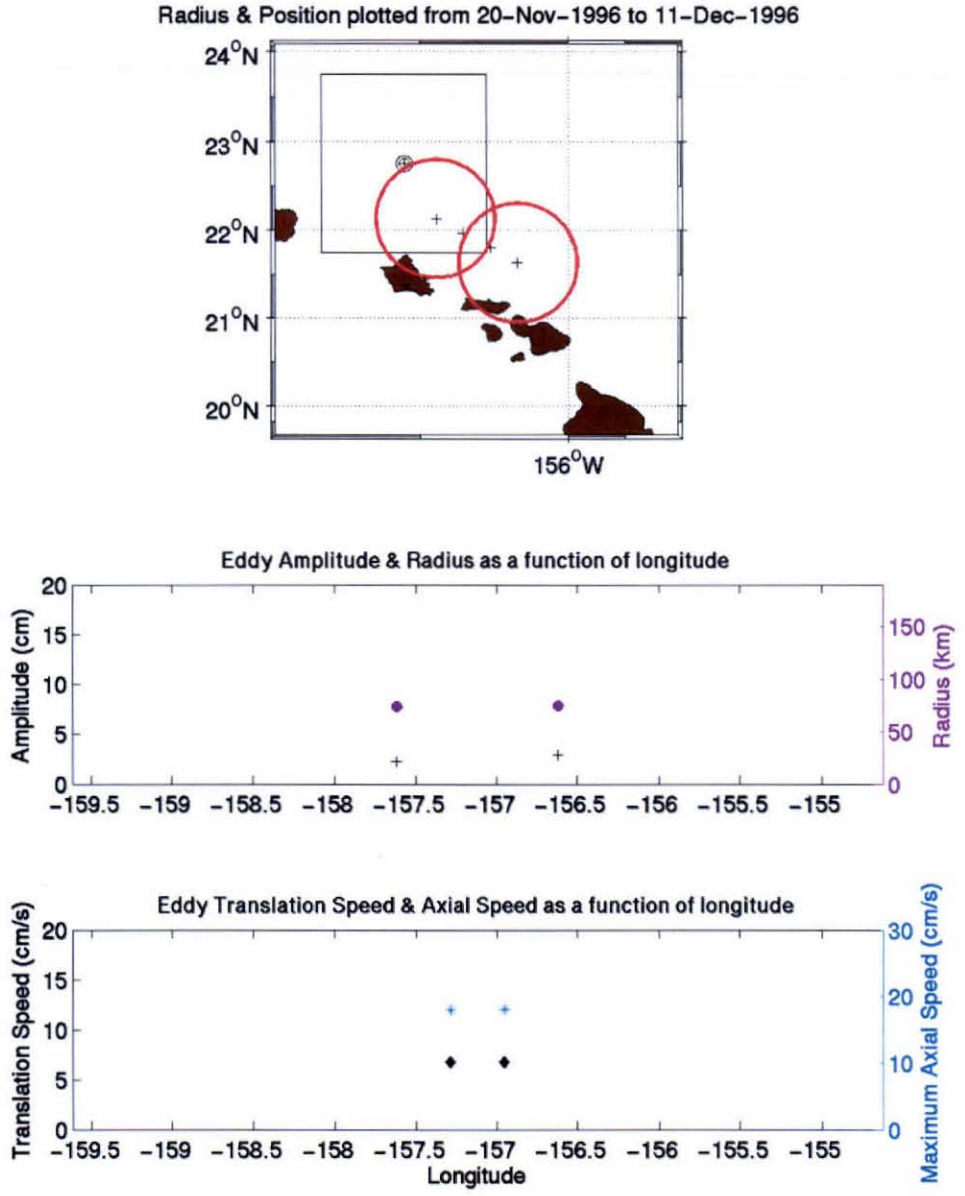

EID: 19A

This questionable eddy was short-lived and traveled up the island chain but did not display circular characteristics associated with other eddies.

Eddy: 20A Dates in ALOHA box: 29-Jan-1997 to 26-Feb-1997

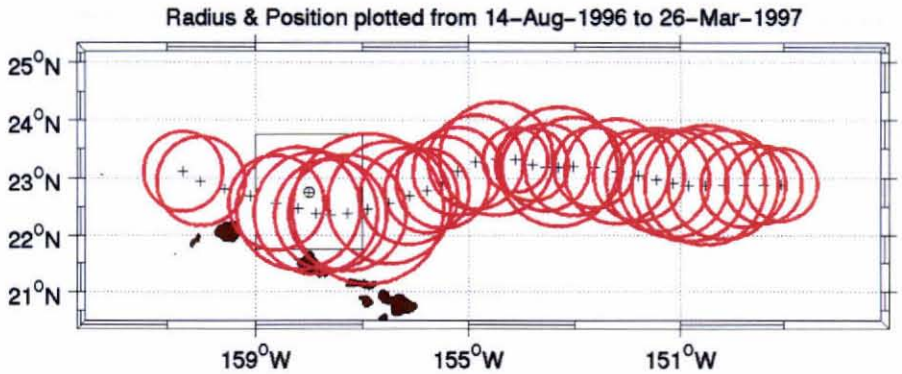

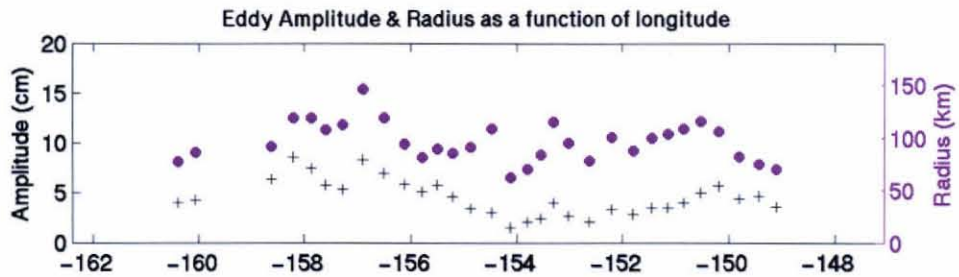

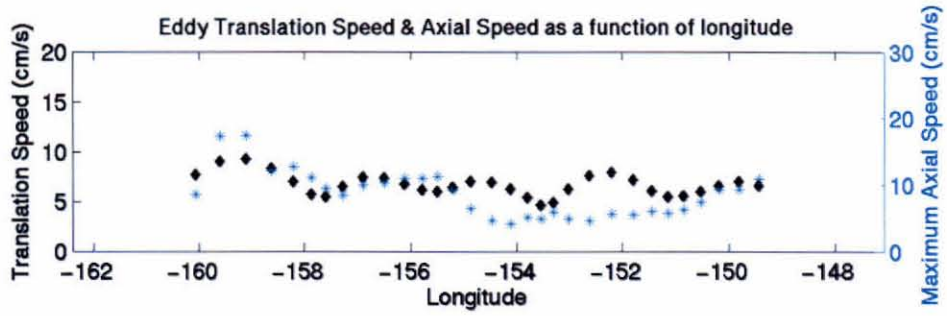

EID: 20A

This eddy formed at 149W and translated unimpeded to the west until it reached 154W where it was drawn up next to a cyclonic eddy. This interaction caused it to elongate and split. The track continued to follow the south split and the eddy continued to weaken as it passed ALOHA and came into contact with the island of Oahu.

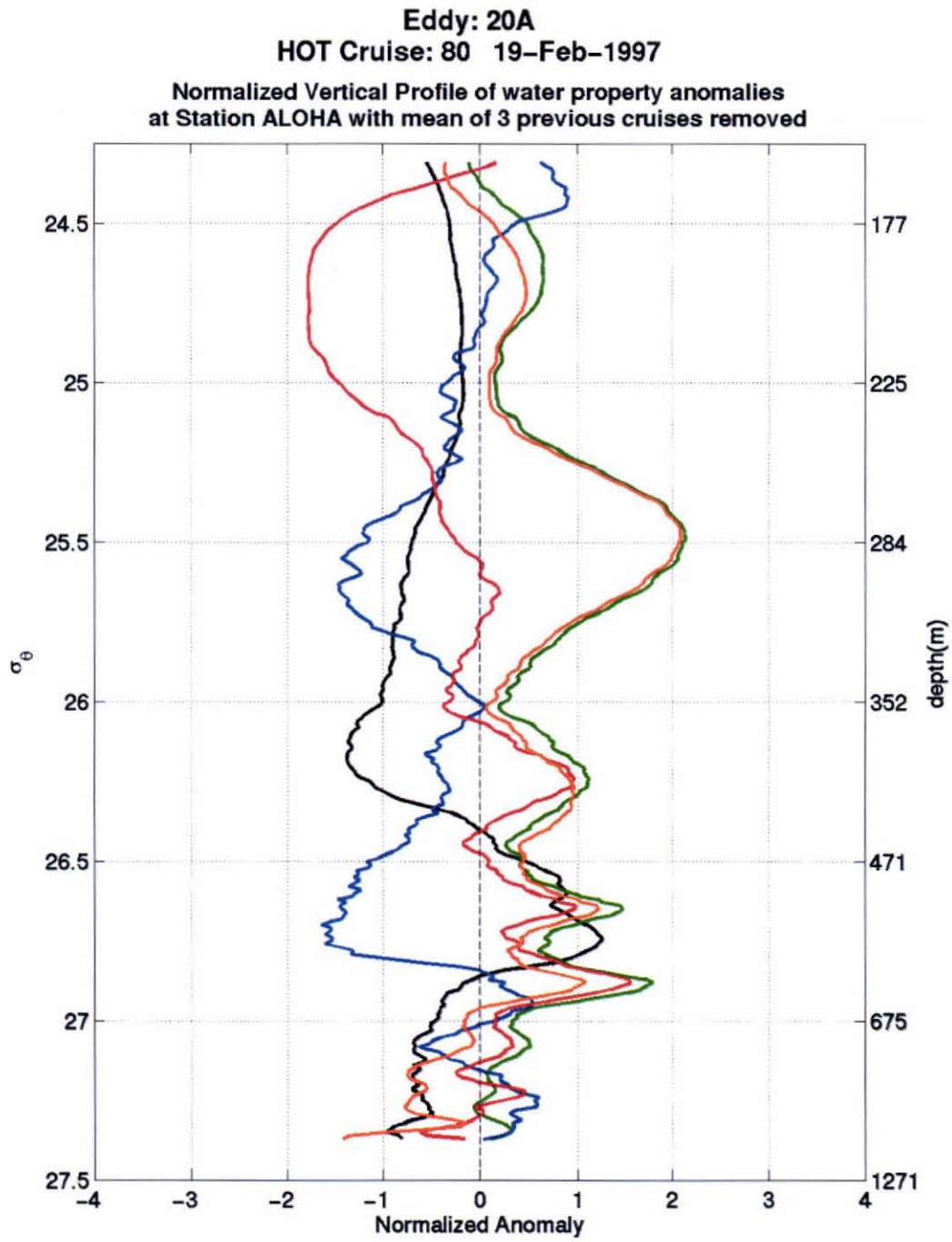
Eddy: 20A
HOT Cruise: 80 19-Feb-1997
Normalized Vertical Profile of water property anomalies
at Station ALOHA with mean of 3 previous cruises removed
24.5
25
25.5
26
26.5
27
27.5
σ_θ
177
225
284
352
471
675
1271
depth(m)
-4
-3
-2
-1
0
1
2
3
4
Normalized Anomaly

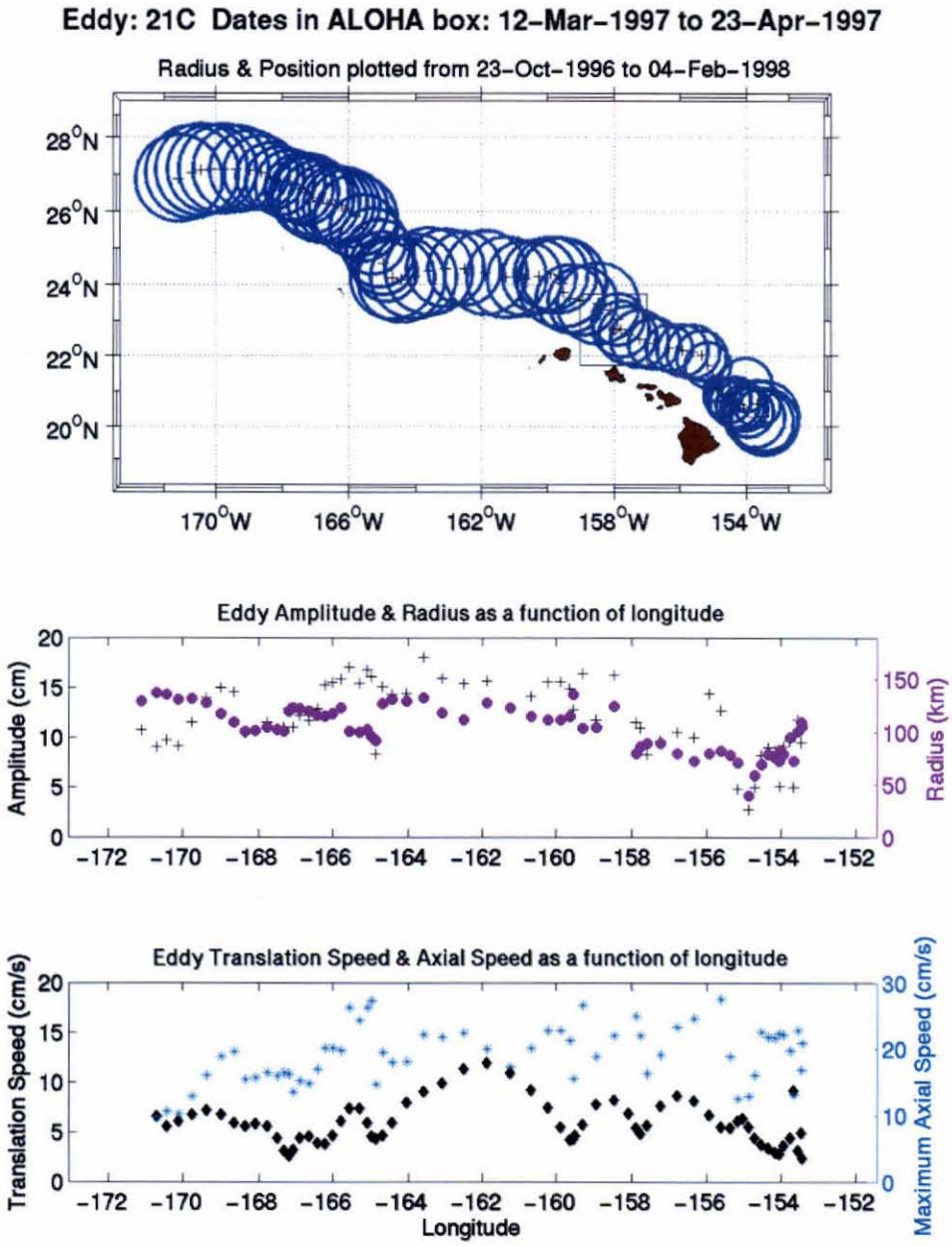

EID: 21C

This eddy formed east of the island of Hawaii, translated northwest along the north side of the island chain and over ALOHA. The eddy continued west until diverted to the north by another eddy. By ALOHA, this eddy was followed close behind by an anticyclonic eddy.

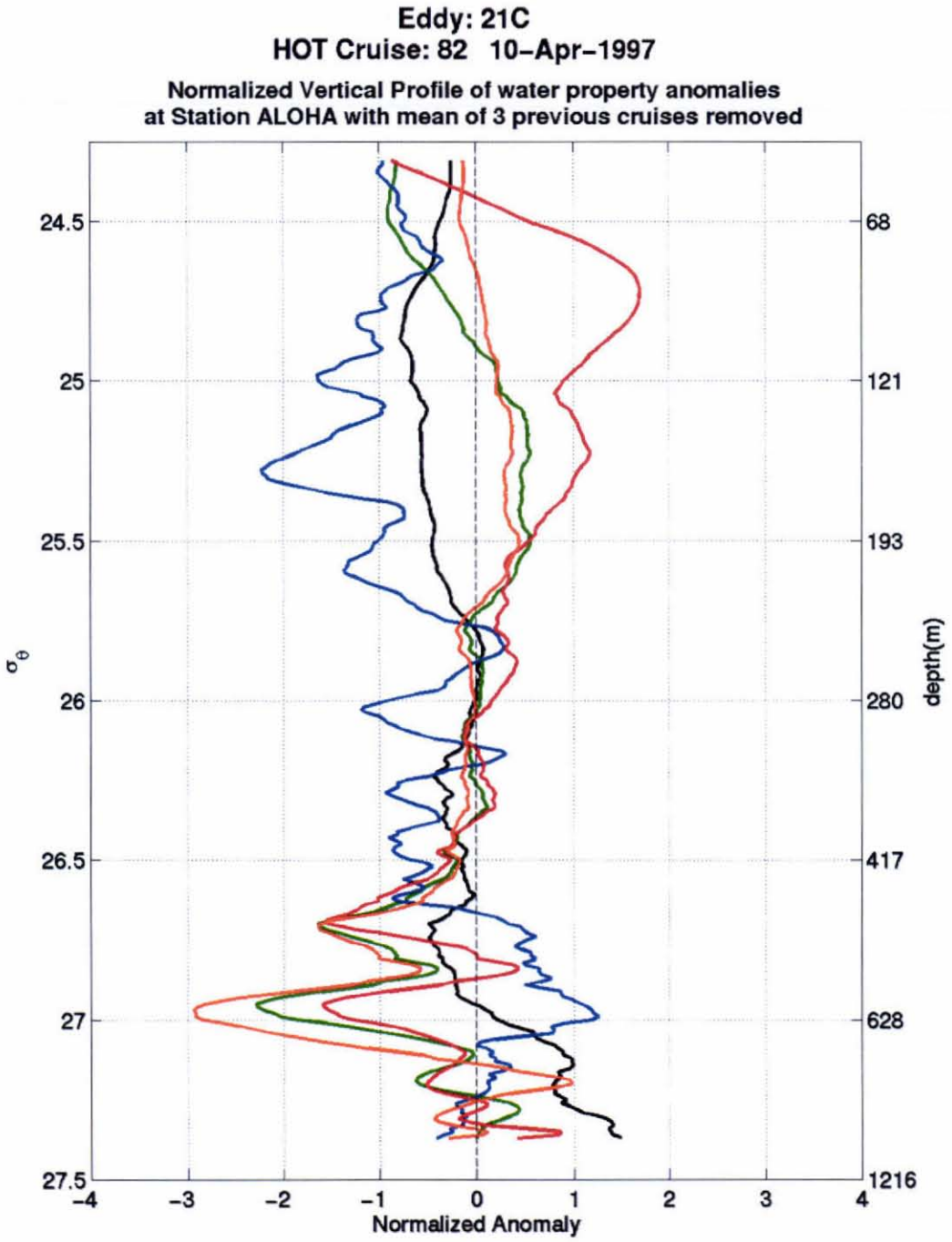
Eddy: 21C
HOT Cruise: 82 10-Apr-1997
Normalized Vertical Profile of water property anomalies
at Station ALOHA with mean of 3 previous cruises removed
24.5
25
25.5
26
26.5
27
27.5
σ_θ
68
121
193
280
417
628
1216
depth(m)
-4
-3
-2
-1
0
1
2
3
4
Normalized Anomaly

Eddy: 22A Dates in ALOHA box: 30-Apr-1997 to 11-Jun-1997

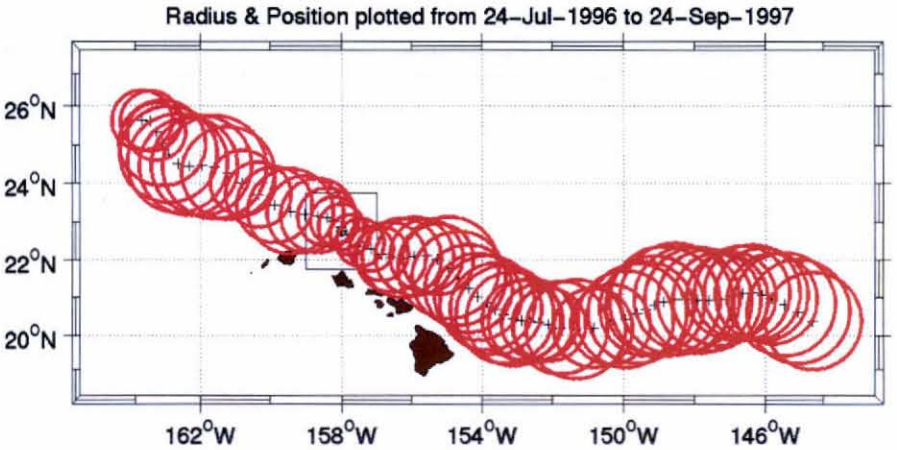

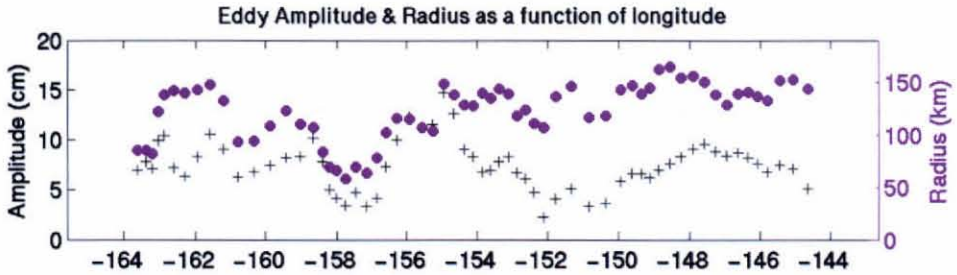

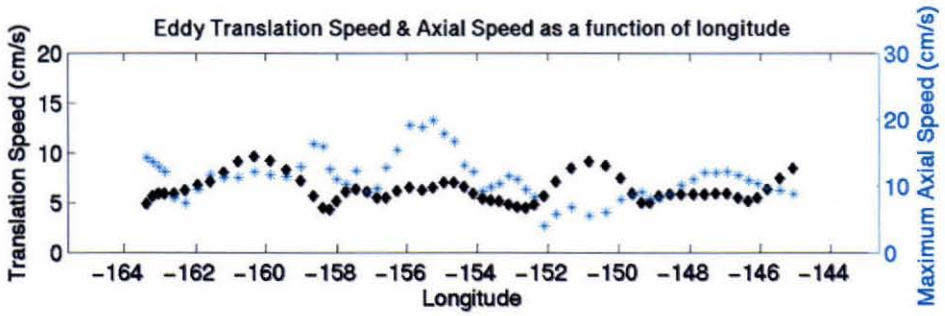

EID: 22A

This eddy formed around 21N and 145W and translated west until it encountered the Hawaiian islands, then it moved NW, possibly due to eddy-island interactions and also eddy-eddy interactions when it appeared to be squeezed north between two cyclonic eddies. Decreases in intensity (amplitude and radius) over ALOHA, then gets larger again, eventually dissipates NW of the islands.

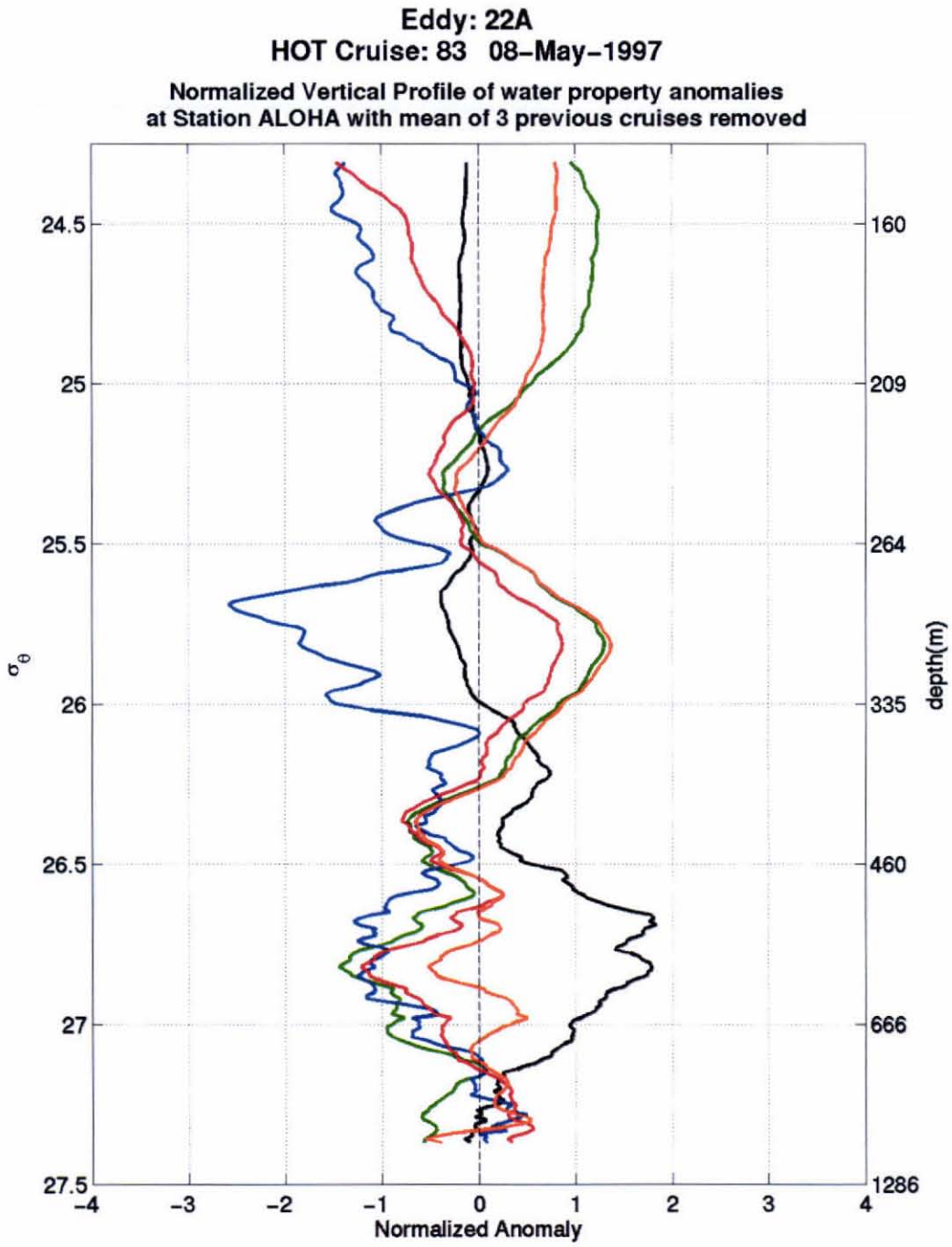
Eddy: 22A
HOT Cruise: 83 08-May-1997
Normalized Vertical Profile of water property anomalies
at Station ALOHA with mean of 3 previous cruises removed
24.5
25
25.5
26
26.5
27
27.5
σ_θ
160
209
264
335
460
666
1286
depth(m)
-4
-3
-2
-1
0
1
2
3
4
Normalized Anomaly

Eddy: 23C Dates in ALOHA box: 11-Jun-1997 to 02-Jul-1997

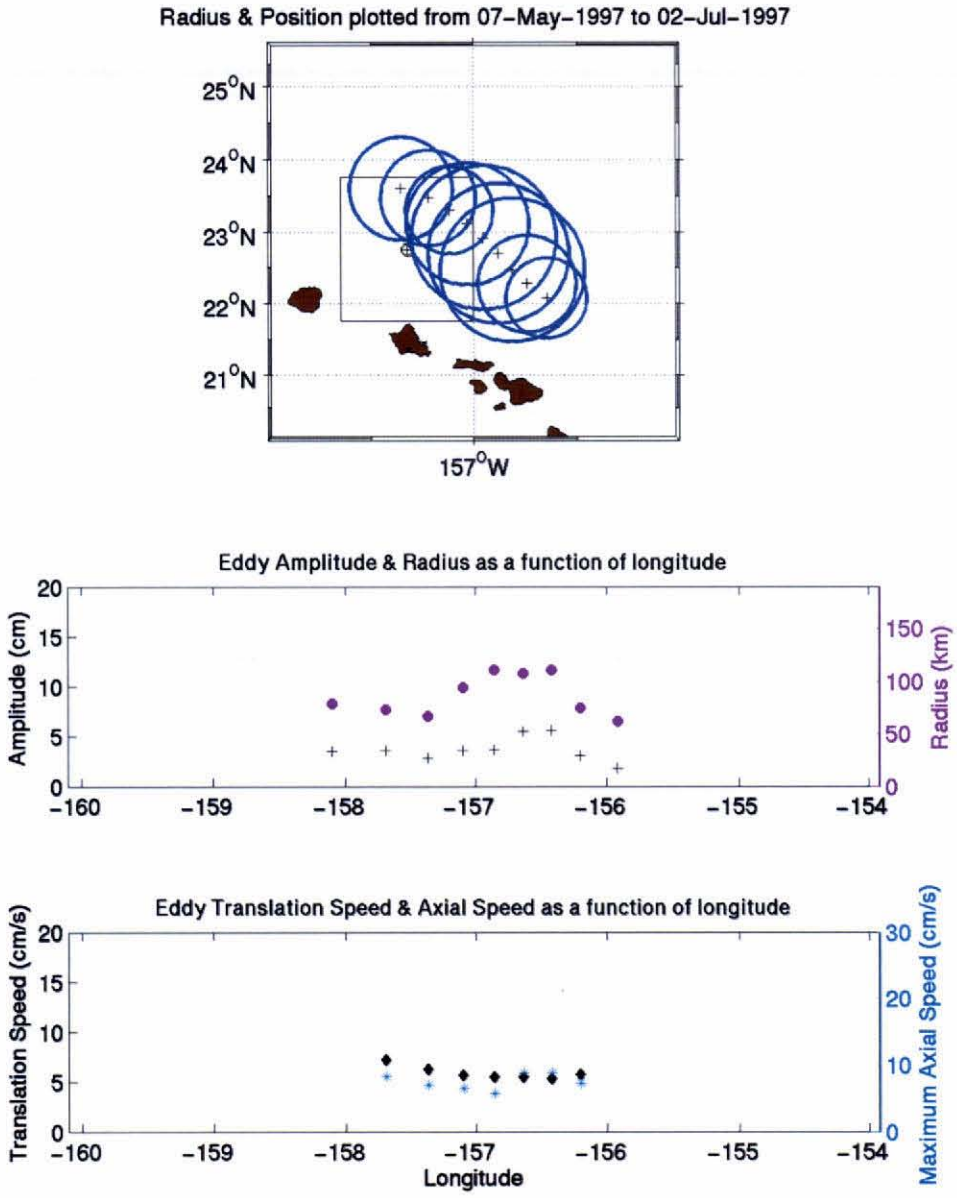

EID: 23C

This eddy was short lived. It formed over Maui, but was squeezed between two anticyclonic eddies and subject to strong eddy-eddy interactions and quickly dissipated.

Eddy: 24A Dates in ALOHA box: 06-Aug-1997 to 27-Aug-1997

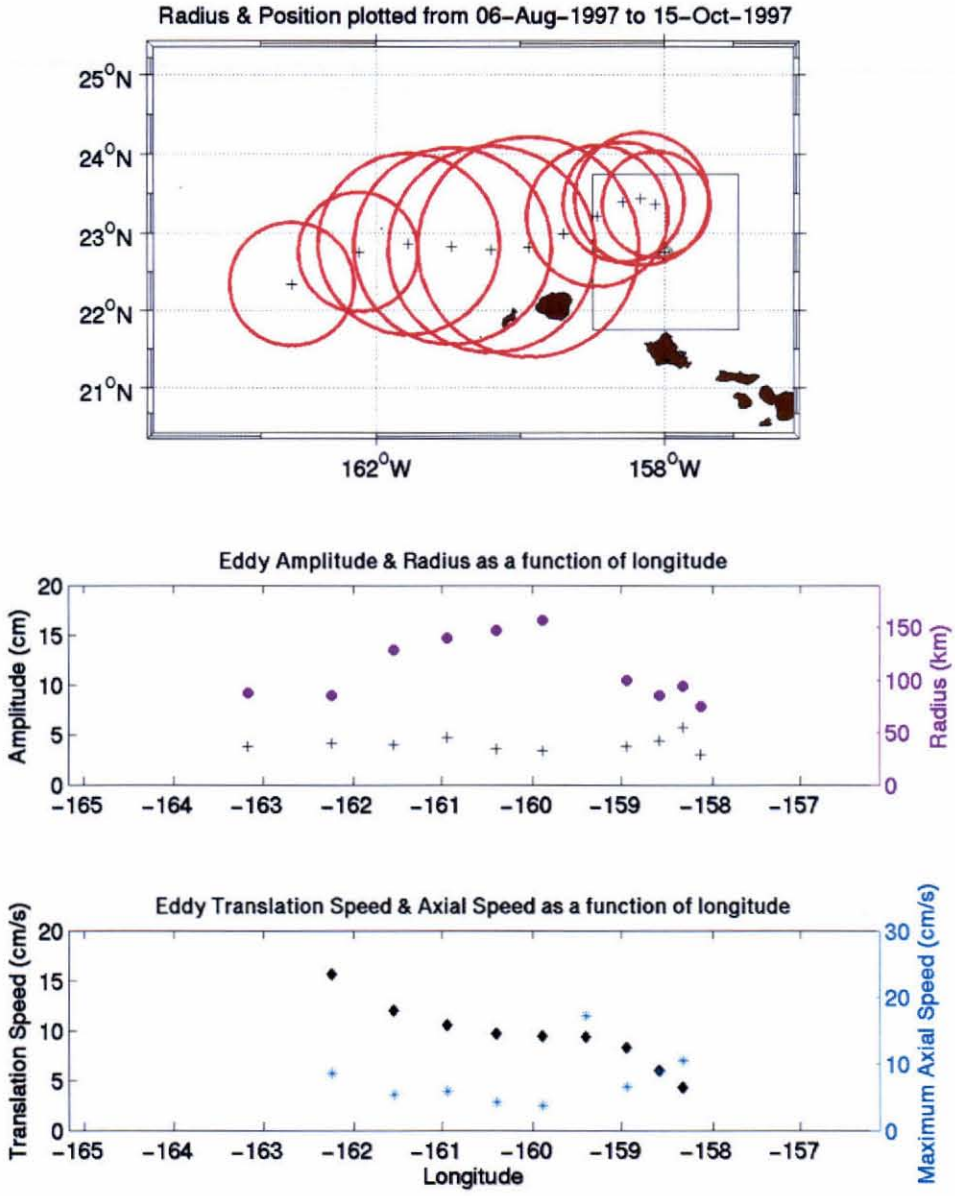

EID: 24A

This eddy was an offshoot of another feature, short lived, small amplitude and large radius, quickly dissipated after grazing ALOHA with its southern edge.

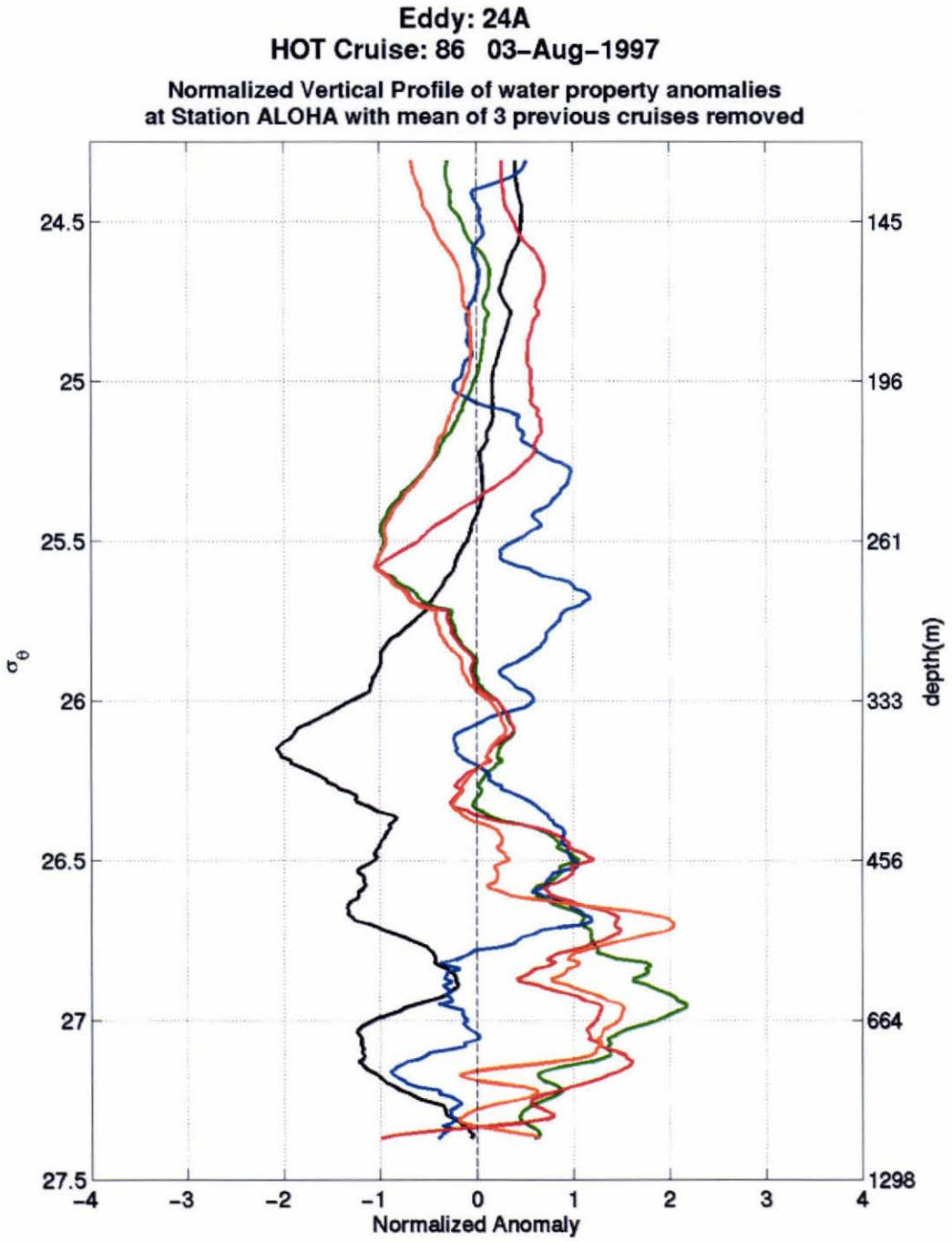
Eddy: 24A
HOT Cruise: 86 03-Aug-1997
Normalized Vertical Profile of water property anomalies
at Station ALOHA with mean of 3 previous cruises removed
24.5
25
25.5
26
26.5
27
27.5
σ_θ
145
196
261
333
456
664
1298
depth(m)
-4
-3
-2
-1
0
1
2
3
4
Normalized Anomaly

Eddy: 25A Dates in ALOHA box: 24-Sep-1997 to 22-Oct-1997

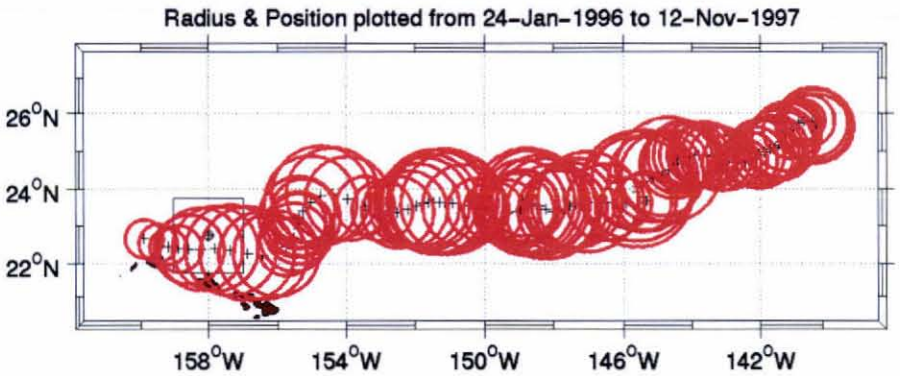

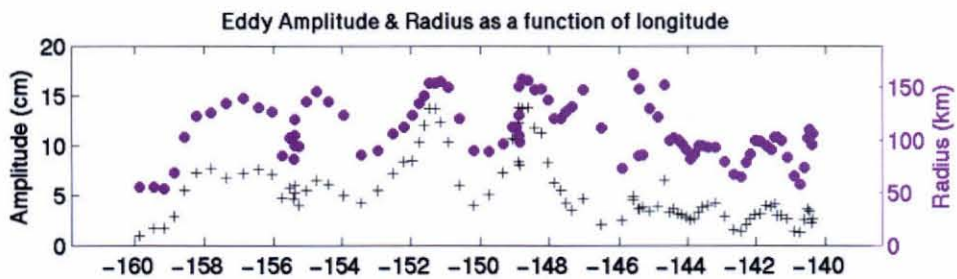

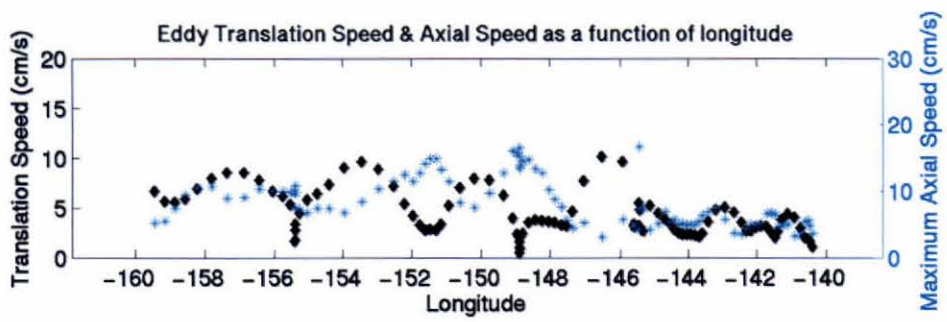

EID: 25A

This eddy was very long-lived. It formed near 24N and 141W and appeared to draw smaller eddies into it as it traveled west. There was an abrupt direction change to the south and then it turned west again as it encountered the island of Maui. From there it traveled along islands until dissipating over Kauai.

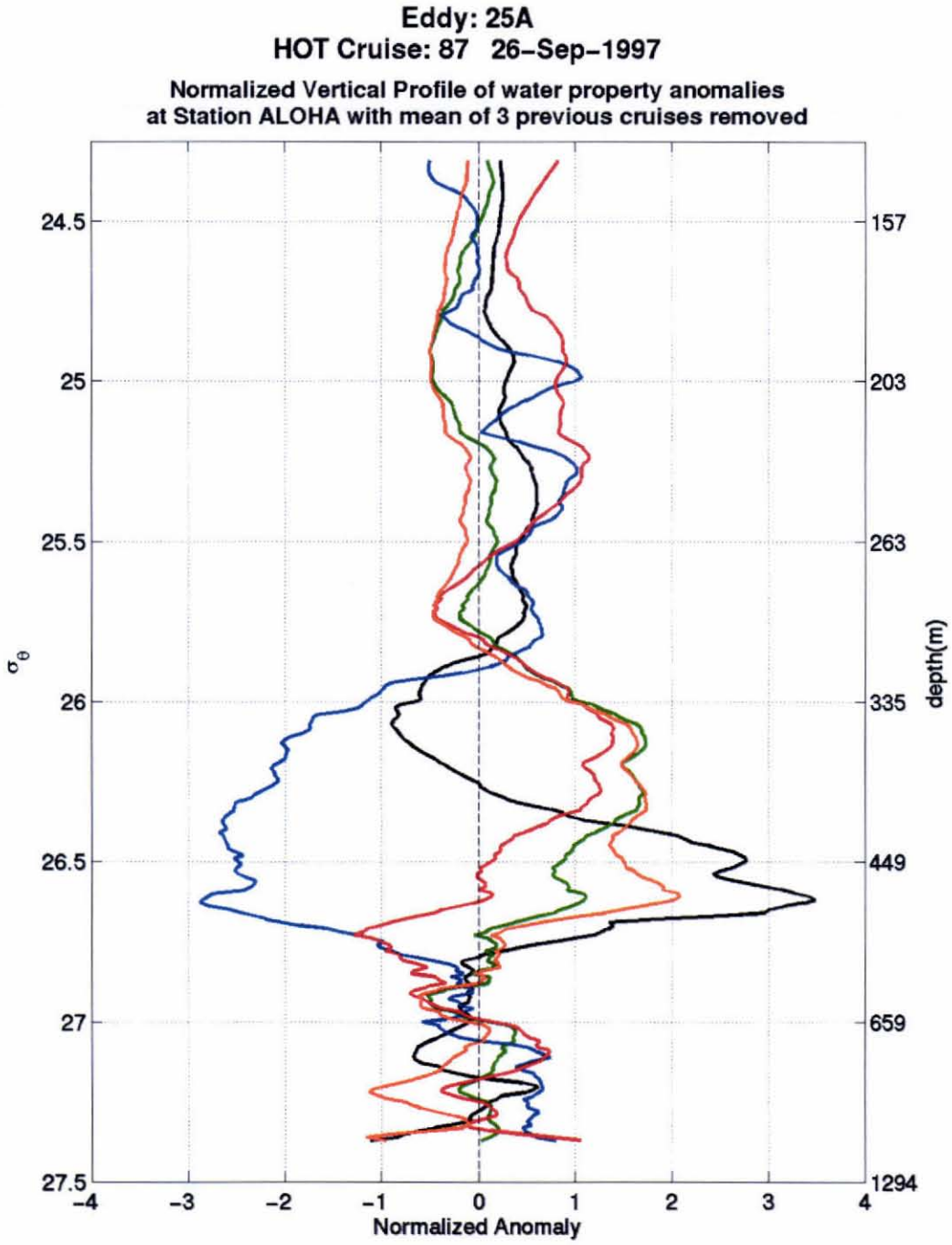
Eddy: 25A
HOT Cruise: 87 26-Sep-1997
Normalized Vertical Profile of water property anomalies
at Station ALOHA with mean of 3 previous cruises removed
24.5
25
25.5
26
26.5
27
27.5
σ_θ
157
203
263
335
449
659
1294
depth(m)
-4
-3
-2
-1
0
1
2
3
4
Normalized Anomaly

Eddy: 26C Dates in ALOHA box: 07-Jan-1998 to 21-Jan-1998

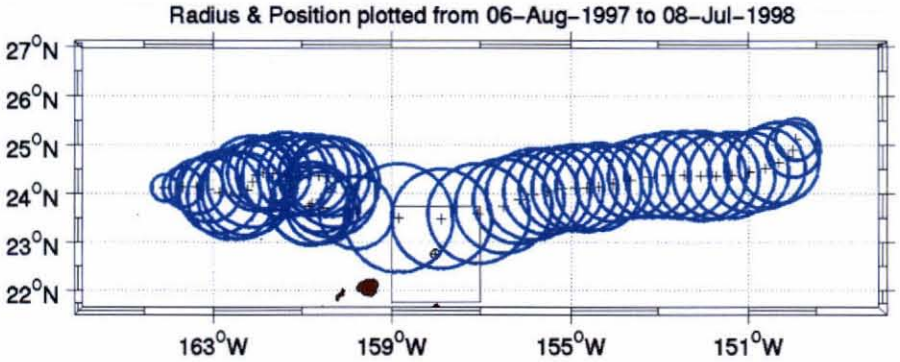

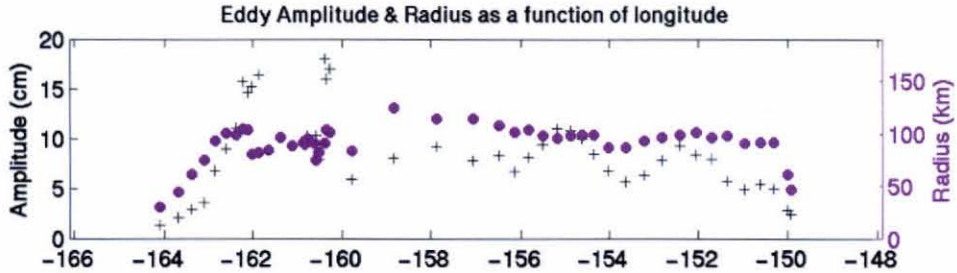

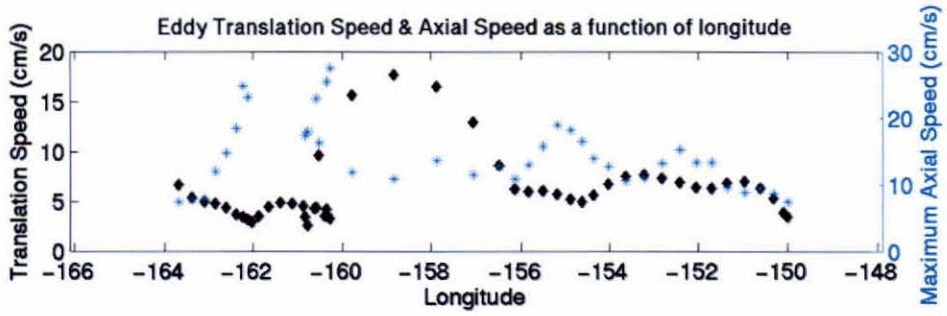

EID: 26C

This eddy formed at 25N and 150W and traveled steadily west until it passed north of ALOHA. Once over Kauai, the eddy experienced a decrease in translation speed and increase in amplitude. It appears that two anticyclonic eddies surrounded this eddy and effectively broke it apart.

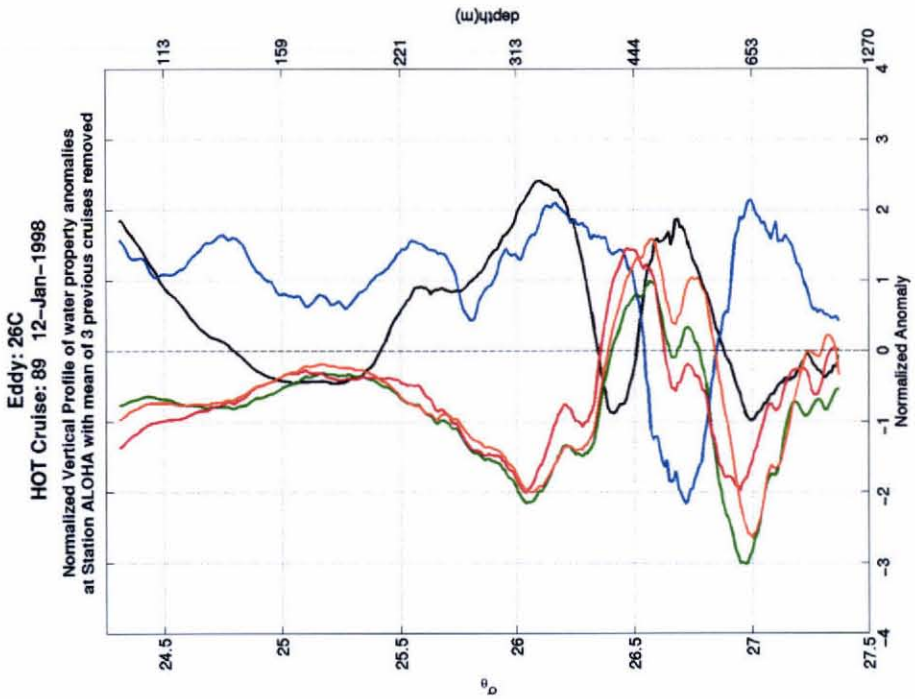
Eddy: 26C
HOT Cruise: 89 12-Jan-1998
Normalized Vertical Profile of water property anomalies
at Station ALOHA with mean of 3 previous cruises removed
depth(m)
113
159
221
313
444
653
1270
Normalized Anomaly
θ_D

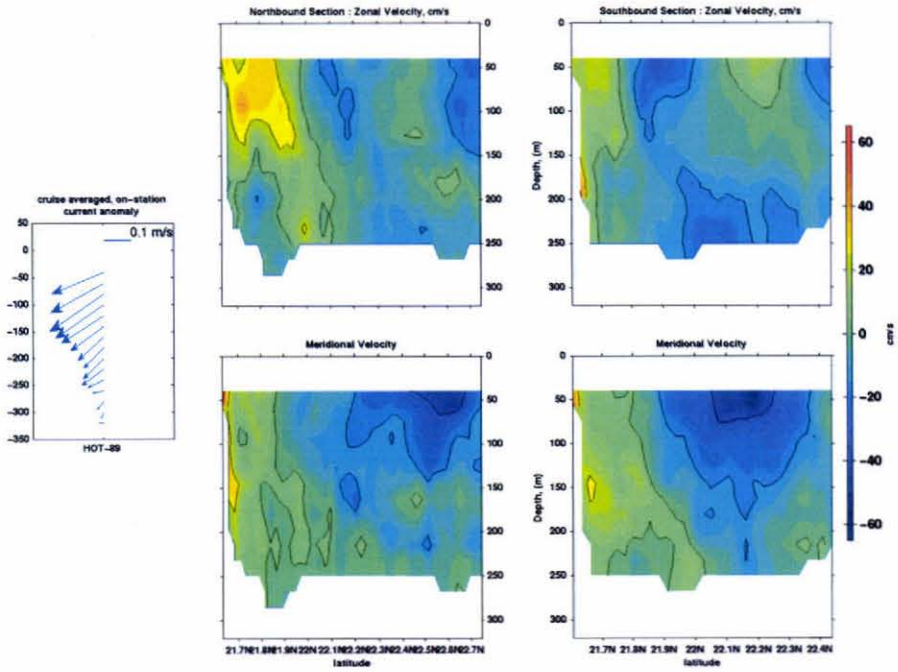
cruise averaged, on-station
current anomaly
0.1 m/s
HOT-89
Northbound Section : Zonal Velocity, cm/s
Southbound Section : Zonal Velocity, cm/s
Meridional Velocity
Meridional Velocity
Depth, (m)
latitude
cm/s

Eddy: 27C Dates in ALOHA box: 18-Feb-1998 to 11-Mar-1998

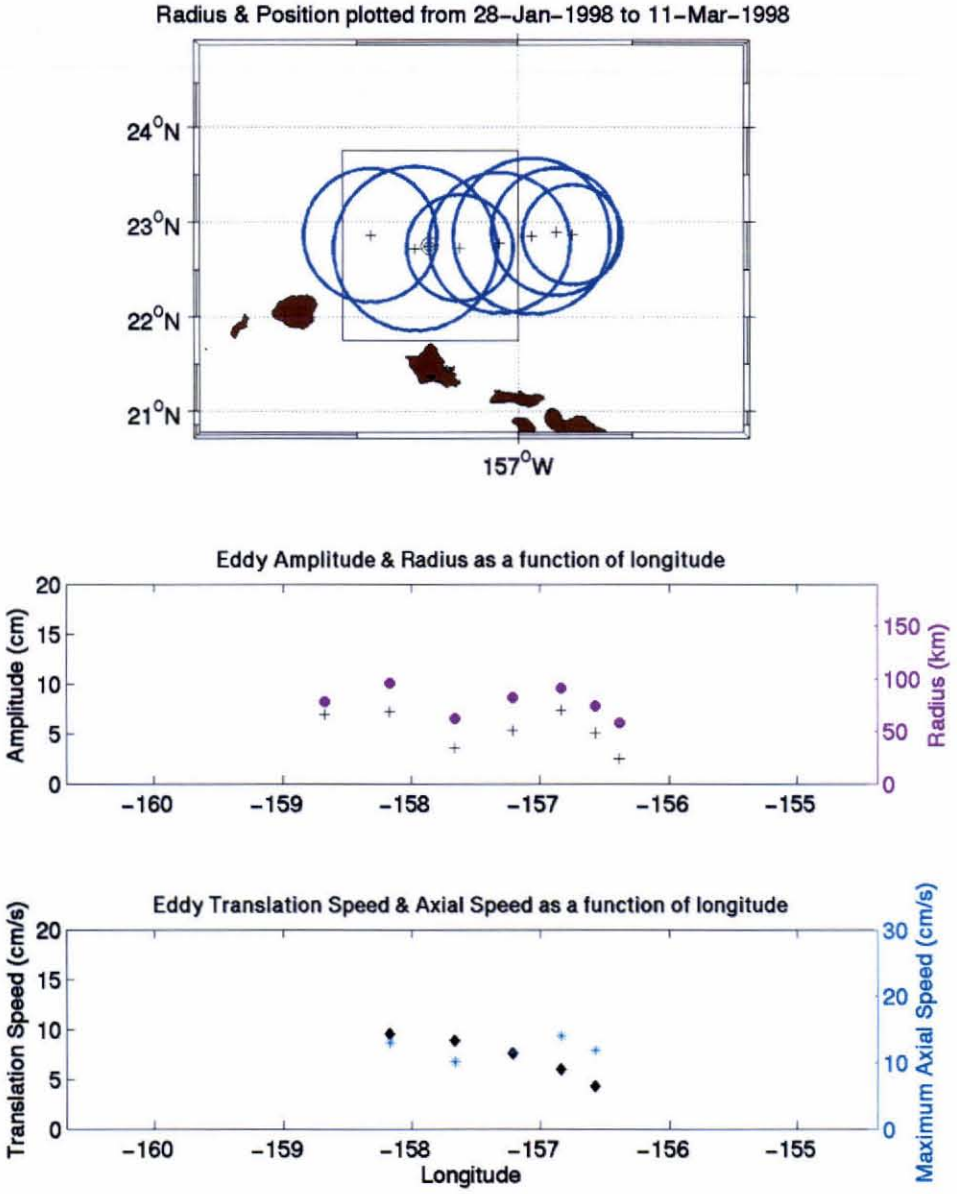

EID: 27C

This questionable, short-lived, eddy formed from a dissipating eddy and was quickly reabsorbed into another feature.

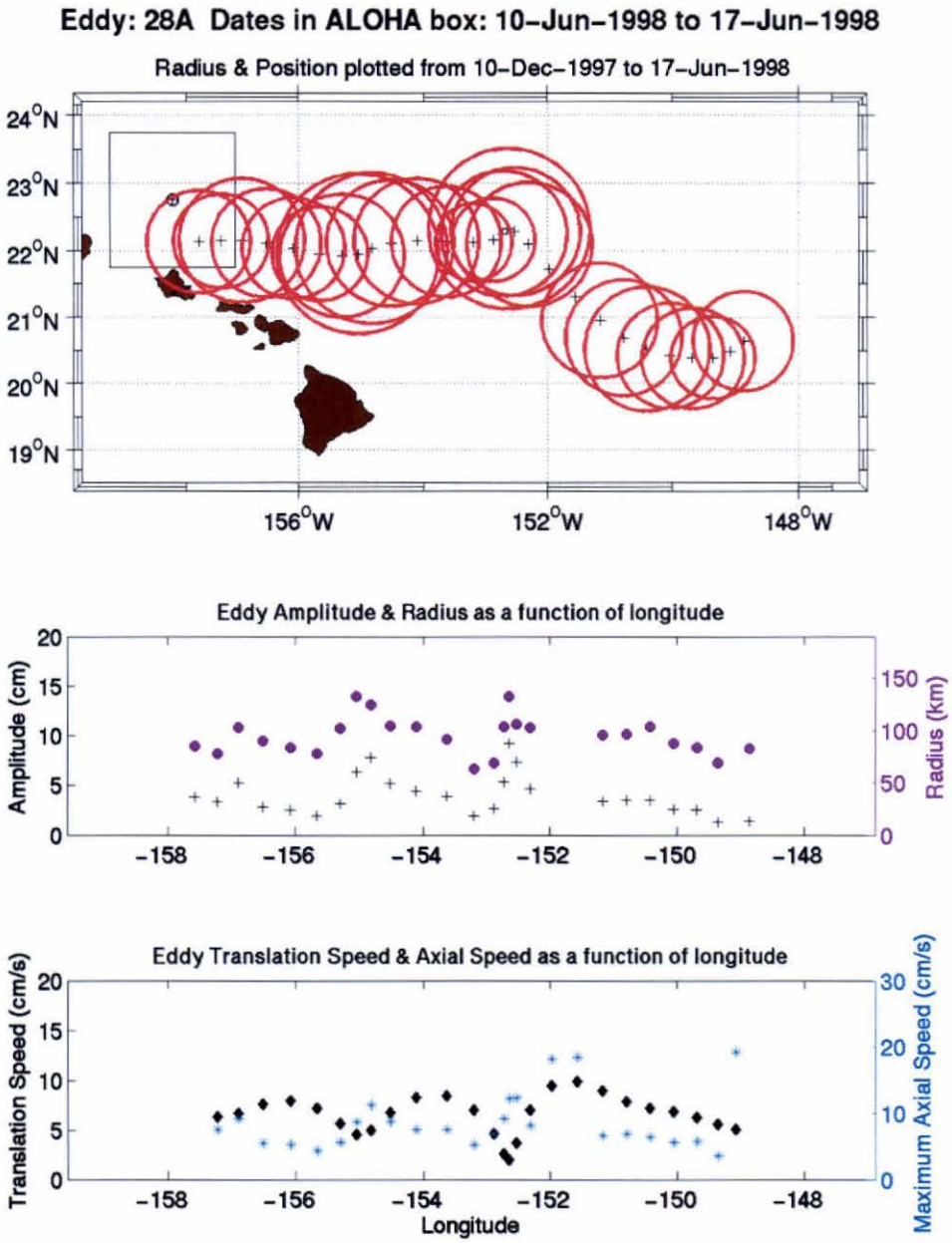

EID: 28A

This eddy formed at 149W, east of the Big Island and was characterized by an abrupt direction change at 152W, at which time it also experienced a sharp decrease in amplitude and radius, and a decrease in translation and axial speeds. This appears to be the result of this eddy merging with some other feature. Weak eddy center approached southeast of ALOHA when track was dropped because eddy dissipated.

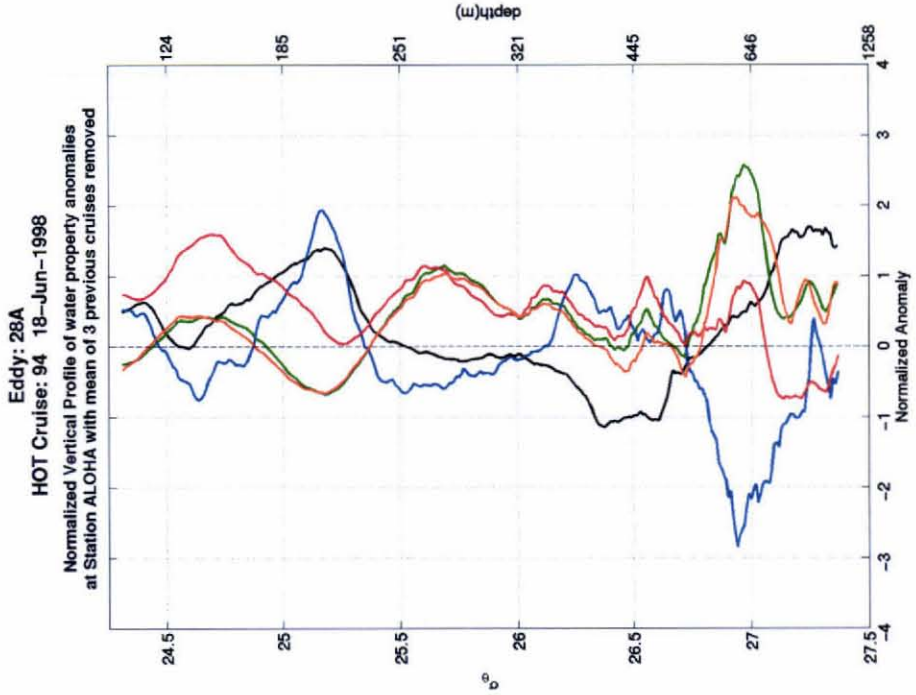
Eddy: 28A
HOT Cruise: 94 18–Jun–1998
Normalized Vertical Profile of water property anomalies
at Station ALOHA with mean of 3 previous cruises removed
depth(m)
124
185
251
321
445
646
1258
Normalized Anomaly
σθ

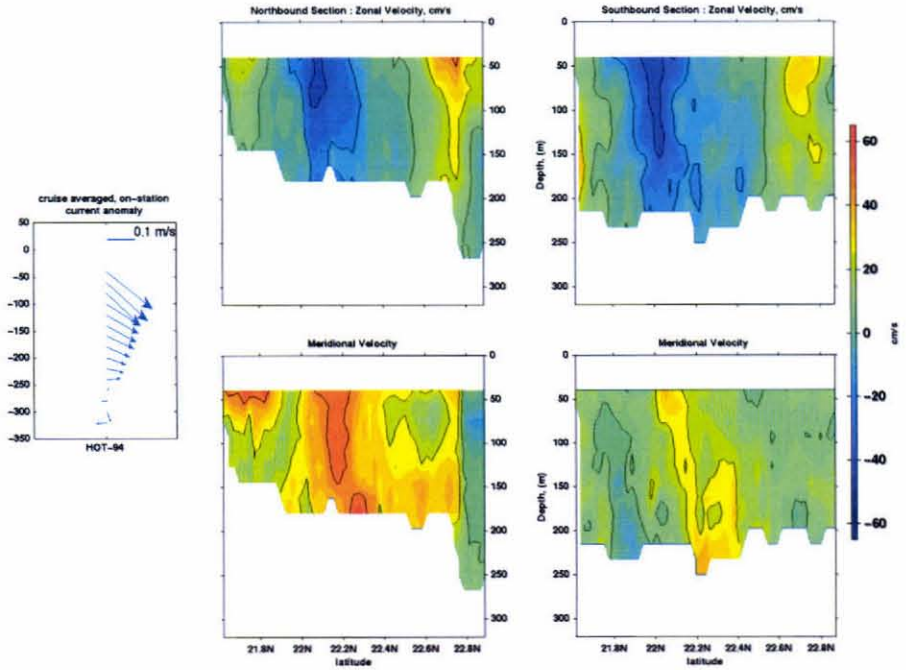
cruise averaged, on-station
current anomaly
0.1 m/s
HOT-94
Northbound Section : Zonal Velocity, cm/s
Southbound Section : Zonal Velocity, cm/s
Meridional Velocity
Meridional Velocity
Depth, (m)
latitude
cm/s

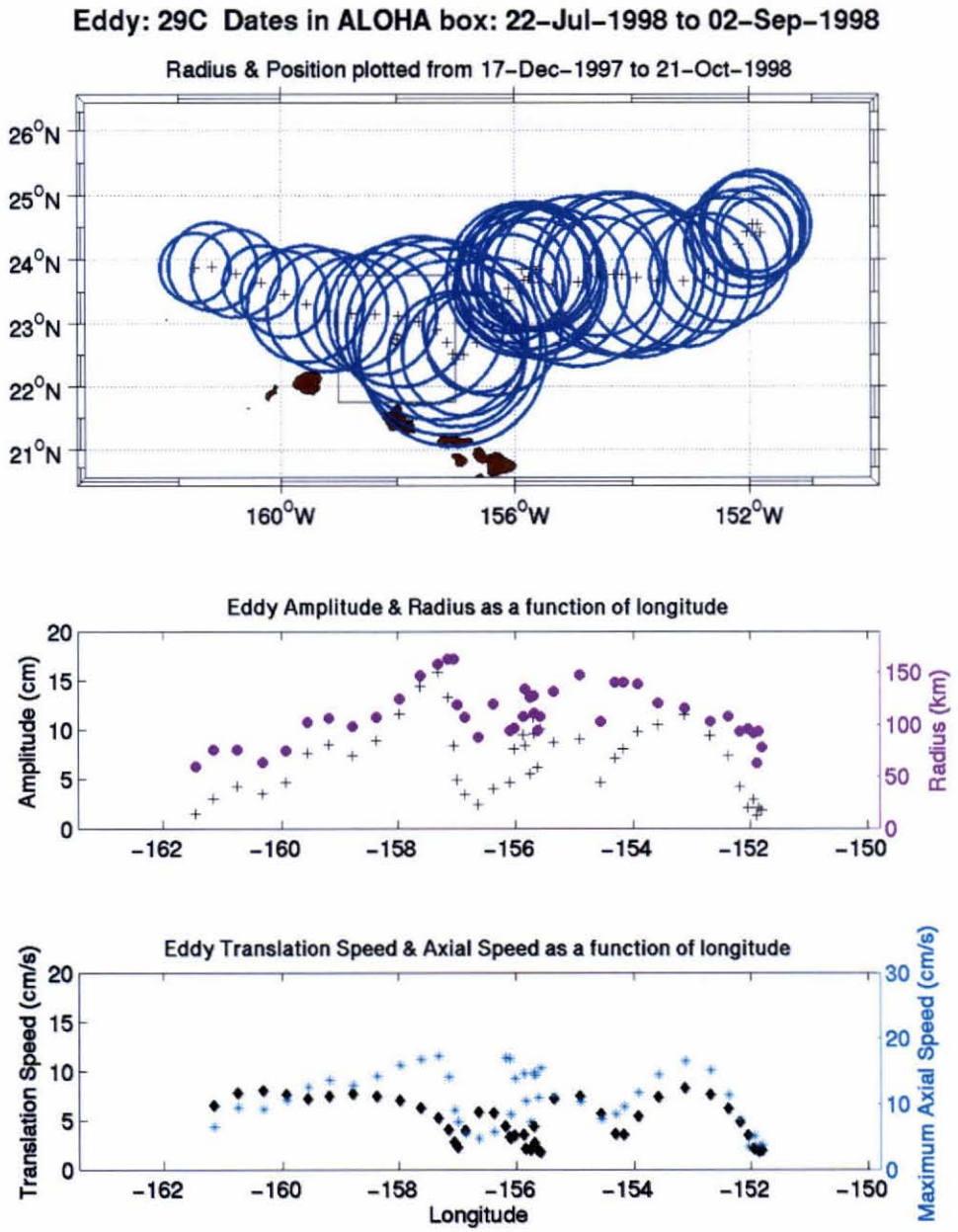

EID: 29C

This eddy formed at 152W and experienced drastic direction change to the SW over Maui, due to the eddy splitting. Track follows south split over ALOHA, as eddy steadily decreases and dissipates.

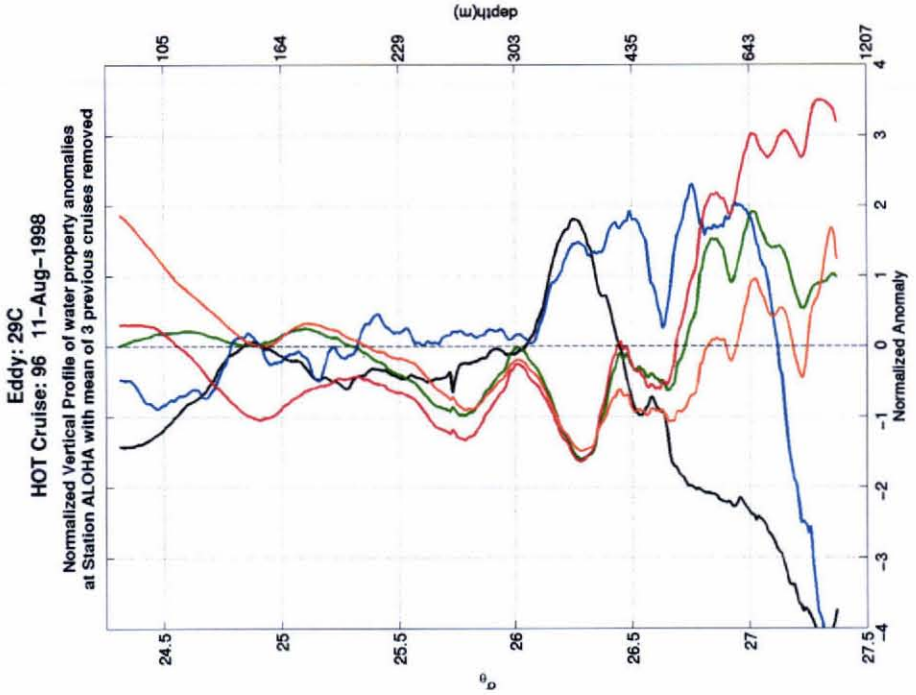
Eddy: 29C
HOT Cruise: 96 11-Aug-1998
Normalized Vertical Profile of water property anomalies
at Station ALOHA with mean of 3 previous cruises removed
depth(m)
105
164
229
303
435
643
1207
Normalized Anomaly
24.5
25
25.5
26
26.5
27
27.5

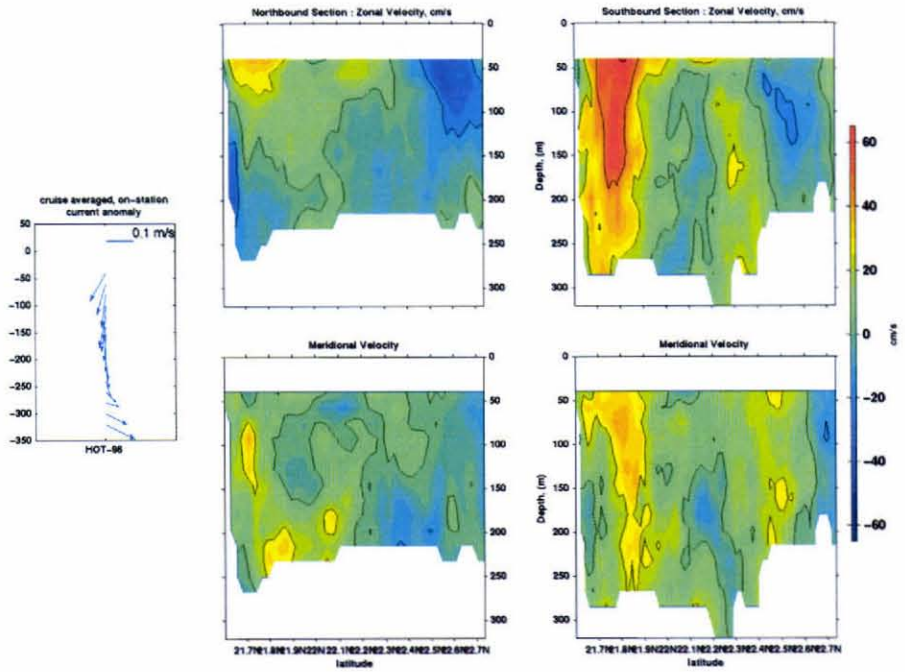
cruise averaged, on-station
current anomaly
0.1 m/s
HOT-96
Northbound Section : Zonal Velocity, cm/s
Southbound Section : Zonal Velocity, cm/s
Meridional Velocity
Meridional Velocity
Depth, (m)
latitude
cm/s

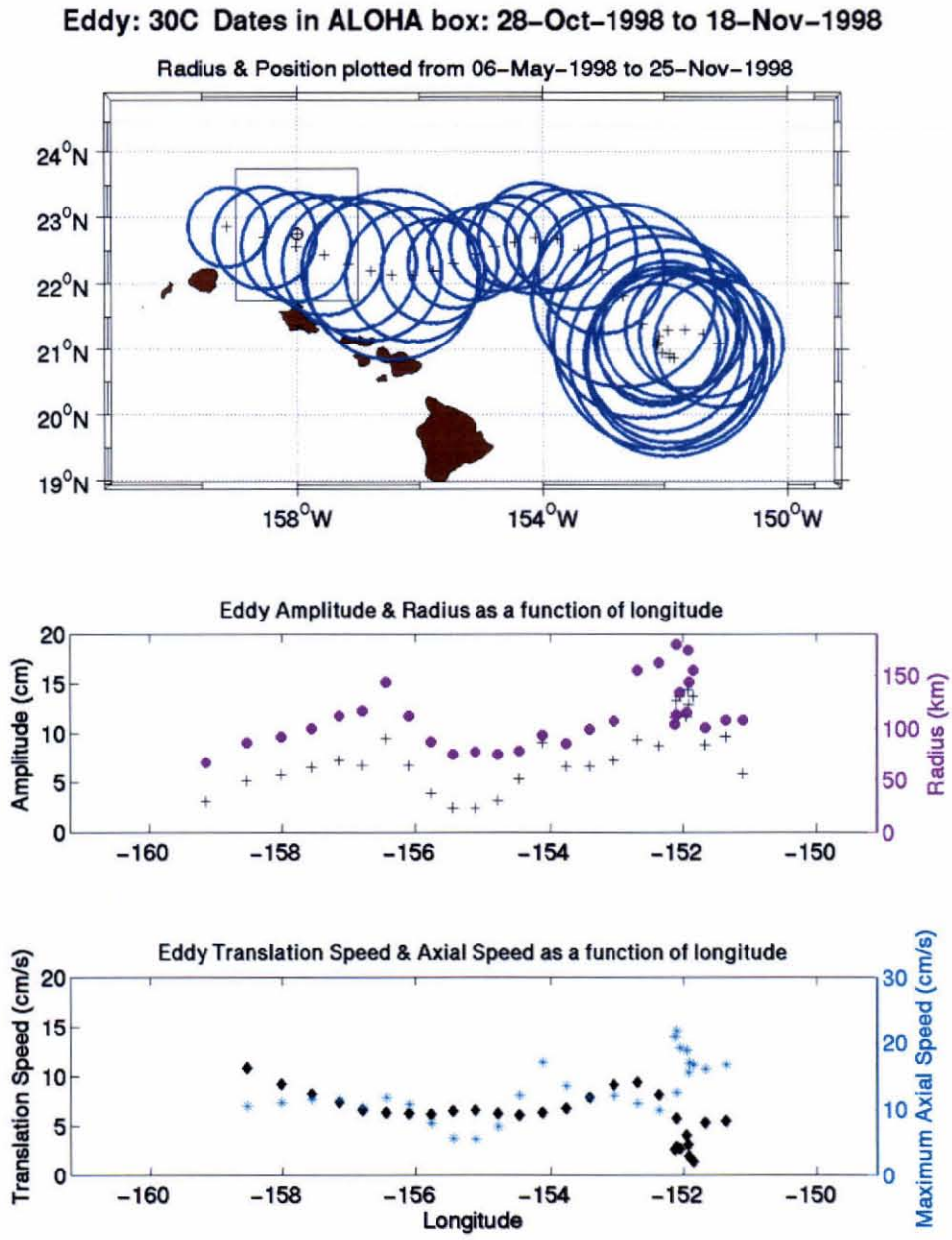

EID: 30C

This eddy spent time spinning up east of the Big Island (152W) before moving northwest. Direction change at 154W to due west occurred because of eddy interaction with an anticyclonic eddy. Eddy moved NW over Maui, Molokai and Oahu and dissipated over Kauai.

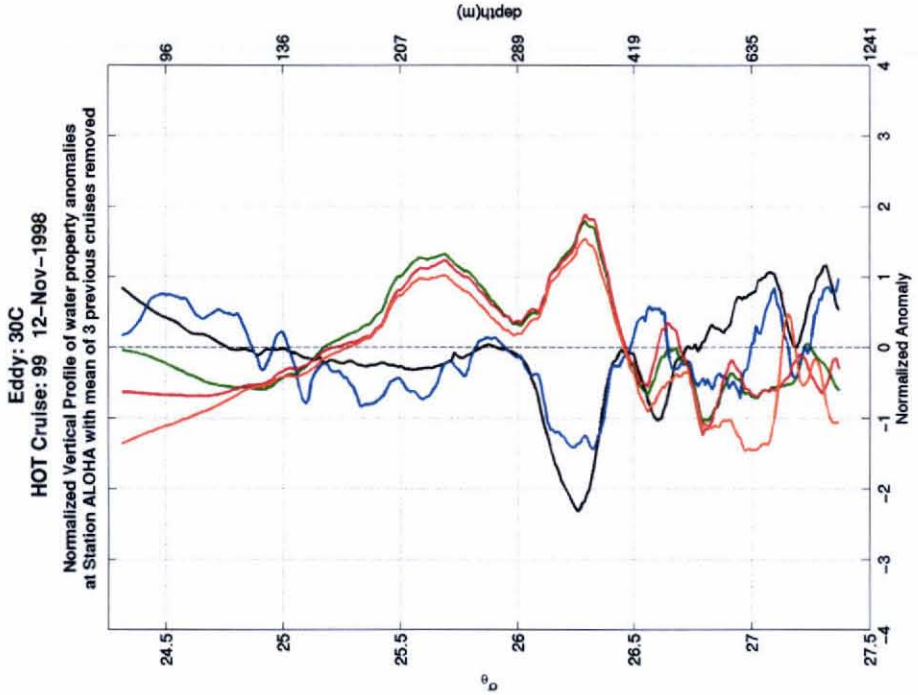
Eddy: 30C
HOT Cruise: 99 12-Nov-1998
Normalized Vertical Profile of water property anomalies
at Station ALOHA with mean of 3 previous cruises removed
depth(m)
96
136
207
289
419
635
1241
Normalized Anomaly
θ_D

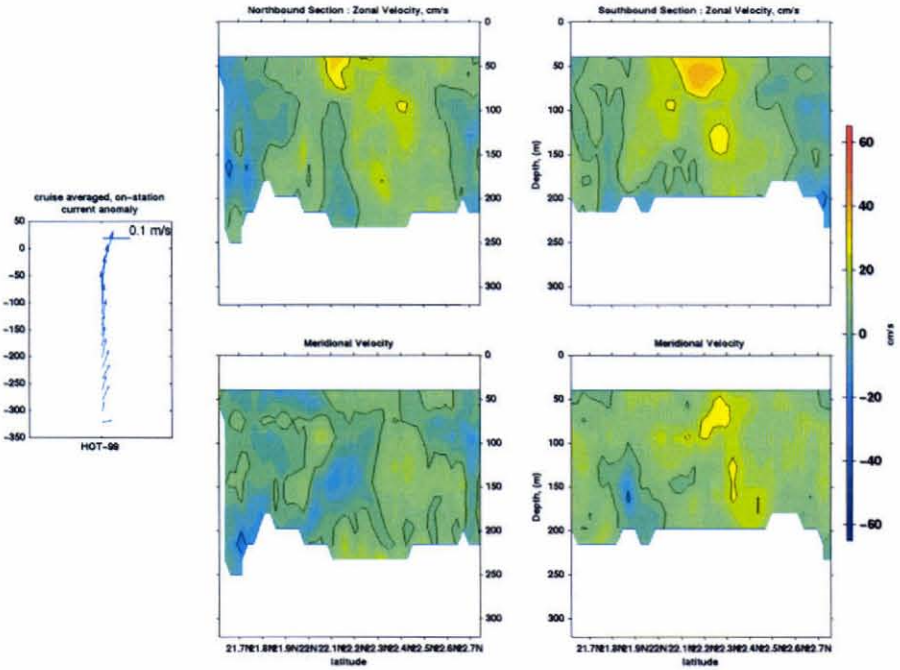
cruise averaged, on-station
current anomaly
0.1 m/s
HOT-99
Northbound Section : Zonal Velocity, cm/s
Southbound Section : Zonal Velocity, cm/s
Meridional Velocity
Meridional Velocity
Depth, (m)
latitude
cm/s

Eddy: 31A Dates in ALOHA box: 02-Dec-1998 to 23-Dec-1998

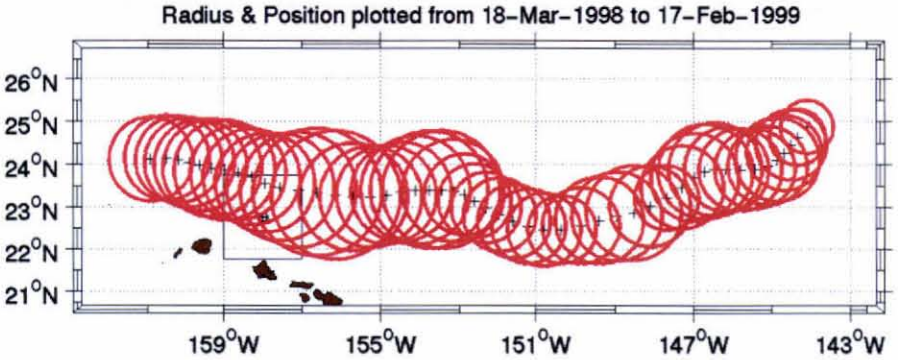

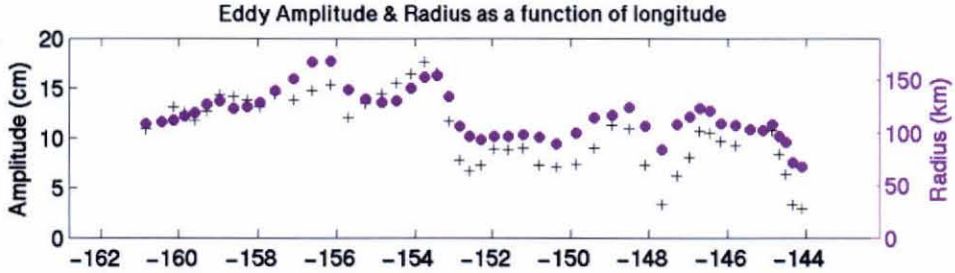

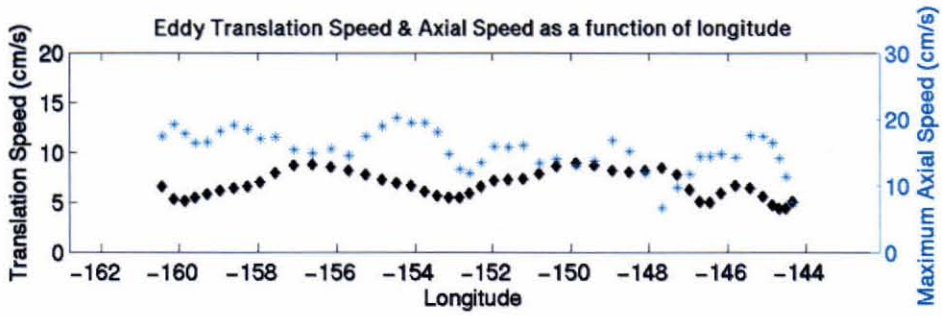

EID: 31A

This eddy lasted almost a year in duration. The change in direction from SW to west at 147W occurred because of the presence of two cyclonic eddies, one on either side of this eddy. Amplitude and radius both increased as it approached ALOHA. Eddy dissipated northwest of Kauai.

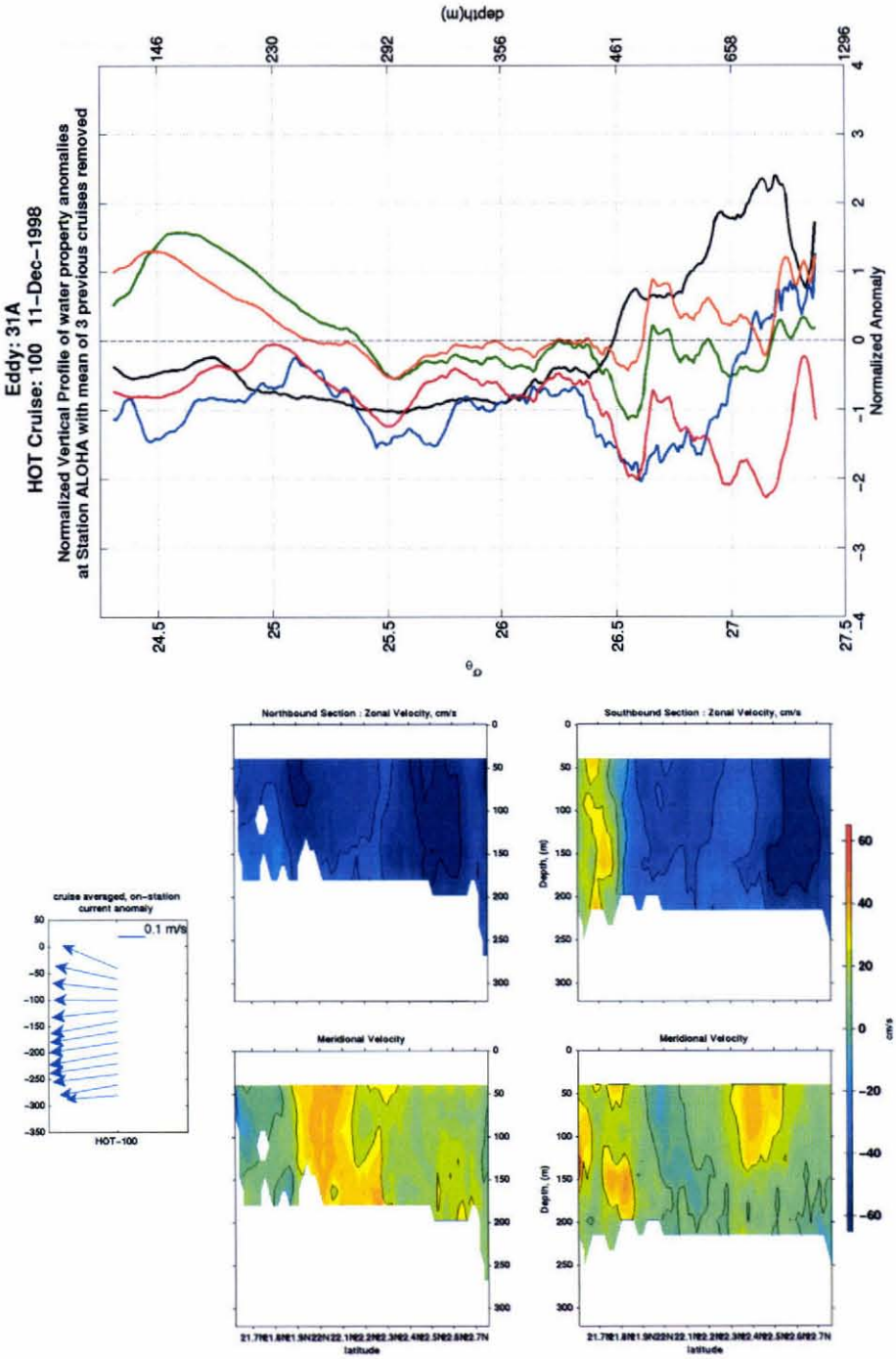
Eddy: 31A
HOT Cruise: 100 11-Dec-1998
Normalized Vertical Profile of water property anomalies
at Station ALOHA with mean of 3 previous cruises removed
depth(m)
146
230
292
356
461
658
1296
Normalized Anomaly
σ_θ
cruise averaged, on-station
current anomaly
0.1 m/s
HOT-100
Northbound Section : Zonal Velocity, cm/s
Southbound Section : Zonal Velocity, cm/s
Meridional Velocity
Meridional Velocity
Depth, (m)
latitude
cm/s

Eddy: 32A Dates in ALOHA box: 27-Jan-1999 to 24-Feb-1999

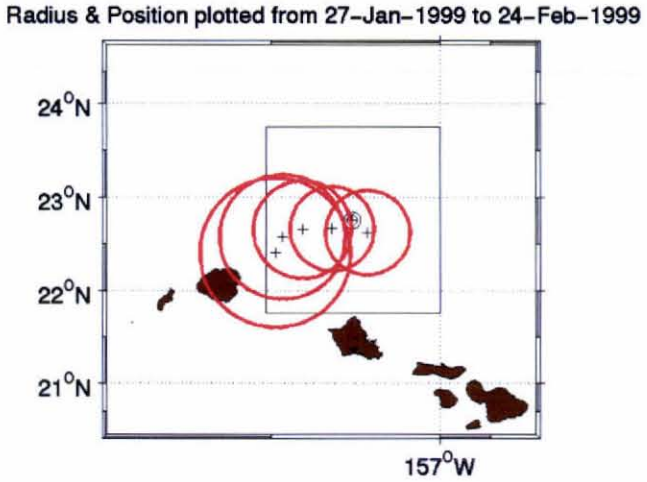

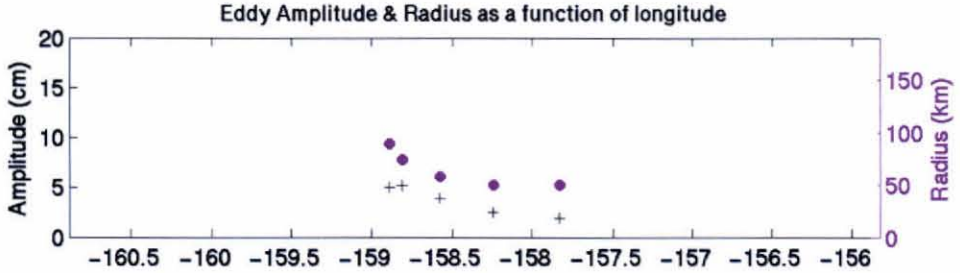

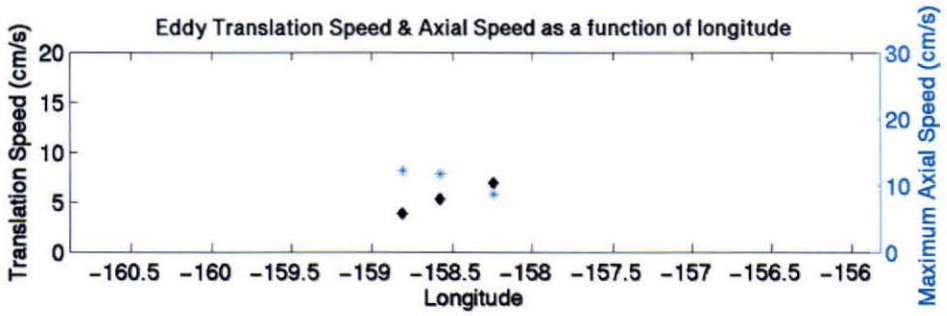

EID: 32A

This eddy spun up in the box surrounding ALOHA, and is short-lived. Probably formed from interaction of two other anticyclones in the region, neither of which affected ALOHA. Questionable eddy, does have large surface anomalies in water property profile.

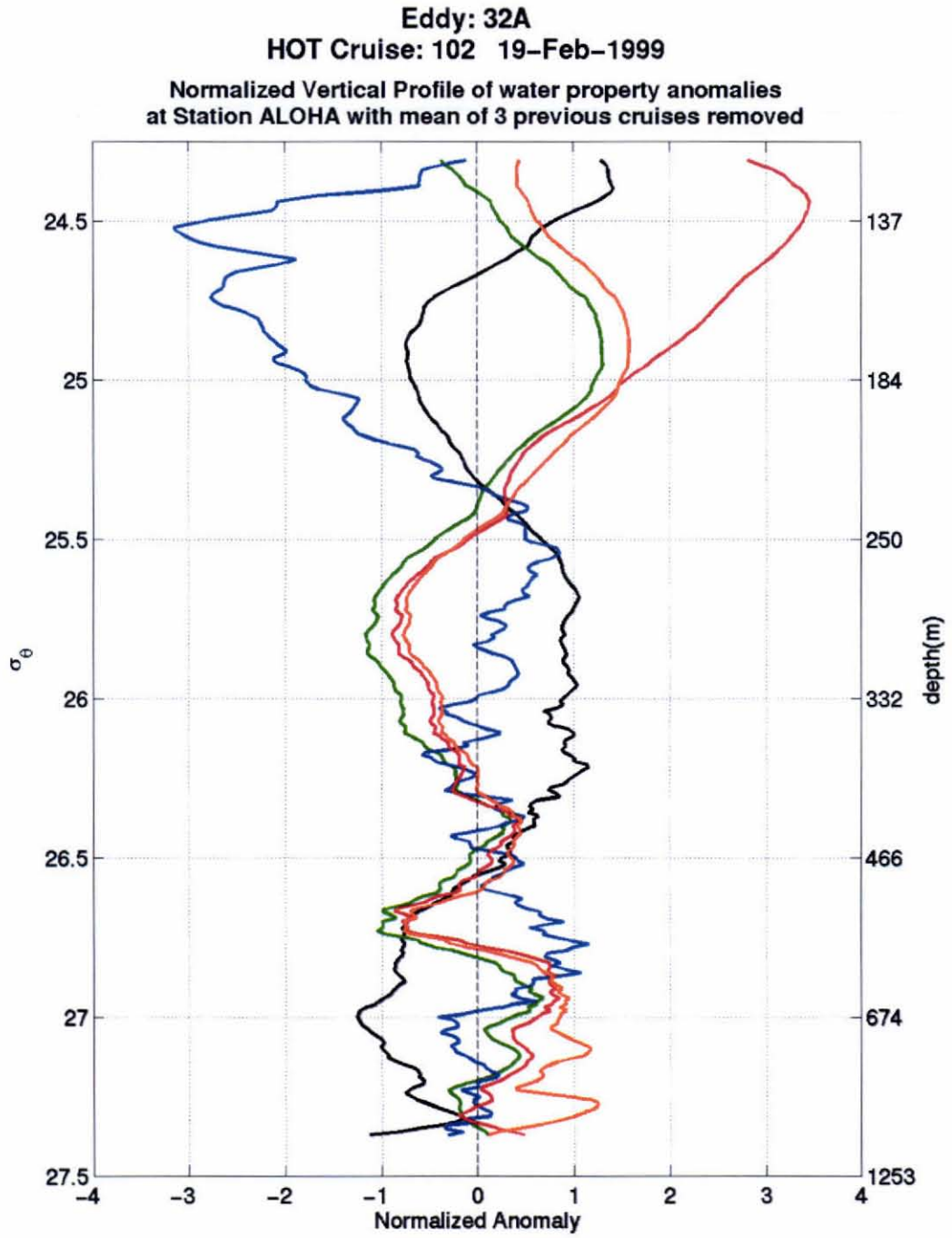
Eddy: 32A
HOT Cruise: 102 19-Feb-1999
Normalized Vertical Profile of water property anomalies
at Station ALOHA with mean of 3 previous cruises removed
24.5
25
25.5
26
26.5
27
27.5
σ_θ
137
184
250
332
466
674
1253
depth(m)
-4
-3
-2
-1
0
1
2
3
4
Normalized Anomaly

Eddy: 33C Dates in ALOHA box: 05-May-1999 to 19-May-1999

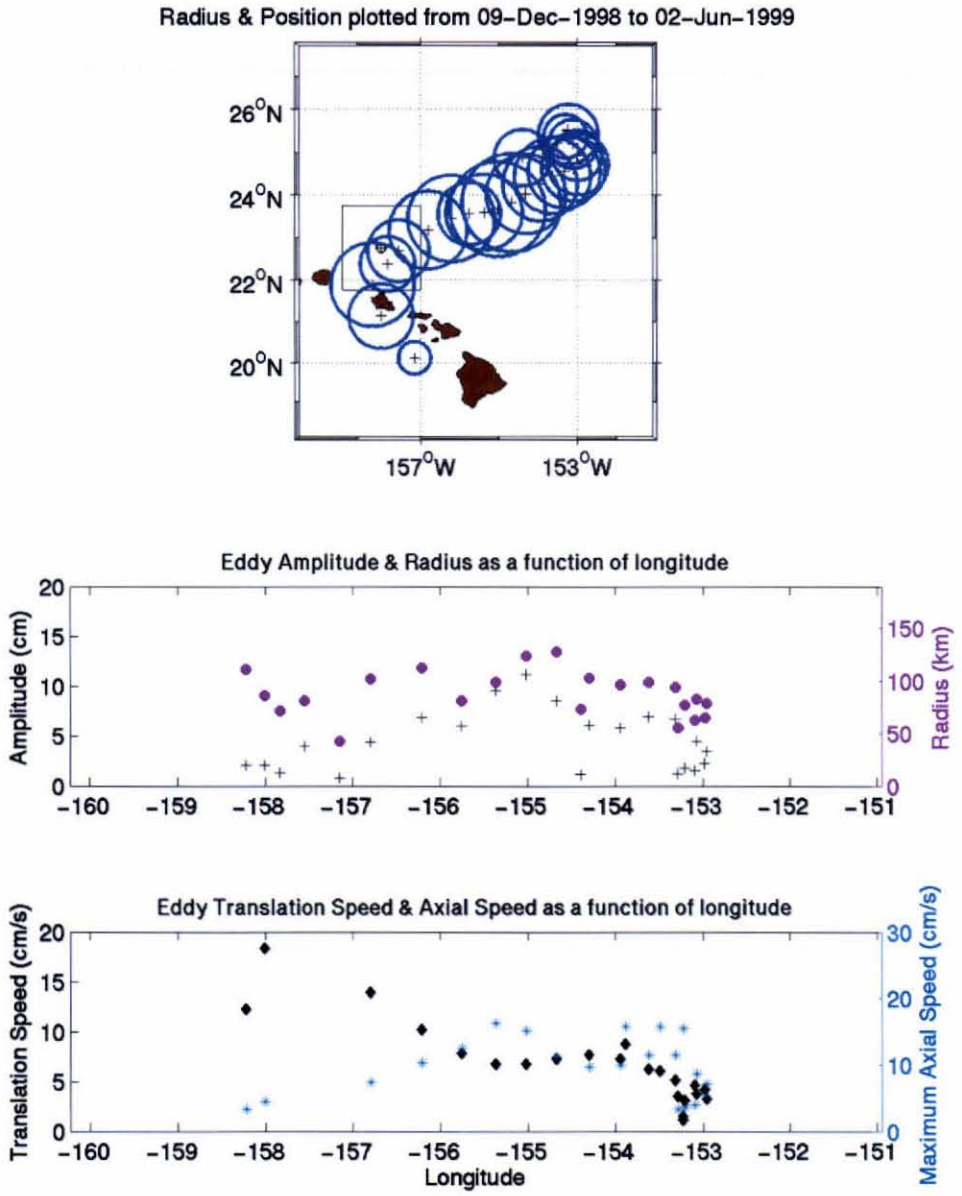

EID: 33C

This eddy formed further to the north, almost 26N, and at 153W. As it moved steadily to the southwest, it passed by ALOHA and collided with Oahu. Its remnant was tracked through the Kauai Channel, but this behavior could not be seen visually.

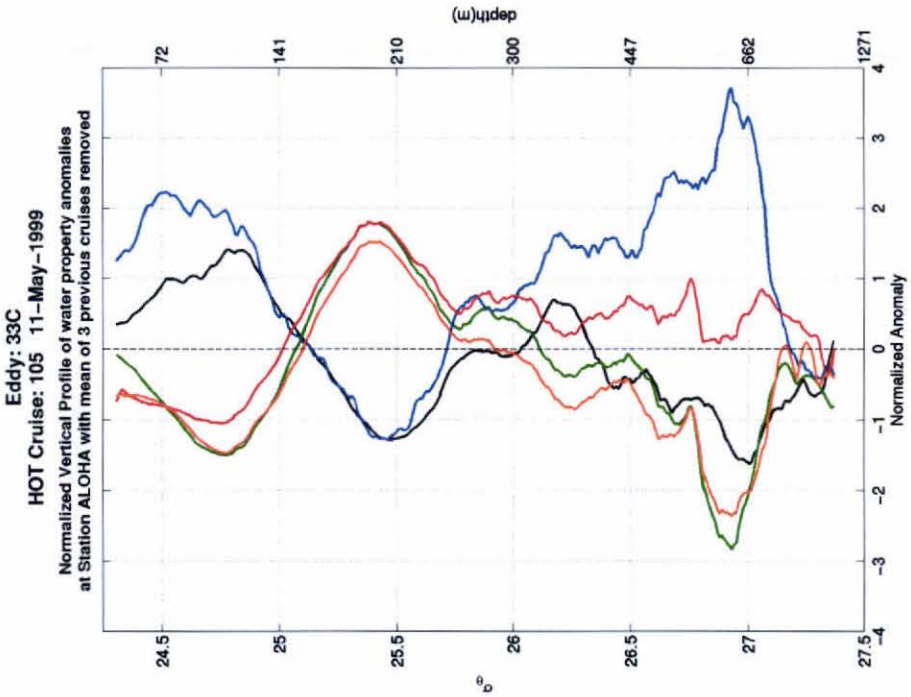
Eddy: 33C
HOT Cruise: 105 11-May-1999
Normalized Vertical Profile of water property anomalies
at Station ALOHA with mean of 3 previous cruises removed
depth(m)
72
141
210
300
447
662
1271
Normalized Anomaly
σ_θ

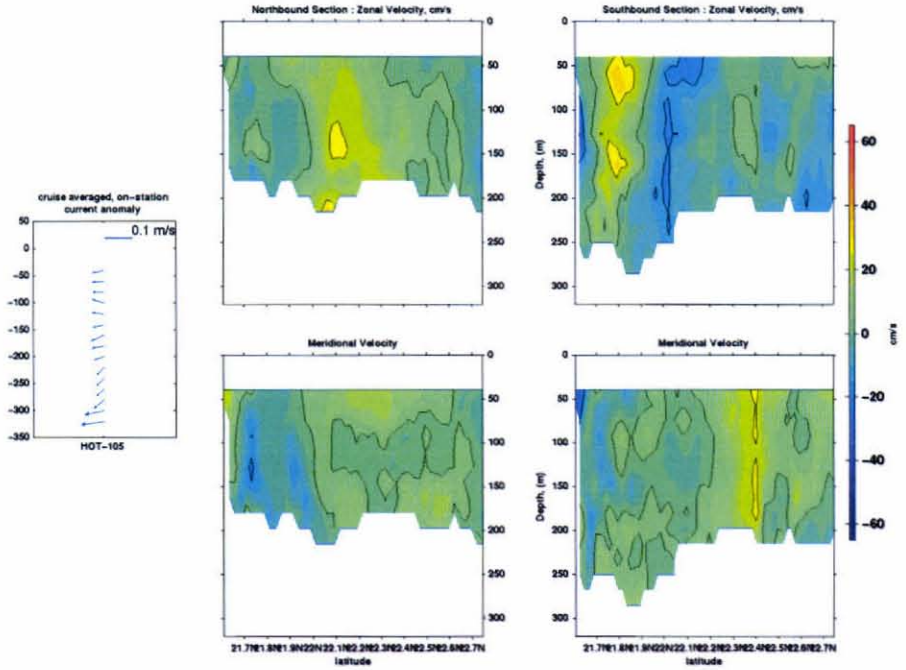
cruise averaged, on-station
current anomaly
0.1 m/s
HOT-105
Northbound Section : Zonal Velocity, cm/s
Southbound Section : Zonal Velocity, cm/s
Meridional Velocity
Meridional Velocity
Depth, (m)
latitude
cm/s

Eddy: 34A Dates in ALOHA box: 23-Jun-1999 to 21-Jul-1999

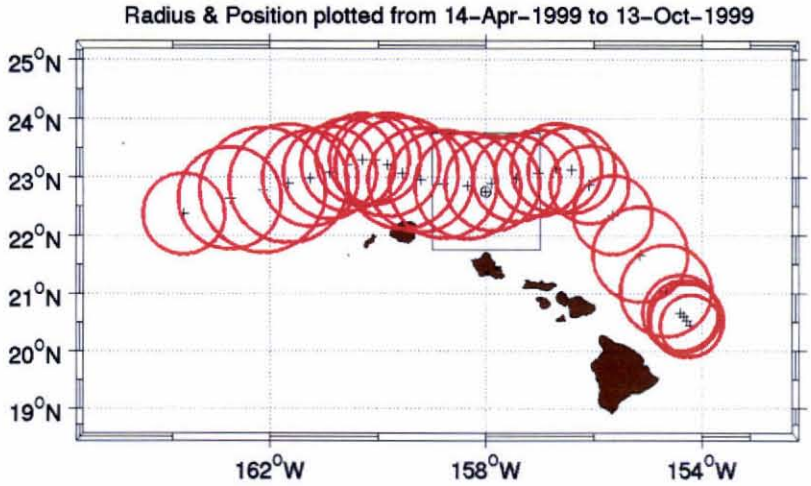

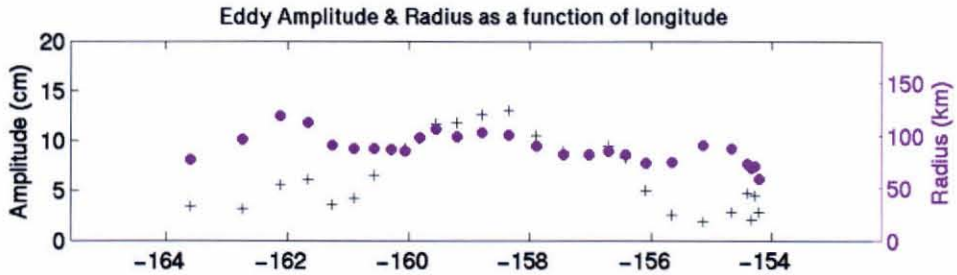

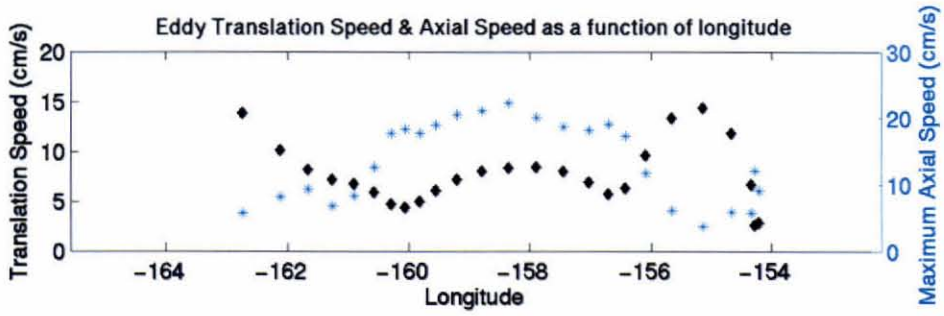

EID: 34A

This eddy was stationary for the first five weeks as it spun up on the northeast side of the Big Island. It was then drawn into a larger eddy that was forming to the NW. The propagation speed increased as it was "sucked" into the larger eddy. The eddy eventually dissipates due to eddy-eddy, eddy-island interactions and perhaps due to not re-gaining stability after the two features merged.

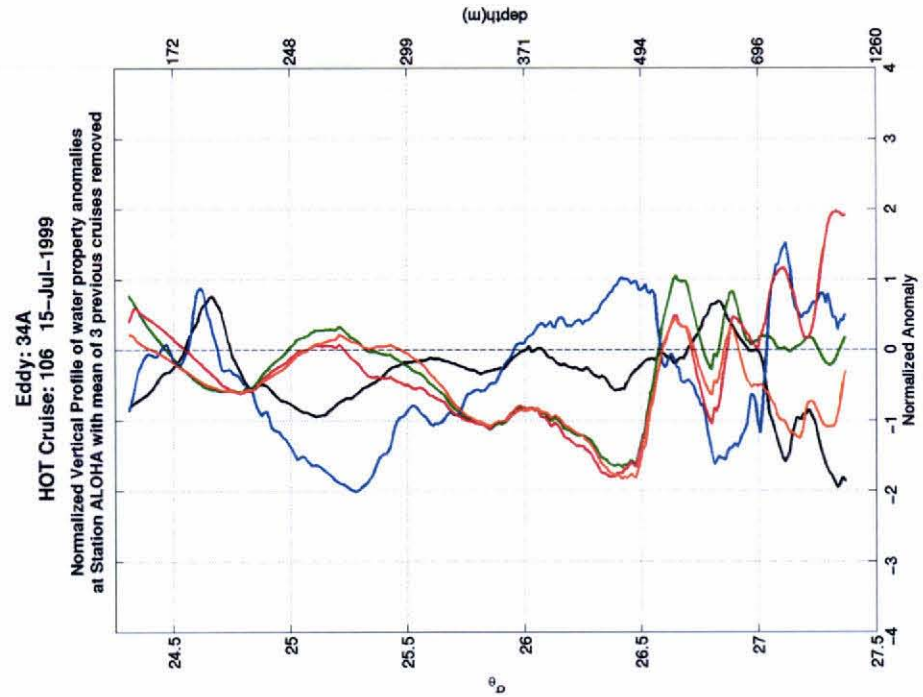
Eddy: 34A
HOT Cruise: 106 15-Jul-1999
Normalized Vertical Profile of water property anomalies
at Station ALOHA with mean of 3 previous cruises removed
depth(m)
172
248
299
371
494
696
1260
Normalized Anomaly
θ_D

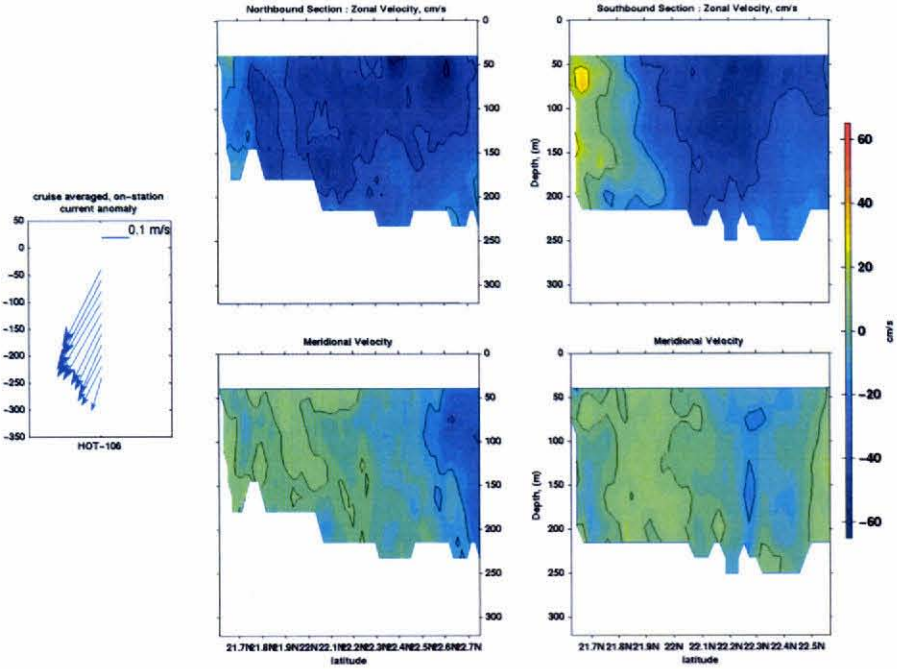
cruise averaged, on-station
current anomaly
0.1 m/s
HOT-106
Northbound Section : Zonal Velocity, cm/s
Southbound Section : Zonal Velocity, cm/s
Meridional Velocity
Meridional Velocity
Depth, (m)
latitude
cm/s

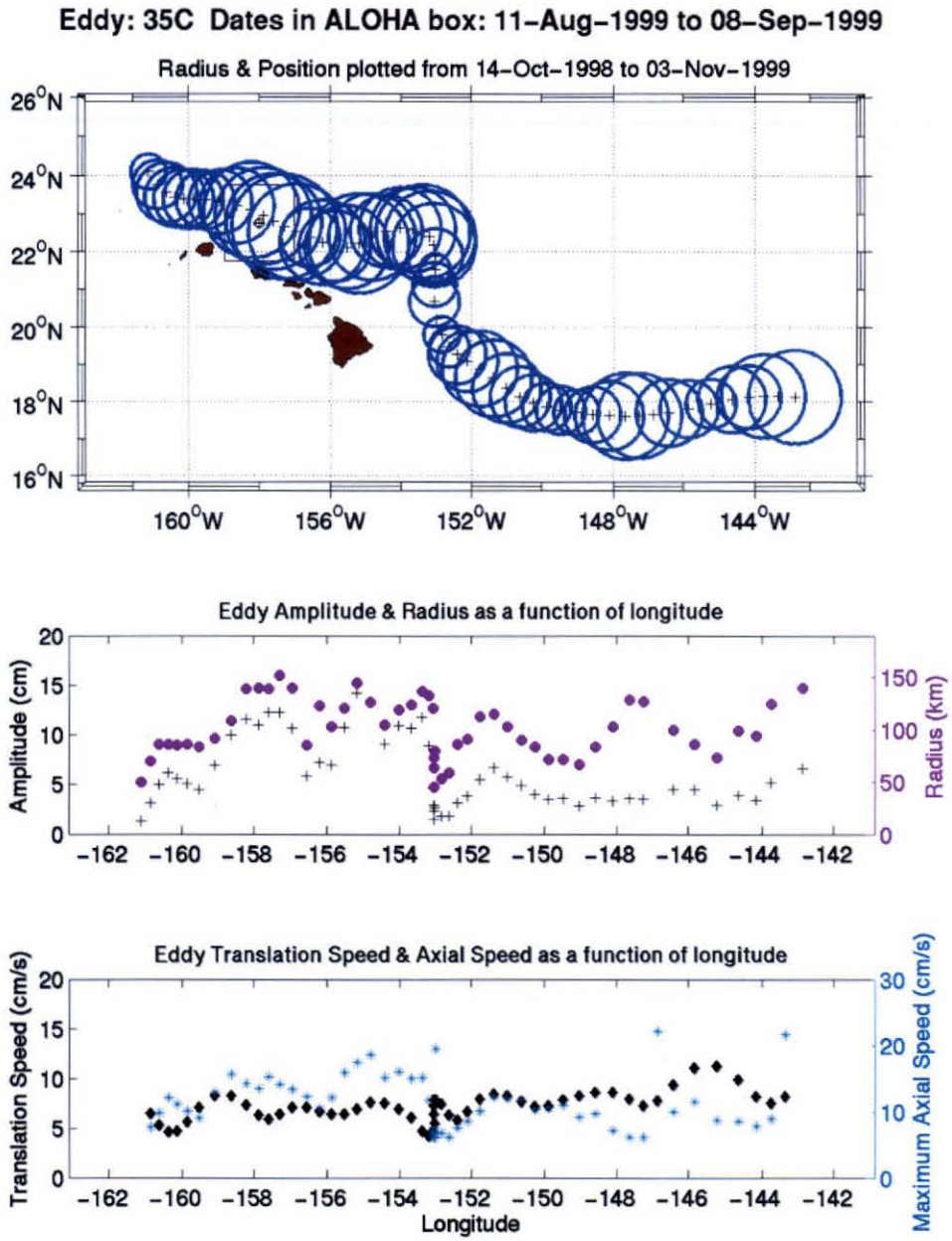

EID: 35C

This eddy lasted almost a year and was formed at 17N and 143W. It moved west until forced north by an anticyclonic eddy, then forced west again at 22N due to another eddy-eddy interaction. Large size over ALOHA may indicate some island interaction. Center passes right over ALOHA, would expect relatively large anomalies in water properties, which do appear at 24.75σ_θ level.

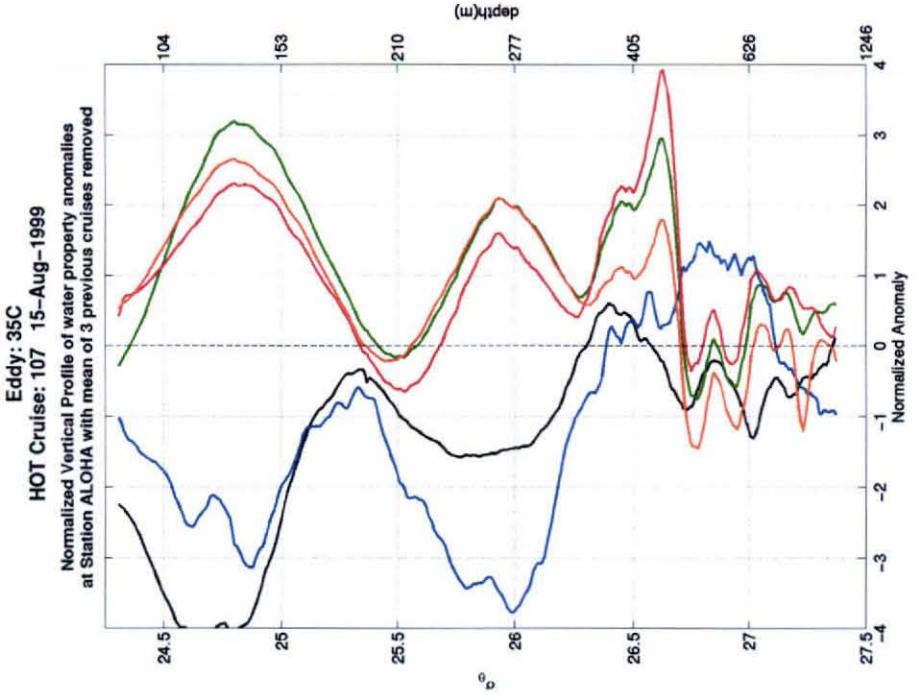
Eddy: 35C
HOT Cruise: 107 15-Aug-1999
Normalized Vertical Profile of water property anomalies
at Station ALOHA with mean of 3 previous cruises removed
depth(m)
104
153
210
277
405
626
1246
Normalized Anomaly
24.5
25
25.5
26
26.5
27
27.5
θ_p

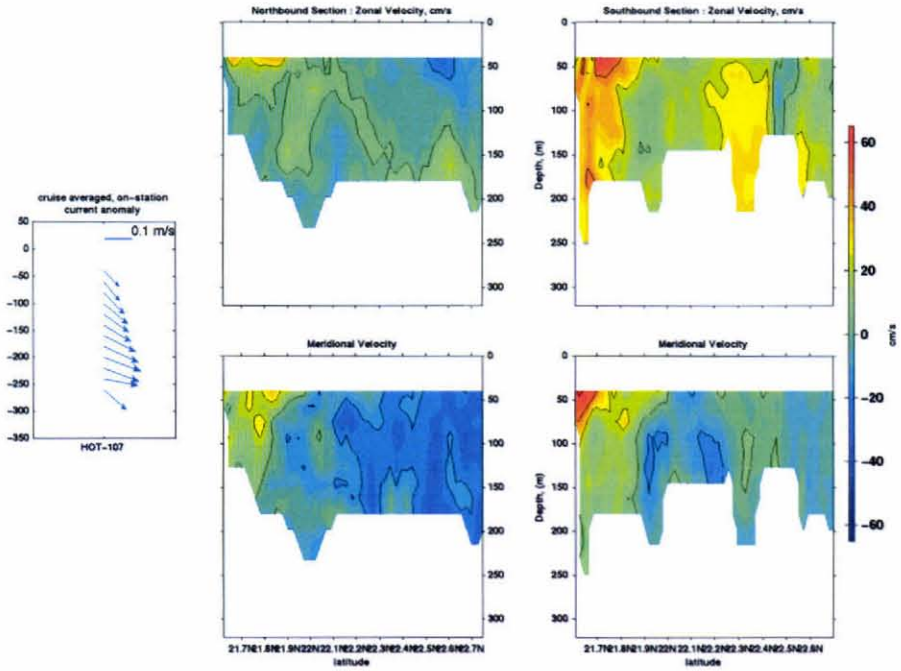
cruise averaged, on-station
current anomaly
0.1 m/s
HOT-107
Northbound Section : Zonal Velocity, cm/s
Southbound Section : Zonal Velocity, cm/s
Meridional Velocity
Meridional Velocity
Depth, (m)
latitude
cm/s

Eddy: 36A Dates in ALOHA box: 06-Oct-1999 to 06-Oct-1999

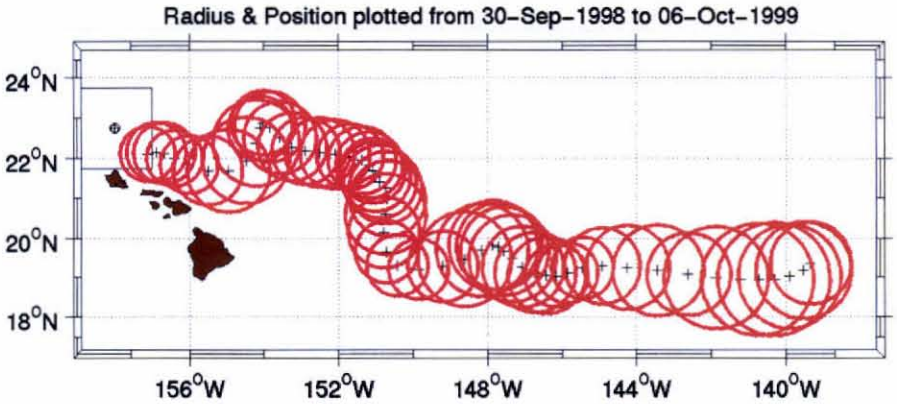

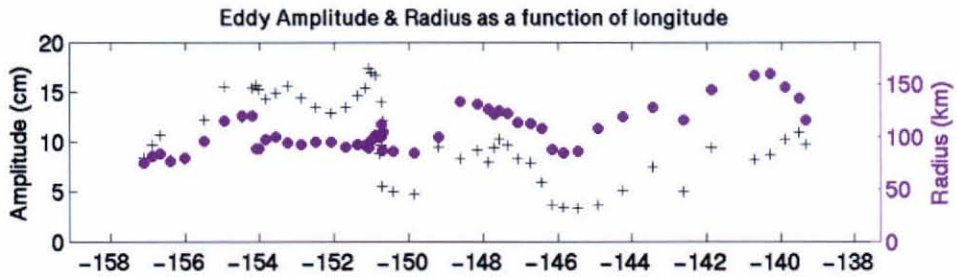

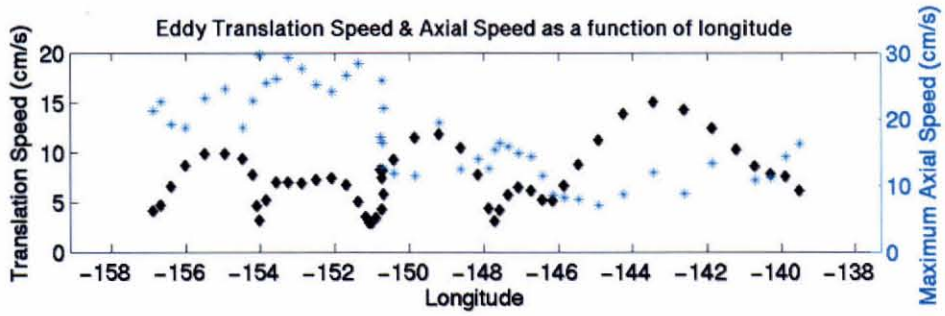

EID: 36A

This eddy formed 19N and 139W and traveled west until forced north by interaction with two cyclonic eddies. It resumes westward movement until more eddy-eddy interactions cause a deviation in direction and the eddy starts to break up. It eventually dissipates and passed over ALOHA at the end of its lifetime of almost a year.

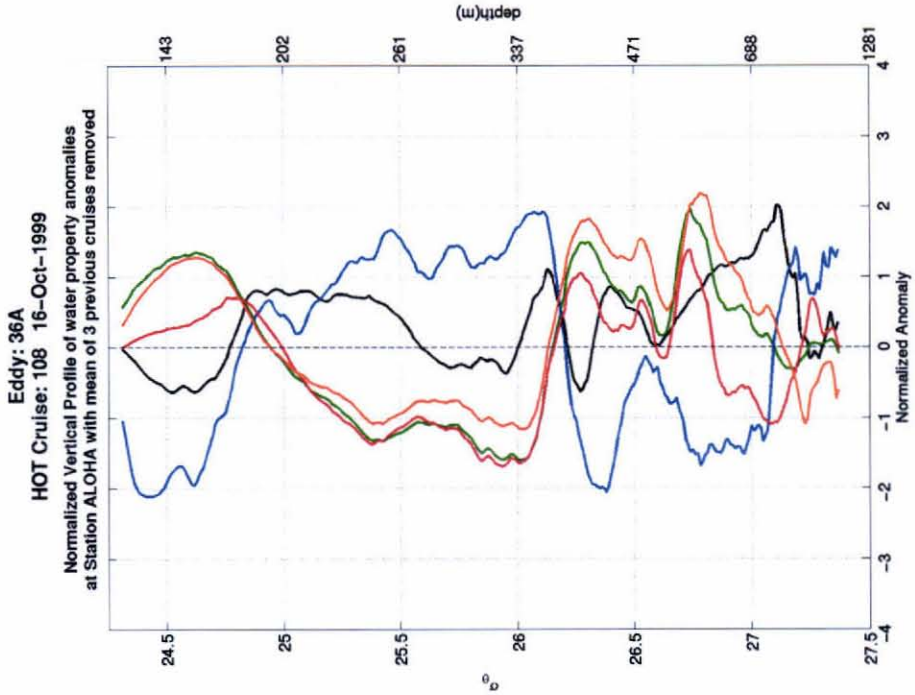
Eddy: 36A
HOT Cruise: 108 16-Oct-1999
Normalized Vertical Profile of water property anomalies
at Station ALOHA with mean of 3 previous cruises removed
depth(m)
143
202
261
337
471
688
1281
Normalized Anomaly
σ_θ

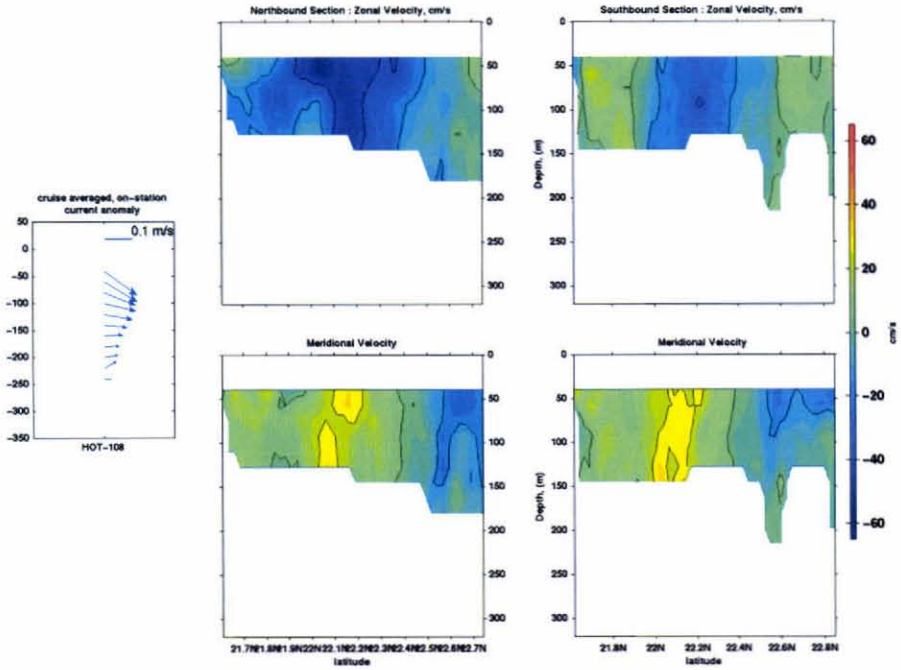
cruise averaged, on-station
current anomaly
0.1 m/s
HOT-108
Northbound Section : Zonal Velocity, cm/s
Southbound Section : Zonal Velocity, cm/s
Meridional Velocity
Meridional Velocity
Depth, (m)
latitude
cm/s

Eddy: 37C Dates in ALOHA box: 10-Nov-1999 to 12-Jan-2000

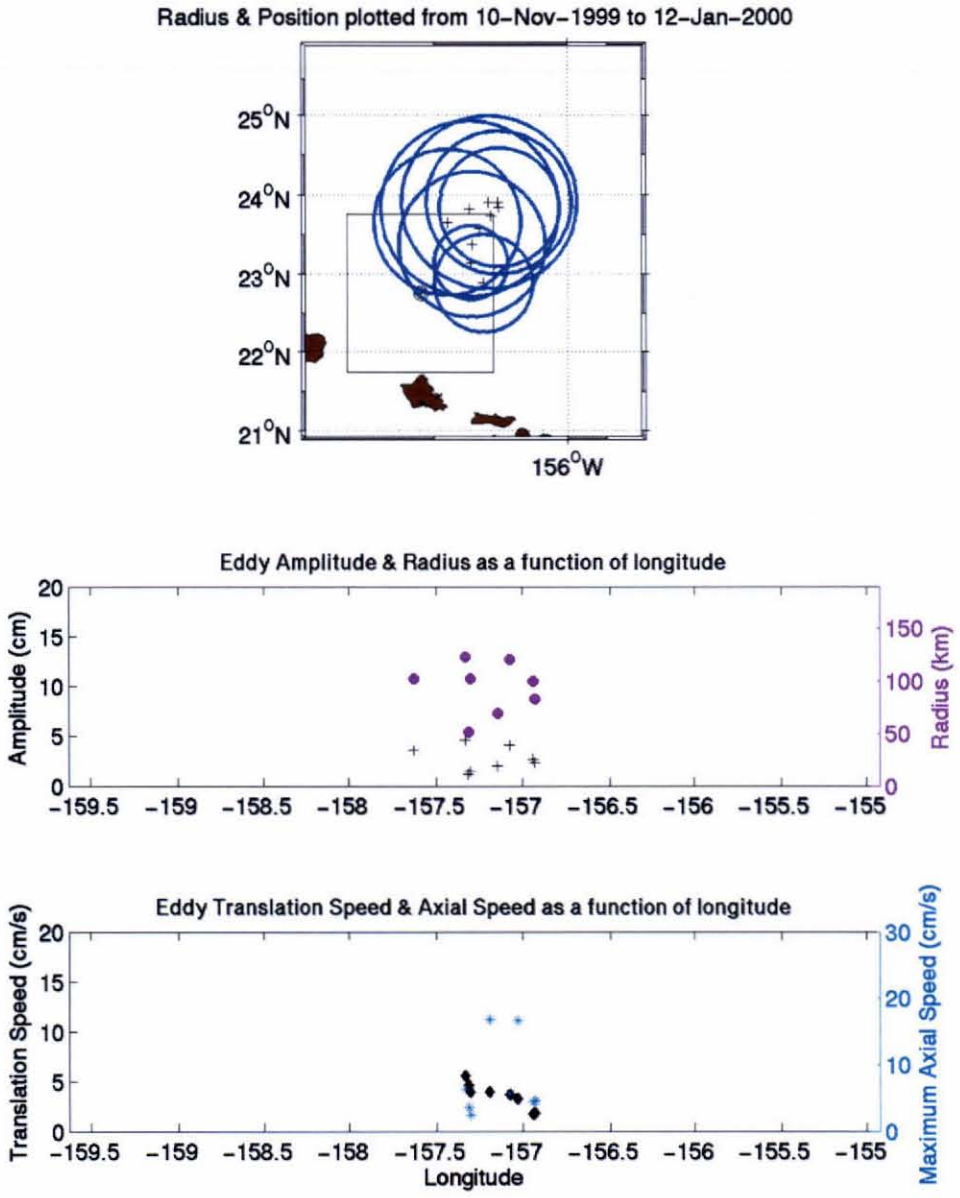

EID: 37C

This eddy was short-lived and stationary, spending all 10 weeks of its lifetime northeast of ALOHA. It appeared to be the remnant of an eddy that split several times due to continual eddy-eddy interaction. The relatively large water property anomalies associated with the timing of the passage of this feature are most likely due to some other mechanism.

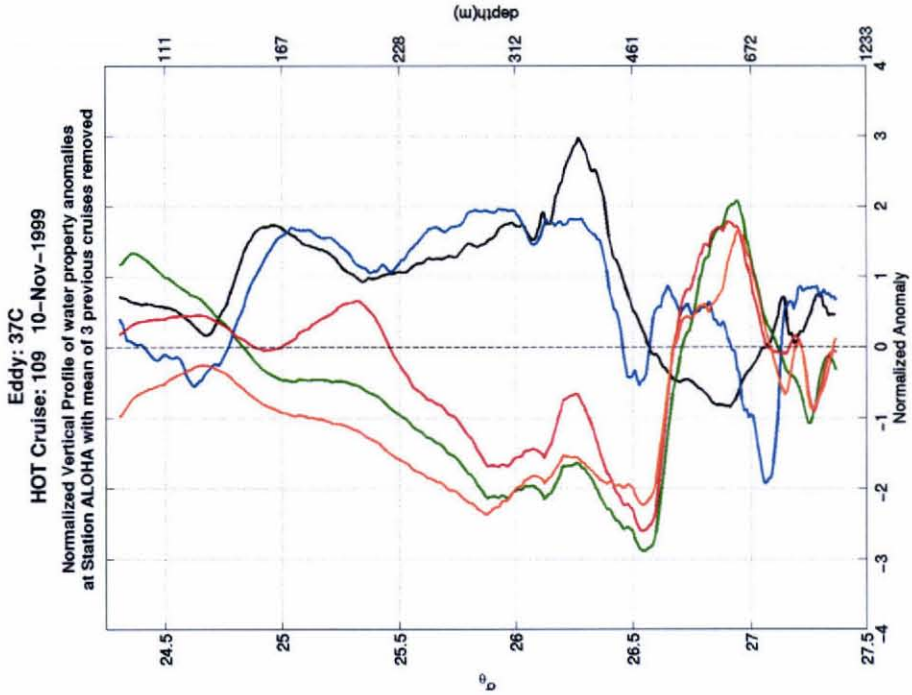
Eddy: 37C
HOT Cruise: 109 10-Nov-1999
Normalized Vertical Profile of water property anomalies
at Station ALOHA with mean of 3 previous cruises removed
depth(m)
111
167
228
312
461
672
1233
Normalized Anomaly
θ_p

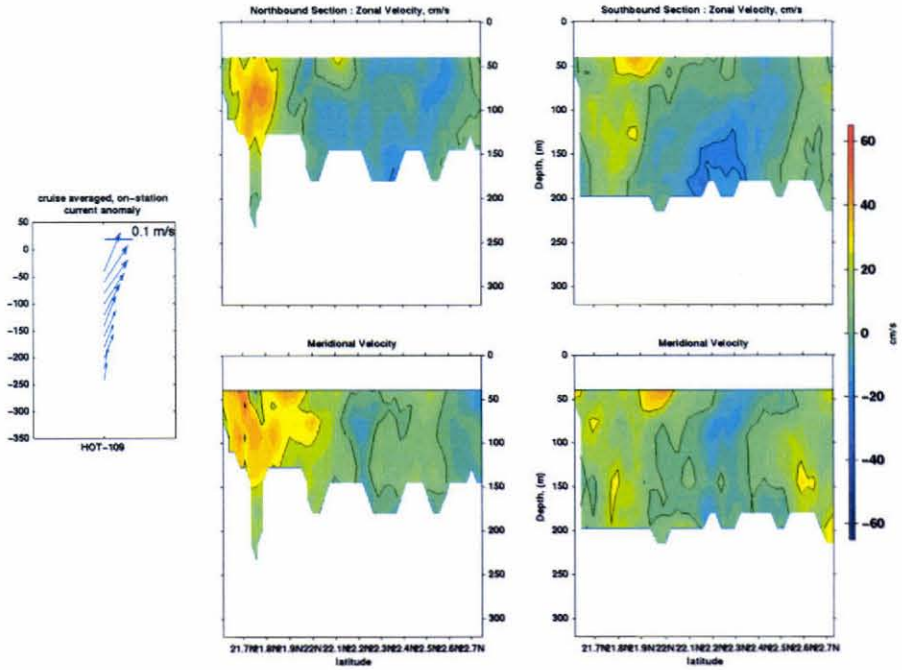
cruise averaged, on-station
current anomaly
0.1 m/s
HOT-109
Northbound Section : Zonal Velocity, cm/s
Southbound Section : Zonal Velocity, cm/s
Meridional Velocity
Meridional Velocity
Depth, (m)
latitude
cm/s

Eddy: 38C Dates in ALOHA box: 01-Dec-1999 to 22-Dec-1999

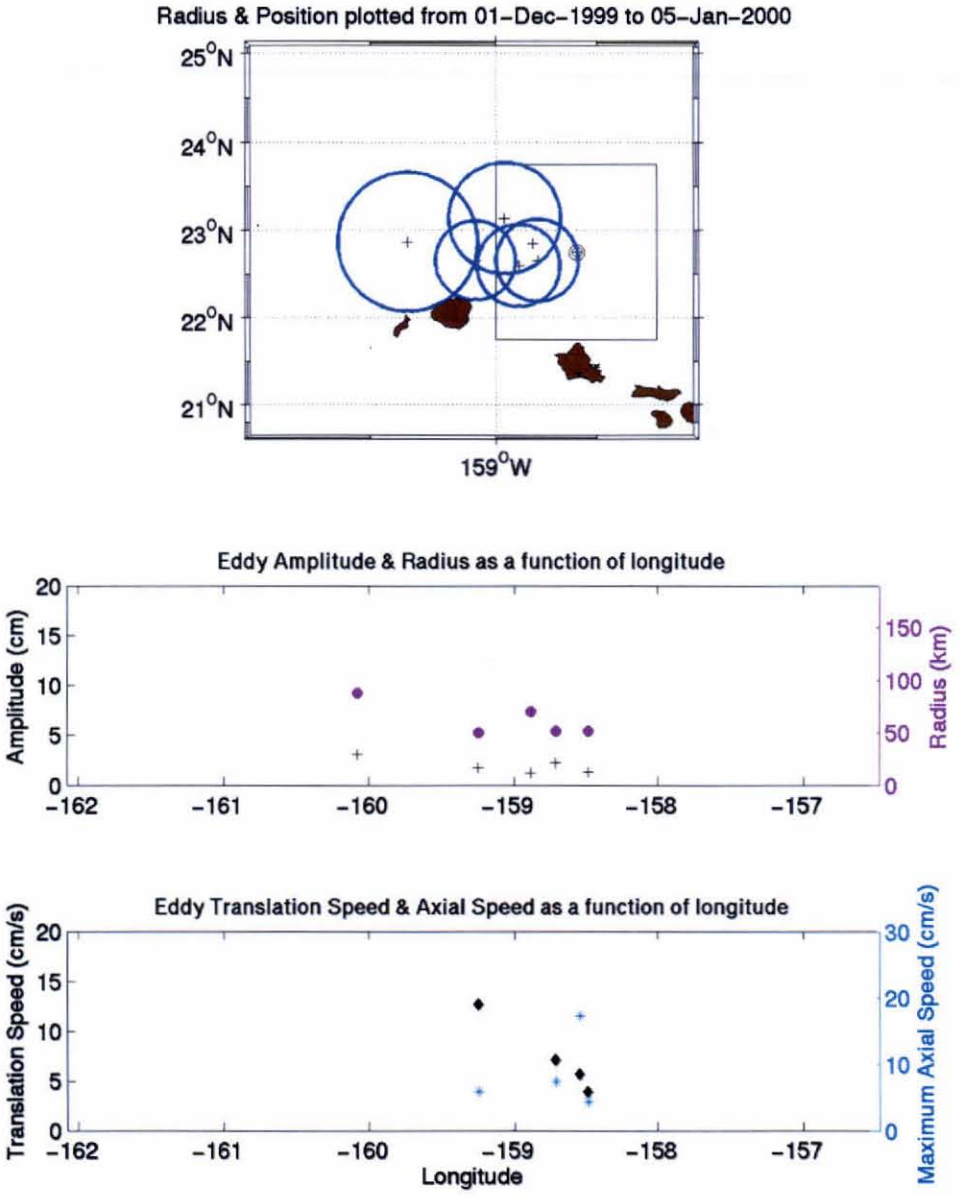

EID: 38C

This eddy should be similar to 37C because it appears to come from the same source, which splits again due to an anticyclone that comes by west of ALOHA. This feature is also short-lived and questionable.

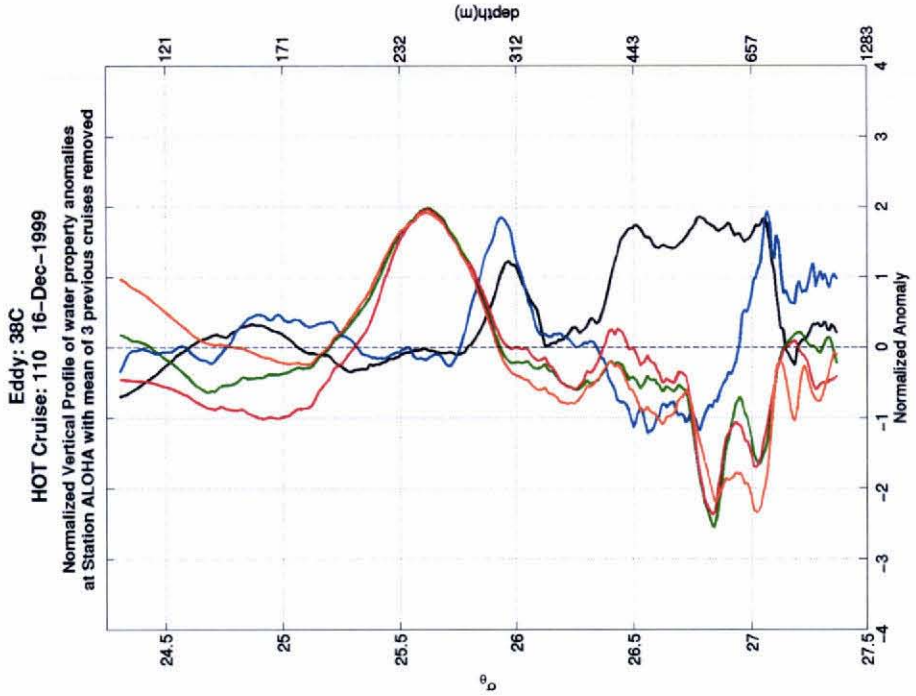
Eddy: 38C
HOT Cruise: 110 16-Dec-1999
Normalized Vertical Profile of water property anomalies
at Station ALOHA with mean of 3 previous cruises removed
depth(m)
121
171
232
312
443
657
1283
Normalized Anomaly
θ_σ

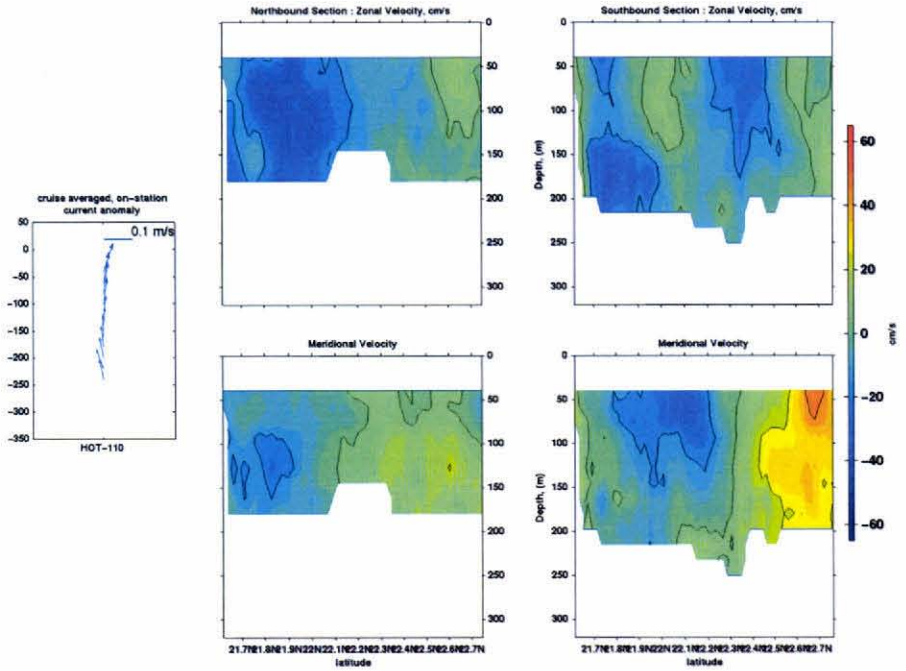
cruise averaged, on-station
current anomaly
0.1 m/s
HOT-110
Northbound Section : Zonal Velocity, cm/s
Southbound Section : Zonal Velocity, cm/s
Meridional Velocity
Meridional Velocity
Depth, (m)
latitude
cm/s

Eddy: 39A Dates in ALOHA box: 12-Jan-2000 to 26-Jan-2000

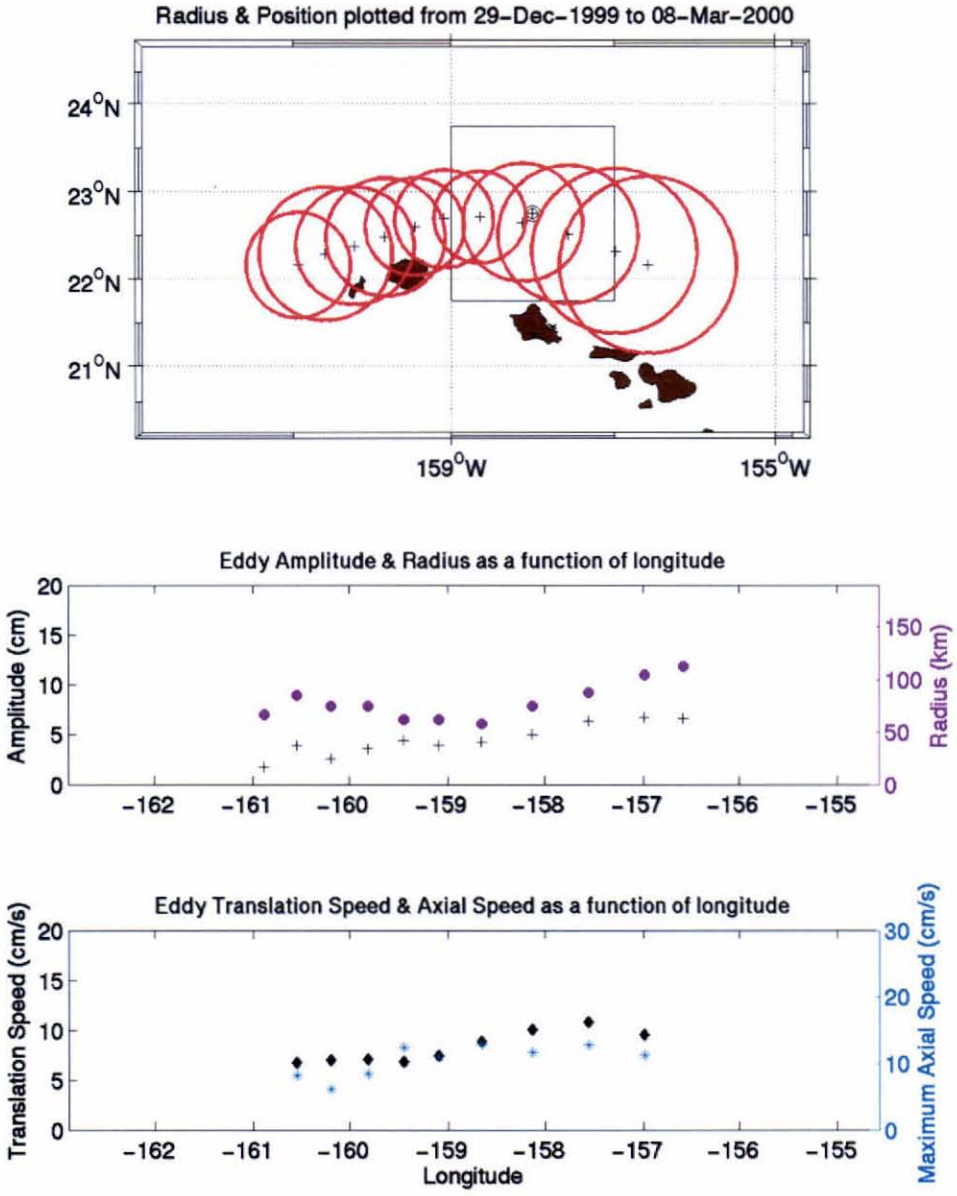

EID: 39A

This eddy comes together over Maui due to eddy-eddy (and probably also eddy-island) interactions, which also cause it to split just before ALOHA, then recombine and dissipate past Kauai. Do not expect much of a signal because of all the interactions.

Eddy: 40C Dates in ALOHA box: 02-Feb-2000 to 23-Feb-2000

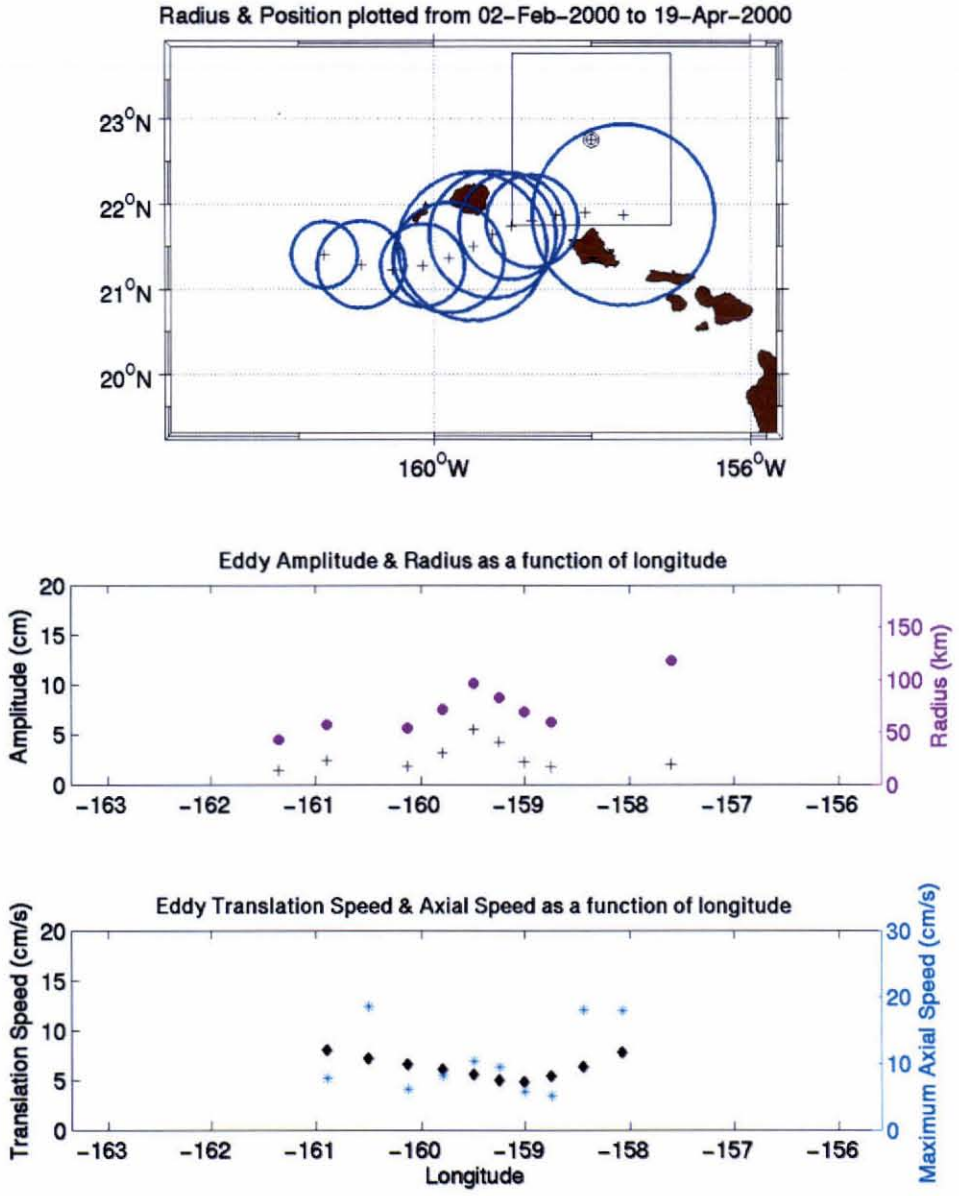

EID: 40C

This eddy is a weak structure that appears to come up through Kaiwi Channel, past ALOHA then back down through Kauai Channel, but this is highly unlikely. This feature is probably not an eddy.

Eddy: 41C Dates in ALOHA box: 29-Mar-2000 to 26-Apr-2000

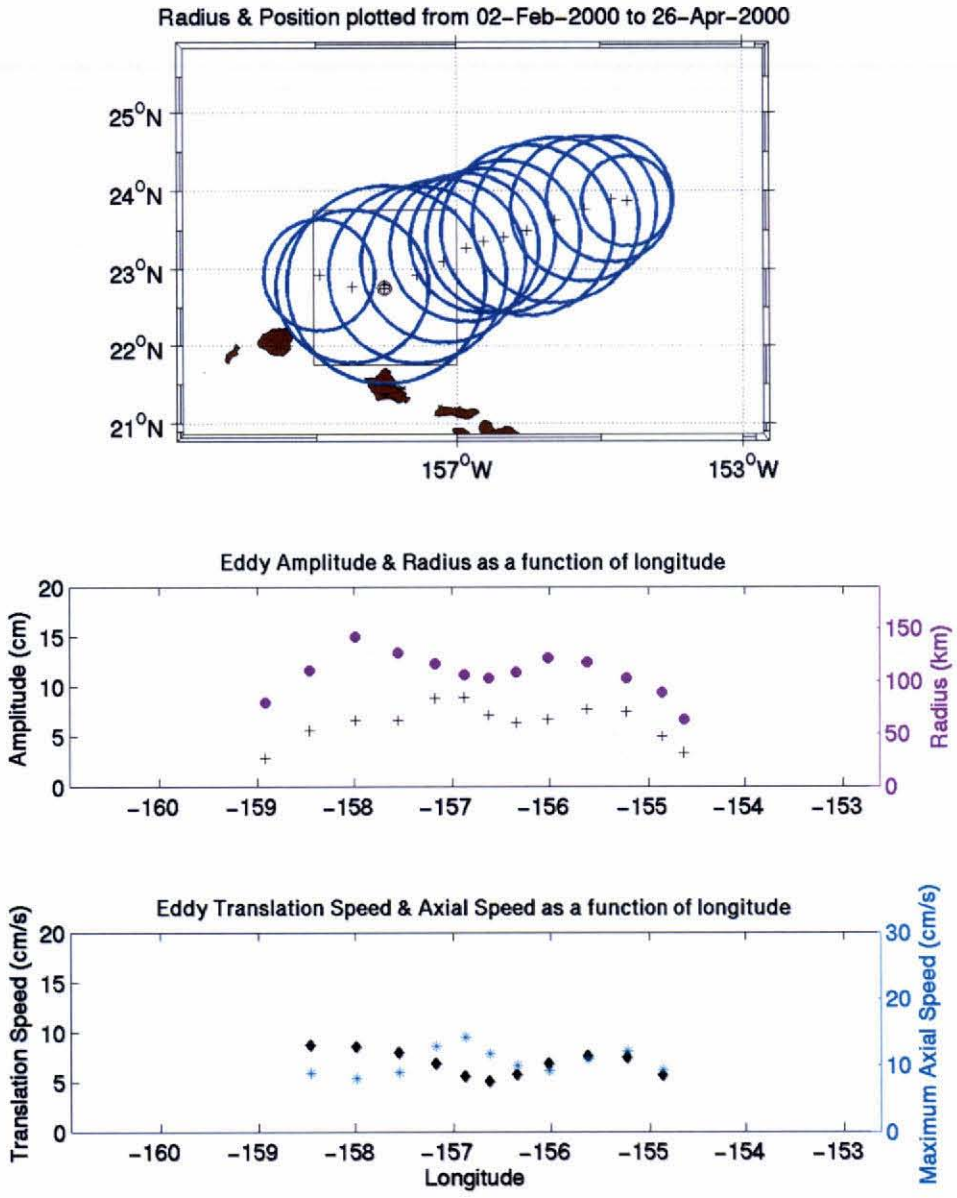

EID: 41C

This eddy is a month long feature that moves southwest from its formation location (24N, 155W). A large anticyclonic eddy was located immediately west of this eddy and is probably responsible for the southwest trajectory. Eddy dissipates after encountering Oahu and Kauai.

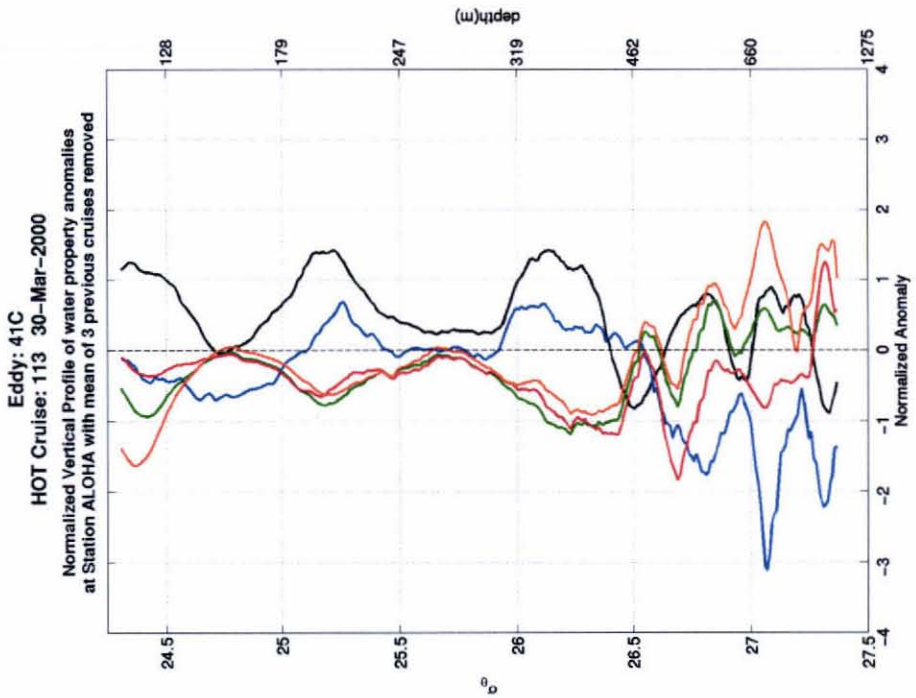
Eddy: 41C
HOT Cruise: 113 30-Mar-2000
Normalized Vertical Profile of water property anomalies
at Station ALOHA with mean of 3 previous cruises removed
depth(m)
128
179
247
319
462
660
1275
Normalized Anomaly
σ_θ

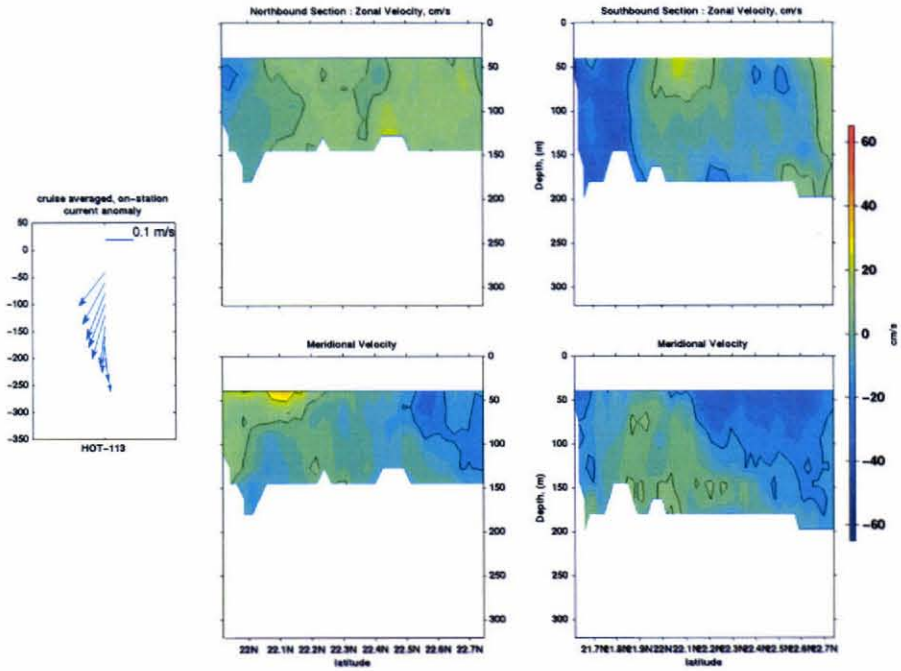
cruise averaged, on-station
current anomaly
0.1 m/s
HOT-113
Northbound Section : Zonal Velocity, cm/s
Southbound Section : Zonal Velocity, cm/s
Meridional Velocity
Meridional Velocity
Depth, (m)
latitude
cm/s

Eddy: 42A Dates in ALOHA box: 09-Aug-2000 to 30-Aug-2000

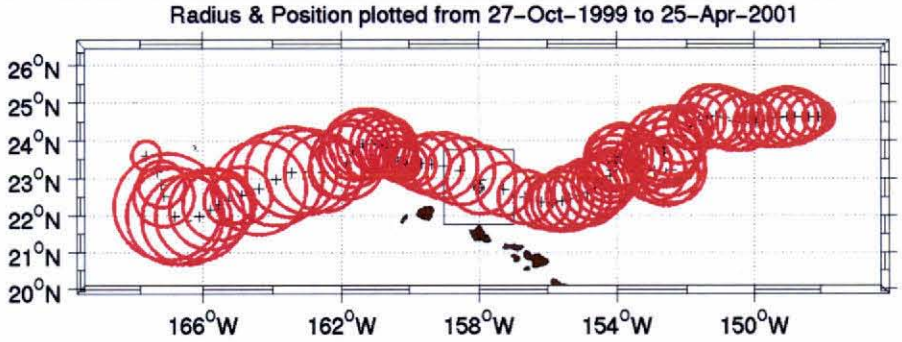

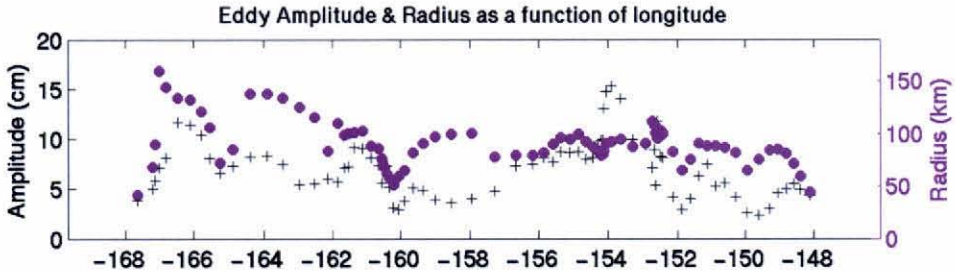

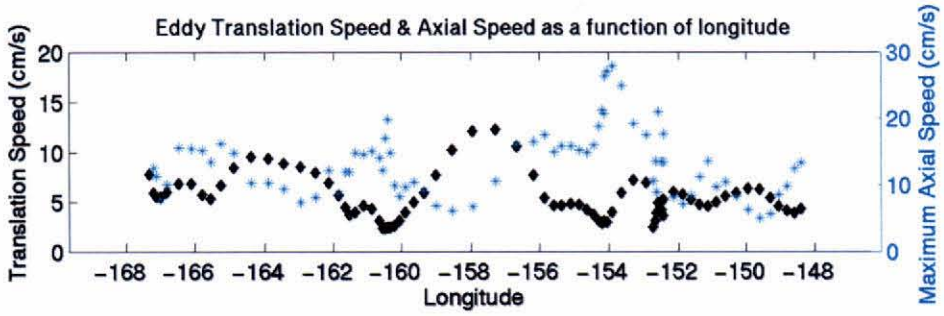

EID: 42A

This eddy was formed from two merging eddies and lasted a year and a half. It moved quickly through ALOHA after several obscure direction changes due to eddy-eddy interactions. The eddy traveled northwest past islands, then changed direction to the southwest after encountering other features, and eventually dissipated at 167W.

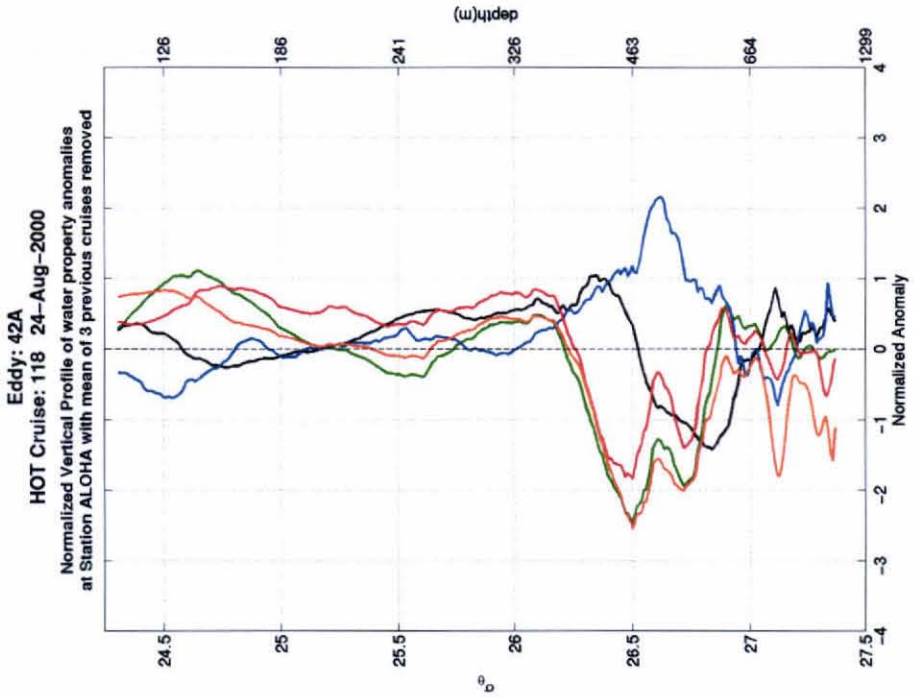
Eddy: 42A
HOT Cruise: 118 24-Aug-2000
Normalized Vertical Profile of water property anomalies
at Station ALOHA with mean of 3 previous cruises removed
depth(m)
126
186
241
326
463
664
1299
Normalized Anomaly
θ_D

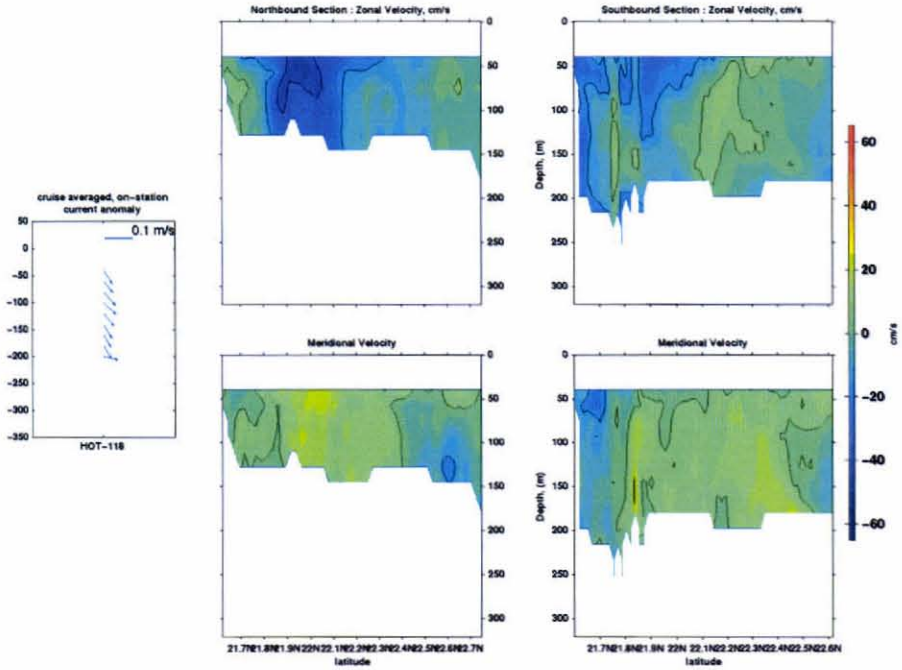
cruise averaged, on-station
current anomaly
0.1 m/s
HOT-118
Northbound Section : Zonal Velocity, cm/s
Southbound Section : Zonal Velocity, cm/s
Meridional Velocity
Meridional Velocity
Depth, (m)
latitude
cm/s

Eddy: 43A Dates in ALOHA box: 08-Nov-2000 to 08-Nov-2000

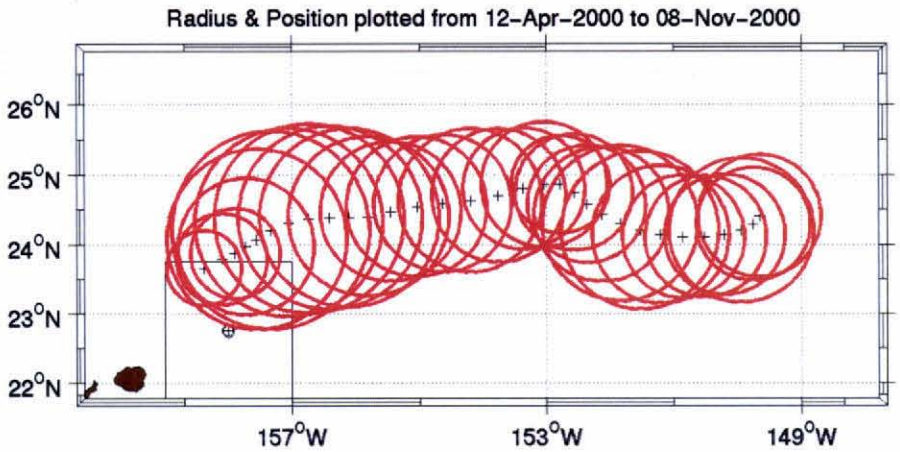

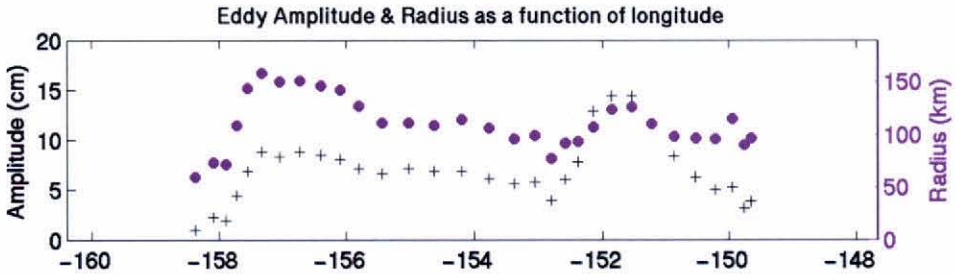

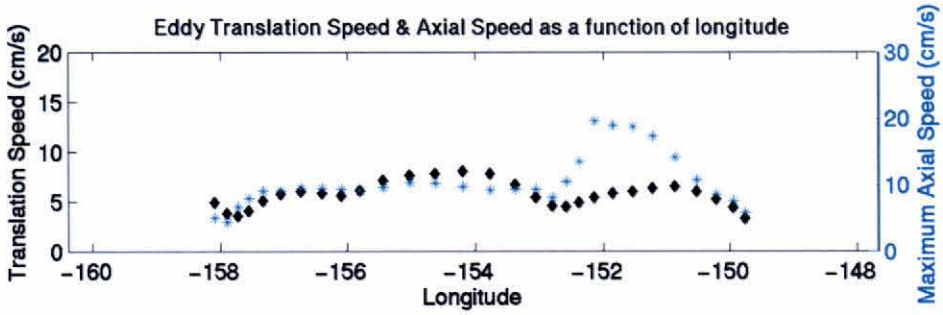

EID: 43A

This eddy formed at 150W, traveled west to north of ALOHA, dissipates as it arrives and is drawn up into another eddy. Barely grazes ALOHA with its southwest edge and therefore expect minimal impact on ALOHA from this eddy.

Eddy: 44A Dates in ALOHA box: 20-Dec-2000 to 14-Feb-2001

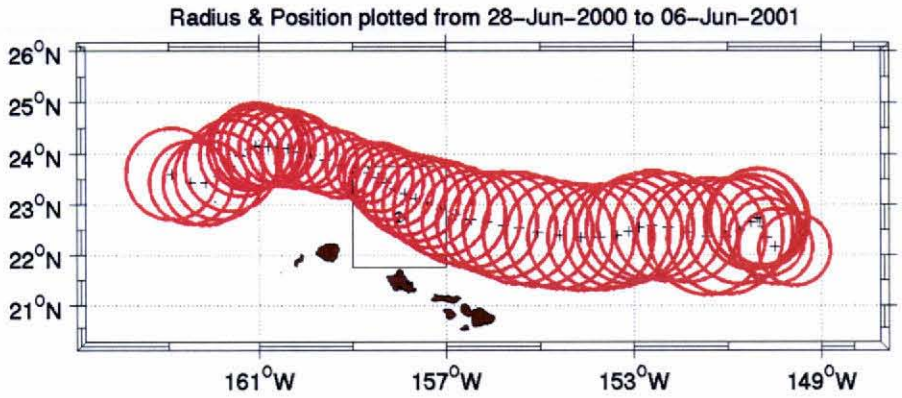

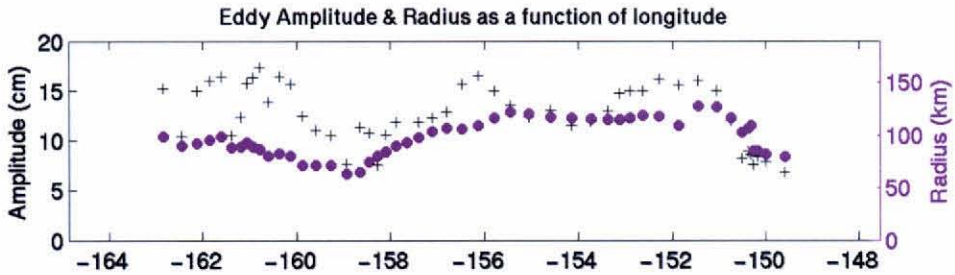

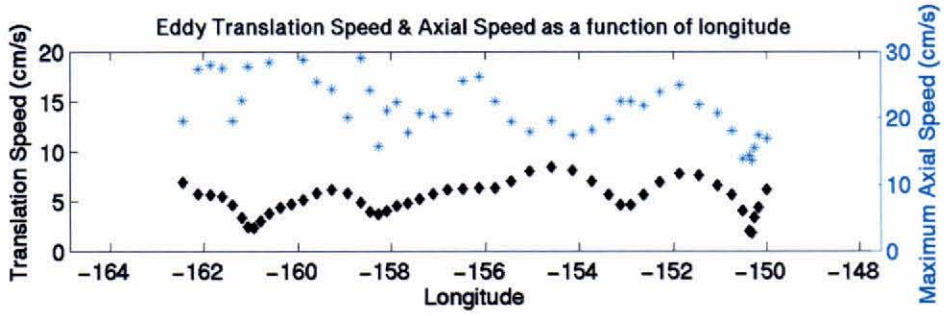

EID: 44A

This eddy spun up at 150W as the result of two merging eddies and moves west towards ALOHA, northwest over ALOHA, then southwest once past Kauai. This final direction change was due to interaction with another eddy. The northwest trajectory north of the islands maybe due to meridional advection by the mean flow.

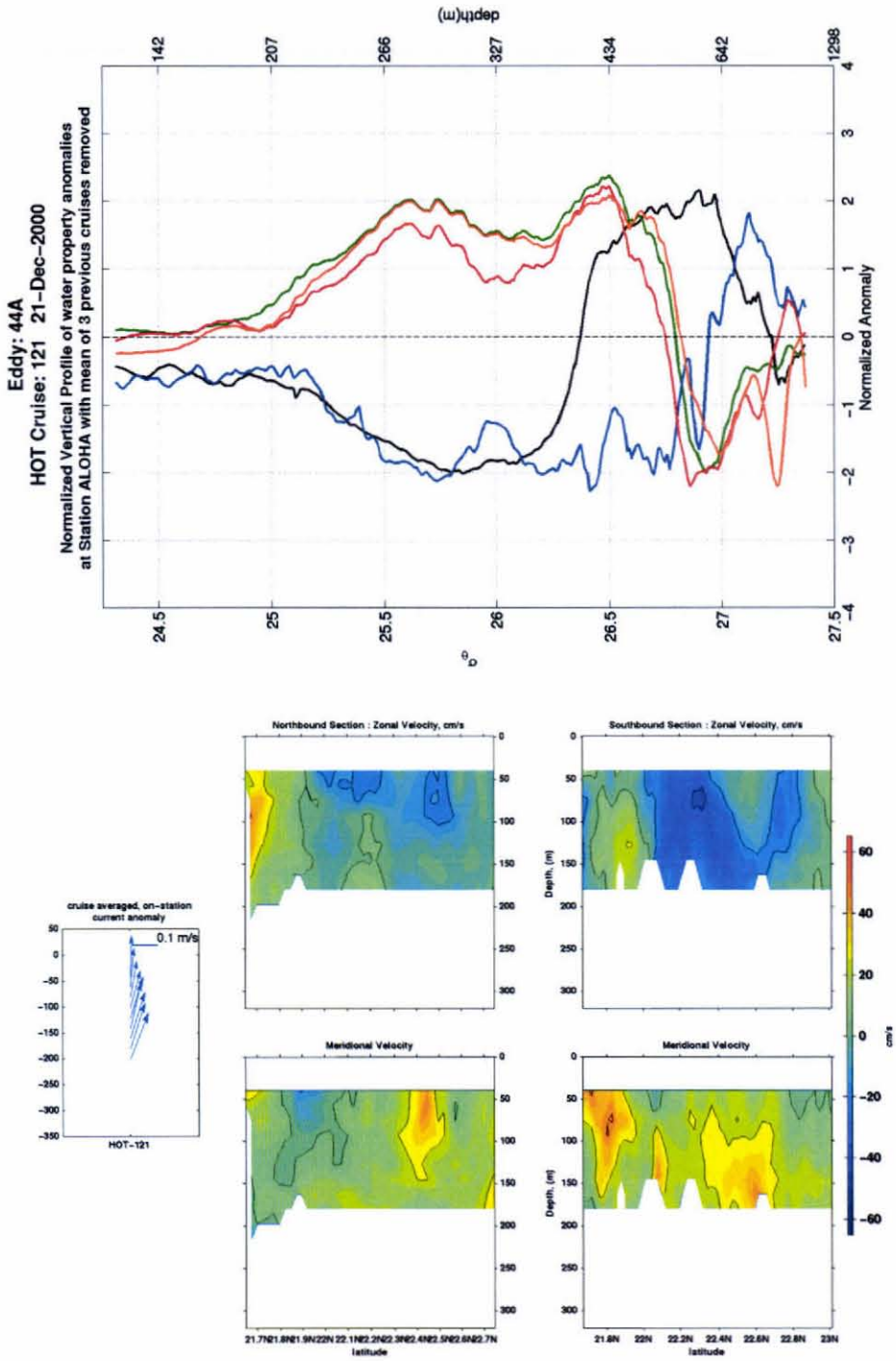
Eddy: 44A
HOT Cruise: 121 21-Dec-2000
Normalized Vertical Profile of water property anomalies
at Station ALOHA with mean of 3 previous cruises removed
depth(m)
142
207
266
327
434
642
1298
Normalized Anomaly
σ_θ
cruise averaged, on-station
current anomaly
0.1 m/s
HOT-121
Northbound Section : Zonal Velocity, cm/s
Southbound Section : Zonal Velocity, cm/s
Meridional Velocity
Meridional Velocity
Depth, (m)
latitude
cm/s

Eddy: 45A Dates in ALOHA box: 11-Apr-2001 to 25-Apr-2001

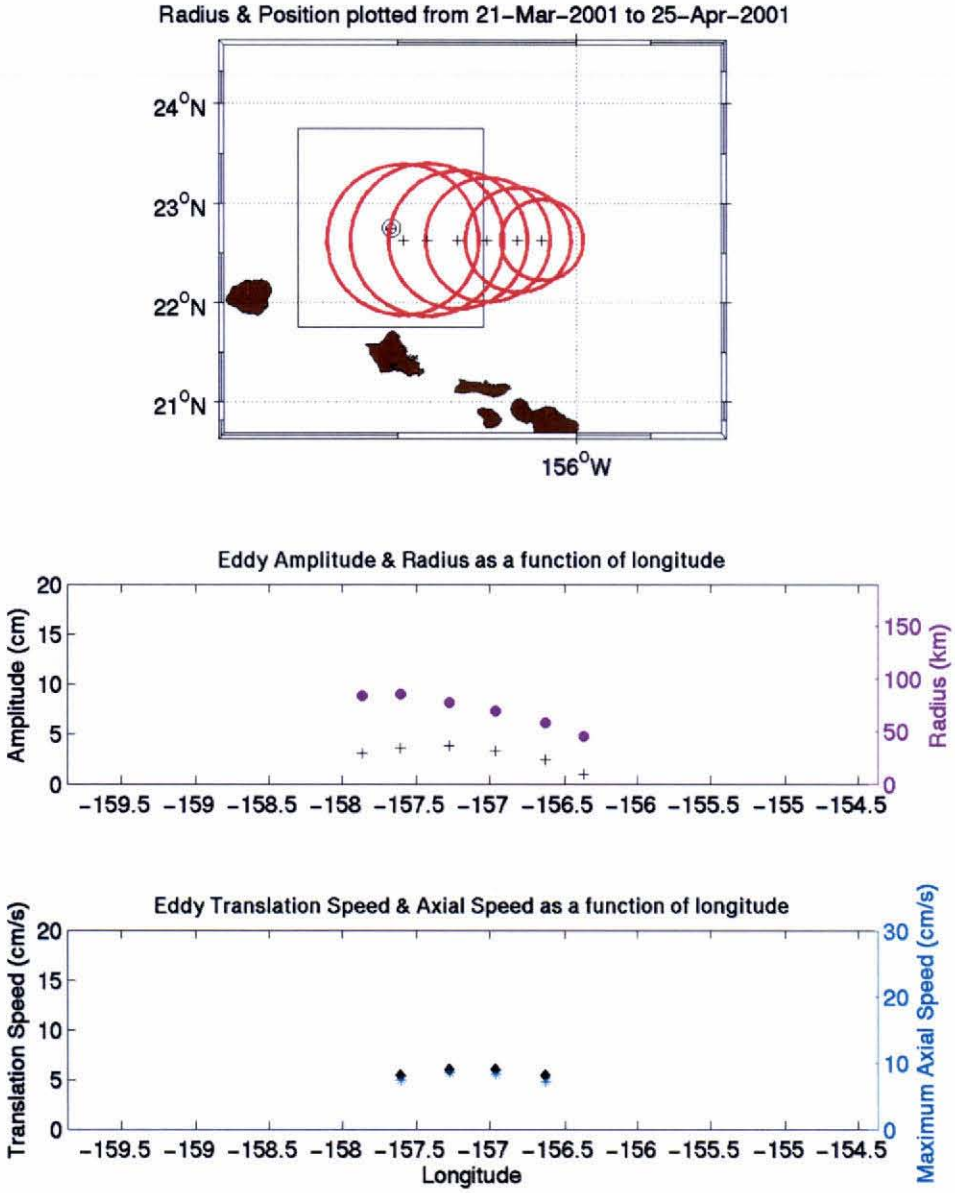

EID: 45A

This questionable eddy is short-lived with a small amplitude, dissipated before it passed ALOHA, probably not truly an eddy.

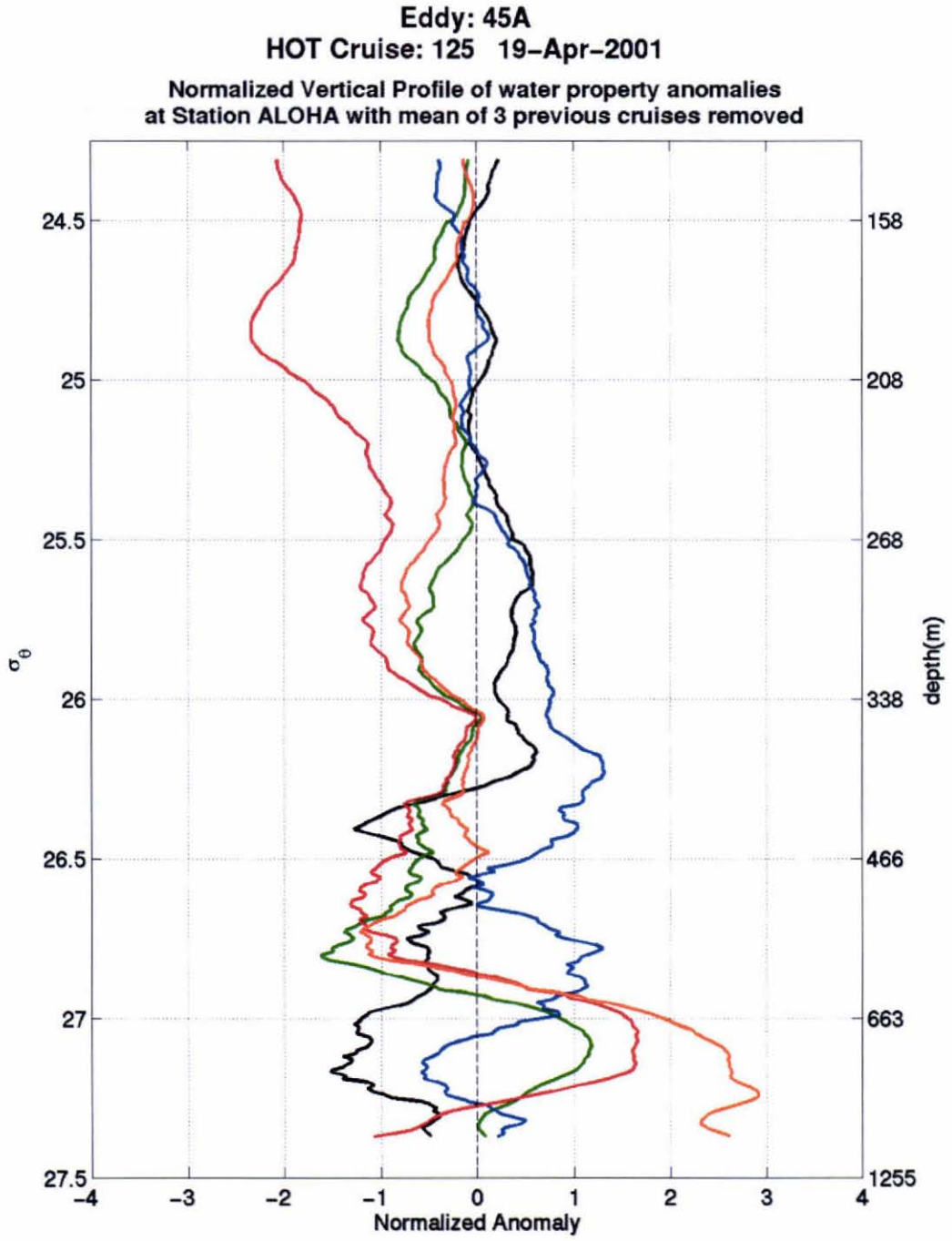
Eddy: 45A
HOT Cruise: 125 19-Apr-2001
Normalized Vertical Profile of water property anomalies
at Station ALOHA with mean of 3 previous cruises removed
24.5
25
25.5
26
26.5
27
27.5
σ_θ
158
208
268
338
466
663
1255
depth(m)
-4
-3
-2
-1
0
1
2
3
4
Normalized Anomaly

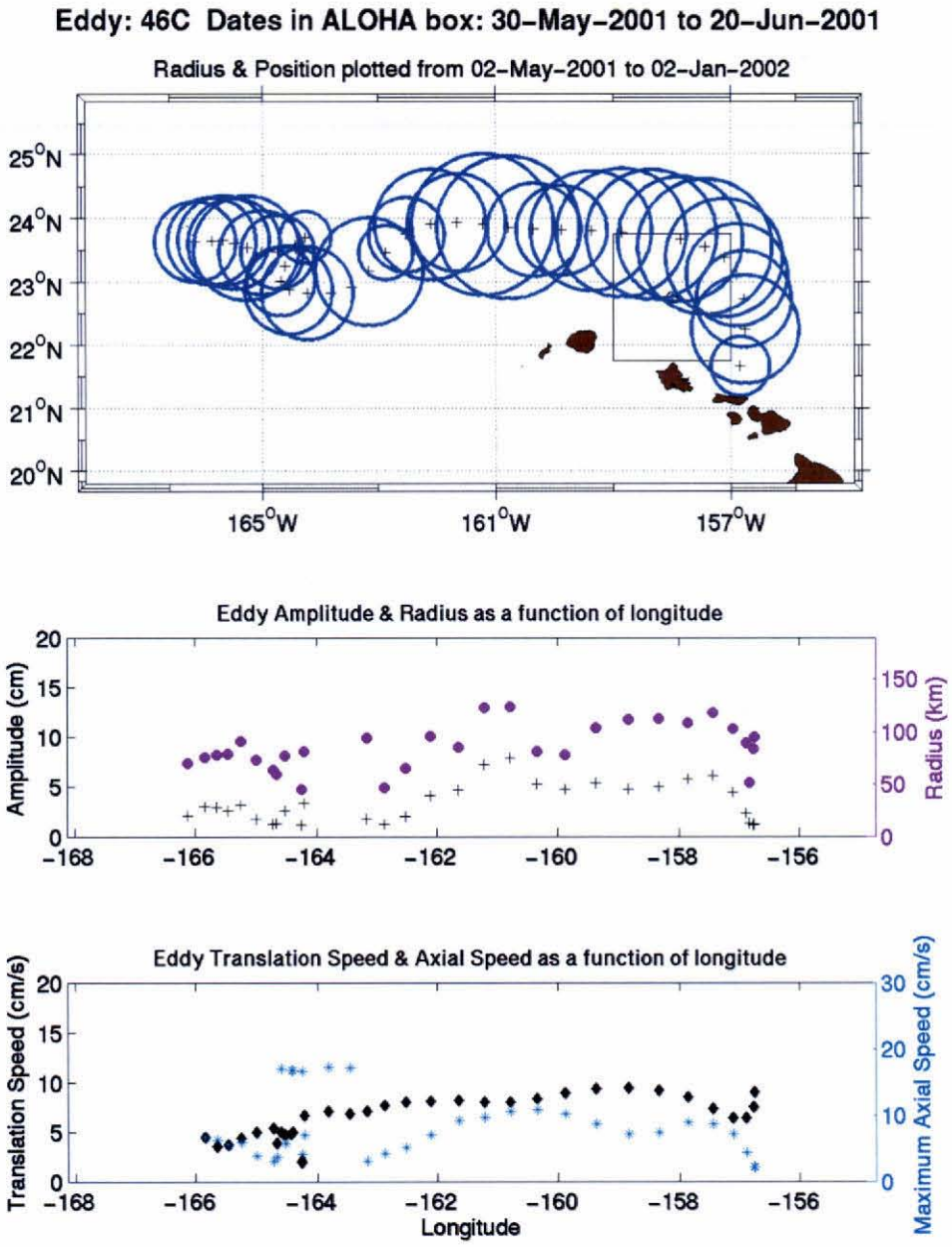

EID: 46C

This eddy formed from eddy-eddy or eddy-island (or combination of both) interactions north of Maui. Continuous interaction with other features throughout its lifetime prevent this feature from ever achieving steady state. It never develops the idealistic circular structure and its erratic behavior probably accounts for the radical changes in radius determined by the algorithm.

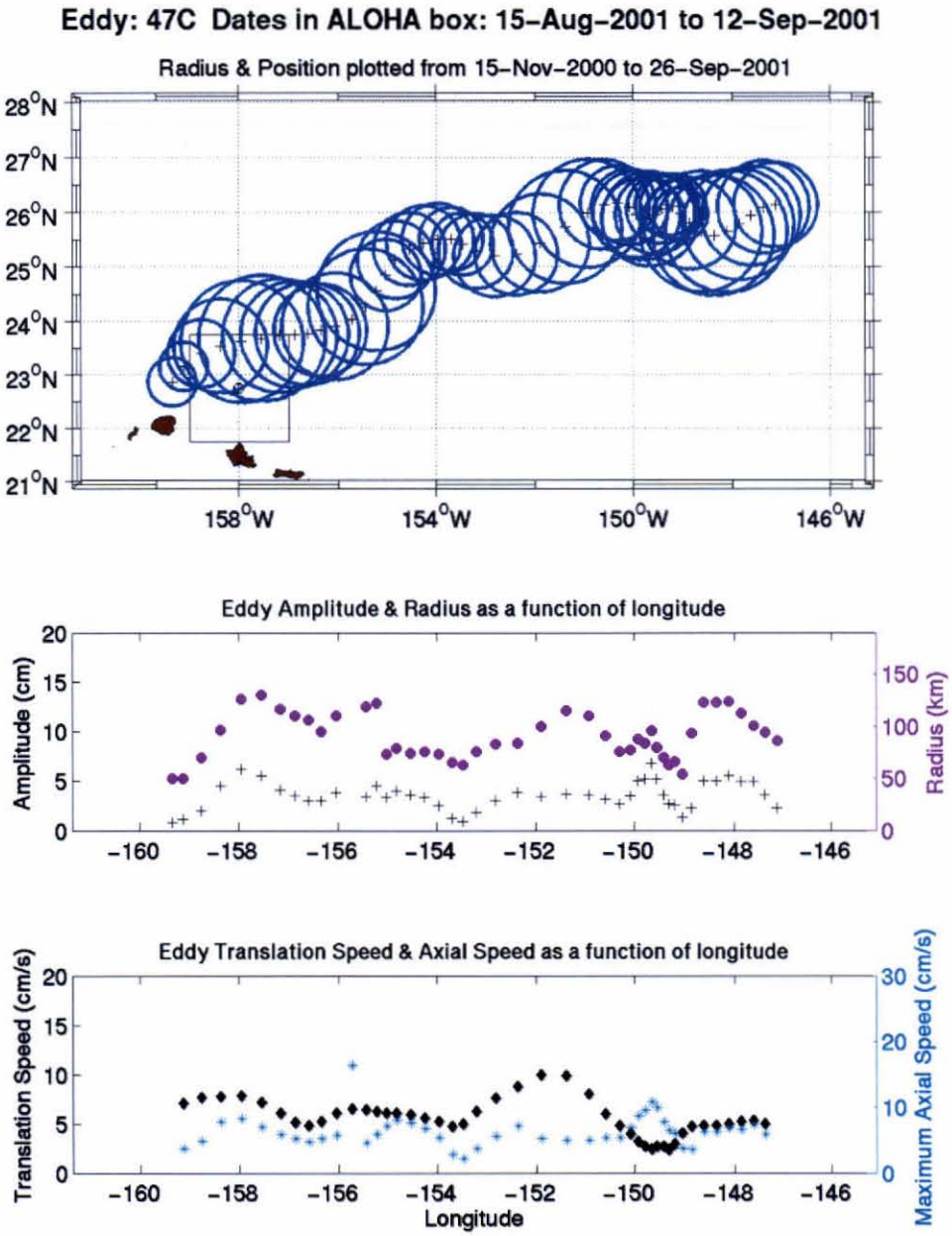

EID: 47C

This eddy formed northeast of ALOHA at 26N, 147W. It formed between two anticyclonic eddies, and the direction change to the southwest was a result of eddy-eddy interactions. It was then forced south when it butted up against an anticyclonic eddy located to the west. The tracked position and calculated radius does not encompass the whole eddy as it passes over ALOHA. Visually, the center of the eddy passes closer to ALOHA and the southern part of the eddy may be interacting with the islands.

Eddy: 48C Dates in ALOHA box: 10-Oct-2001 to 07-Nov-2001

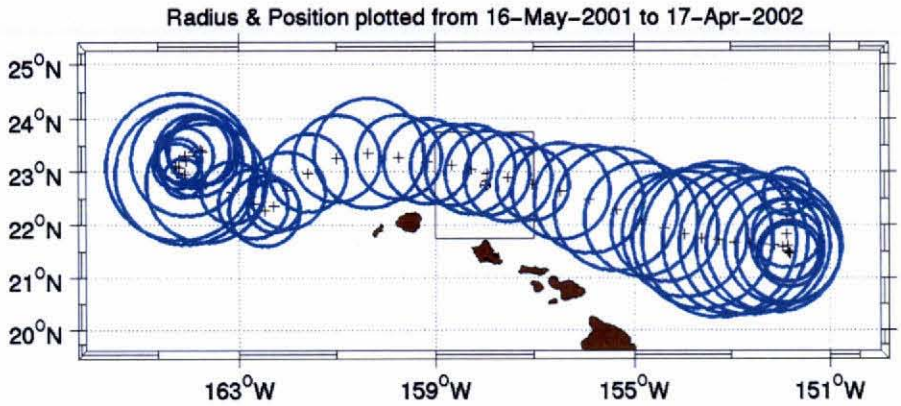

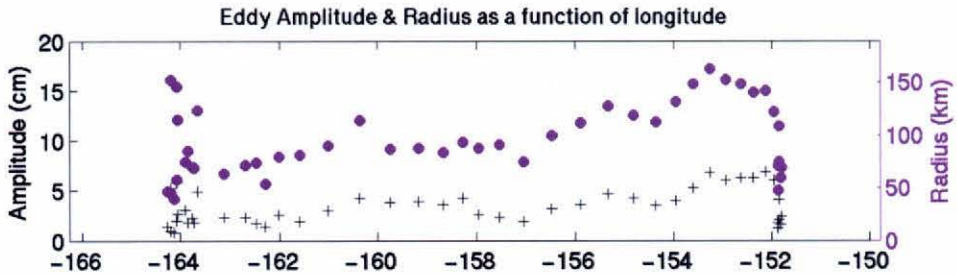

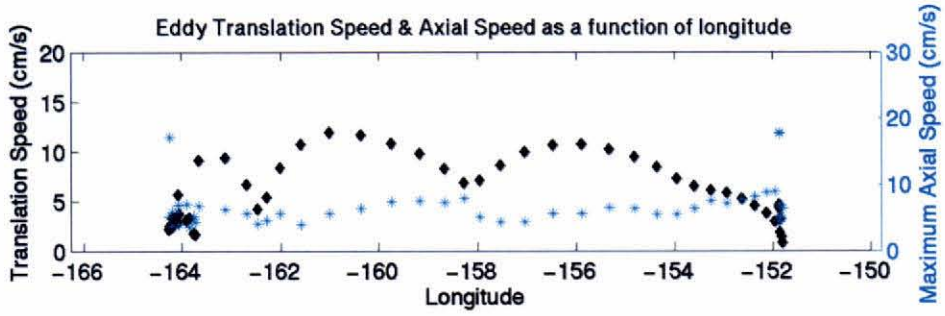

EID: 48C

This eddy was stationary for the first two months while it was spinning up. It then moved northwest over island chain, passed over ALOHA and then experienced a large size change at 164W. Eddy-eddy interactions ultimately cause it to break up.

Eddy: 49A Dates in ALOHA box: 26-Dec-2001 to 06-Feb-2002

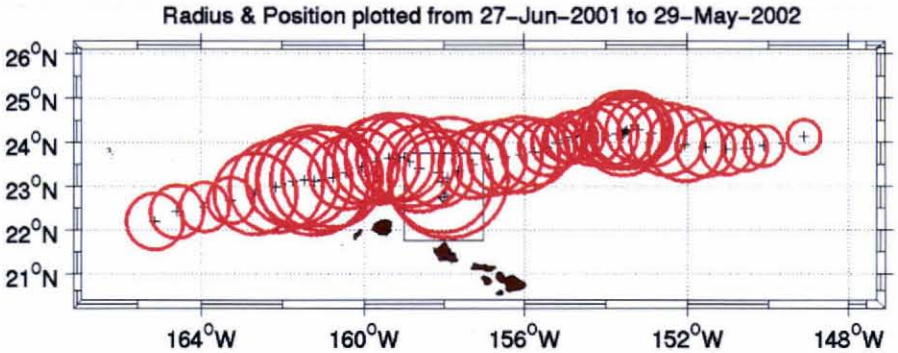

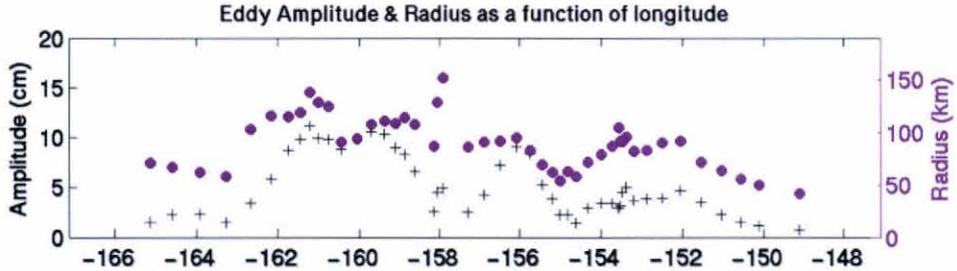

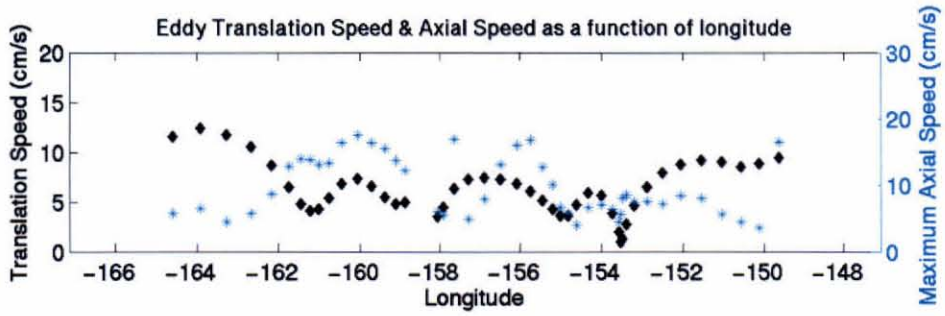

ID: 49A

This eddy formed around 150W, translates west, briefly increases size over ALOHA, continues west and eventually dissipates when a cyclonic eddy moves in to the east of it. One of the few cases where no significant interactions with other eddies were observed, would expect a bolus anomaly, vertical profile shows a large anomaly at the $27\sigma_\theta$ level.

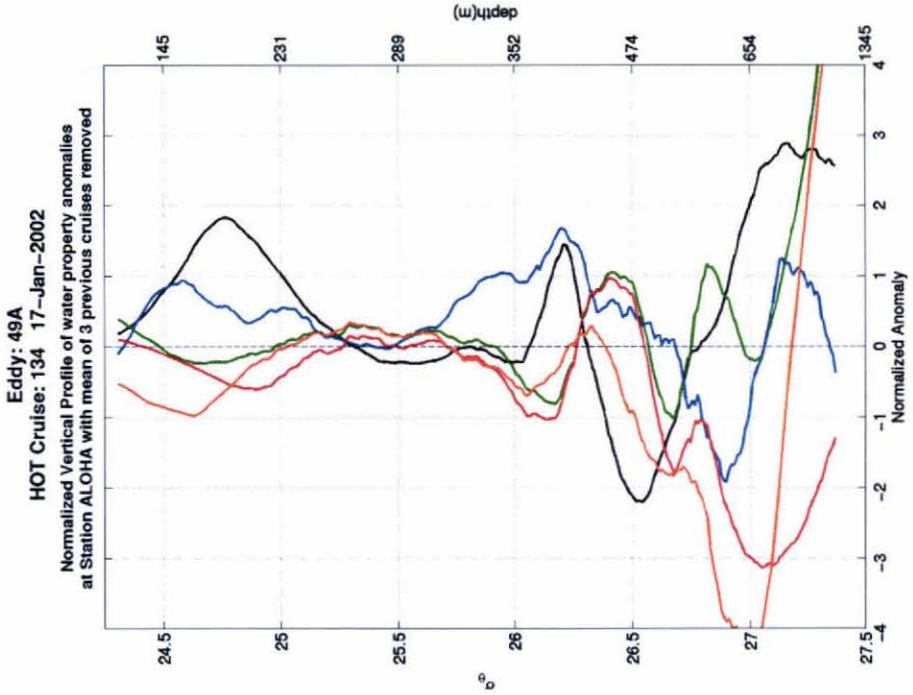
Eddy: 49A
HOT Cruise: 134 17-Jan-2002
Normalized Vertical Profile of water property anomalies
at Station ALOHA with mean of 3 previous cruises removed
depth(m)
145
231
289
352
474
654
1345
Normalized Anomaly
σθ

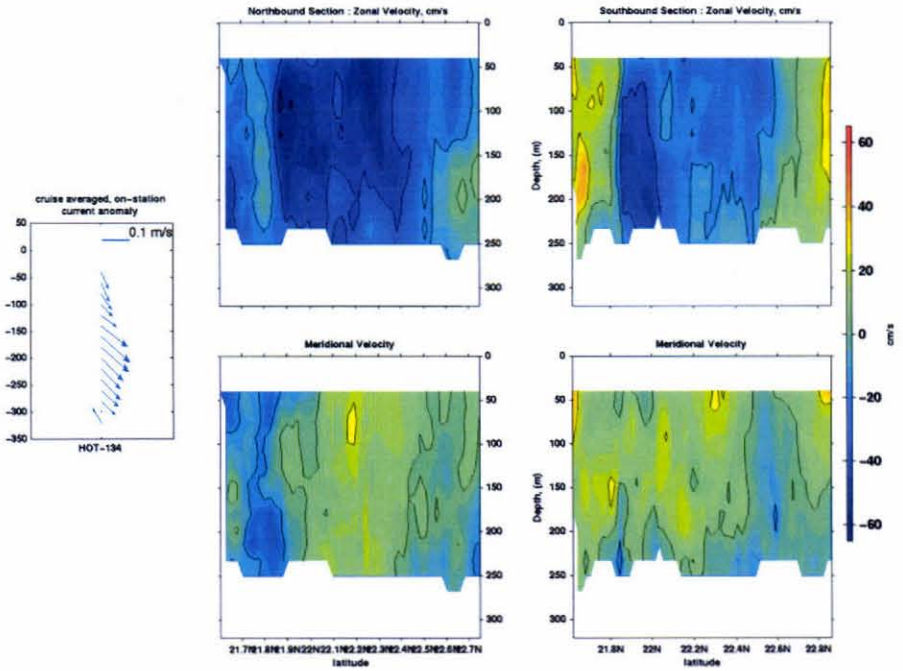
cruise averaged, on-station
current anomaly
0.1 m/s
HOT-134
Northbound Section : Zonal Velocity, cm/s
Southbound Section : Zonal Velocity, cm/s
Meridional Velocity
Meridional Velocity
Depth, (m)
latitude
cm/s

Eddy: 50C Dates in ALOHA box: 08-May-2002 to 10-Jul-2002

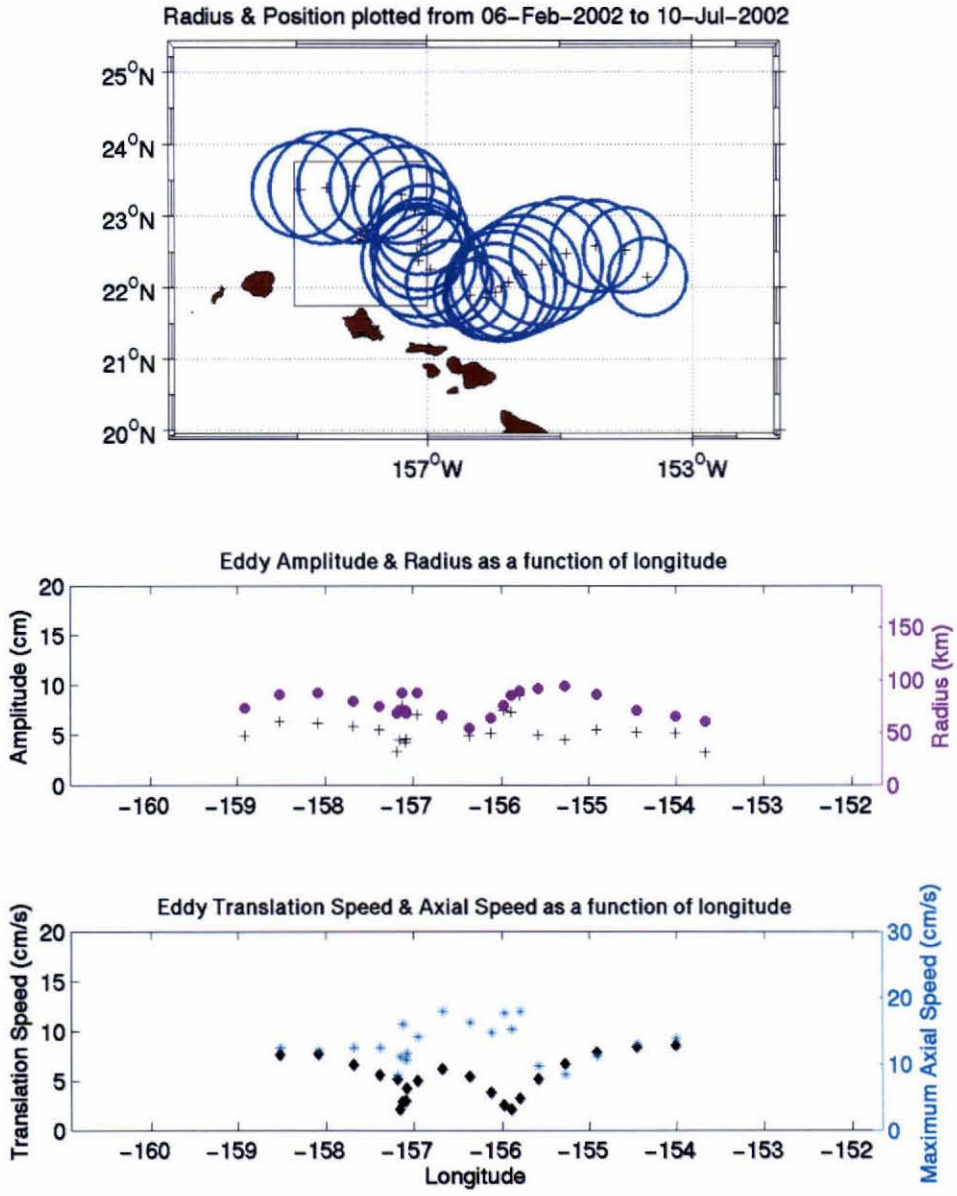

EID: 50C

This eddy formed from two merging eddies, probably island interaction and eddy interaction with an anticyclone that comes in to the east causes the eddy to change direction. It dissipates quickly just west of ALOHA, the HOT cruise catches the very end of this feature and the leading edge of the anticyclone following behind it (51A), so vertical profile signal is probably a mixture of the two features.

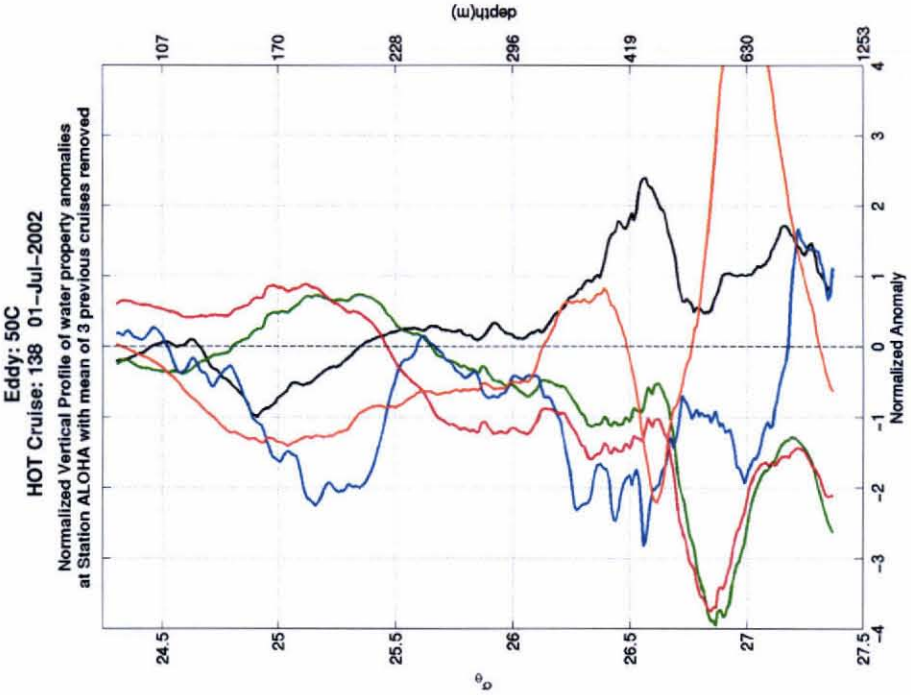
Eddy: 50C
HOT Cruise: 138 01-Jul-2002
Normalized Vertical Profile of water property anomalies
at Station ALOHA with mean of 3 previous cruises removed
depth(m)
107
170
228
296
419
630
1253
Normalized Anomaly
σ_θ

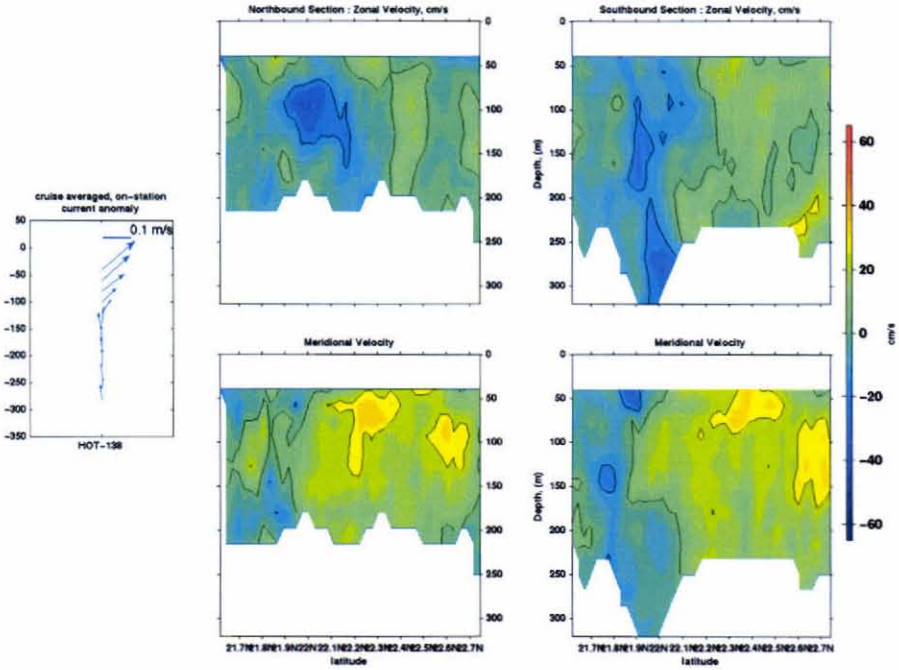
cruise averaged, on-station
current anomaly
0.1 m/s
HOT-138
Northbound Section : Zonal Velocity, cm/s
Southbound Section : Zonal Velocity, cm/s
Meridional Velocity
Meridional Velocity
Depth, (m)
latitude
cm/s

Eddy: 51A Dates in ALOHA box: 03–Jul–2002 to 24–Jul–2002

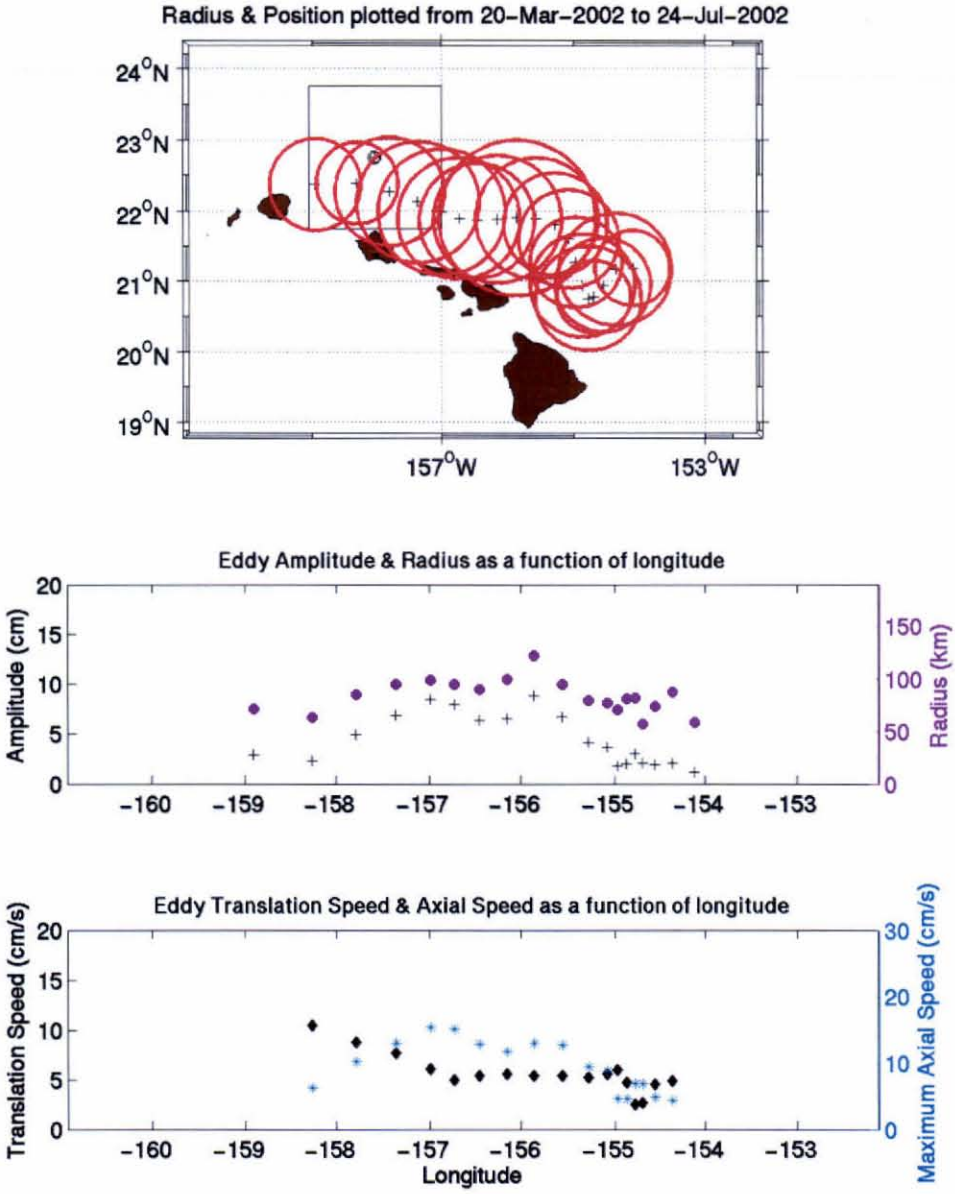

EID: 51A

This eddy formed on northeast side of Big Island, appears to be the remnant of an eddy that collided with the Big Island and broke up, then reformed. This eddy definitely interacts with the islands as it travels up the chain to ALOHA. See HOT cruise note in the 50C notes. This eddy is also followed behind by another cyclonic eddy.

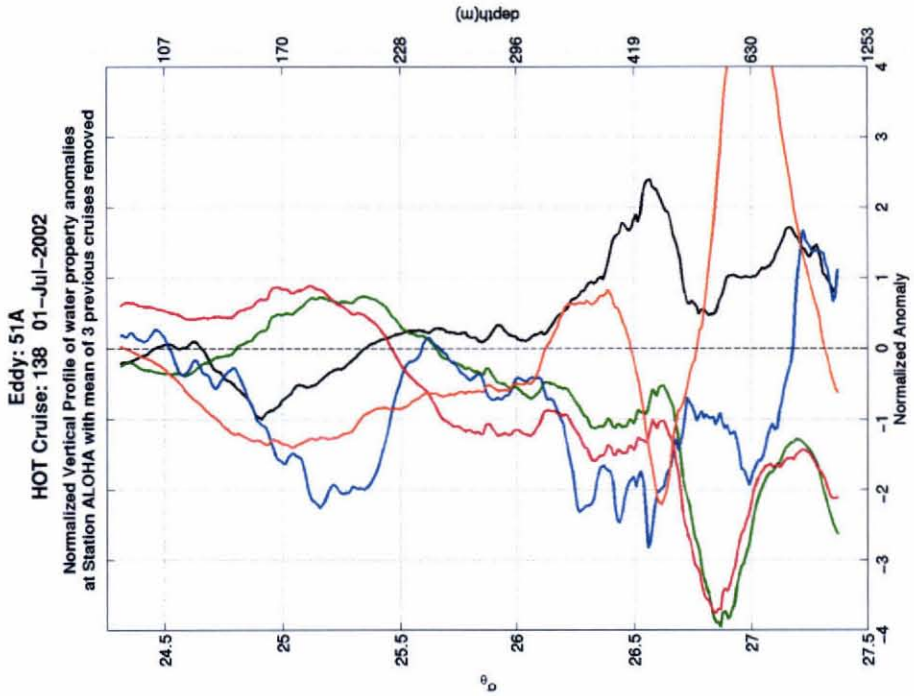
Eddy: 51A
HOT Cruise: 138 01-Jul-2002
Normalized Vertical Profile of water property anomalies
at Station ALOHA with mean of 3 previous cruises removed
depth(m)
107
170
228
296
419
630
1253
Normalized Anomaly
σ_θ

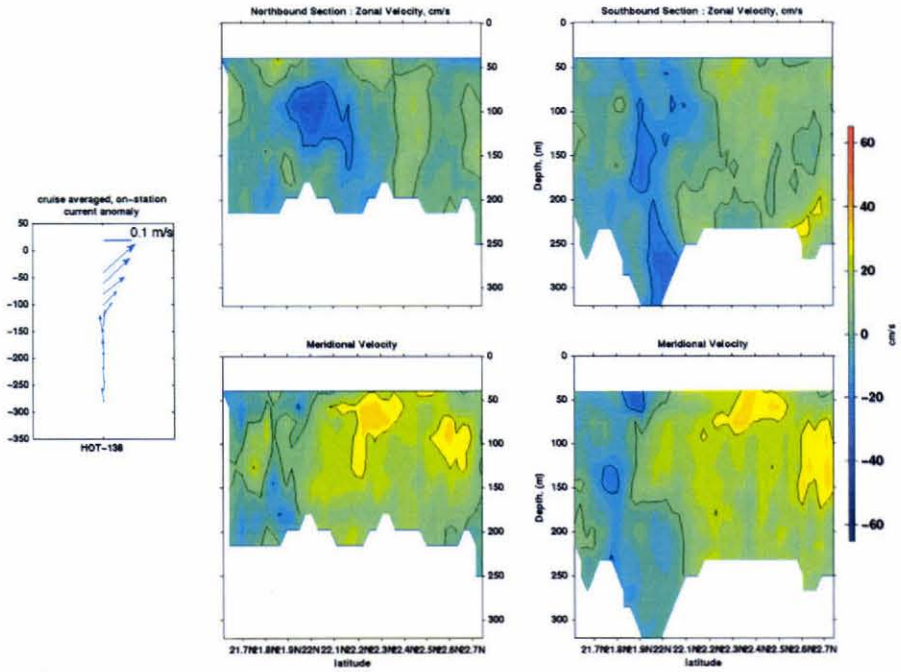
cruise averaged, on-station
current anomaly
0.1 m/s
HOT-138
Northbound Section : Zonal Velocity, cm/s
Southbound Section : Zonal Velocity, cm/s
Meridional Velocity
Meridional Velocity
Depth, (m)
latitude
cm/s

Eddy: 52C Dates in ALOHA box: 07-Aug-2002 to 28-Aug-2002

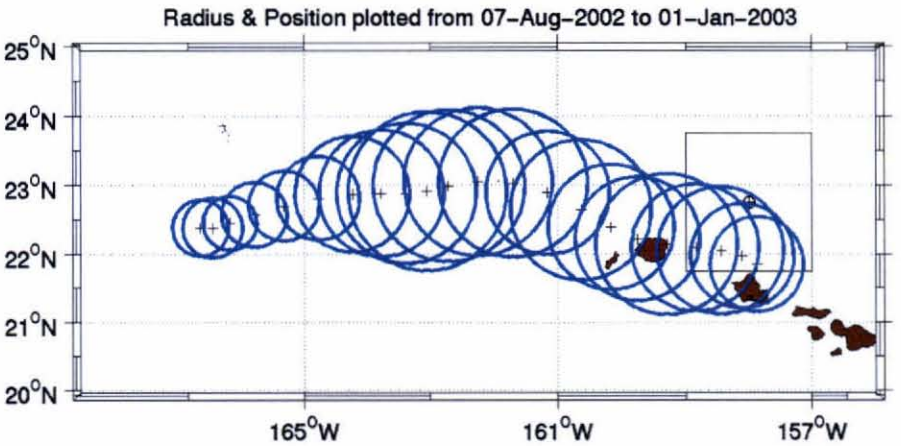

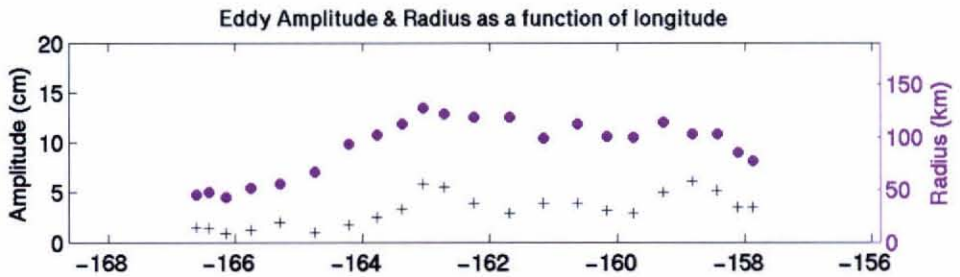

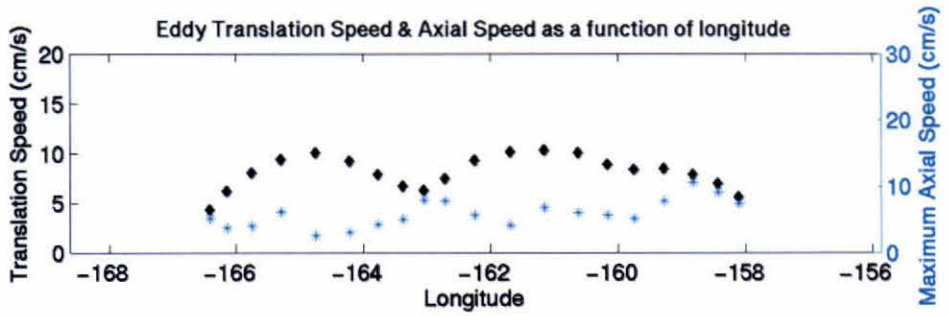

EID: 52C

This eddy starts off Oahu because it's the remnant of an eddy that dissipated when it hit Oahu be reformed. It continues close to the islands (strong eddy-island interaction), then travels west and eventually dissipates. The north edge of this eddy brushes Station ALOHA, and due to the nature of the eddy, there aren't large anomalies in the vertical profile of water properties.

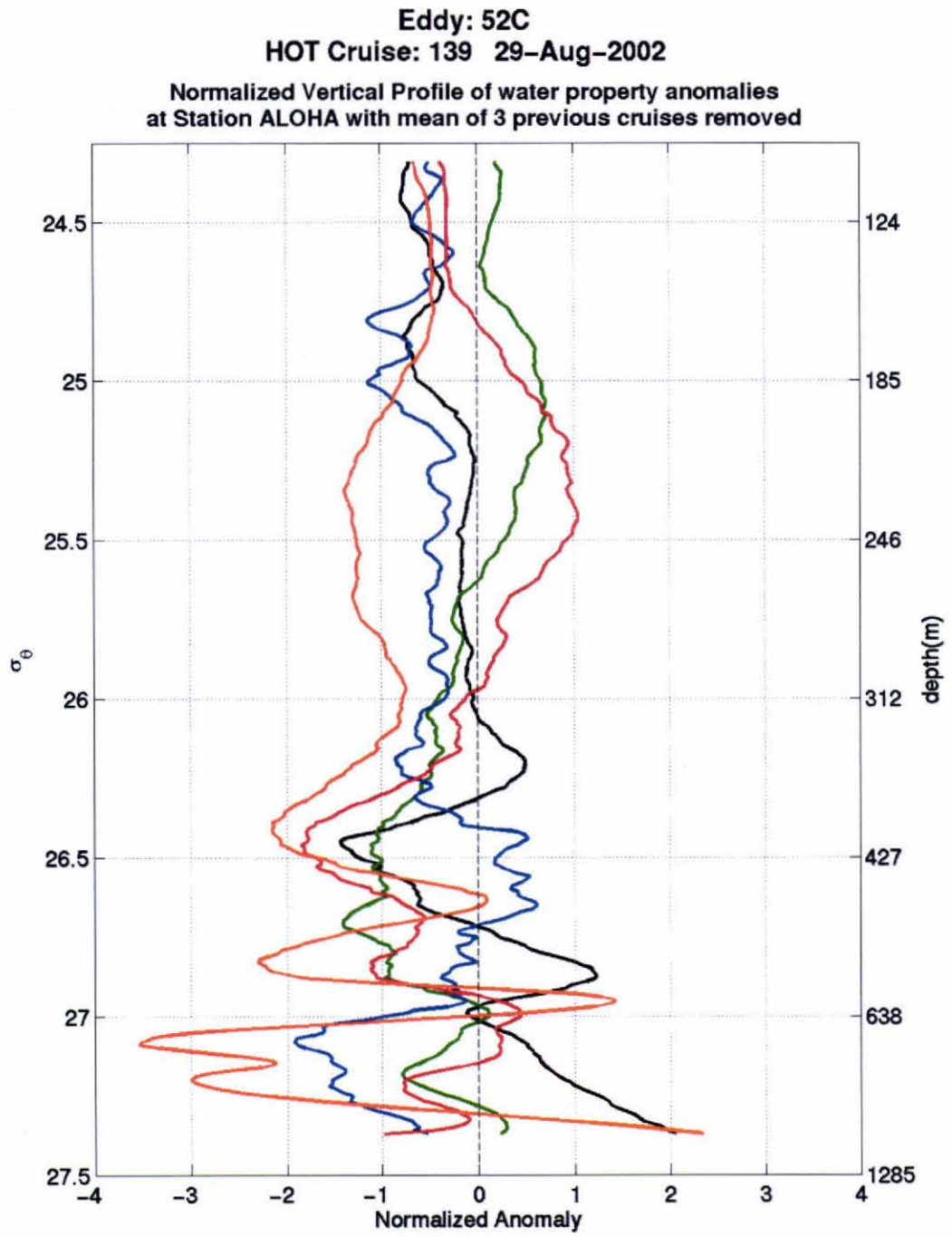
Eddy: 52C
HOT Cruise: 139 29-Aug-2002
Normalized Vertical Profile of water property anomalies
at Station ALOHA with mean of 3 previous cruises removed
24.5
25
25.5
26
26.5
27
27.5
σ_θ
124
185
246
312
427
638
1285
depth(m)
-4
-3
-2
-1
0
1
2
3
4
Normalized Anomaly

Eddy: 53A Dates in ALOHA box: 04-Sep-2002 to 30-Oct-2002

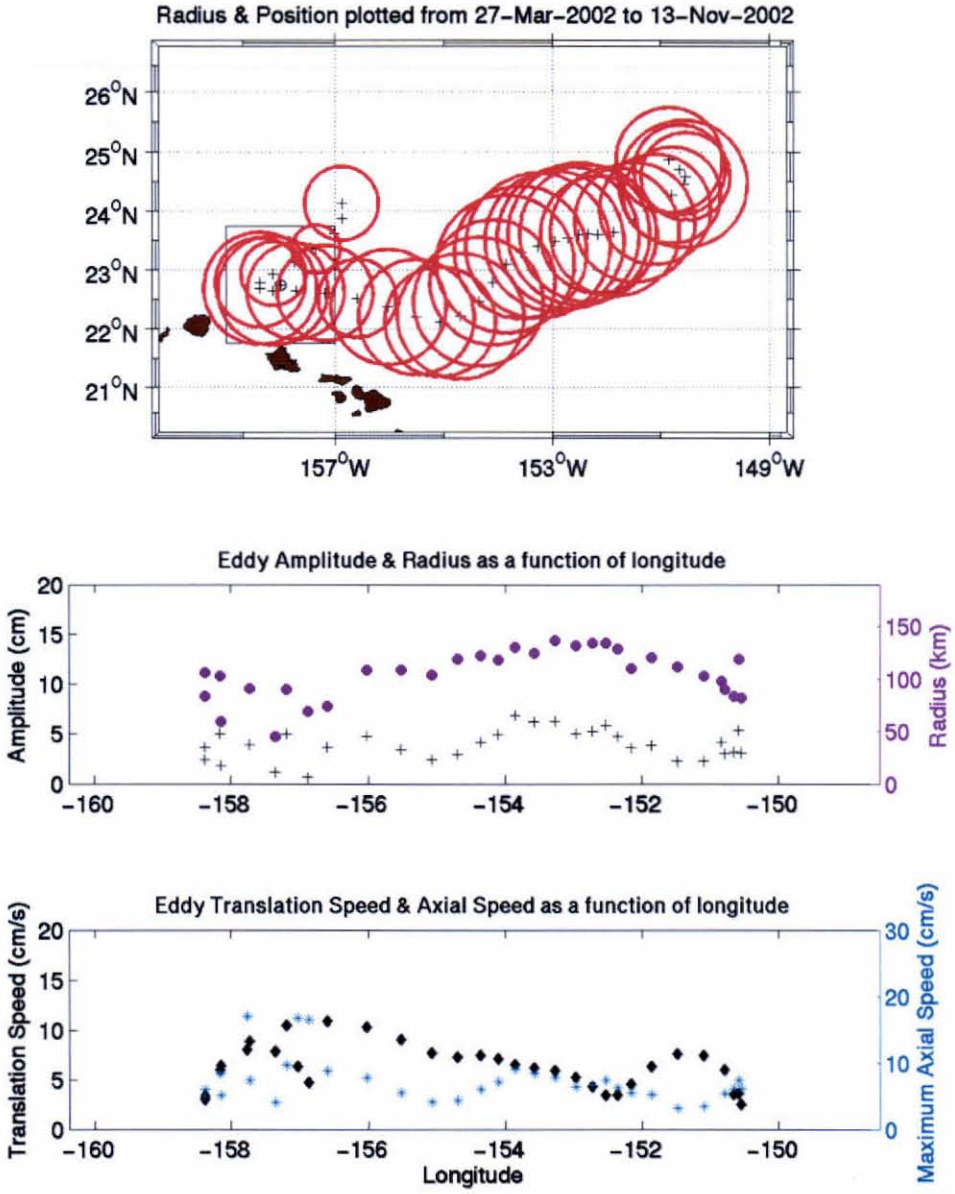

EID: 53A

This eddy formed at 25N and 151W and was drawn southwest due to the presence of cyclonic eddies. It spent an extended amount of time in the box surrounding ALOHA because of its interaction with two merging anticyclonic eddies also in the region. The presence of these other eddies caused the tracking algorithm to jump features, as can be seen by the time steps of this eddy in Appendix A2 that don't make sense.

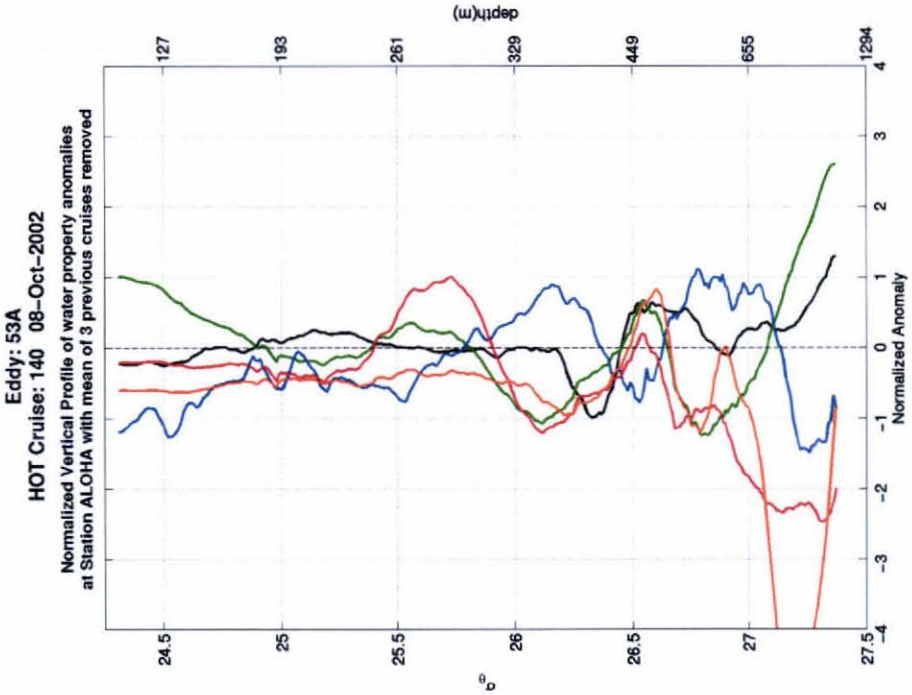
Eddy: 53A
HOT Cruise: 140 08-Oct-2002
Normalized Vertical Profile of water property anomalies
at Station ALOHA with mean of 3 previous cruises removed
depth(m)
127
193
261
329
449
655
1294
Normalized Anomaly
σ_θ

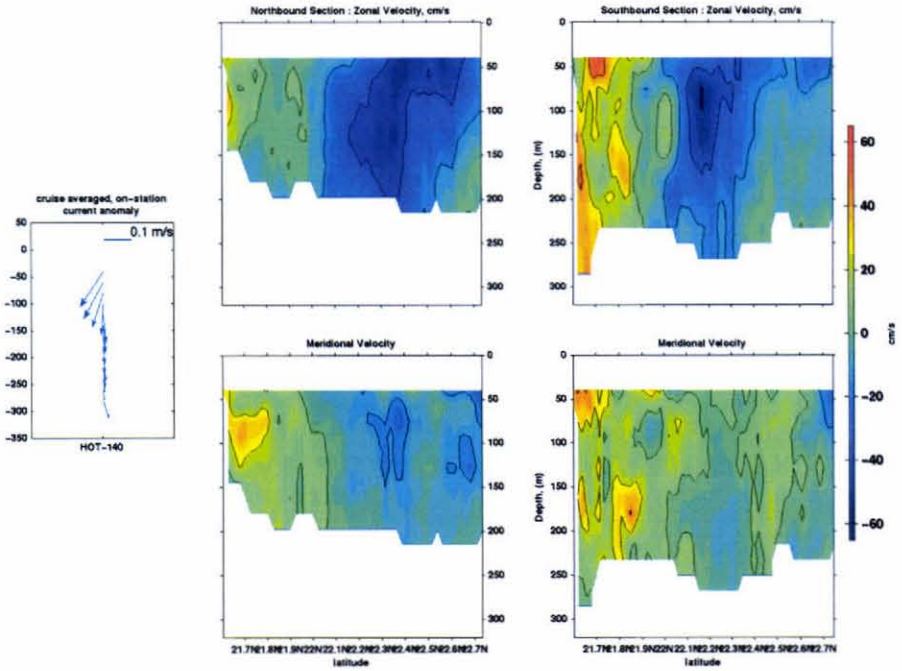
cruise averaged, on-station
current anomaly
0.1 m/s
HOT-140
Northbound Section : Zonal Velocity, cm/s
Southbound Section : Zonal Velocity, cm/s
Meridional Velocity
Meridional Velocity
Depth, (m)
latitude
cm/s

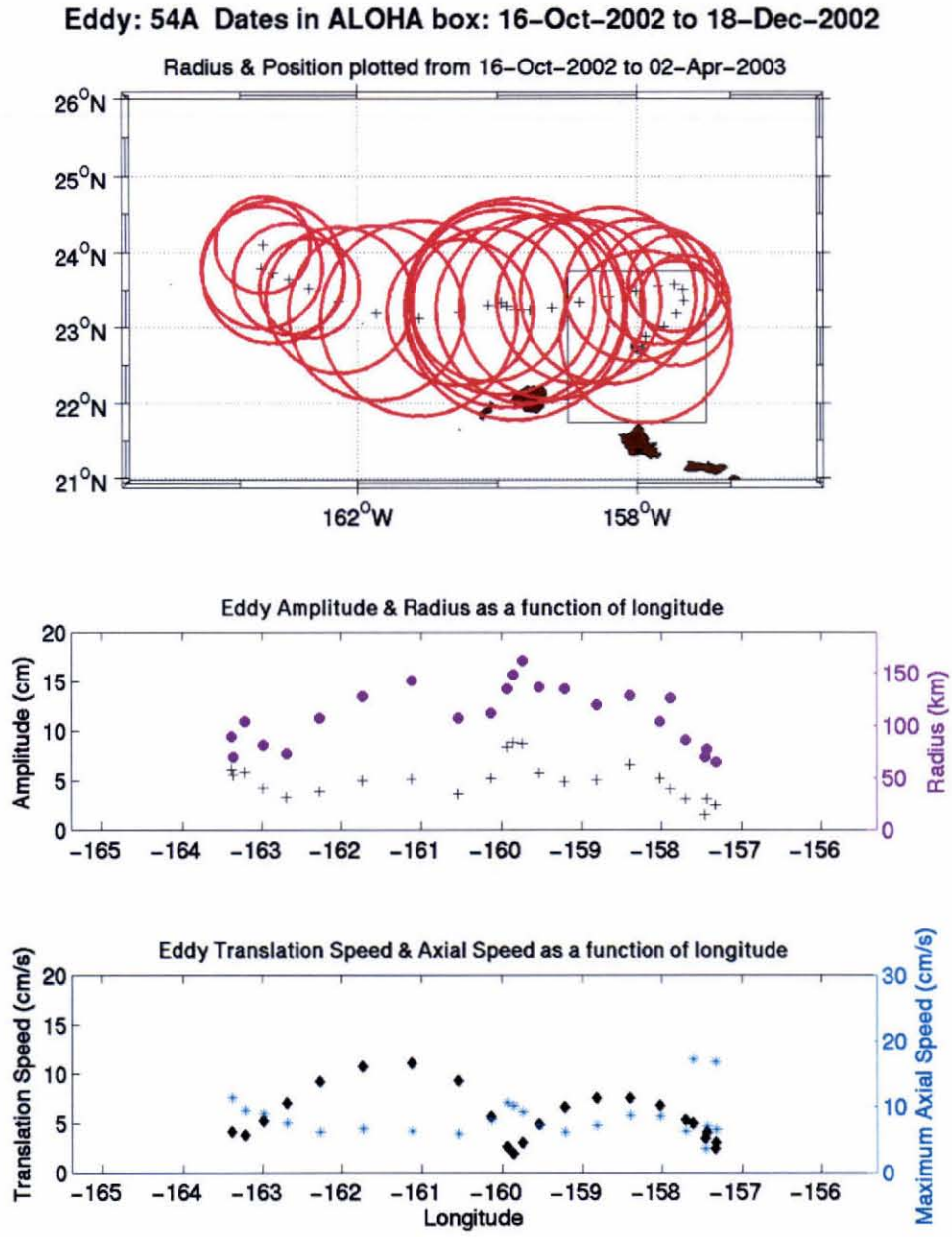

EID: 54A

This eddy was formed by the merging of the remnants of two other features (one of which was 53A). Once this eddy gets organized, it moves west, interacting with Kauai as it passes by and is eventually drawn up into another eddy.

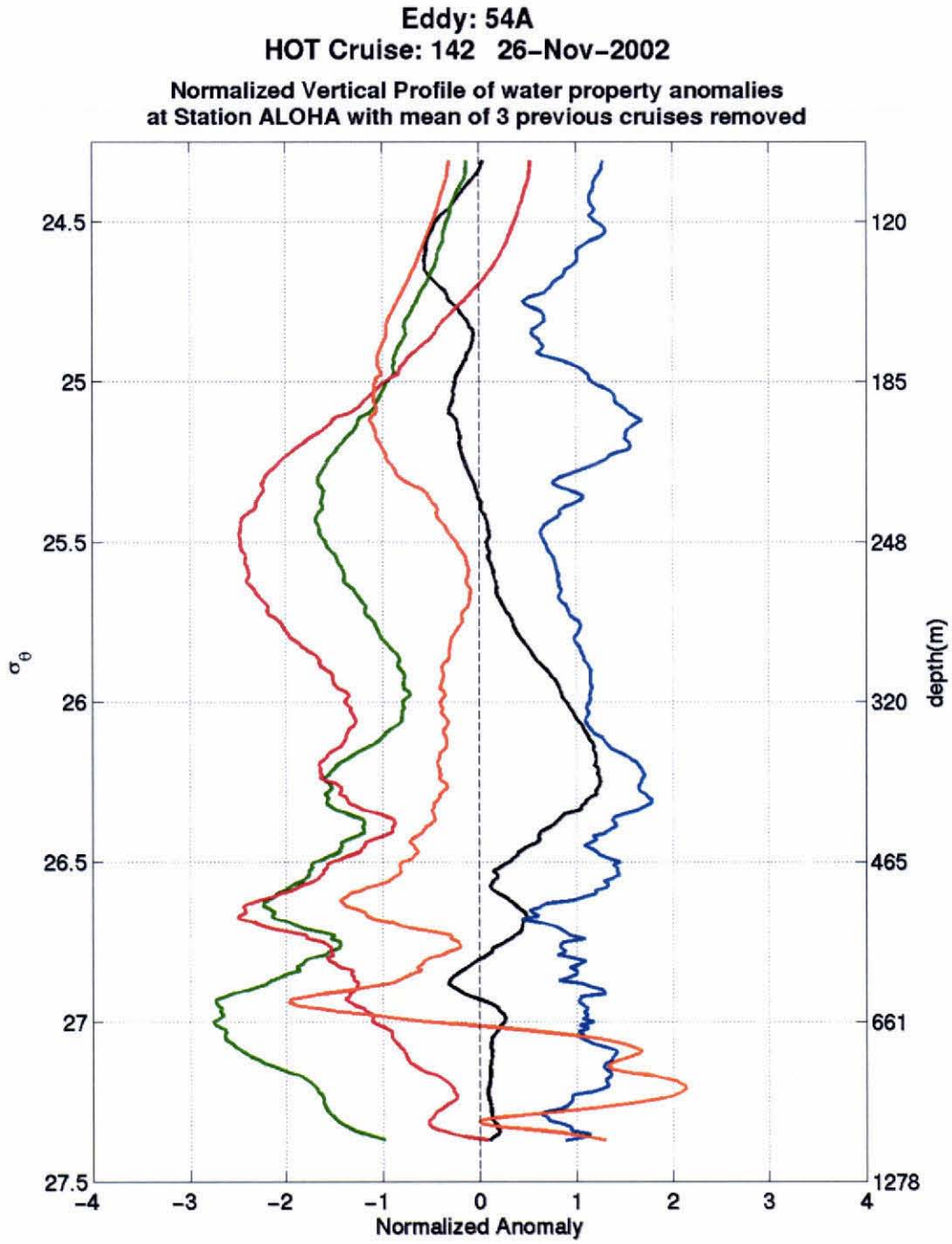
Eddy: 54A
HOT Cruise: 142 26-Nov-2002
Normalized Vertical Profile of water property anomalies
at Station ALOHA with mean of 3 previous cruises removed
24.5
25
25.5
26
26.5
27
27.5
σ_θ
120
185
248
320
465
661
1278
depth(m)
-4
-3
-2
-1
0
1
2
3
4
Normalized Anomaly

Eddy: 55C Dates in ALOHA box: 22-Jan-2003 to 19-Feb-2003

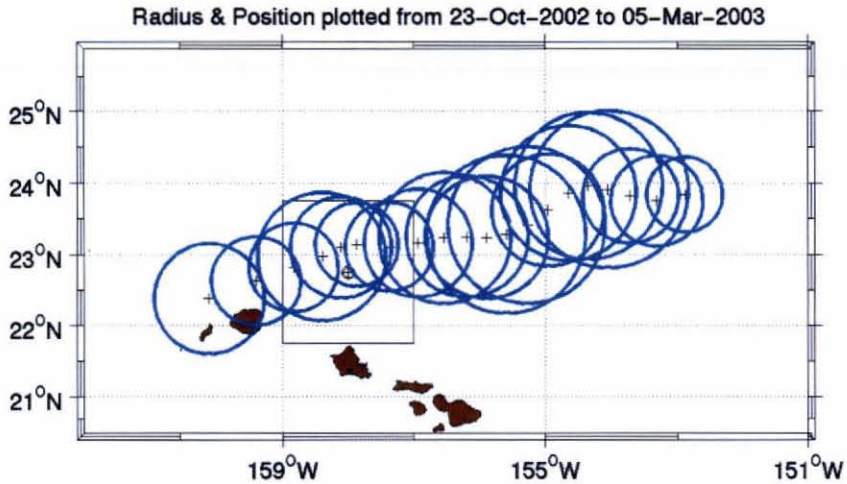

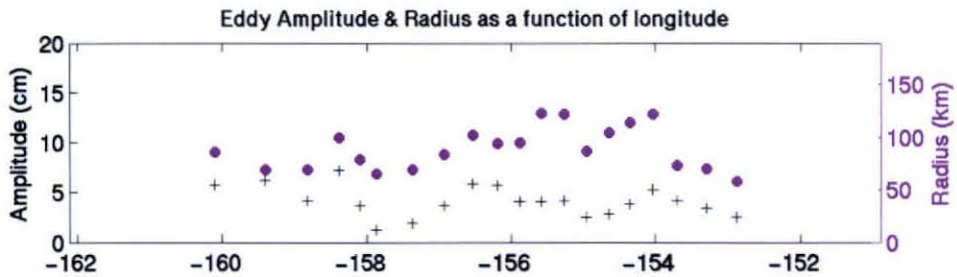

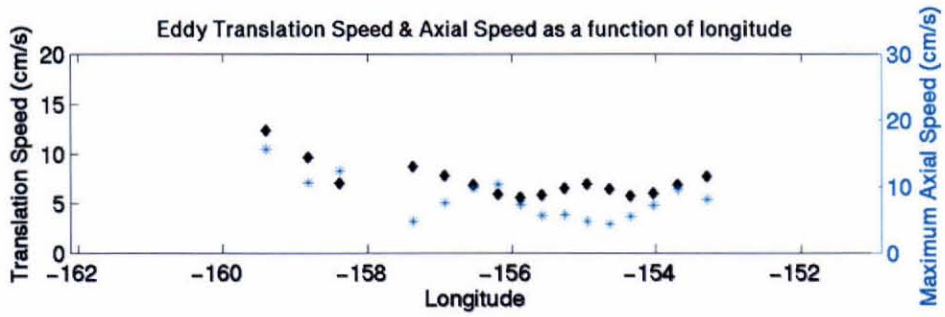

EID: 55C

This eddy formed at 24N, 153W and quickly increased in size when another cyclonic eddy that was forming east of the Big Island was drawn up into it. It passes over ALOHA and then dissipates due to a collision with Kauai.

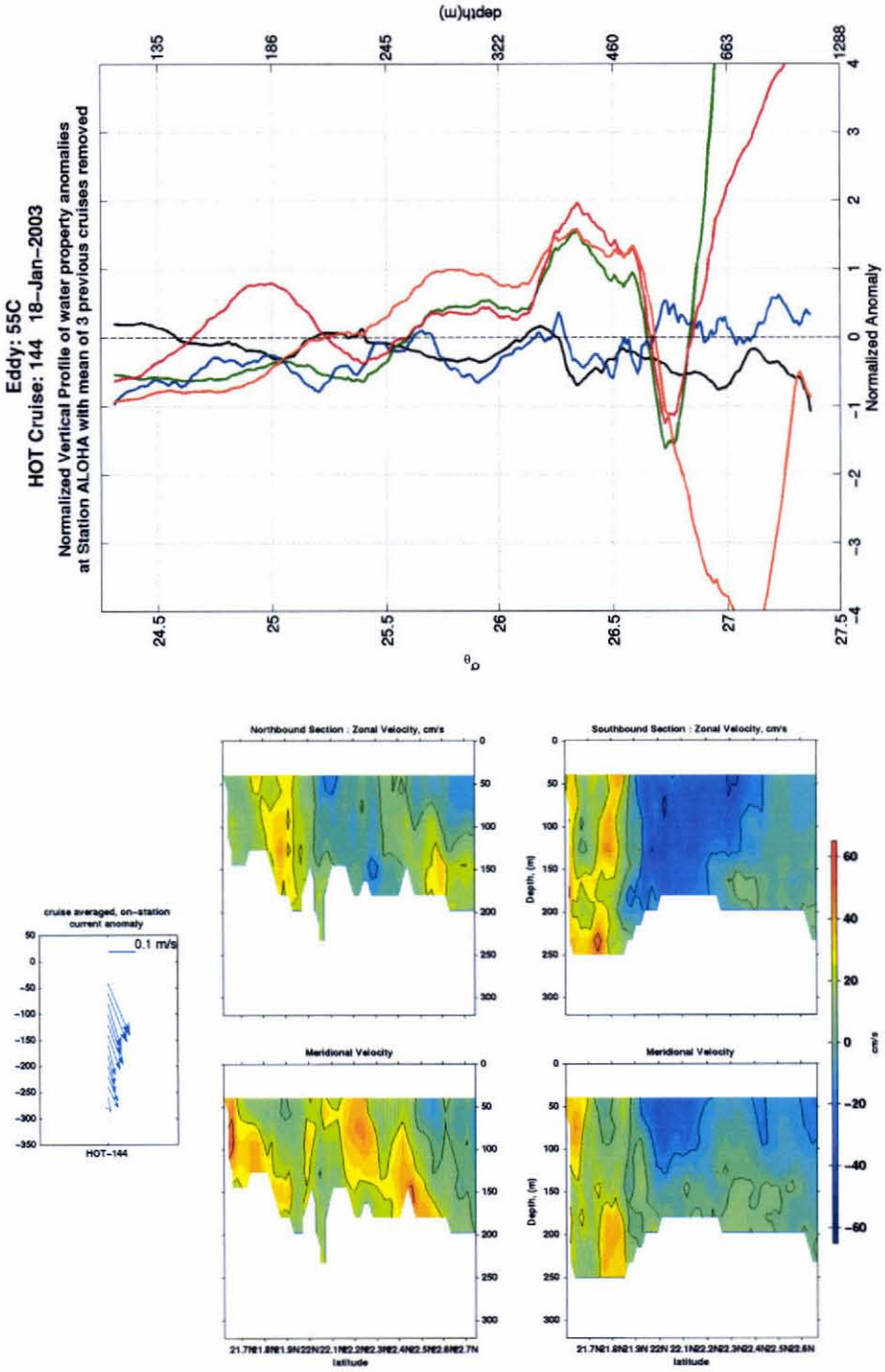
Eddy: 55C
HOT Cruise: 144 18-Jan-2003
Normalized Vertical Profile of water property anomalies
at Station ALOHA with mean of 3 previous cruises removed
depth(m)
135
186
245
322
460
663
1288
Normalized Anomaly
θ_p
cruise averaged, on-station
current anomaly
0.1 m/s
HOT-144
Northbound Section : Zonal Velocity, cm/s
Southbound Section : Zonal Velocity, cm/s
Meridional Velocity
Meridional Velocity
Depth, (m)
latitude
cm/s

Eddy: 56C Dates in ALOHA box: 26-Mar-2003 to 23-Apr-2003

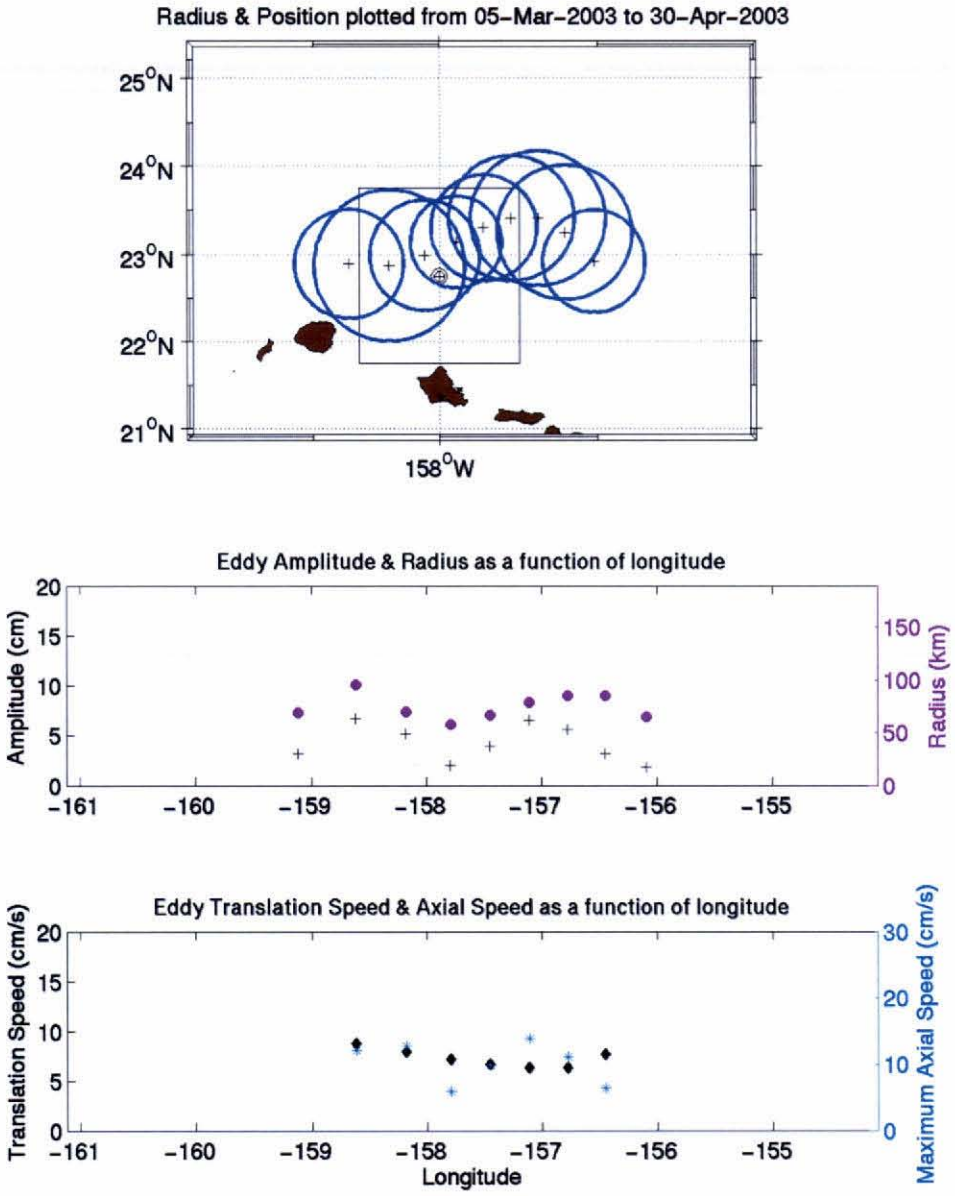

EID: 56C

This eddy may be the remainder of an eddy that formed over a year before, but there is no noticeable bolus transport anomaly to back up this observation. The eddy merged with another eddy over Kauai and then quickly dissipates.

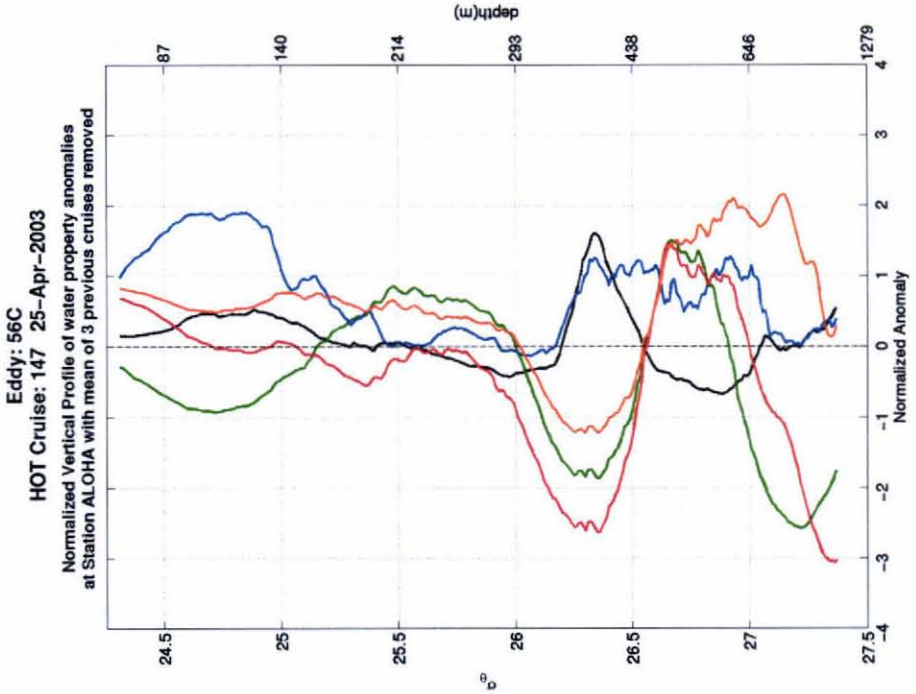
Eddy: 56C
HOT Cruise: 147 25-Apr-2003
Normalized Vertical Profile of water property anomalies
at Station ALOHA with mean of 3 previous cruises removed
depth(m)
87
140
214
293
438
646
1279
Normalized Anomaly
θ_σ

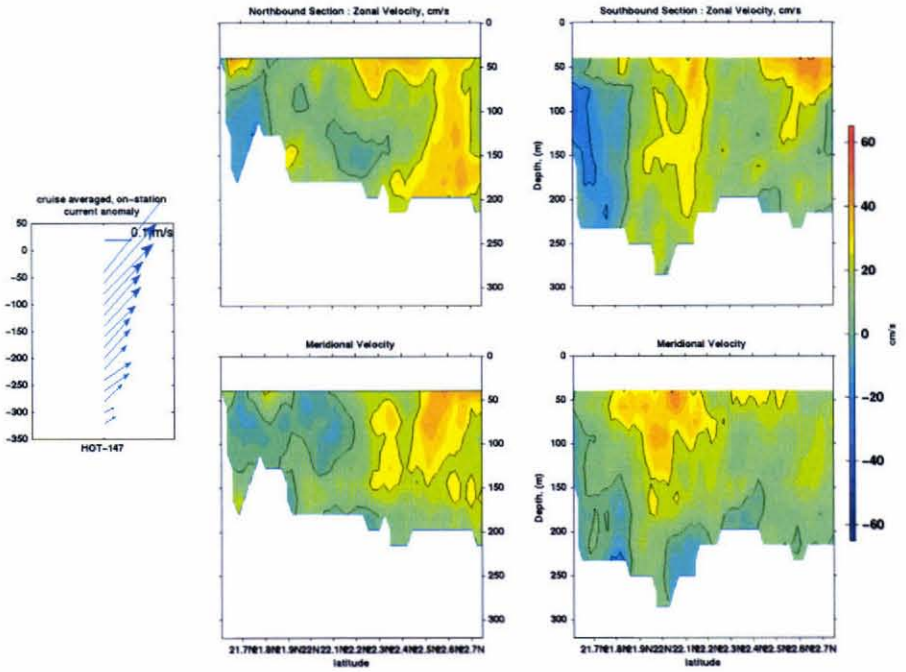
cruise averaged, on-station
current anomaly
0.1m/s
HOT-147
Northbound Section : Zonal Velocity, cm/s
Southbound Section : Zonal Velocity, cm/s
Meridional Velocity
Meridional Velocity
Depth, (m)
latitude
cm/s

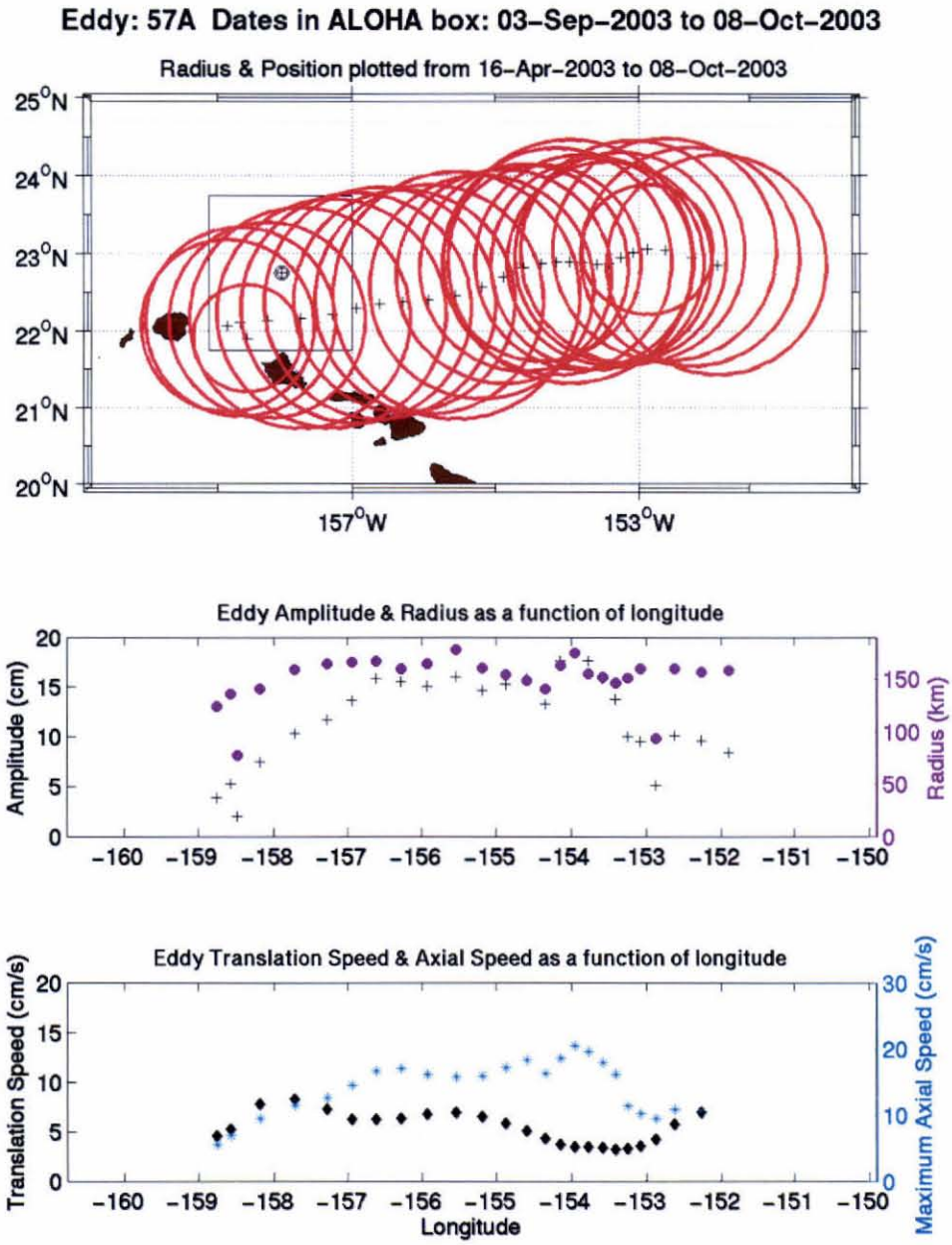

EID: 57A

Two anticyclones merge, split, merge, split, merge again and is then tracked as this eddy. This eddy then travels directly into the islands of Oahu and Kauai and breaks up. Visually it appears that a remnant makes it through the Kauai Channel, but the track stops on the north side of the channel.

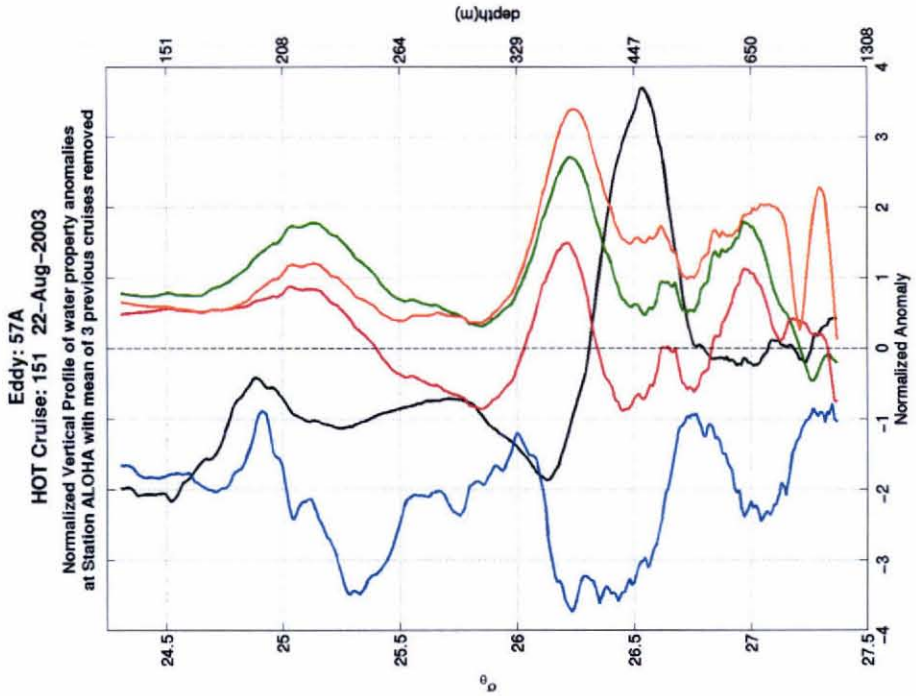
Eddy: 57A
HOT Cruise: 151 22-Aug-2003
Normalized Vertical Profile of water property anomalies
at Station ALOHA with mean of 3 previous cruises removed
depth(m)
151
208
264
329
447
650
1308
Normalized Anomaly
σθ

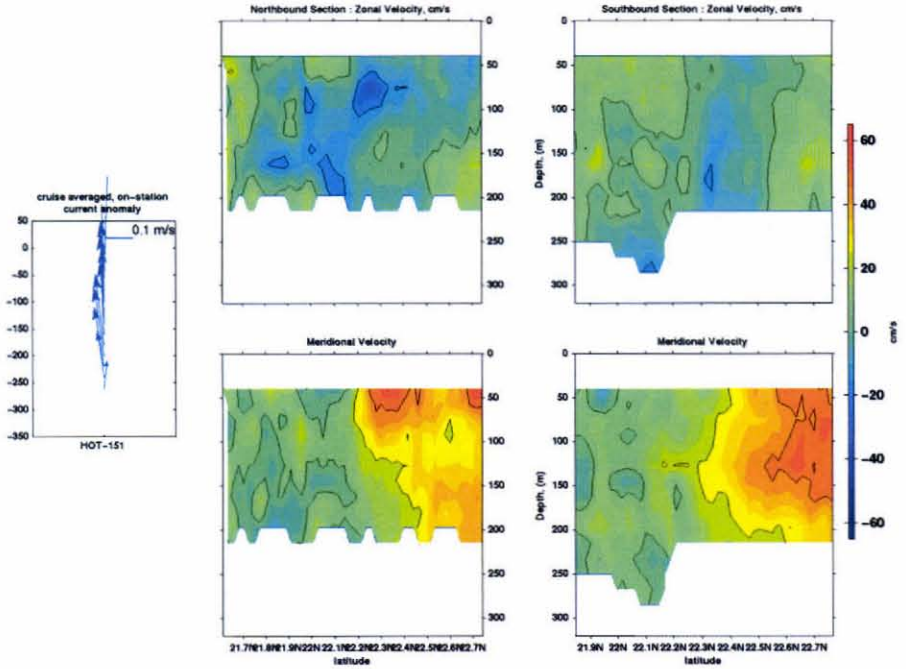
cruise averaged, on-station
current anomaly
0.1 m/s
HOT-151
Northbound Section : Zonal Velocity, cm/s
Southbound Section : Zonal Velocity, cm/s
Meridional Velocity
Meridional Velocity
Depth, (m)
latitude
cm/s

Eddy: 58C Dates in ALOHA box: 17-Dec-2003 to 31-Dec-2003

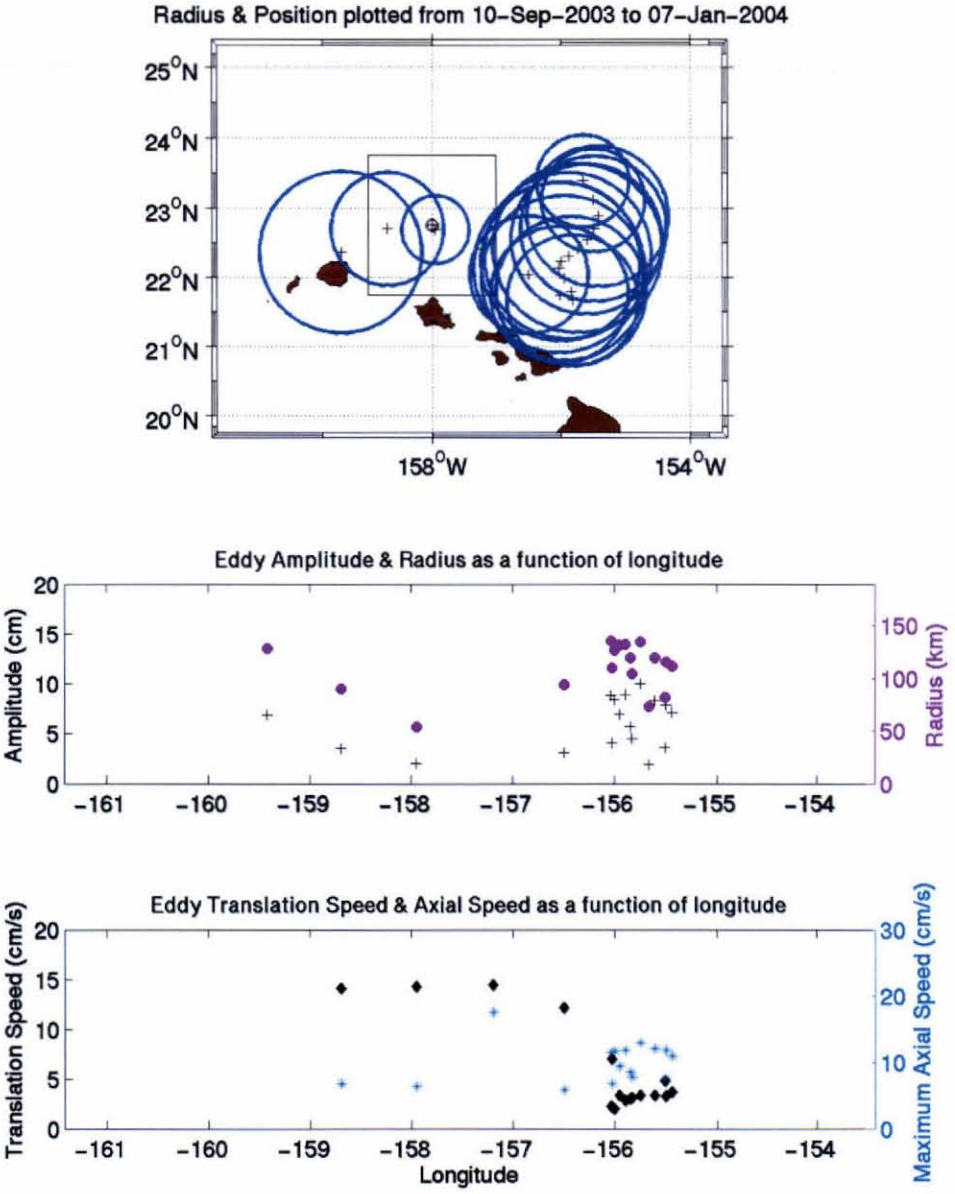

EID: 58C

This eddy formed west of 57A but then rotated clockwise over 57A and then was tracked. It travels south and collides with Maui and breaks up. A remnant of this feature is tracked over ALOHA and west to Kauai for 3 weeks, but at that point, it's not really still an eddy.

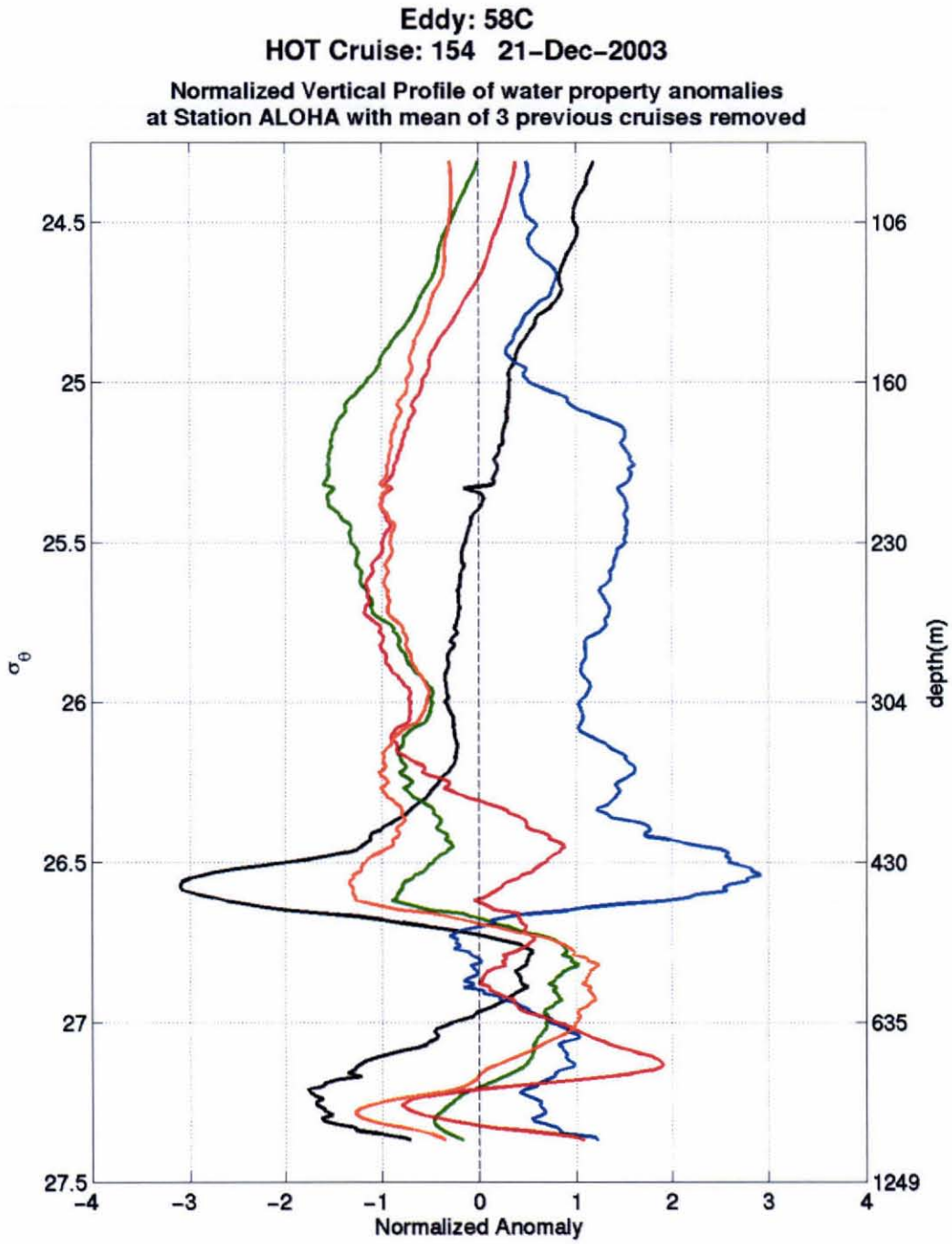
Eddy: 58C
HOT Cruise: 154 21-Dec-2003
Normalized Vertical Profile of water property anomalies
at Station ALOHA with mean of 3 previous cruises removed
24.5
25
25.5
26
26.5
27
27.5
σ_θ
106
160
230
304
430
635
1249
depth(m)
-4
-3
-2
-1
0
1
2
3
4
Normalized Anomaly

Eddy: 59C Dates in ALOHA box: 24-Mar-2004 to 07-Apr-2004

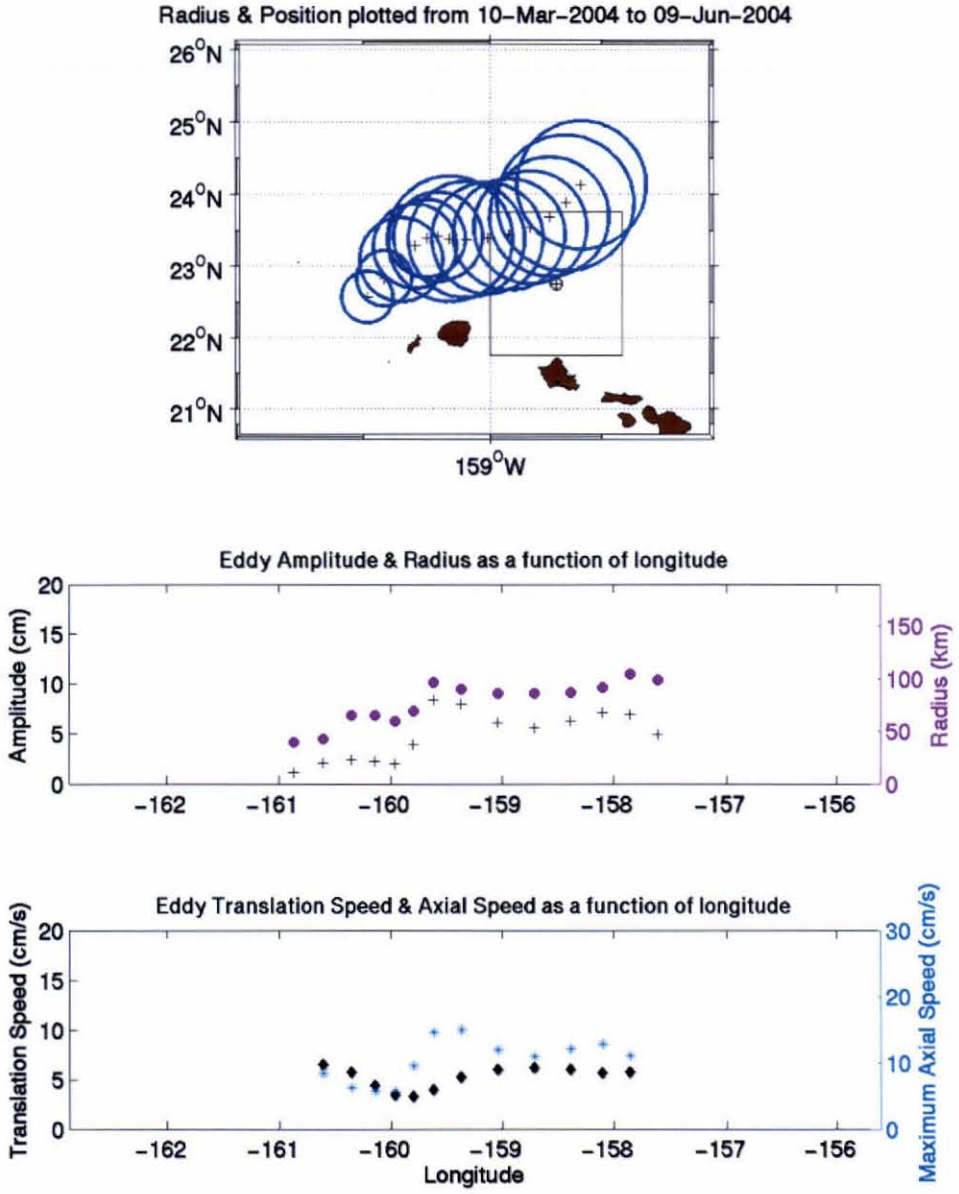

EID: 59C

This eddy may have been a longer lived feature but it's hard to tell because of eddy-eddy interactions. The eddy intensifies and moves south due to an anticyclonic eddy to the west. This anticyclonic eddy also causes 59C to break up west of Kauai.

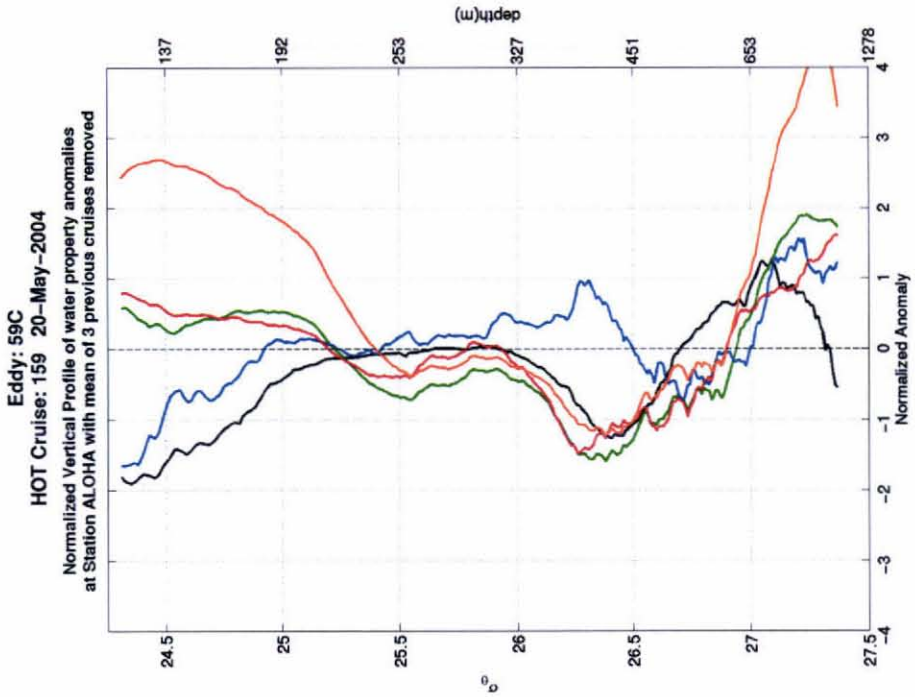
Eddy: 59C
HOT Cruise: 159 20-May-2004
Normalized Vertical Profile of water property anomalies
at Station ALOHA with mean of 3 previous cruises removed
depth(m)
137
192
253
327
451
653
1278
Normalized Anomaly
σ_θ

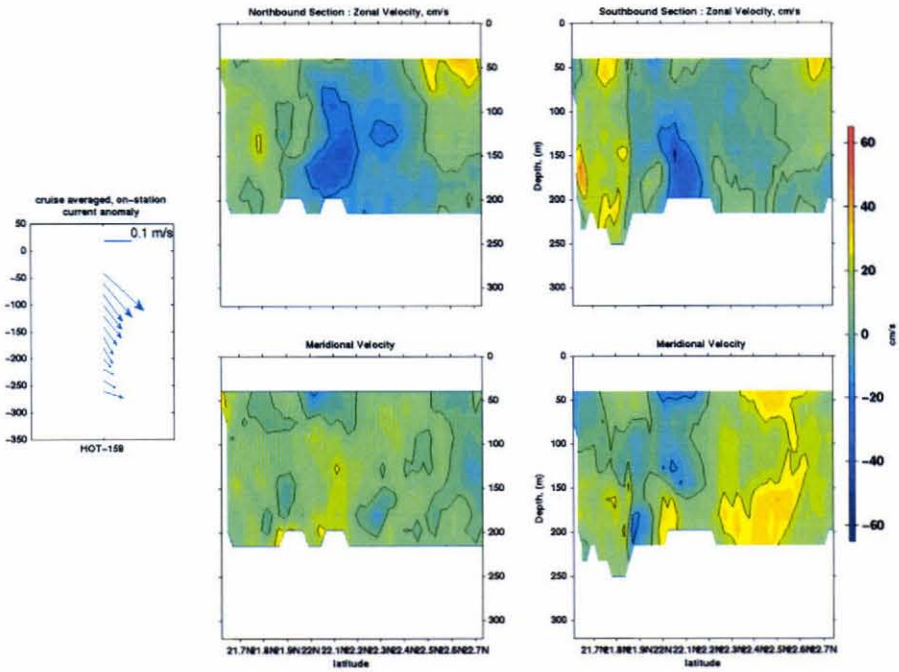
cruise averaged, on-station
current anomaly
0.1 m/s
HOT-159
Northbound Section : Zonal Velocity, cm/s
Southbound Section : Zonal Velocity, cm/s
Meridional Velocity
Meridional Velocity
Depth, (m)
latitude
cm/s

Eddy: 60A Dates in ALOHA box: 19-May-2004 to 30-Jun-2004

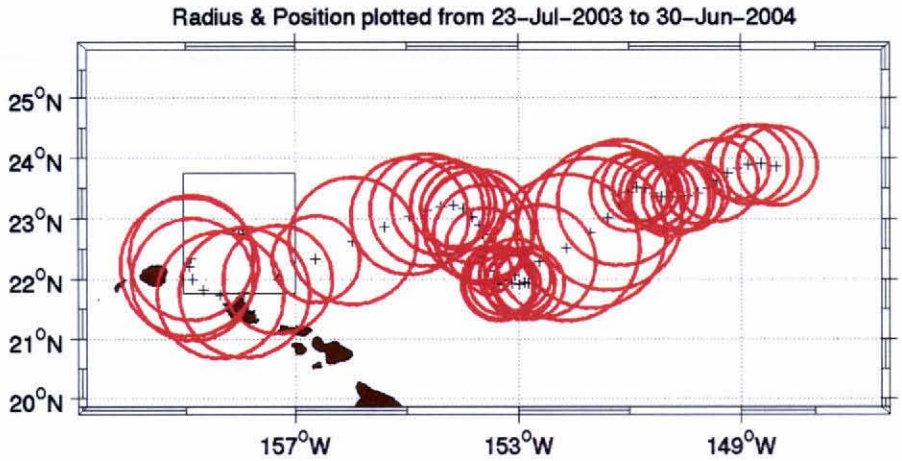

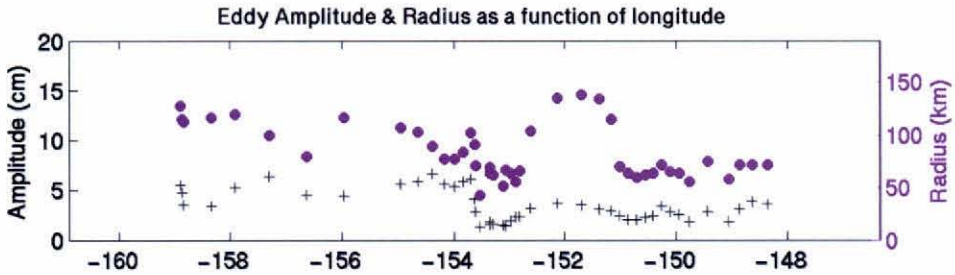

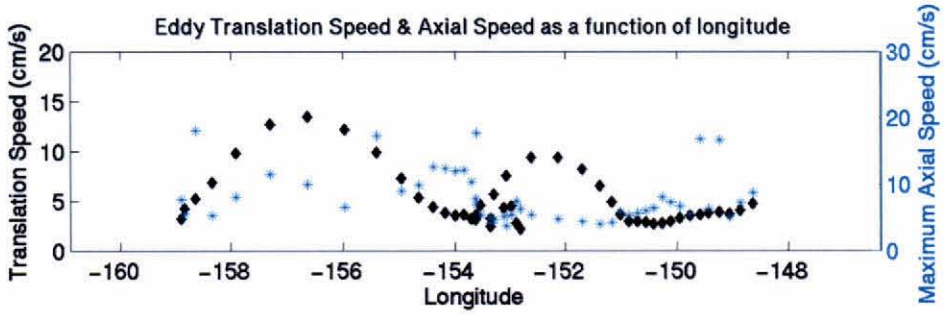

EID: 60A

This eddy formed at 148W and is characterized by several changes in direction and associated changes in radius and translation speed. Most of these changes can be attributed to various eddy-eddy interactions. The eddy accelerates as it approaches the island chain and it collides with Oahu and breaks up.

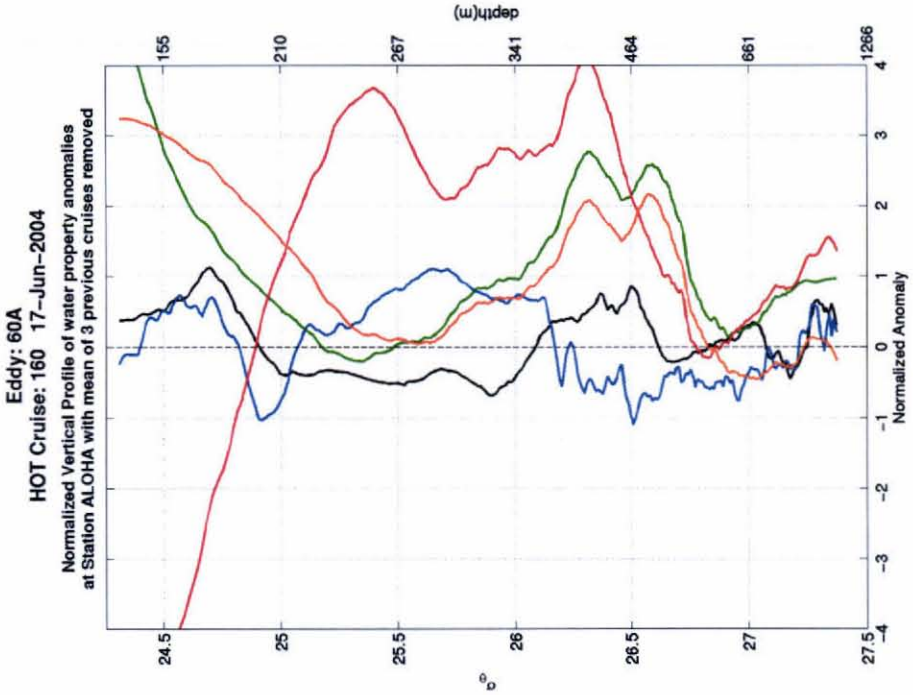
Eddy: 60A
HOT Cruise: 160 17-Jun-2004
Normalized Vertical Profile of water property anomalies
at Station ALOHA with mean of 3 previous cruises removed
depth(m)
155
210
267
341
464
661
1266
Normalized Anomaly
σ_θ

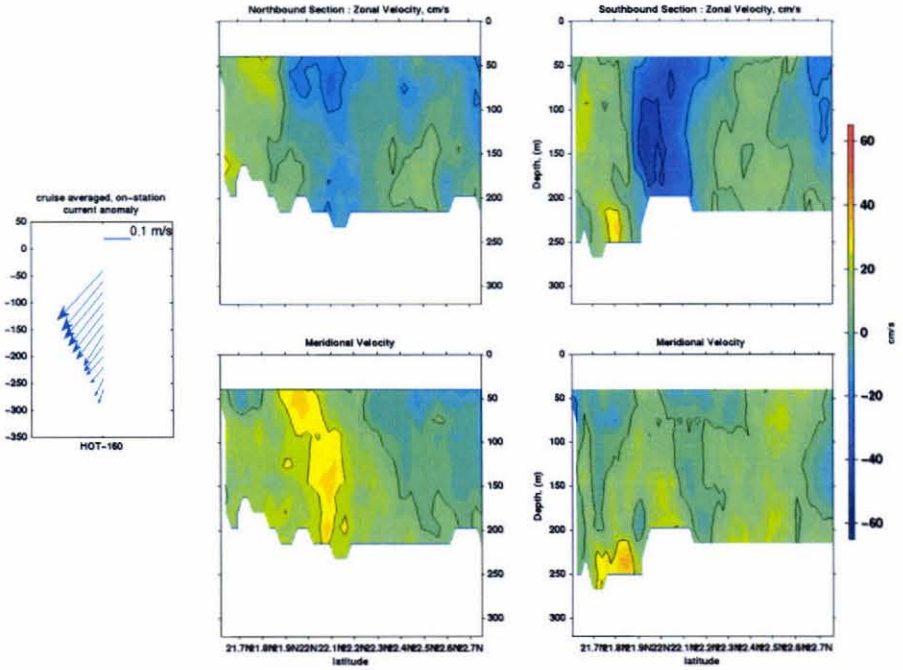
cruise averaged, on-station
current anomaly
0.1 m/s
HOT-160
Northbound Section : Zonal Velocity, cm/s
Southbound Section : Zonal Velocity, cm/s
Meridional Velocity
Meridional Velocity
Depth, (m)
latitude
cm/s

Eddy: 61C Dates in ALOHA box: 04-Aug-2004 to 01-Sep-2004

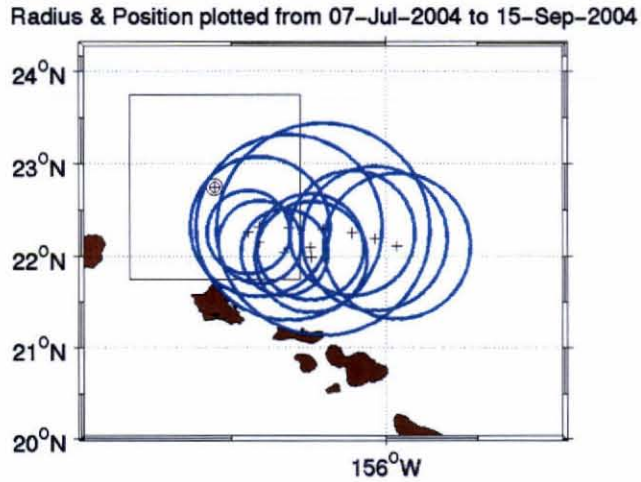

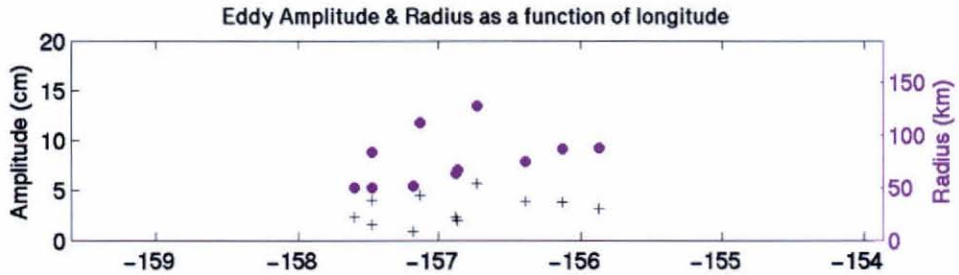

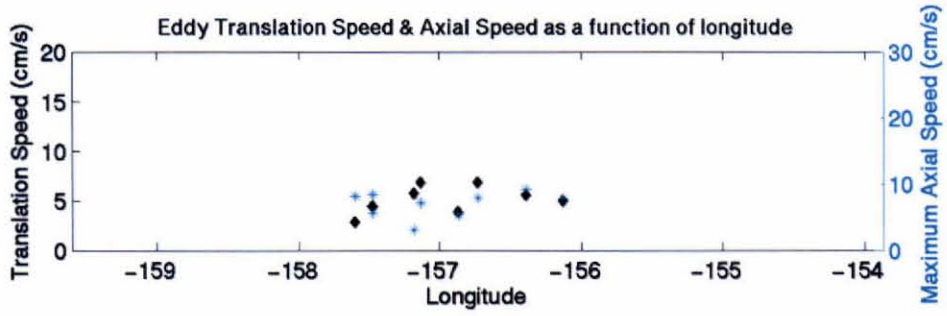

EID: 61C

This weak eddy formed east of the Big Island but wasn't tracked until it intensified north of Maui where it elongates and deforms until it breaks apart due to interactions with other eddies.

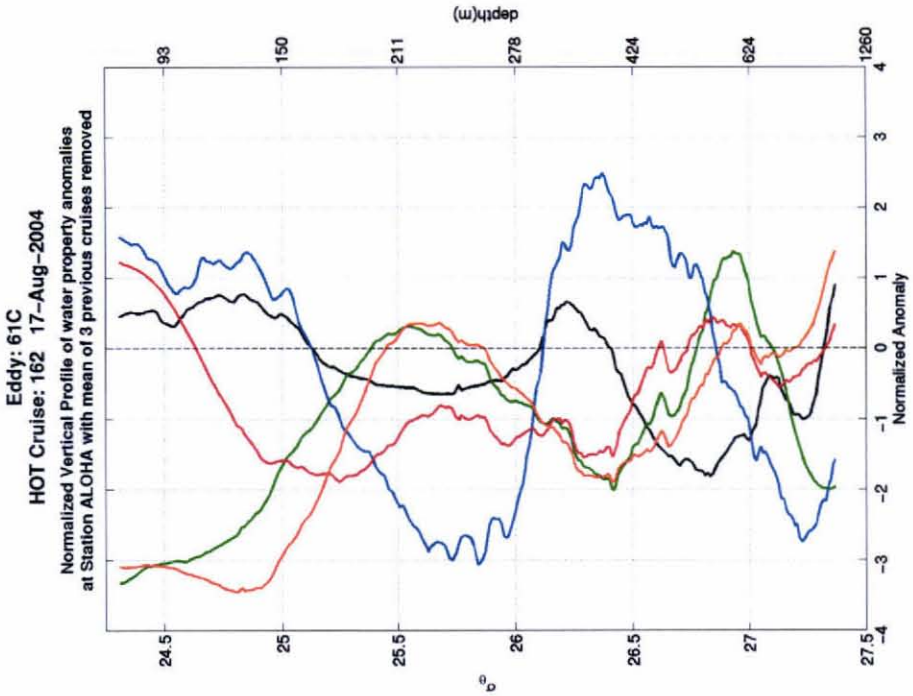
Eddy: 61C
HOT Cruise: 162 17-Aug-2004
Normalized Vertical Profile of water property anomalies
at Station ALOHA with mean of 3 previous cruises removed
depth(m)
93
150
211
278
424
624
1260
Normalized Anomaly
θ_D

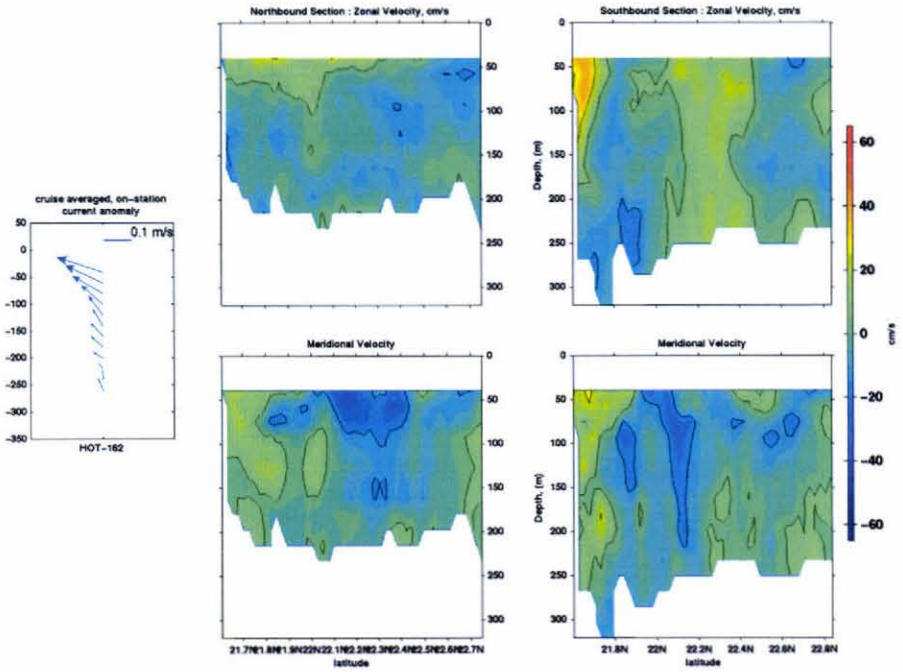
cruise averaged, on-station
current anomaly
0.1 m/s
HOT-162
Northbound Section : Zonal Velocity, cm/s
Southbound Section : Zonal Velocity, cm/s
Meridional Velocity
Meridional Velocity
Depth, (m)
latitude
cm/s

Eddy: 62C Dates in ALOHA box: 02-Mar-2005 to 16-Mar-2005

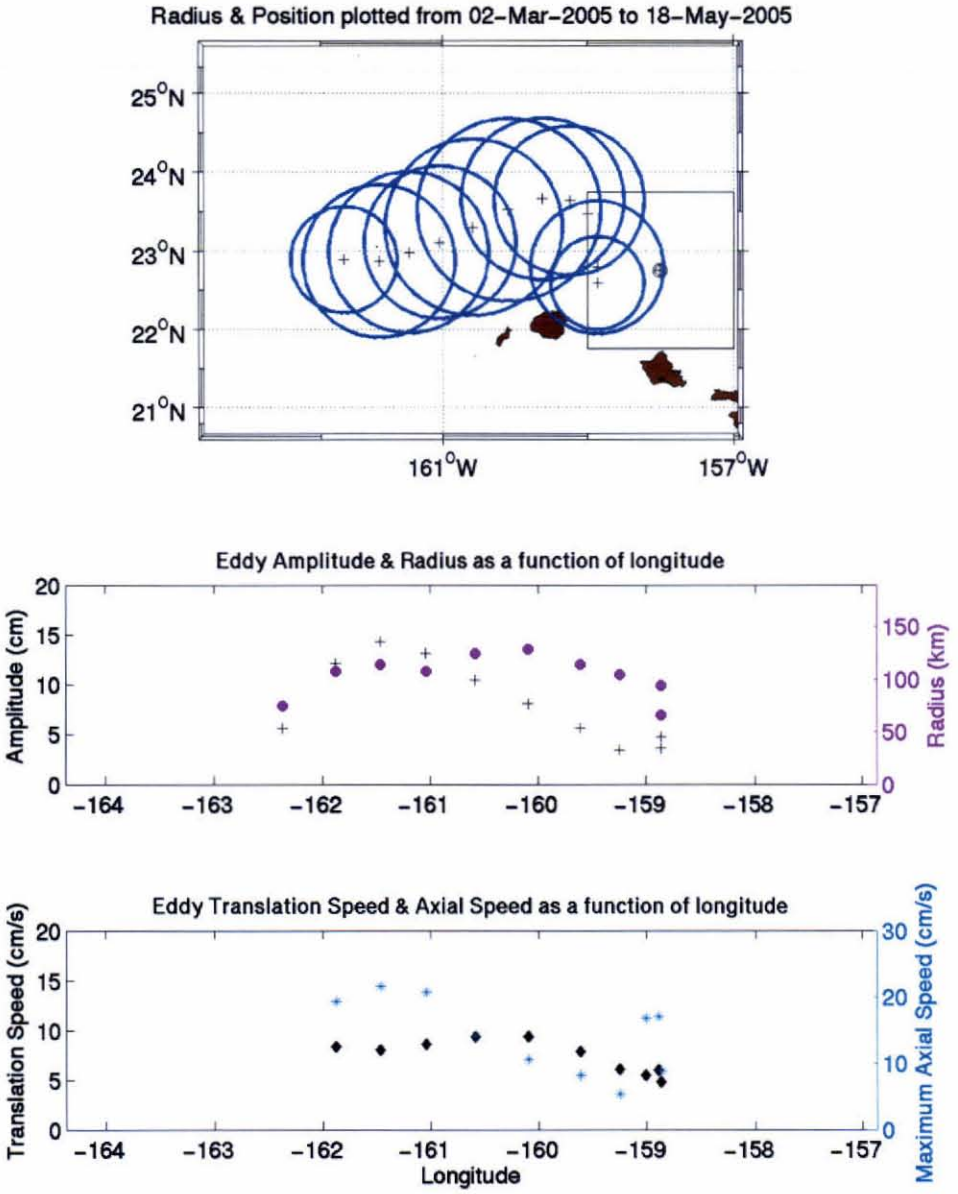

EID: 62C

This eddy is the remnant of a collision of an eddy with the islands after it was forced south by two anticyclones (one on either side). This remnant is weak and not well defined and it quickly dissipates west of Kauai.

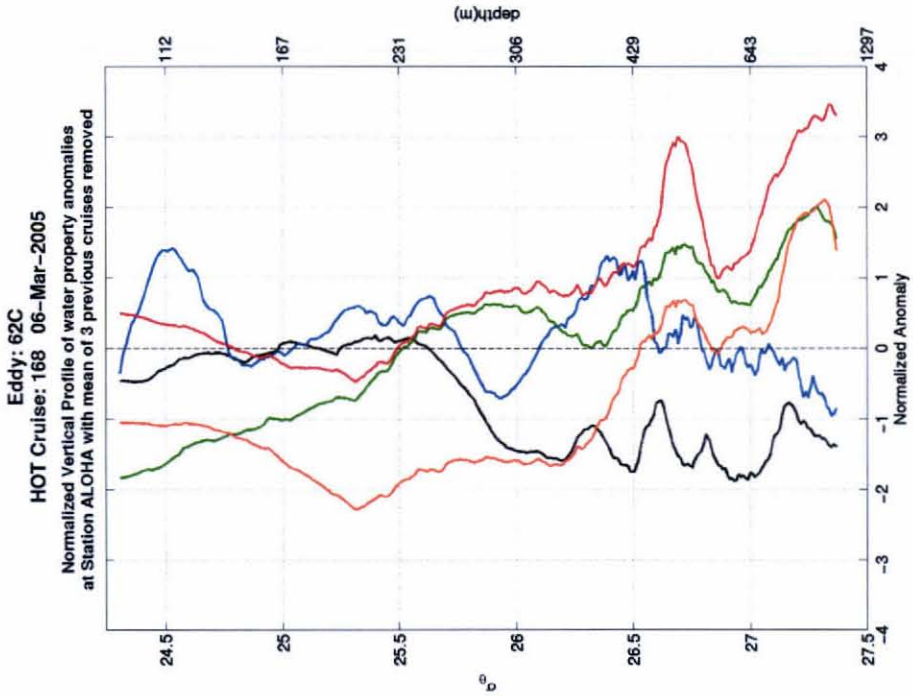
Eddy: 62C
HOT Cruise: 168 06-Mar-2005
Normalized Vertical Profile of water property anomalies
at Station ALOHA with mean of 3 previous cruises removed
depth(m)
112
167
231
306
429
643
1297
Normalized Anomaly
σ_θ

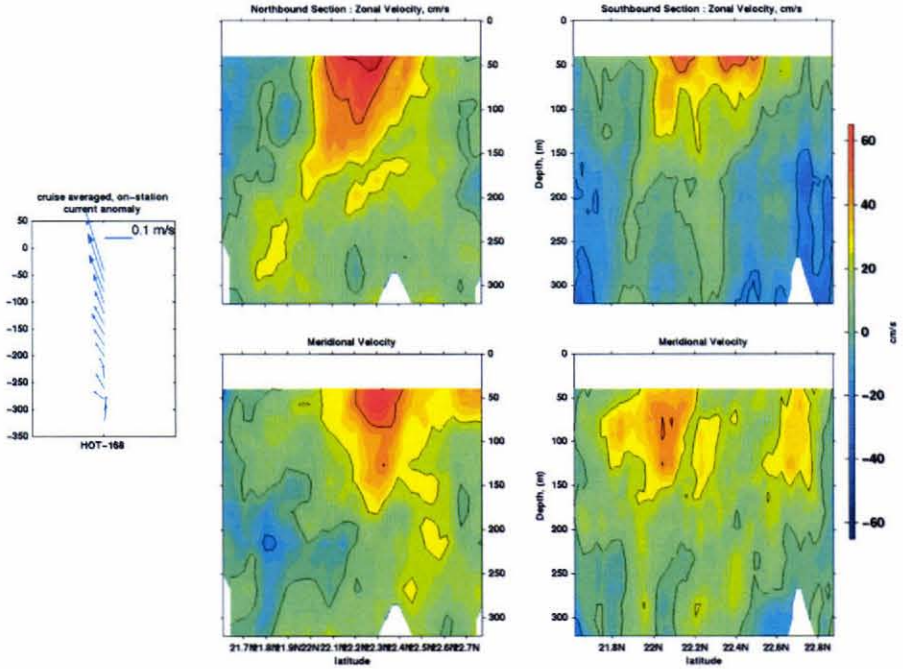
cruise averaged, on-station
current anomaly
0.1 m/s
HOT-168
Northbound Section : Zonal Velocity, cm/s
Southbound Section : Zonal Velocity, cm/s
Meridional Velocity
Meridional Velocity
Depth, (m)
latitude
cm/s

Eddy: 63C Dates in ALOHA box: 23-Feb-2005 to 27-Apr-2005

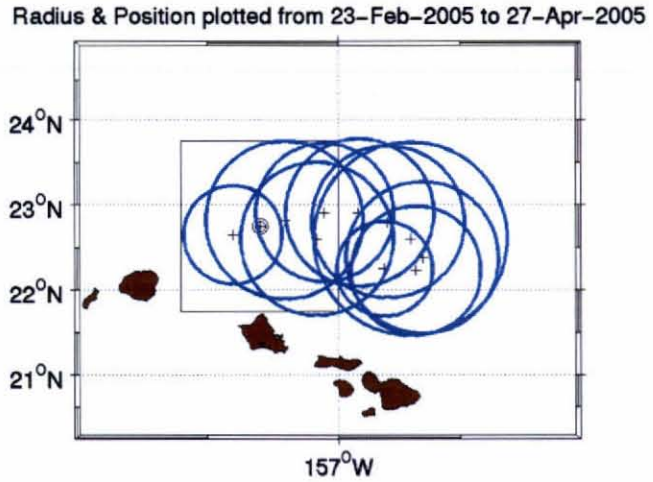

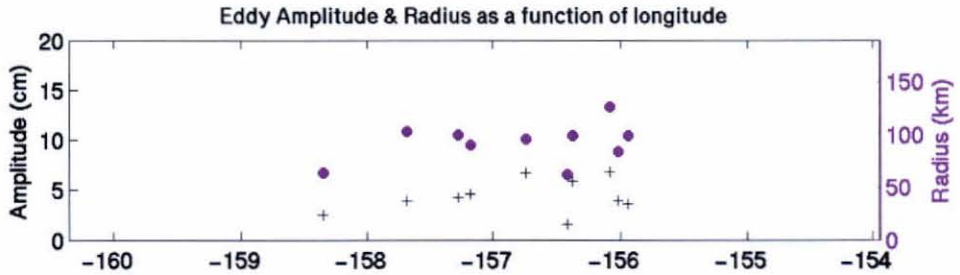

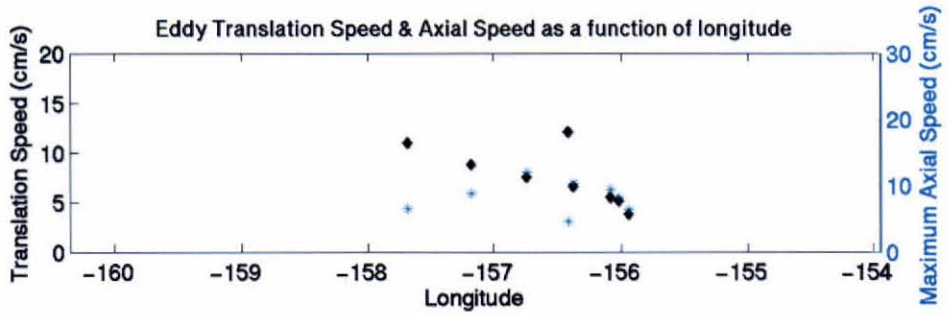

EID: 63C

This eddy is another collision remnant from the same event described for 62C. This feature is short lived and never gains solid, circular shape before it dissipates.

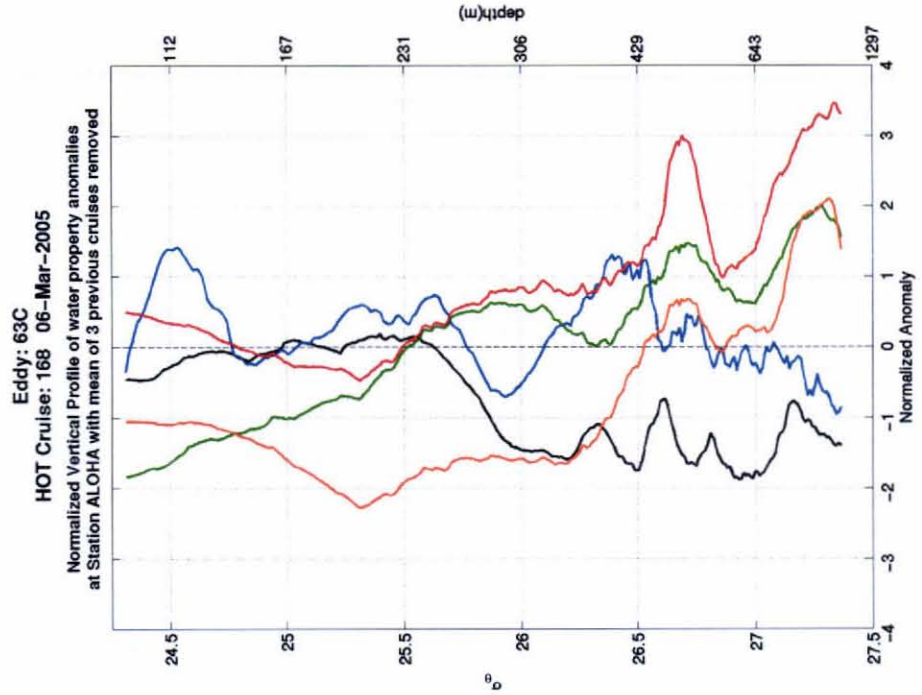
Eddy: 63C
HOT Cruise: 168 06-Mar-2005
Normalized Vertical Profile of water property anomalies
at Station ALOHA with mean of 3 previous cruises removed
depth(m)
112
167
231
306
429
643
1297
Normalized Anomaly
θ_D

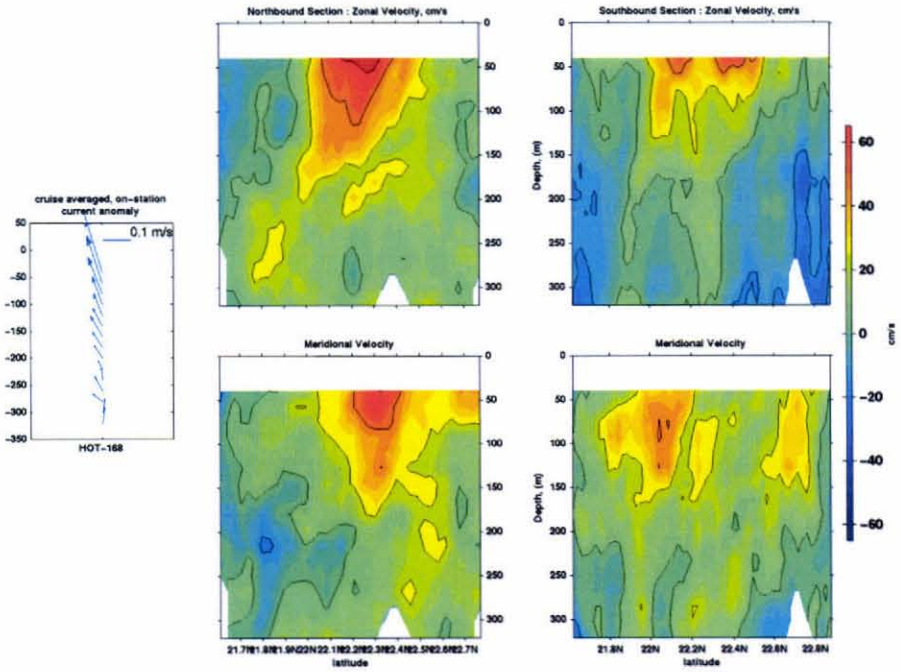
cruise averaged, on-station
current anomaly
0.1 m/s
HOT-168
Northbound Section : Zonal Velocity, cm/s
Southbound Section : Zonal Velocity, cm/s
Meridional Velocity
Meridional Velocity
Depth, (m)
latitude
cm/s

Eddy: 64A Dates in ALOHA box: 16-Mar-2005 to 06-Apr-2005

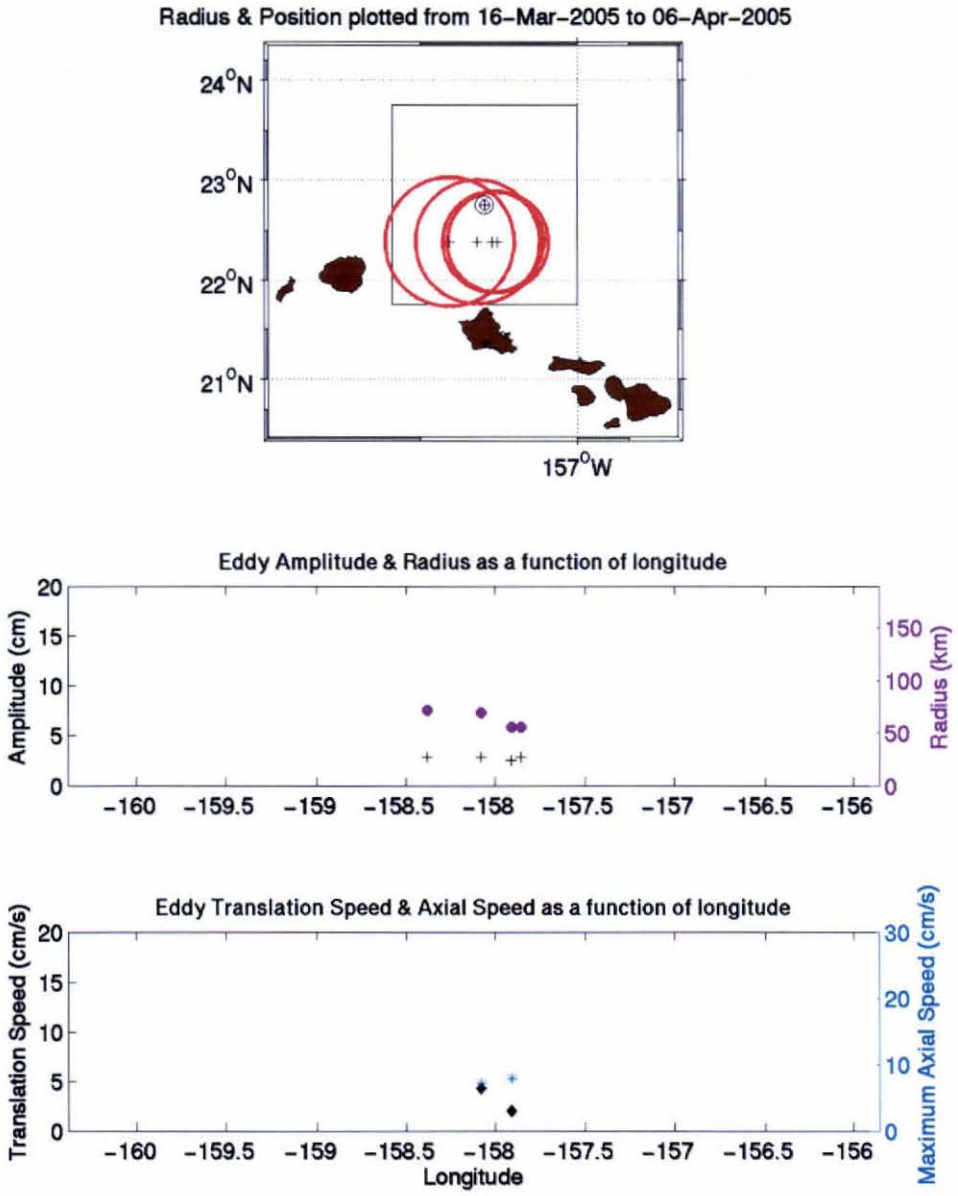

EID: 64A

This weak feature formed north of Oahu and is short-lived. Probably not really an eddy.

Eddy: 65A Dates in ALOHA box: 04-May-2005 to 01-Jun-2005

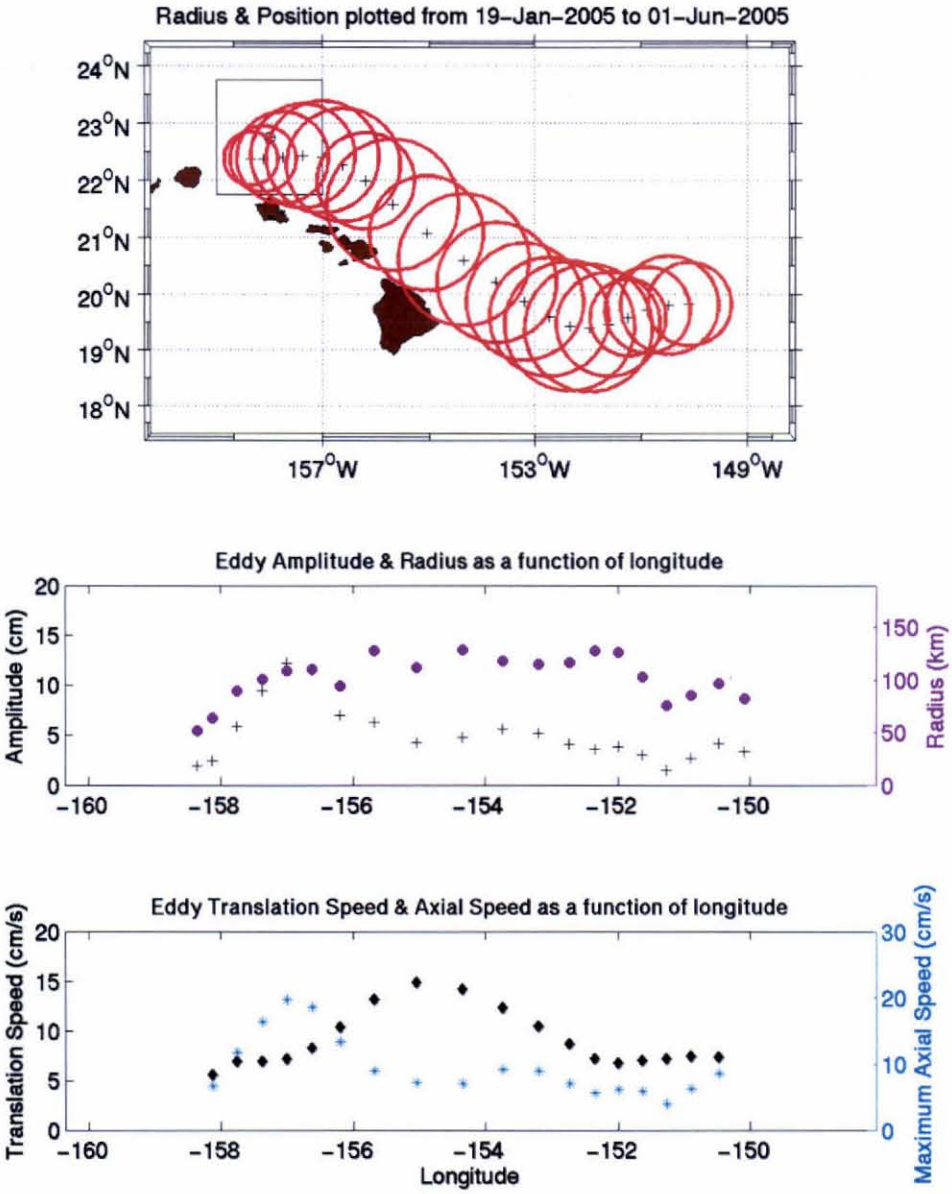

EID: 65A

This eddy formed east of the Big Island at 150W and traveled west, then northwest up the island chain. There are cyclonic eddies ahead and behind it as it moves toward ALOHA. It weakens as it passes ALOHA, its remnant may pass through the Kauai Channel, but the track was dropped.

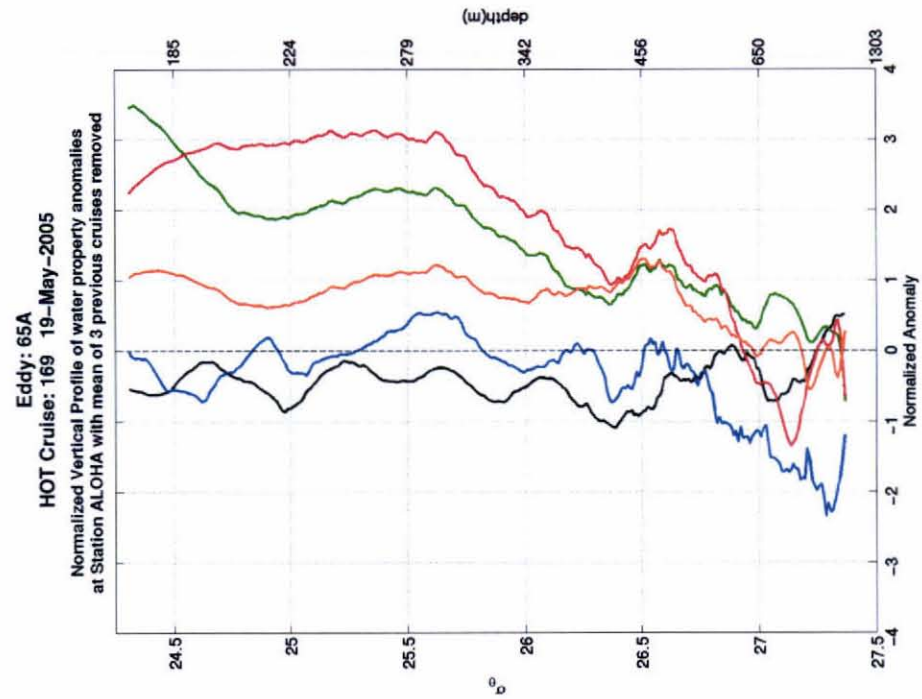
Eddy: 65A
HOT Cruise: 169 19-May-2005
Normalized Vertical Profile of water property anomalies
at Station ALOHA with mean of 3 previous cruises removed
depth(m)
185
224
279
342
456
650
1303
Normalized Anomaly
σθ

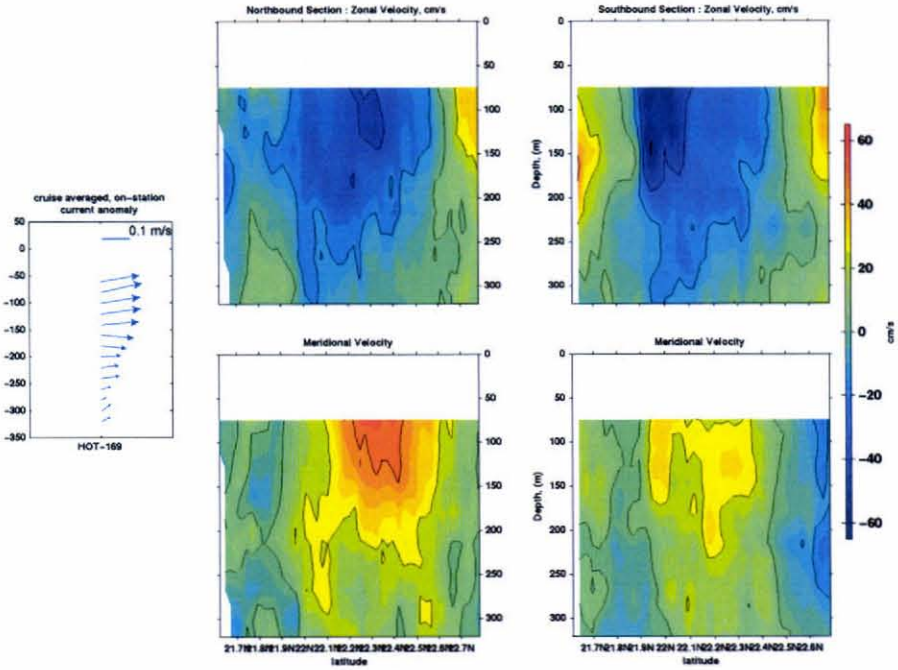
cruise averaged, on-station
current anomaly
0.1 m/s
HOT-169
Northbound Section : Zonal Velocity, cm/s
Southbound Section : Zonal Velocity, cm/s
Meridional Velocity
Meridional Velocity
Depth, (m)
latitude
cm/s

Eddy: 66C Dates in ALOHA box: 15–Jun–2005 to 15–Jun–2005

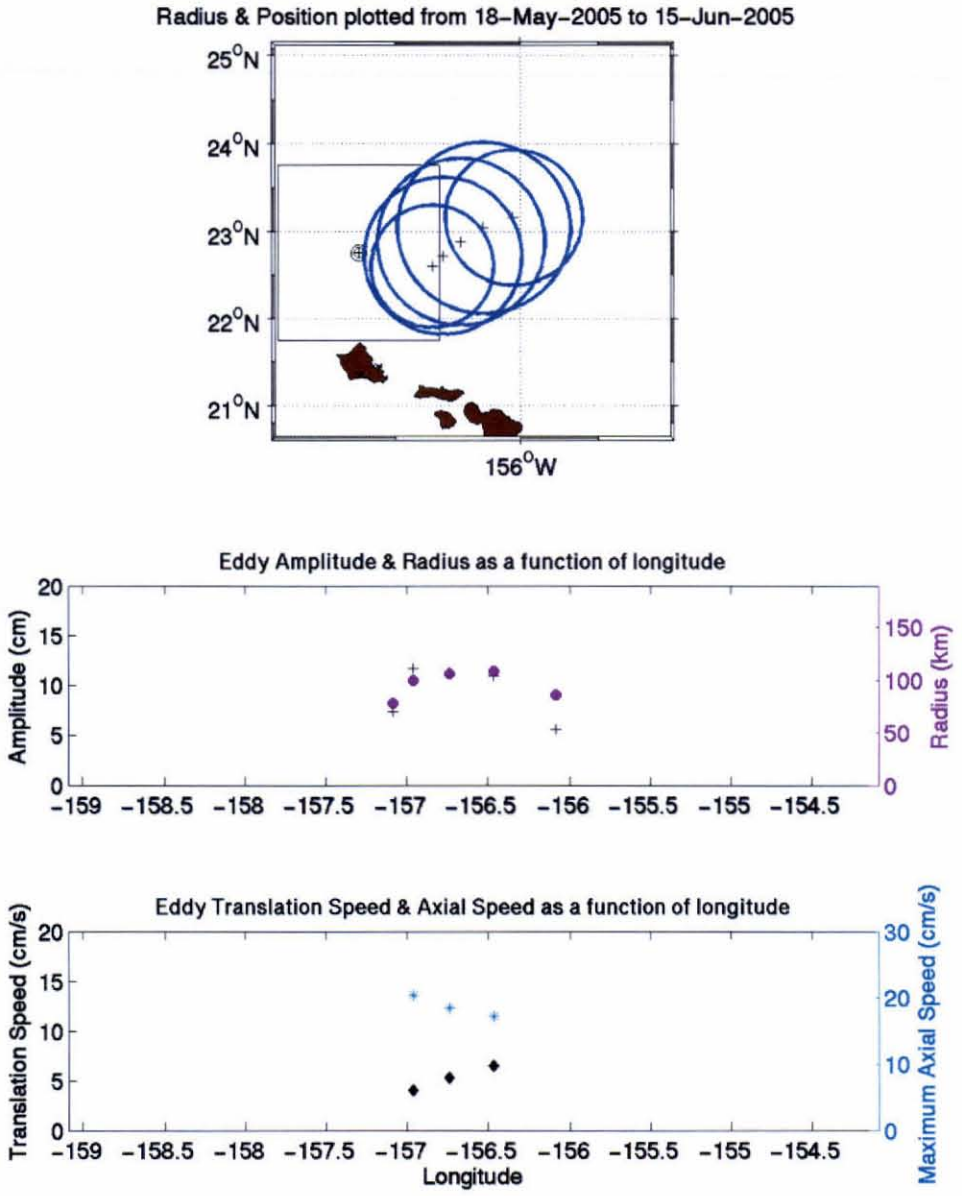

EID: 66C

This eddy is a short-lived offshoot of an eddy from the north that was squeezed down between two anticyclones and collided with the islands. The vertical water property anomalies show an anomaly at the 26.25σ_θ level that may be bolus transport from the eddy that originated to the north.

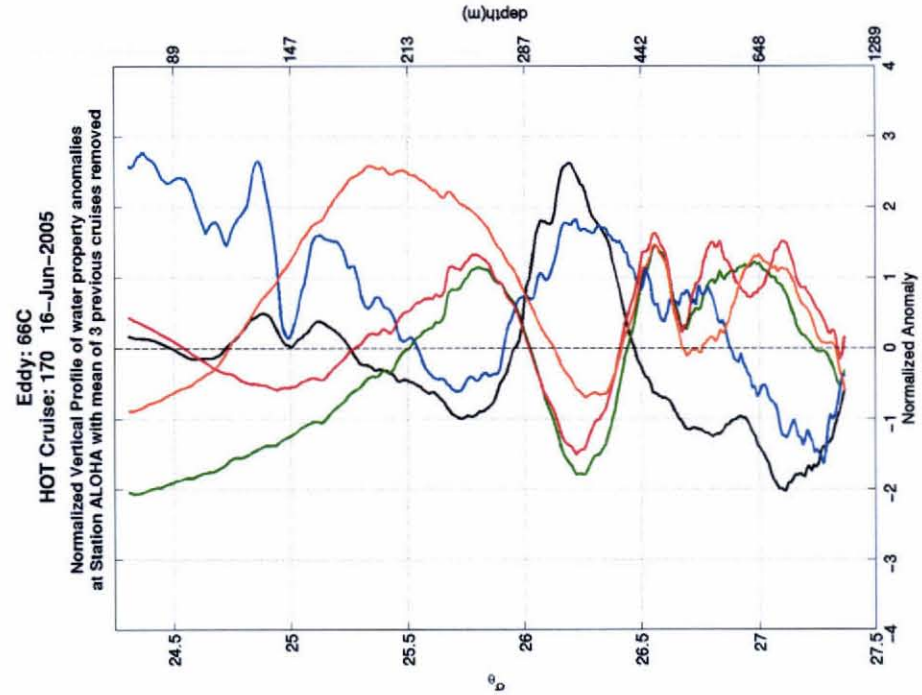
Eddy: 66C
HOT Cruise: 170 16-Jun-2005
Normalized Vertical Profile of water property anomalies
at Station ALOHA with mean of 3 previous cruises removed
depth(m)
89
147
213
287
442
648
1289
Normalized Anomaly
σ_θ

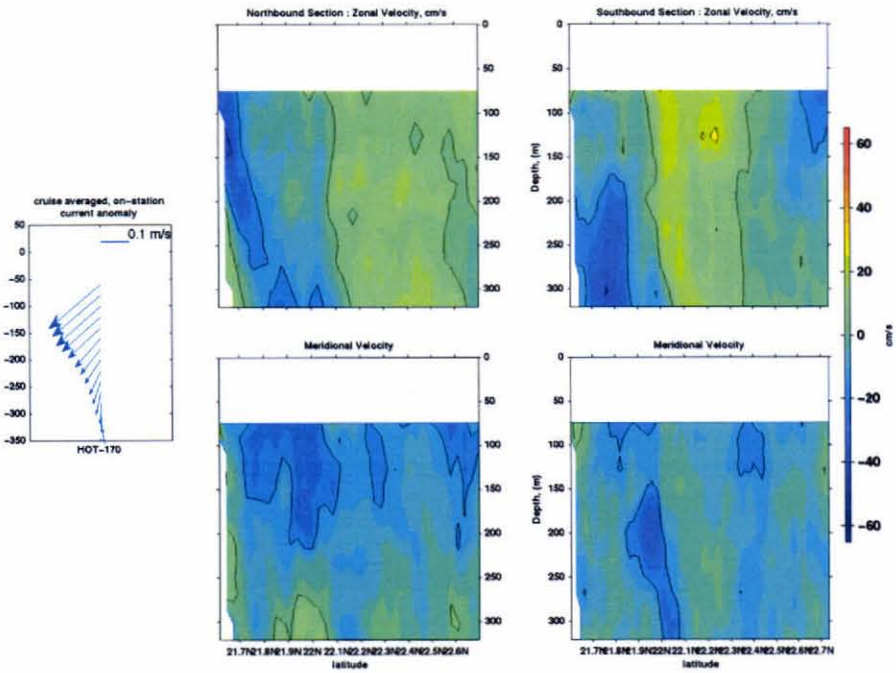
cruise averaged, on-station
current anomaly
0.1 m/s
HOT-170
Northbound Section : Zonal Velocity, cm/s
Southbound Section : Zonal Velocity, cm/s
Meridional Velocity
Meridional Velocity
Depth, (m)
latitude
cm/s

Eddy: 67C Dates in ALOHA box: 29-Jun-2005 to 27-Jul-2005

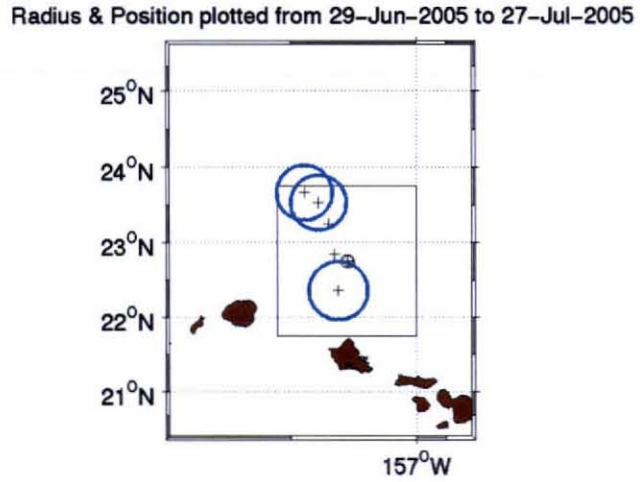

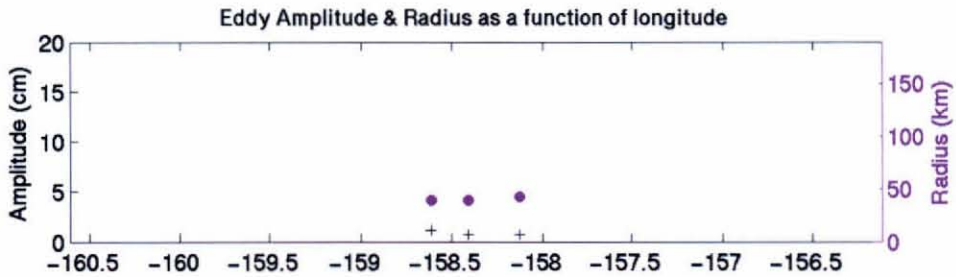

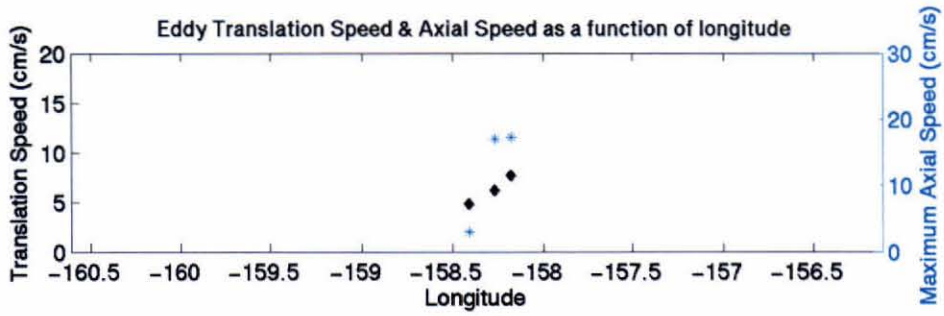

EID: 67C

This short-lived feature is another remnant from the break up described for 66C but this is not really an eddy and should not be further considered.

Eddy: 68A Dates in ALOHA box: 13-Jul-2005 to 17-Aug-2005

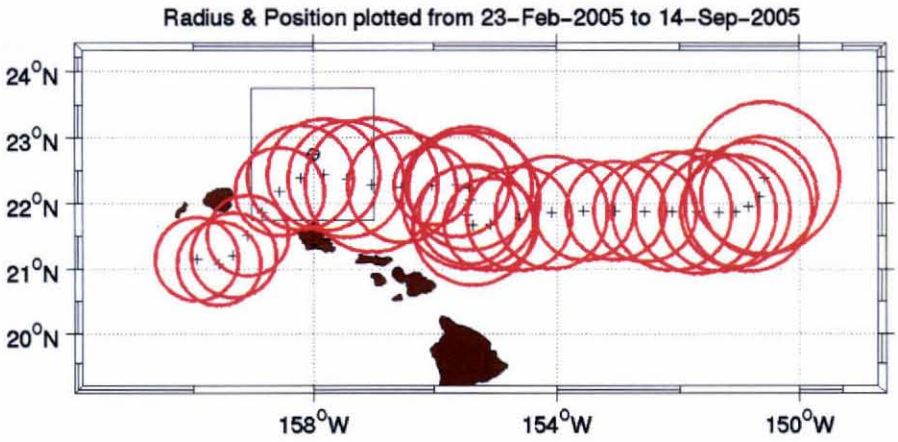

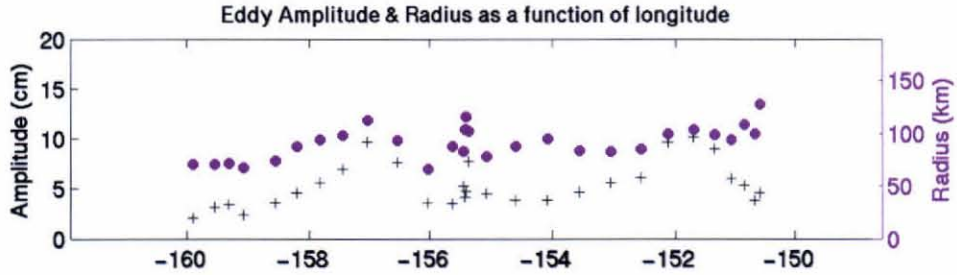

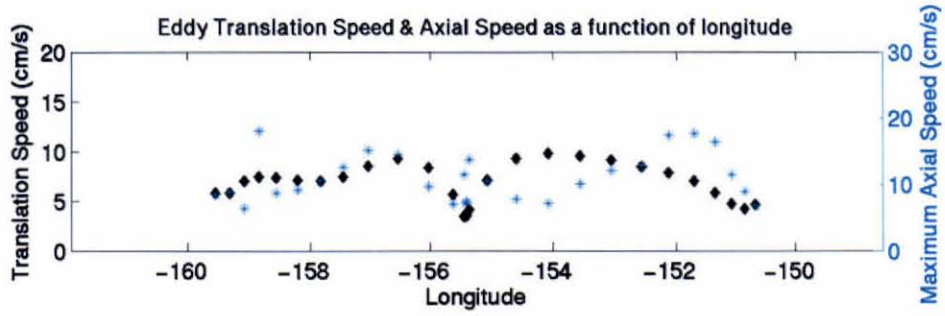

EID: 68A

This eddy formed at 151W and traveled west until it was over Maui, then it was squeezed between two cyclonic eddies and the islands, which shifted it to the north. It then passed to the south of ALOHA, traveled through the Kauai Channel and dissipated.

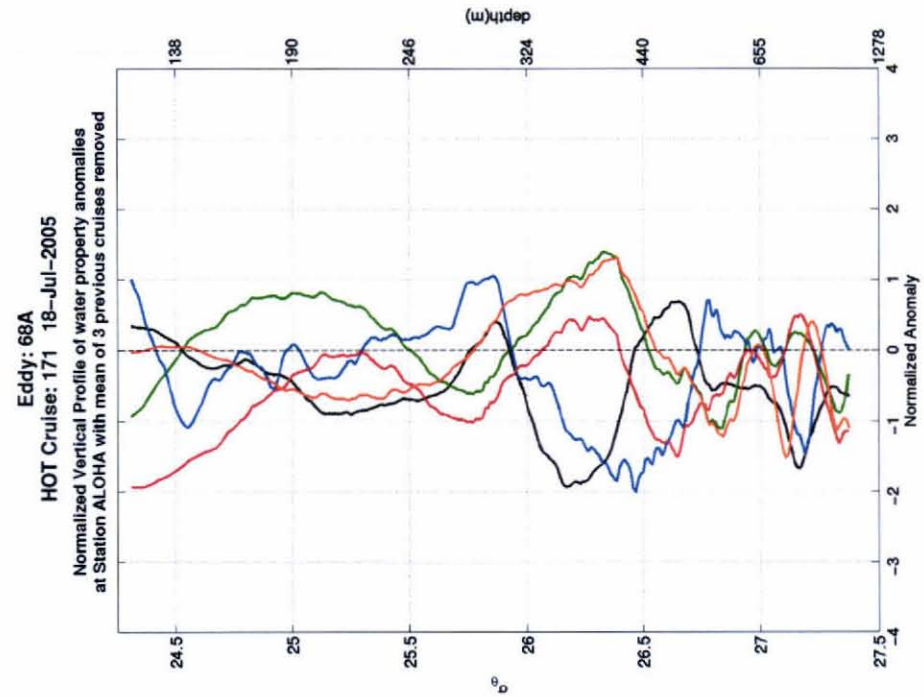
Eddy: 68A
HOT Cruise: 171 18-Jul-2005
Normalized Vertical Profile of water property anomalies
at Station ALOHA with mean of 3 previous cruises removed
depth(m)
138
190
246
324
440
655
1278
Normalized Anomaly
θ_p

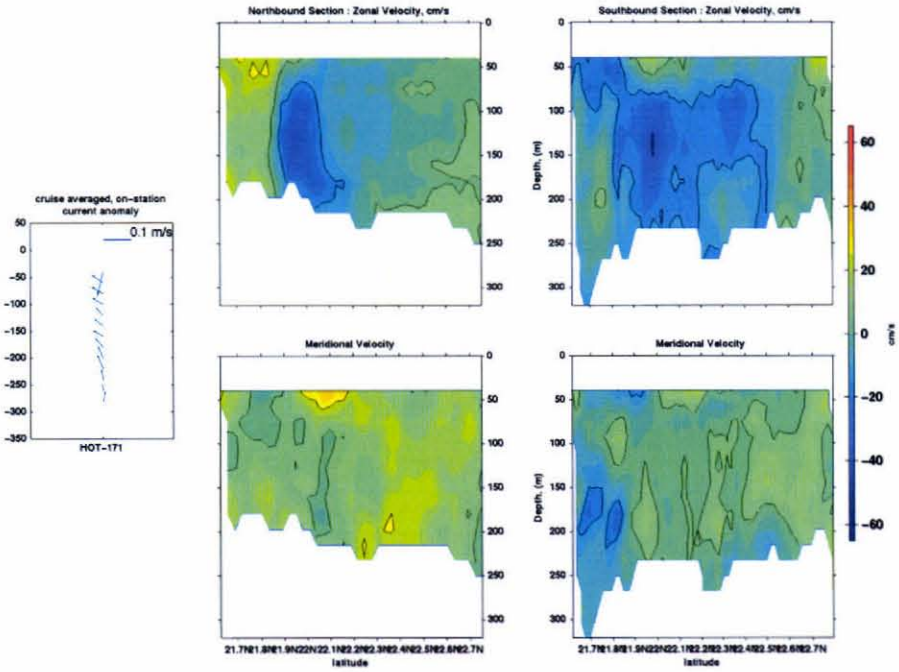
cruise averaged, on-station
current anomaly
0.1 m/s
HOT-171
Northbound Section : Zonal Velocity, cm/s
Southbound Section : Zonal Velocity, cm/s
Meridional Velocity
Meridional Velocity
Depth, (m)
latitude
cm/s

Eddy: 69A Dates in ALOHA box: 14–Sep–2005 to 05–Oct–2005

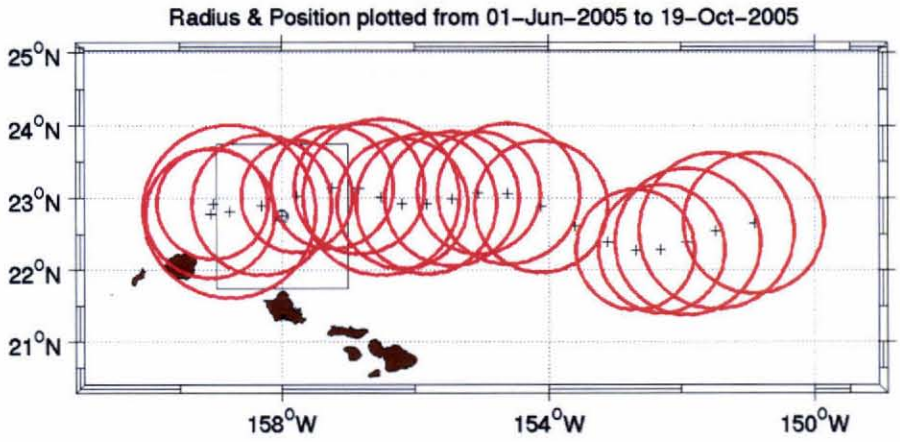

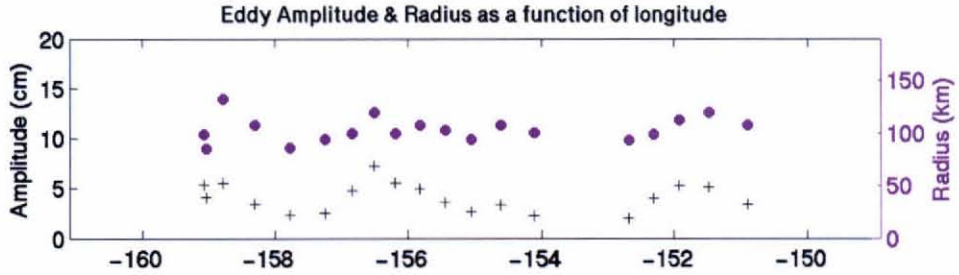

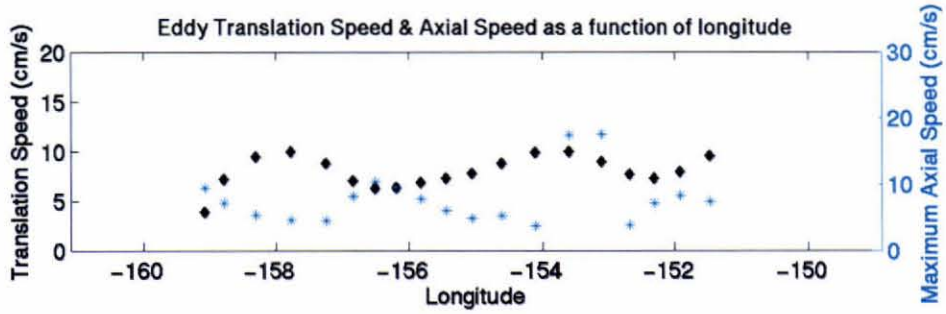

EID: 69A

This eddy formed at 151W and traveled west until it was drawn to the northwest due to a larger anticyclone to the north trying to draw it in. This eddy retained its autonomy and passed over ALOHA, then dissipated when it collided with Kauai.

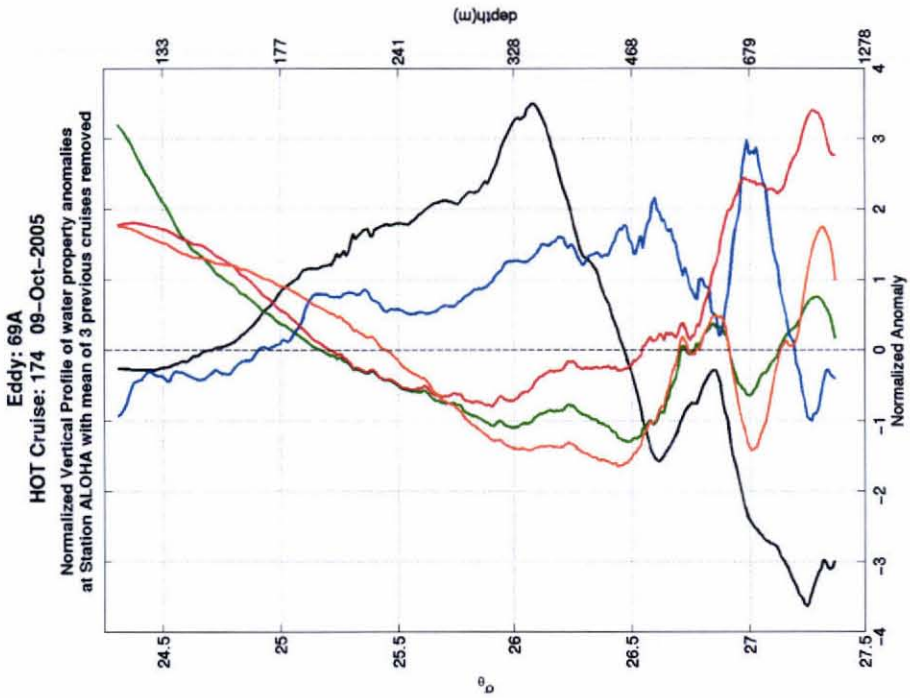
Eddy: 69A
HOT Cruise: 174 09-Oct-2005
Normalized Vertical Profile of water property anomalies
at Station ALOHA with mean of 3 previous cruises removed
depth(m)
133
177
241
328
468
679
1278
Normalized Anomaly
θ_p

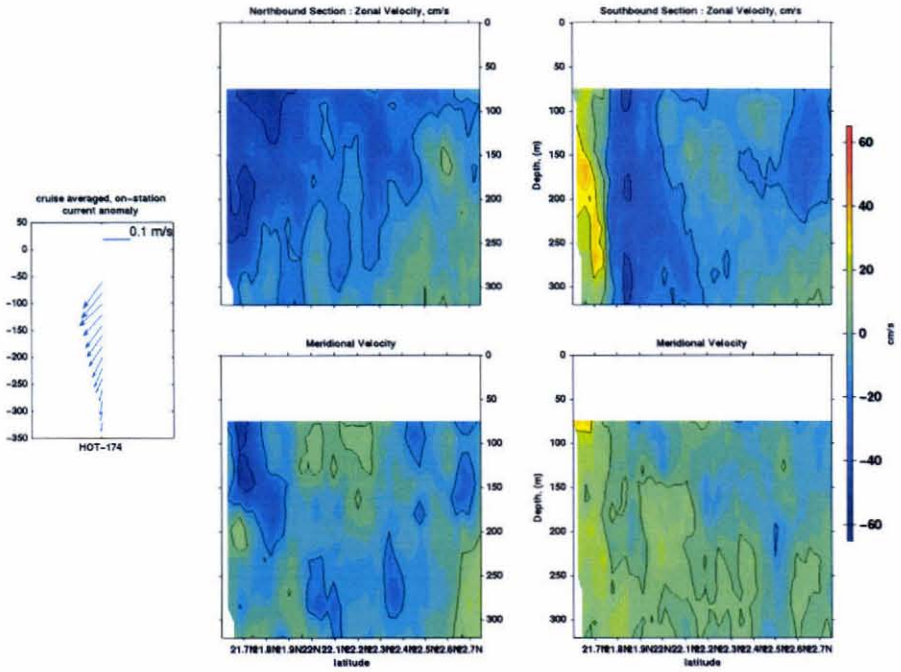
cruise averaged, on-station
current anomaly
0.1 m/s
HOT-174
Northbound Section : Zonal Velocity, cm/s
Southbound Section : Zonal Velocity, cm/s
Meridional Velocity
Meridional Velocity
Depth, (m)
latitude
cm/s

Eddy: 70A Dates in ALOHA box: 09-Nov-2005 to 28-Dec-2005

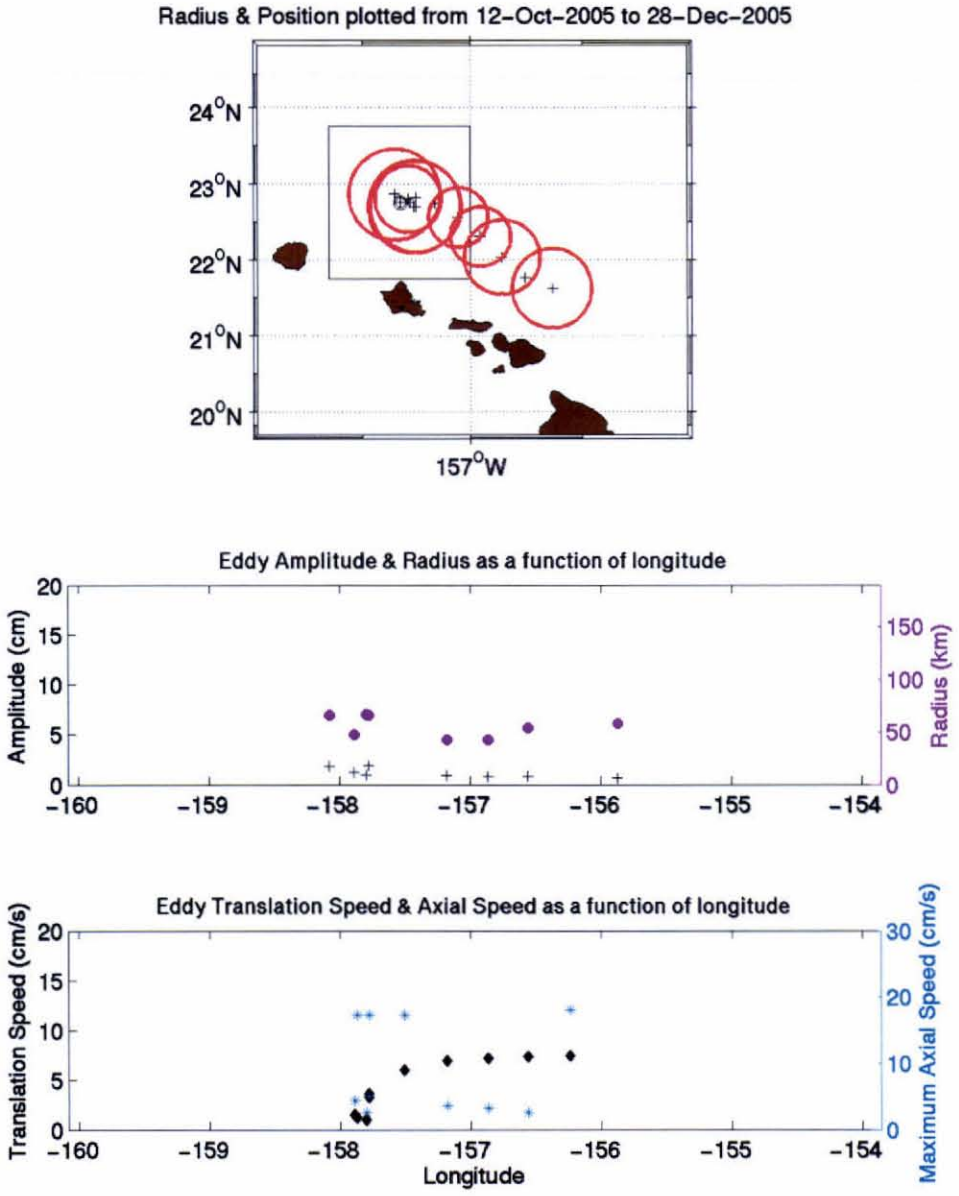

EID: 70A

This eddy is an offshoot of another anticyclone. It traveled up the island chain, then was drawn up into a larger anticyclone to the north after it passed over ALOHA. This eddy never developed good circular structure.

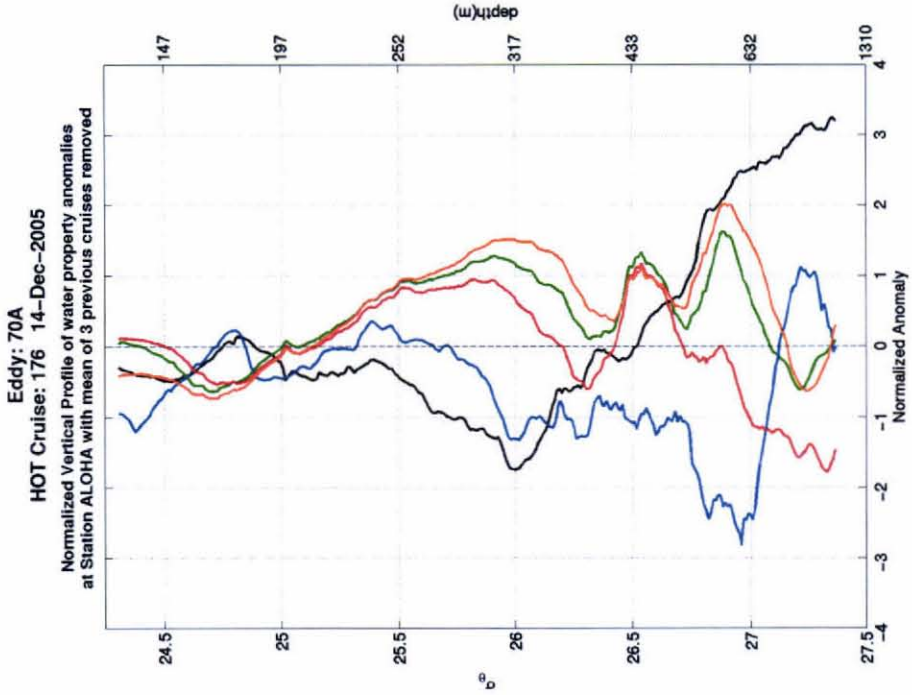
Eddy: 70A
HOT Cruise: 176 14-Dec-2005
Normalized Vertical Profile of water property anomalies
at Station ALOHA with mean of 3 previous cruises removed
depth(m)
147
197
252
317
433
632
1310
Normalized Anomaly
θ_D

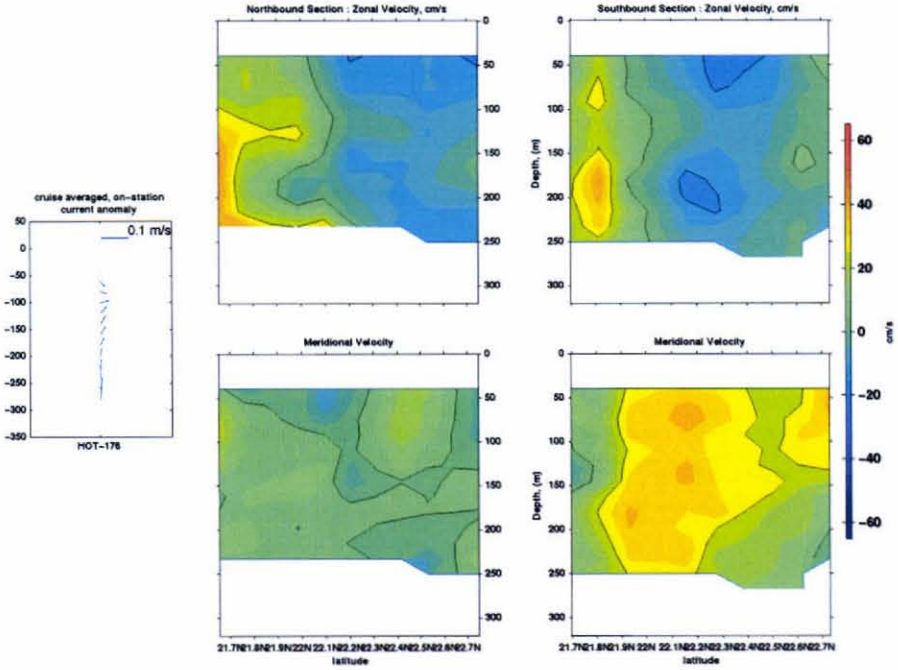
cruise averaged, on-station
current anomaly
0.1 m/s
HOT-176
Northbound Section : Zonal Velocity, cm/s
Southbound Section : Zonal Velocity, cm/s
Meridional Velocity
Meridional Velocity
Depth, (m)
latitude
cm/s

Eddy: 71C Dates in ALOHA box: 08-Feb-2006 to 08-Mar-2006

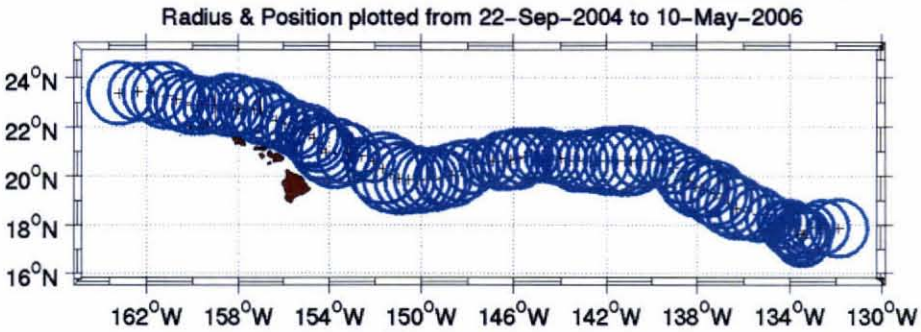

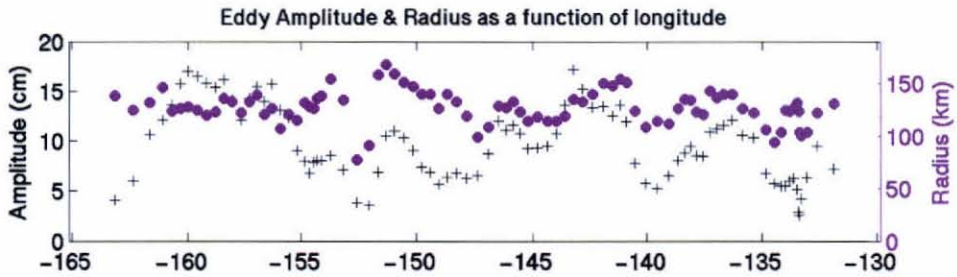

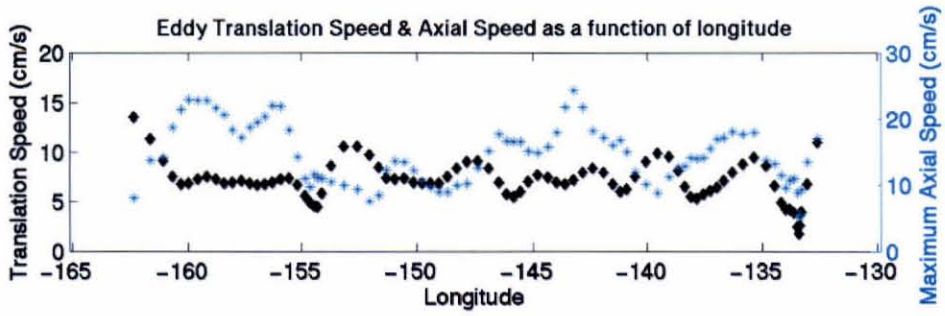

EID: 71C

This eddy was the longest lived feature of the record at almost two years. It spent several weeks spinning up at 18N,133W then traveled northwest until reaching latitude 20N, where it then traveled west until reaching island chain and moving northwest again, over ALOHA, then past Kauai and further west, where it finally splits and dissipates. Throughout its lifetime there are no significant eddy-eddy interactions noticed in the visual analysis. The vertical profile of water property anomalies shows very large anomalies at the 25.5σ_θ level.

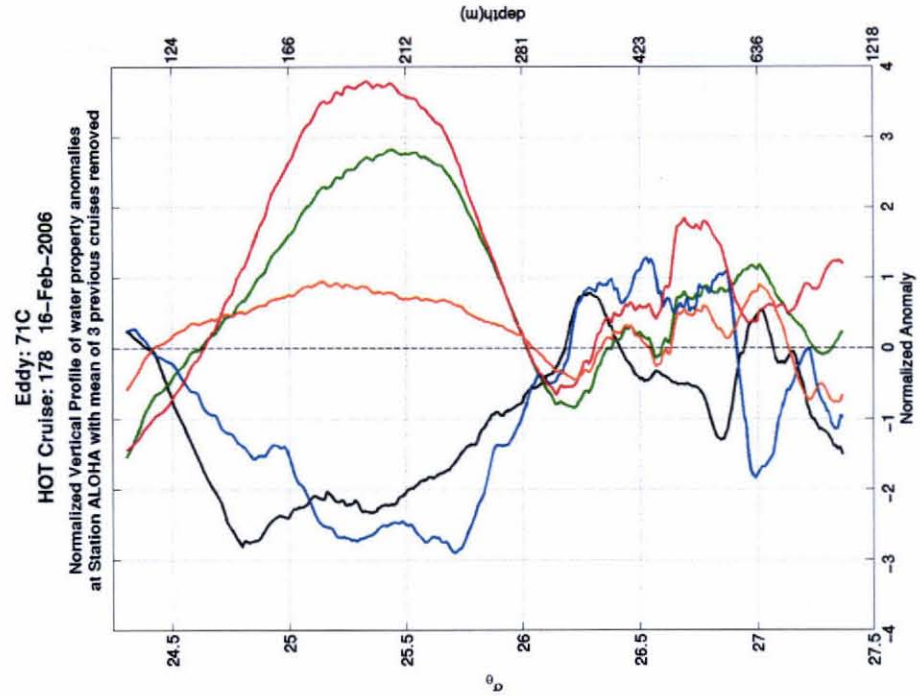
Eddy: 71C
HOT Cruise: 178 16-Feb-2006
Normalized Vertical Profile of water property anomalies
at Station ALOHA with mean of 3 previous cruises removed
depth(m)
124
166
212
281
423
636
1218
Normalized Anomaly
σ_θ

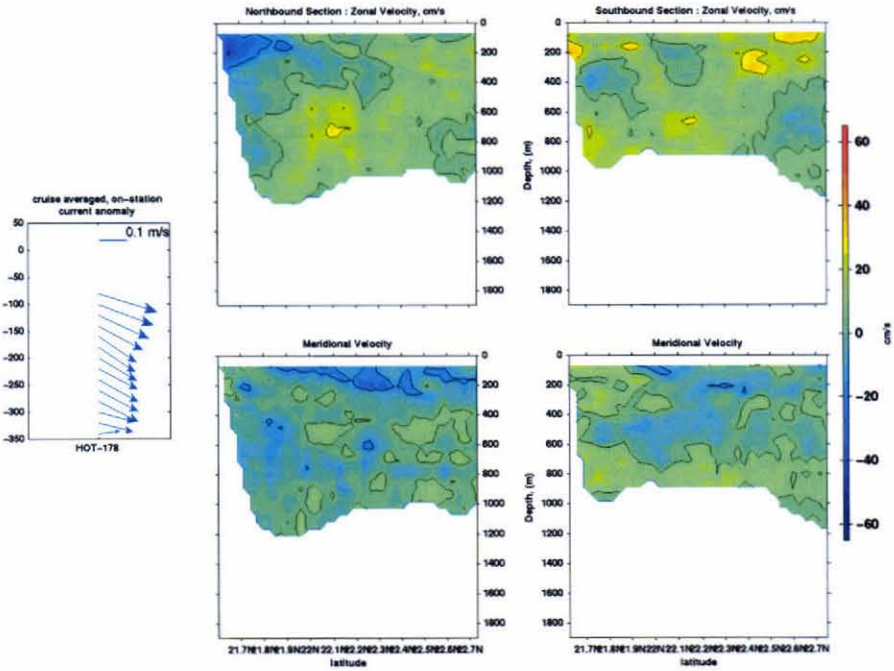
cruise averaged, on-station
current anomaly
0.1 m/s
HOT-178
Northbound Section : Zonal Velocity, cm/s
Southbound Section : Zonal Velocity, cm/s
Meridional Velocity
Meridional Velocity
Depth, (m)
latitude
cm/s

Eddy: 72A Dates in ALOHA box: 22-Mar-2006 to 19-Apr-2006

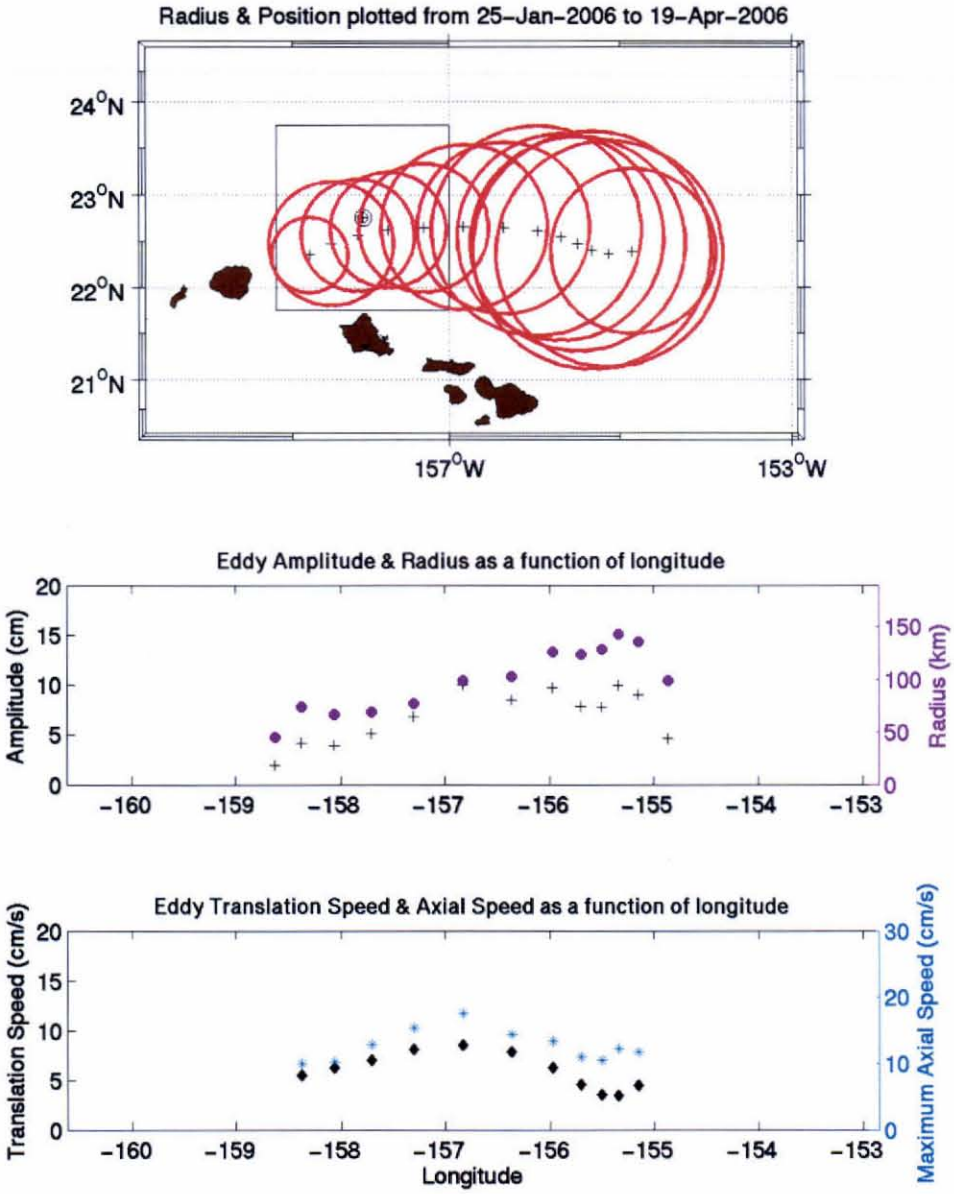

EID: 72A

This eddy is surrounded by two cyclonic eddies (71C to the west and 73C to the east), it passes over ALOHA, then collides with Kauai and dissipates.

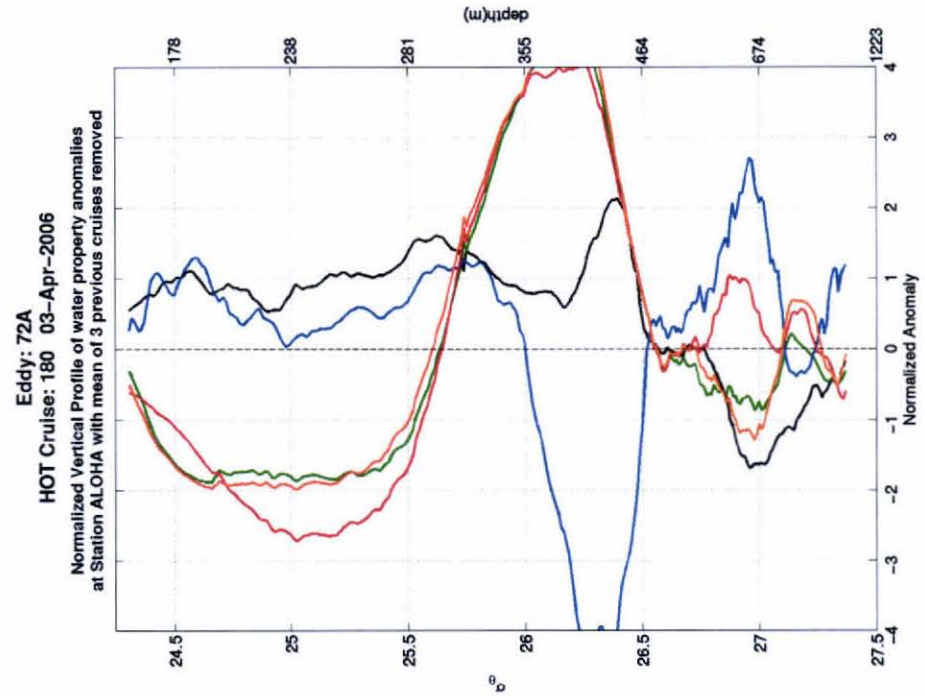
Eddy: 72A
HOT Cruise: 180 03-Apr-2006
Normalized Vertical Profile of water property anomalies
at Station ALOHA with mean of 3 previous cruises removed
depth(m)
178
238
281
355
464
674
1223
Normalized Anomaly
σ_θ

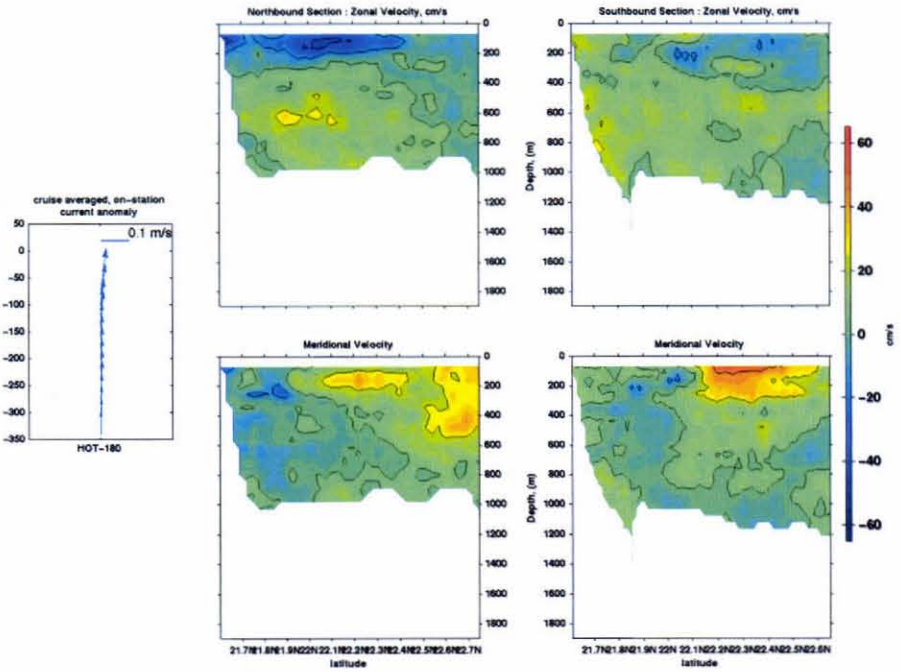
cruise averaged, on-station
current anomaly
0.1 m/s
HOT-180
Northbound Section : Zonal Velocity, cm/s
Southbound Section : Zonal Velocity, cm/s
Meridional Velocity
Meridional Velocity
Depth, (m)
latitude
cm/s

Eddy: 73C Dates in ALOHA box: 03-May-2006 to 31-May-2006

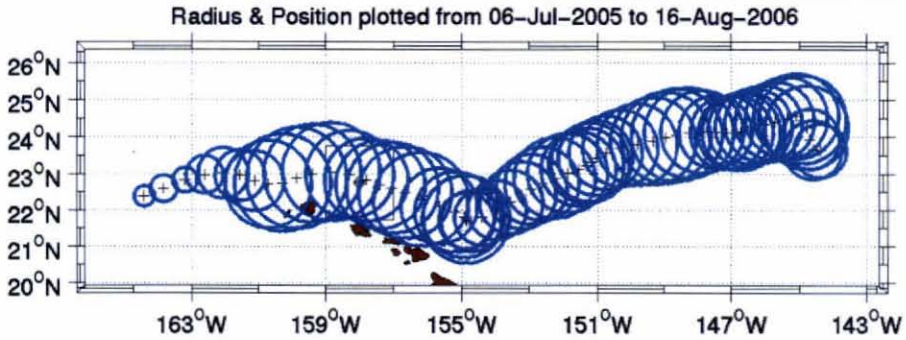

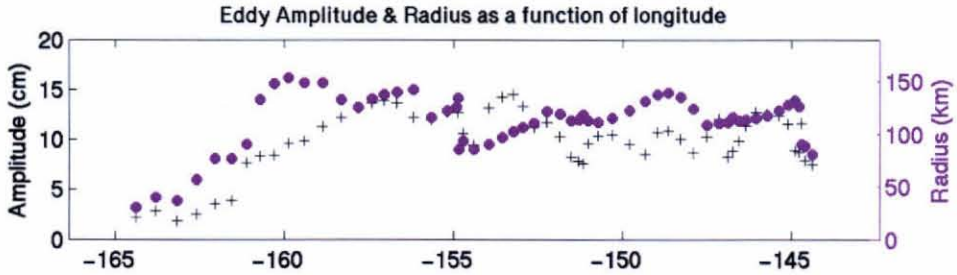

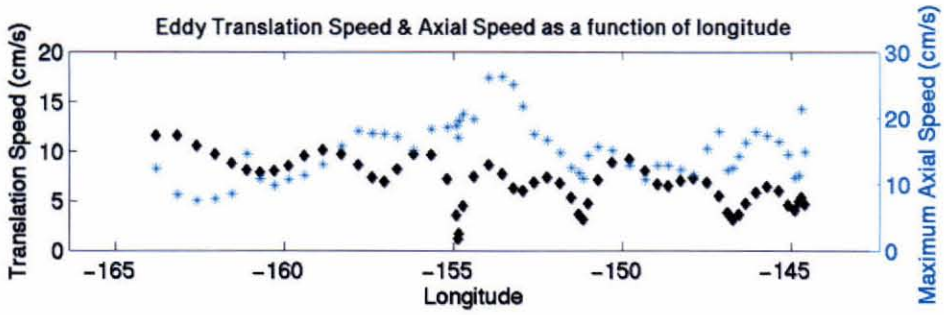

EID: 73C

This eddy was formed from 2 merging cyclones, was forced to the southwest by a large anticyclone, then changes direction to the northwest to follow island chain, follows close behind 72A over ALOHA, then eventually breaks apart west of Kauai due to eddy-eddy interactions.

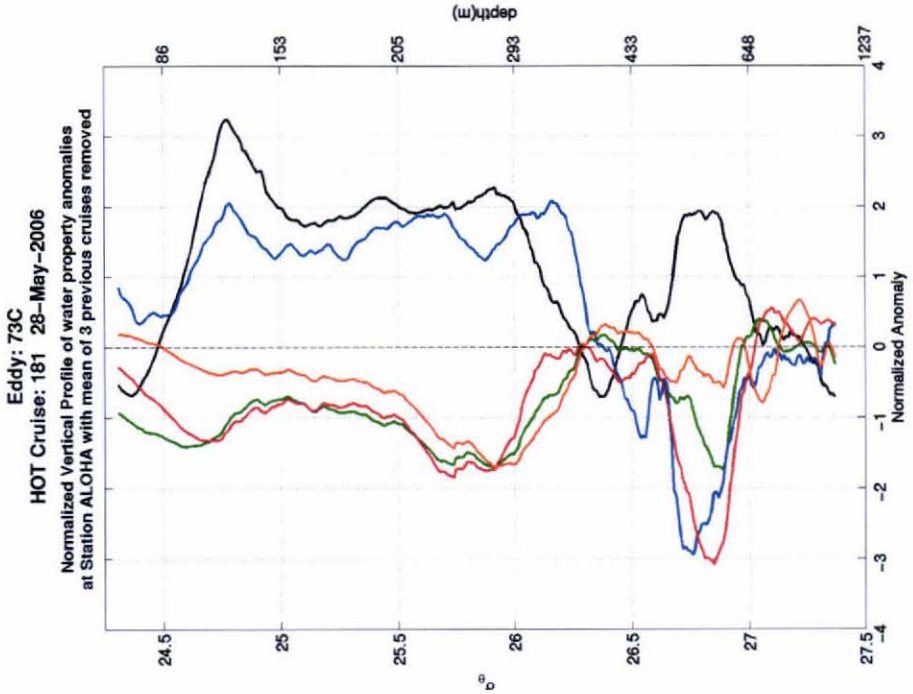
Eddy: 73C
HOT Cruise: 181 28-May-2006
Normalized Vertical Profile of water property anomalies
at Station ALOHA with mean of 3 previous cruises removed
depth(m)
86
153
205
293
433
648
1237
Normalized Anomaly
θ_D

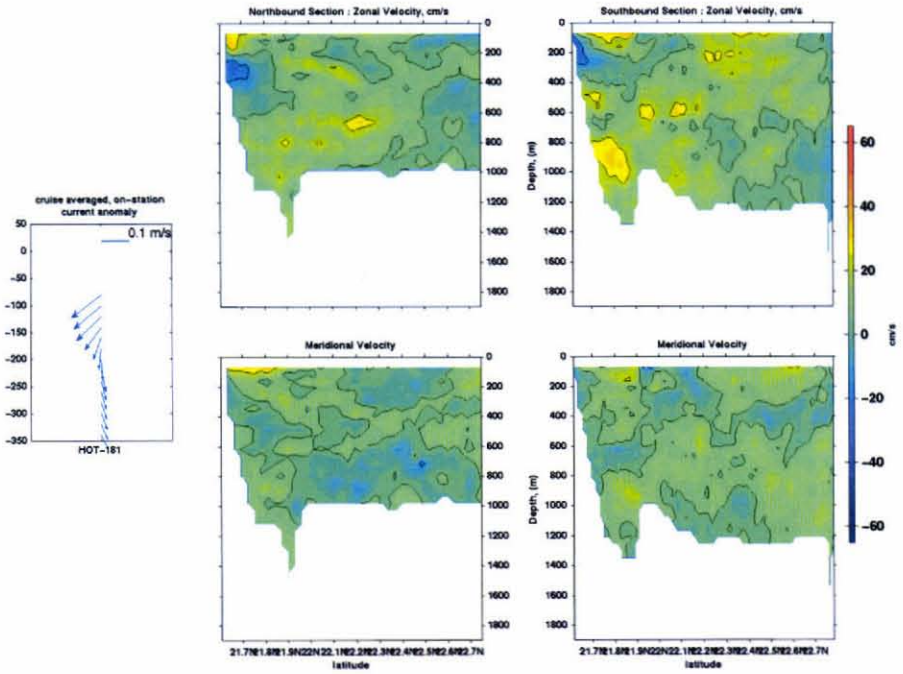
cruise averaged, on-station
current anomaly
0.1 m/s
HOT-181
Northbound Section : Zonal Velocity, cm/s
Southbound Section : Zonal Velocity, cm/s
Meridional Velocity
Meridional Velocity
Depth, (m)
latitude
cm/s

Eddy: 74A Dates in ALOHA box: 28-Jun-2006 to 12-Jul-2006

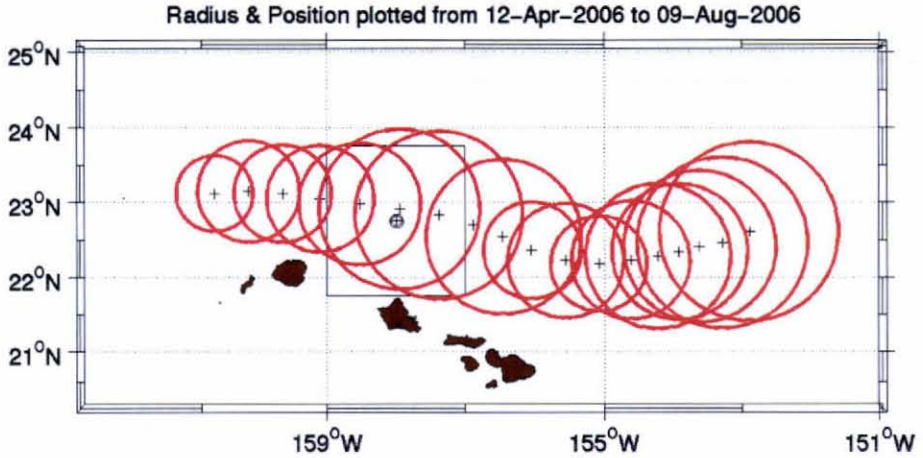

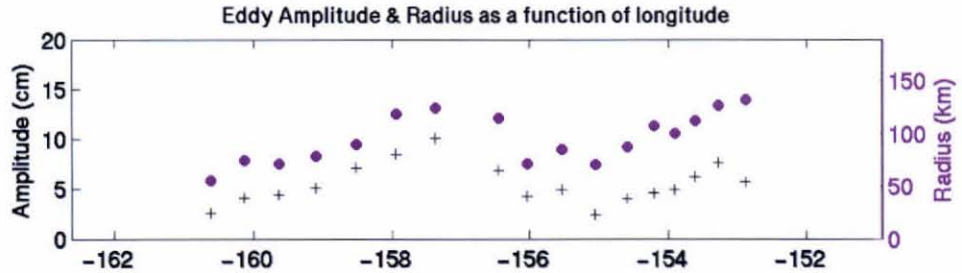

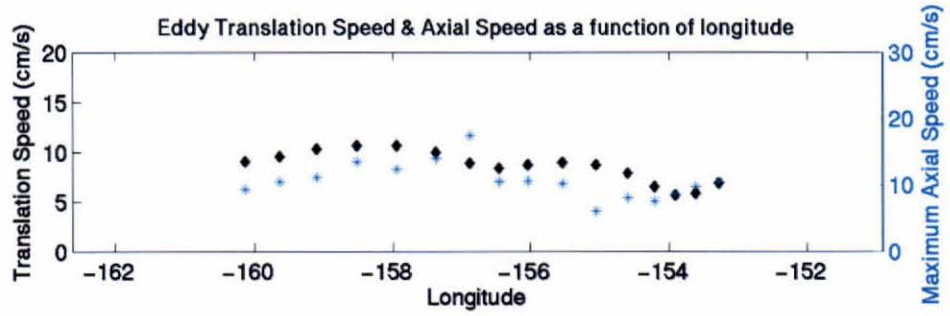

EID: 74A

This eddy may have come from further east, also may interact with 73C on it leading edge. The track was dropped when eddy-eddy interactions with another anticyclone caused it to change direction and dissipate.

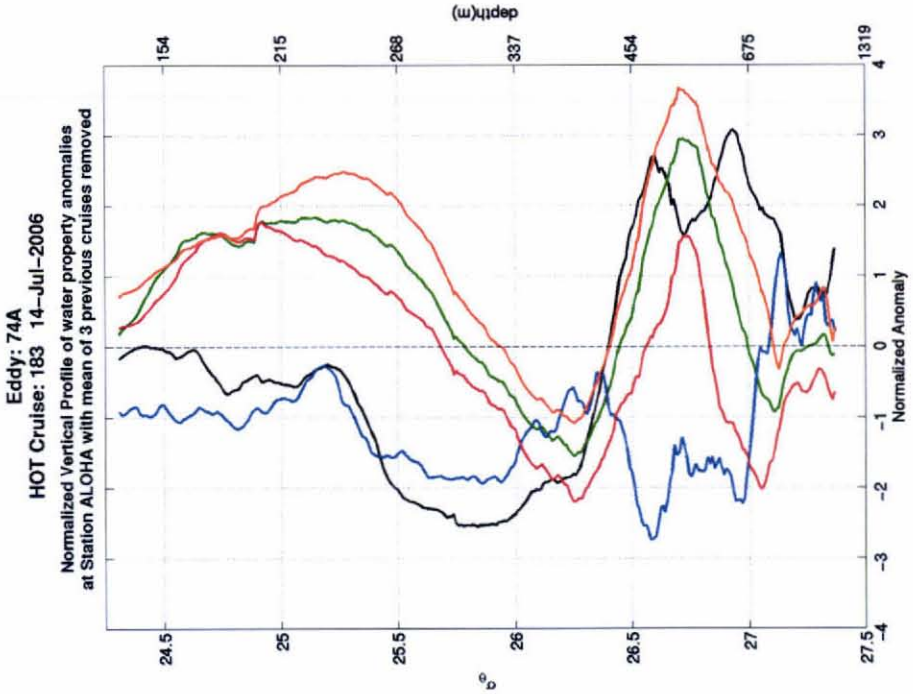
Eddy: 74A
HOT Cruise: 183 14-Jul-2006
Normalized Vertical Profile of water property anomalies
at Station ALOHA with mean of 3 previous cruises removed
depth(m)
154
215
268
337
454
675
1319
Normalized Anomaly
σ_θ

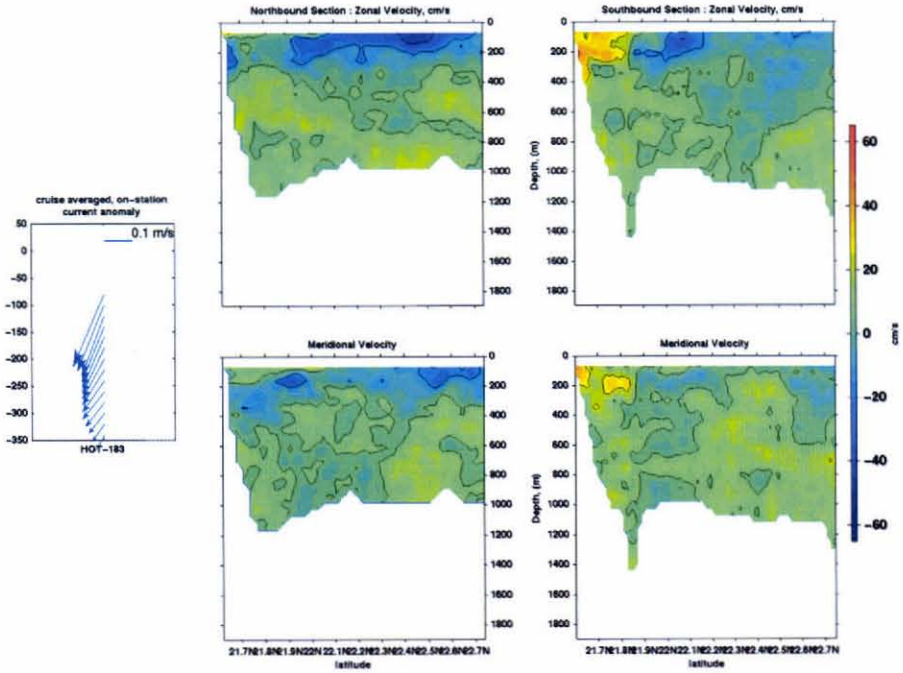
cruise averaged, on-station
current anomaly
0.1 m/s
HOT-183
Northbound Section : Zonal Velocity, cm/s
Southbound Section : Zonal Velocity, cm/s
Meridional Velocity
Meridional Velocity
Depth, (m)
latitude
cm/s

Eddy: 75C Dates in ALOHA box: 02-Aug-2006 to 09-Aug-2006

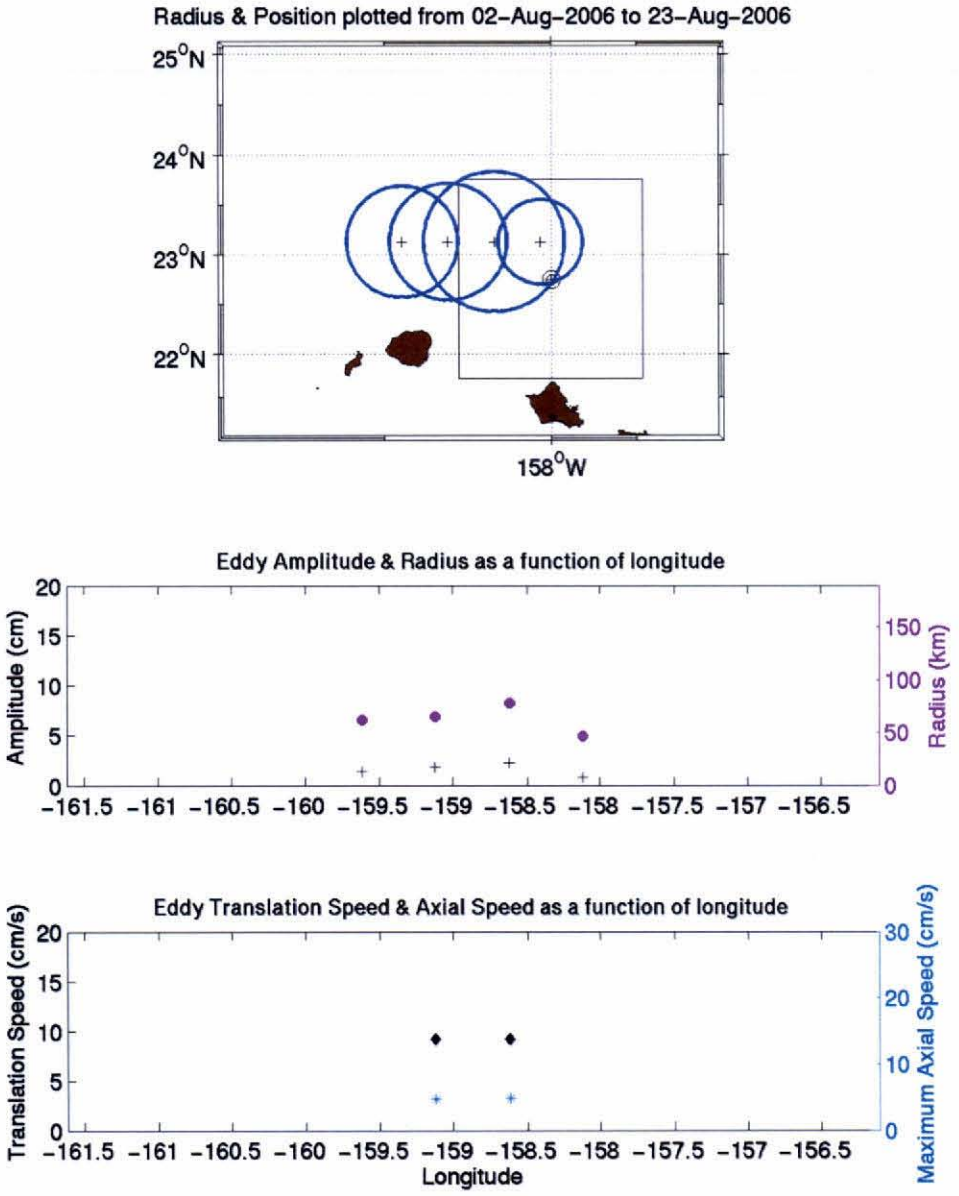

EID: 75C

This small, short-lived eddy forms in the boxed region around ALOHA, probably as the remnant of another feature, but not one that was visually identifiable. Its impact on ALOHA is negligible due to its short lifetime and its position relative to ALOHA makes it so that only the peripheral edge of the "eddy" intersects ALOHA.

Eddy: 76C Dates in ALOHA box: 22-Nov-2006 to 20-Dec-2006

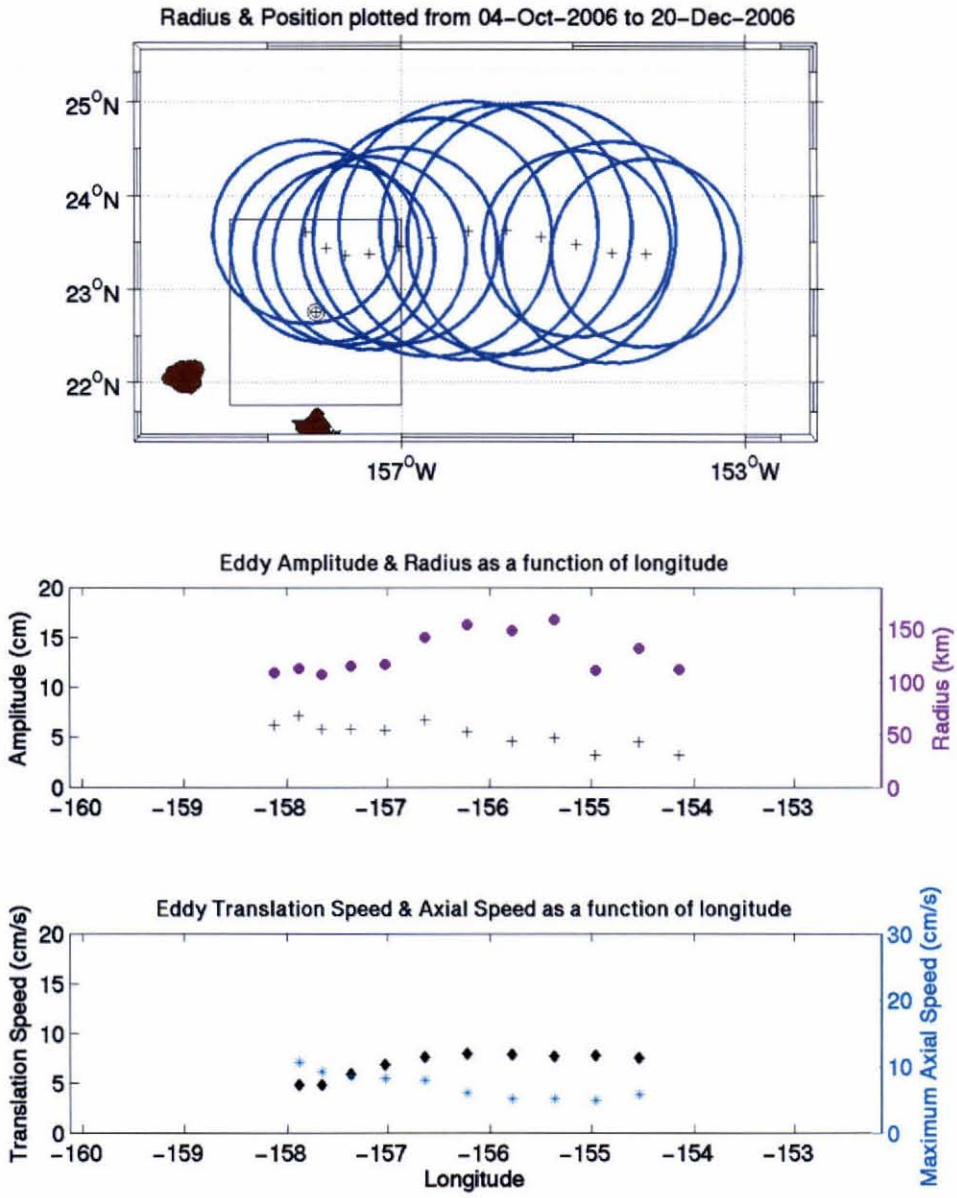

EID: 76C

This eddy may be a split from a previous eddy, if so, there may be associated bolus transport from the original feature. The dissipation of this feature is unknown because it reaches the end of the time-series.

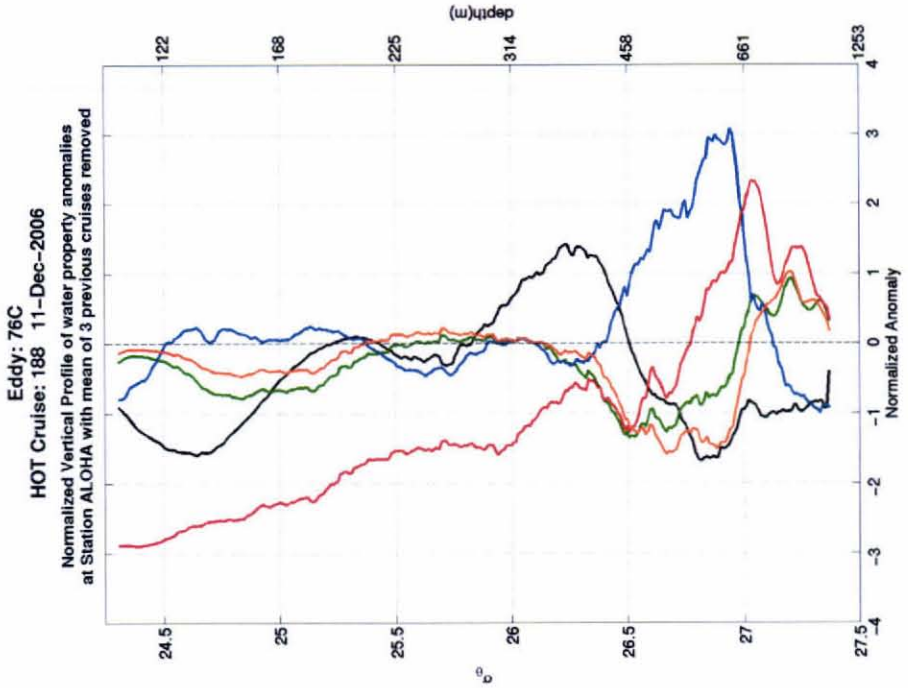
Eddy: 76C
HOT Cruise: 188 11-Dec-2006
Normalized Vertical Profile of water property anomalies
at Station ALOHA with mean of 3 previous cruises removed
depth(m)
122
168
225
314
458
661
1253
Normalized Anomaly
σ_θ

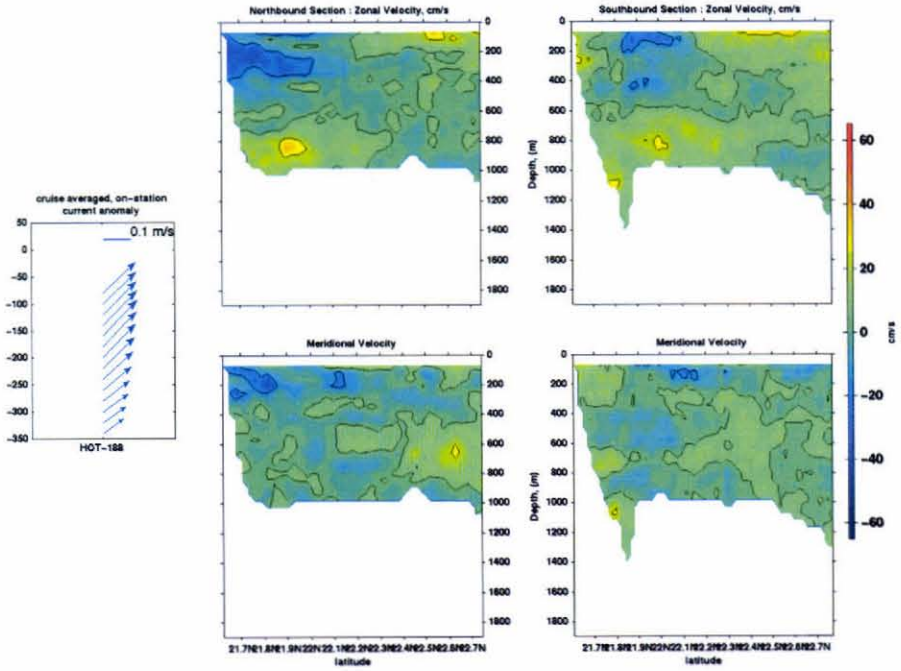
cruise averaged, on-station
current anomaly
0.1 m/s
HOT-188
Northbound Section : Zonal Velocity, cm/s
Southbound Section : Zonal Velocity, cm/s
Meridional Velocity
Meridional Velocity
Depth, (m)
latitude
cm/s

10 APPENDIX III Version 5 (April 2008) eddy identification and tracking algorithm output

This study has analyzed algorithm output from version four (v.4) of the eddy identification and tracking program. Near completion of this study, v.5 was released, so this appendix has been added to summarize the differences between the two versions. Due to the rigorous visual analysis described in Section 3.4.2, the features that appear to be real, concrete eddies are well documented and should stand up to minor adjustments to the algorithm. The second part of this brief analysis quantifies the differences in eddy characteristics (amplitude, radius, translation speed and axial speed) between v.4 and v.5.

Comparison of eddy events

Version 4 contained 76 eddies that impacted Station ALOHA and v.5 identifies 80 eddies. Eddies 03A and 55C from v.4 are each split into two different eddies in v.5. Eight eddies in v.5 were tracked in v.4 but were not considered to be real eddies after the visual analysis and should not be counted, the track numbers and details are found below. Two eddies in v.5, that were not tracked in v.4 were determined by visual analysis to not be real eddies. Two eddies in v.5 that barely grazed Station ALOHA were not considered to have impacted Station ALOHA in v.4 because of differences in the calculation of eddy center and/or radius positioned the eddy edge over ALOHA in v.5 but not in v.4. Four eddies in v.4 (15C, 58C, 67C and 75C) were dropped from the analysis in v.4 and were not tracked at all in v.5. Three other eddies that were tracked in v.4 were not tracked in v.5. 63C was a split from 62C but this split was not tracked in v.5. 40C is a questionable feature that was not tracked in v.5 and 33C was not tracked in v.5 but is a legitimate eddy that should've been tracked.

Specific eddy track details from version 5

- 112230 only tracked in v.4 after it splits north of ALOHA as 03A
- 125117 tracking in v.4 for only 1 time step, weak eddy that is picked up over Maui and dissipates before it gets to Kauai, may be a remnant from something else, difficult to determine visually
- 40762, 57171 were tracked in v.4, but were determined not to be real eddies and were dropped from analysis
- 53568 was tracked in v.4, but was dropped at the timestep before it entered ALOHA box, looks like an eddy that broke up and shouldn't be counted in the analysis anyway (no circular structure)
- 66549 is tracked similarly to v.4, its first timestep puts it directly north of Oahu, south of ALOHA, then it passes through Kauai channel and continues west. It was not counted as an eddy in v.4 because the radius was smaller at the first timestep, and so its radius did not overlap with ALOHA, so it was not flagged for retention

- 177269 was tracked longer in v.4, but again was not flagged for retention because of the slight difference in radius measurement
- 179968 not a real eddy, wasn't tracked in v.4
- 87997 is a split from 58C that is not tracked in v.4, the track begins west of ALOHA as the eddy is leaving the box
- 83743 jumps features from an eddy that was tracked in v.4 to some other feature that looks like a remnant from an eddy breaking up, should not be counted
- 195639 is tracked in v.4 but is dropped before the box. The part of the eddy tracked in ALOHA looks like there isn't any eddy left to track and shouldn't be counted.
- 205324 was tracked in v.4 but was determined not to be an eddy

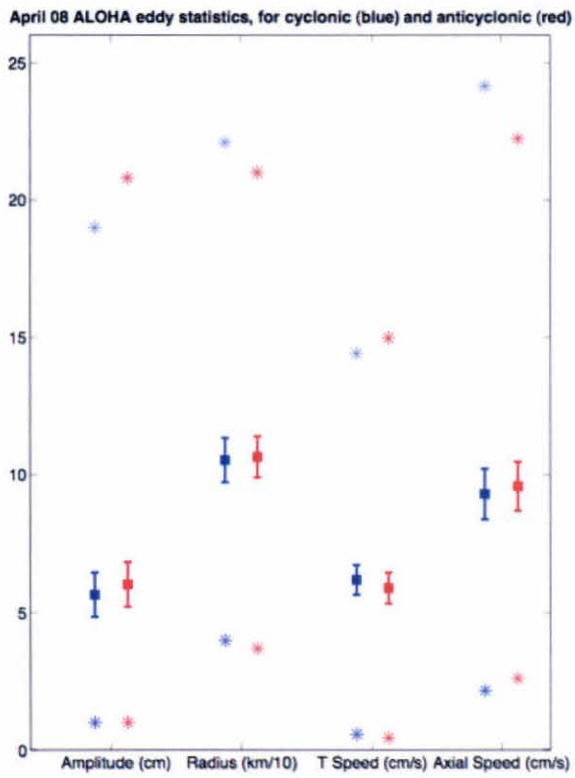

Figure III.1*:* ALOHA eddy statistics from v.5 of the eddy identification and tracking algorithm, including amplitude (cm), radius (km/10), translation speed (cm) and axial speed (cm). Squares denote the mean, the error bars denote the standard deviation of the mean based on 80 eddy events and the stars indicate maximum and minimum values of each distribution.

Comparison of eddy characteristics

Figure III.1 shows the eddy statistics for ALOHA eddies from the v.5 output. The mean amplitude is ~1 cm less than the mean amplitude from v.4 and the radius is ~4 km larger but the statistics for all eddy characteristics are not significantly different (Table III.1). Visual comparison of select eddy events between v.4 and v.5 show no noticeable indication of differences in eddy characteristics. There is not an apparent bias for larger measurements of eddies characteristics in one version versus the other version.

Table III.1: Mean and standard error of the mean for ALOHA eddies in v.5, similar to Table 4.1.

v.5 ALOHA eddy statistics	Cyclonic	Anticyclonic
Amplitude (cm)	5.66 ± 3.6	6.02 ± 3.6
Radius (km)	105.0 ± 35.6	106 ± 33.3
Translation Speed (cm s^{-1})	6.19 ± 2.4	5.88 ± 2.5
Axial Speed (cm s^{-1})	9.3 ± 4.0	9.57 ± 4